UNIVERSIDADE ESTADUAL PAULISTA
"JÚLIO DE MESQUITA FILHO"
Campus de São José do Rio Preto

Luiz Fernando Gonçalves

Campos de vetores suaves por partes: Aspectos teóricos e aplicações

São José do Rio Preto

2020

Luiz Fernando Gonçalves

Campos de vetores suaves por partes: Aspectos teóricos e aplicações

Tese apresentada como parte dos requisitos para obtenção do título de Doutor em Matemática, junto ao Programa de Pós-Graduação em Matemática, do Instituto de Biociências, Letras e Ciências Exatas da Universidade Estadual Paulista "Júlio de Mesquita Filho", Câmpus de São José do Rio Preto.

Financiadora: CAPES

Orientador: Prof. Dr. Tiago de Carvalho

Coorientador: Prof. Dr. Luis Fernando de Osorio Mello

São José do Rio Preto

2020

G635c

Gonçalves, Luiz Fernando

Campos de vetores suaves por partes : aspectos teóricos e aplicações / Luiz Fernando Gonçalves. -- São José do Rio Preto, 2020

195 f.

Tese (doutorado) - Universidade Estadual Paulista (Unesp), Instituto de Biociências Letras e Ciências Exatas, São José do Rio Preto

Orientador: Tiago de Carvalho

Coorientador: Luis Fernando de Osorio Mello

1. Campos de vetores suaves por partes. 2. Singularidades típicas. 3. Conjuntos minimais e caóticos. 4. Ciclos limite. 5. Coeficientes de Lyapunov. I. Título.

Sistema de geração automática de fichas catalográficas da Unesp. Biblioteca do Instituto de Biociências Letras e Ciências Exatas, São José do Rio Preto. Dados fornecidos pelo autor(a).

Essa ficha não pode ser modificada.

Luiz Fernando Gonçalves

Campos de vetores suaves por partes: Aspectos teóricos e aplicações

Tese apresentada como parte dos requisitos para obtenção do título de Doutor em Matemática, junto ao Programa de Pós-Graduação em Matemática, do Instituto de Biociências, Letras e Ciências Exatas da Universidade Estadual Paulista "Júlio de Mesquita Filho", Câmpus de São José do Rio Preto.

BANCA EXAMINADORA

Prof. Dr. Tiago de Carvalho (Orientador)
Universidade de São Paulo (FFCLRP/USP)

Profa. Dra. Regilene Delazari dos Santos Oliveira
Universidade de São Paulo (ICMC/USP)

Prof. Dr. Durval José Tonon
Universidade Federal de Goiás

Prof. Dr. Claudio Aguinaldo Buzzi
UNESP - São José do Rio Preto

Prof. Dr. Claudio Gomes Pessoa
UNESP - São José do Rio Preto

São José do Rio Preto

22 de Janeiro de 2020

A meus amados pais José e Ilma;

A meus grandes amigos;

A meus mestres;

Dedico.

Agradecimentos

À Universidade Estadual Paulista "Júlio de Mesquita Filho" (UNESP), em especial ao membros do Programa de Pós Graduação em Matemática do Instituto de Biociências, Letras e Ciências Exatas (IBILCE), pela oportunidade e realização deste trabalho.
Aos professores do IBILCE, pelos ensinamentos e conselhos que foram de grande importância em minha formação.
Ao meu orientador, Tiago de Carvalho, pelos ensinamentos e dedicação.
Ao meu coorientador, Luis Fernando Mello, pelo exemplo profissional e conselhos.
Aos meus colegas do Doutorado em Matemática do IBILCE.
À minha amada mãe que sempre me apoiou e encorajou nesta caminhada.
Ao meu amado pai, pelo exemplo e incentivo.
Aos meus grandes amigos e familiares pelo carinho e apoio.
O presente trabalho foi realizado com apoio da Coordenação de Aperfeiçoamento de Pessoal de Nível Superior - Brasil (CAPES) - Código de Financiamento 001, à qual agradeço.
Enfim, a todos que contribuíram, meus sinceros agradecimentos.

"In the broad light of day mathematicians check their equations and their proofs, leaving no stone unturned in their search for rigour. But, at night, under the full moon, they dream, they float among the stars and wonder at the mystery of the heavens: they are inspired. Without dreams there is no art, no mathematics, no life."

(Michael Atiyah, 2010, p.1)

Resumo

Nesta tese abordaremos aspectos qualitativos e dinâmicos de problemas envolvendo campos de vetores suaves por partes, também conhecidos como campos descontínuos. Primeiramente, apresentamos aplicações da teoria de campos de vetores descontínuos em modelos de tratamento intermitente de Cancer e Vírus da Imunodeficiência Humana onde exibimos a existência de singularidades típicas e órbitas periódicas. Ainda no contexto de aplicações, revisitamos um modelo predador-presa descontínuo de modo a concluir que o mesmo tem um comportamento caótico através da existência de uma órbita de Shilnikov. Posteriormente, respondemos questões sobre existência de conjuntos minimais e caóticos para campos de vetores descontínuos na esfera bidimensional. Em seguida, partimos ao estudo de bifurcação de ciclos limites em campos de vetores descontínuos tri e bidimensionais. No primeiro caso, perturbamos um campo descontínuo tangente a uma folheação por toros de modo a gerar uma quantidade finita ou infinita de ciclos limites. No segundo caso, estudamos uma família de campos descontínuos apresentando uma dobra-dobra invisível de costura, sua ciclicidade e a relação entre os coeficientes de Lyapunov desta família e sua regularização. Além disso, estudamos campos vetoriais suaves por partes Hamiltonianos contendo uma dobra-dobra invisível de costura donde apresentamos uma fórmula explícita para o cálculo dos cinco primeiros coeficientes de Lyapunov, além de explorar os diagramas de bifurcação gerados pelo desdobramento desta singularidade.

Palavras-chave: Campo de vetores suaves por partes. Singularidades típicas. Conjuntos minimais e caóticos. Ciclos limites. Coeficientes de Lyapunov. Órbita de Shilnikov.

Abstract

In this work we discuss qualitative and dynamic features of problems involving piecewise smooth vector fields, also known as discontinuous vector fields. Firstly, we present applications of discontinuous vector field theory in Human Immunodeficiency Virus and Cancer intermittent treatment models where we exhibit typical singularities and periodic orbits. Moreover, we revisit a discontinuous predator-prey model in order to conclude that it has a chaotic behavior through the existence of a Shilnikov orbit. Next, we answer questions about the existence of minimal and chaotic sets in the bidimensional sphere for discontinuous vector fields. Subsequently, we investigate the creation of limit cycles in three and two-dimensional discontinuous vector fields. In the first case, we perturb a discontinuous vector field tangent to a foliation composed by topological nested tori to generate a finite or infinite number of limit cycles. In the second case, we analyze a family of discontinuous vector fields containing a crossing invisible fold-fold, their cyclicity and the relation between the Lyapunov coefficients of this family and their regularization. Also, we study general piecewise Hamiltonian vector fields presenting a crossing invisible fold-fold where we give an explicit formula for the computation of the five first Lyapunov coefficients in addition to the investigation of the bifurcation diagrams.

Keywords: Piecewise smooth vector fields. Typical singularities. Minimal and chaotic sets. Limit cycles. Lyapunov coefficients. Shilnikov orbit.

List of Figures

List of Tables

Summary

Introduction

Ordinary Differential Equations (ODE's) are important mathematical tools for investigating natural phenomena. However, we know that many of them do not admit explicit solutions and this motivated great mathematicians to look for different alternatives to understand such solutions. Consequently, the way in which Ordinary Differential Equations were studied changed dramatically in the late $19th$ century. This fact is due to Henri Poincaré after the publication of his work *Mémoire sur les courbes definies par une équation différentielle* (see [100]) in which he introduces a new technique for the study of ODE's that was the basis of which today we call the Qualitative Theory of Ordinary Differential Equations. This theory gives us important and significant results and tools for studying the behavior of the orbits of the differential equation and the analysis of its phase portrait, without knowing its explicit solutions, through geometric, topological, analytical aspects, among others.

Several and important models used in applied problems, related to engineering and biology, are described by systems that are not completely differentiable, but in different parts, where a law of evolution is suddenly interrupted by another law of evolution that will begin to govern such system. The modeling of such systems consists of different vector fields defined in distinct regions separated by a switching manifold and are known as piecewise smooth vector fields, discontinuous systems or Filippov systems.

Pioneering studies initiated by Andronov [5] and Filippov [47] led to a theoretical foundation for this kind of problem and developed certain conventions for the transition of orbits between different regions, in order to define the basic objects of Qualitative Theory of Differential Equations and investigation of their dynamics. Currently, there is a wide literature on discontinuous vector fields. See, for example, the book [37] for main theory and applications, [16, 40, 82] for applications in mechanical models, [28, 32, 76] on circuits electrical, [39, 71] in relay systems, among others.

The study of minimal sets and limit sets is of great importance in the context of qualitative theory, as they help us to understand the behavior of a dynamic system. In the context of vector field flows in compact sets of the plane, and even in the sphere, the Poincaré-Bendixson Theorem establishes that the limit set of a trajectory must be an equilibrium point, a graph or a periodic orbit. Denjoy in [36] proves that if we consider in the torus (or a connected two-dimensional compact manifold) a flow of class C^2 then the minimal sets are trivial, that is, fixed points, closed orbits or all the torus, in which case the flow is topologically equivalent to an irrational flow. However, a C^1 flow can present non-trivial minimal sets, a fact that was also shown by Denjoy in [36] (see also [22, 63, 102]).

Minimal trivial sets significant in the theory of dynamical systems are isolated periodic orbits, that is, limit cycles. Studies involving bifurcations of limit cycles and the maximum number of limit cycles that can bifurcate in a family of vector fields, that is, their ciclicity, are some of the topics most covered in the qualitative theory, both for their mathematical relevance and for their applications in real models. Such an object is the subject of Hilbert's famous $16th$ problem (see [65]) which seeks for an upper bound for the number of limit cycles in planar polynomial vector fields. The appearance of non-trivial minimal sets requires a lower regularity than that required in the Denjoy-Schwartz Theorem, that is, vector fields of class C^1 or even discontinuous as can be seen in [18], [19], and [36].

The occurrence of non-trivial minimal sets in certain systems is linked to the presence of complex behaviors, such as chaotic dynamics. Chaos can be understood through the existence of an invariant compact set in which trajectories by their initial conditions exhibit transitivity and sensitive dependence (see [67, 89]) and can be traced by studying the existence of previously known objects being chaotic as this is the case of Shilnikov's homoclinic orbit, a trajectory connecting a hyperbolic equilibrium of saddle-focus type to himself (see [67, 103, 104]). Chaotic behaviors in discontinuous vector fields (see Definition 12) have recently been investigated and the first evidence of chaoticity in such systems comes from the work of Jeffrey [31] where new and rich chaotic models appear.

The theory of discontinuous vector fields has been developed taking, at first, parallel to the classical theory. It is known that the Existence and Uniqueness Theorem is not valid in this context since we have no uniqueness of solutions in the orbits defined by means of the sliding field (see Definition 1). The Poincaré-Bendixson Theorem has a version for discontinuous systems (see [19]) as well as the Peixoto Theorem (see [107]). Even a technique that allows us to relate discontinuous to regular systems has been developed. The regularization method, introduced by Sotomayor and Teixeira in [109] consists of the approximation of a discontinuous system by a one parameter family of smooth vector fields, from where we can apply the classical theory to try to obtain information about the piecewise smooth vector field.

As in the regular case, the study of limit cycles is an important problem in discontinuous systems theory. Traditionally, the study of limit cycles in a family of planar vector fields X_λ close to a continuum of periodic orbits or a center-type equilibrium can be replaced by the study of the fixed points of a first return map P_λ or, equivalently, by studying the zeros from the so-called displacement function $\delta_\lambda = P_\lambda - Id$. Such technique is still very useful in the study of crossing limit cycles in discontinuous vector fields and great effort has been devoted to determining the maximum number of limit cycles that can occur in a piecewise smooth vector field, in which even the linear case is already shown intriguing. In the planar case, if the separation curve is not a straight line, for each positive integer n, we can find a piecewise linear system with exactly n limit cycles (see [15, 92]). However, if the separation curve is a straight line, continuous piecewise linear systems can present at most one limit cycle, a fact that was conjectured by Lum and Chua in [86] and proved later in [48]. This result also proved to be valid for sewing planar piecewise linear systems as can be seen in [88]. Discontinuous vector fields, on the other hand, can have three limit cycles (see [84]) and there is a strong belief that three is the maximum number of limit cycles that can appear in crossing piecewise linear systems. There is also the appearance of crossing limit cycles for linear vector fields in which the separation line involves sliding regions as can be seen in [14].

In this way, many authors have contributed to the development of discontinuous vector field theory. Several models related to engineering and biology governed by discontinuous systems occur in families with n parameters that undergo some kind of bifurcation, making it essential to establish the notion of structural stability and the classification of bifurcations for such systems. One of the starting points in this context was the work of Teixeira [116] in which he studies vector fields in two-dimensional manifolds with boundaries. The structural stability of Filippov's vector fields had as precursors the works of Kozlova [77] and Teixeira [118] and, in the study of generic singularities, Teixeira's work in [117]. The classification of one parameter local and global bifurcations of a Filippov planar system was established later by Kuznetsov et al. em [80] and complemented by Guardia et al. in [62] which also begins the study of unfoldings of two parameters generic singularities.

We now present a brief description of the chapters of this work.

In the first chapter, we introduce the terminology and basic concepts of the theory of piecewise smooth vector fields in order to define the fundamental objects of the theory that will be essential in the development of this work.

In chapter two, we present applications of discontinuous vector field theory. We explored models of intermittent treatment of Cancer and Human Immunodeficiency Virus (HIV) and, after, we studied the chaoticity of a discontinuous predator-prey model. In the first case, we studied a system of differential equations in $\mathbb{R}^3$ that models the treatment of leukemia. We explored the transition between the model with or without the treatment given by chemotherapy and/or immunotherapy and we exhibit an interesting behavior next to the switching manifold due to the existence of typical singularities. Some of the singularities found in this work are more complicated than those already shown in the literature (see, for example, [24, 26]) as they are not yet represented by normal forms. This study resulted in the papers I and II from the list of published or submitted papers derived from this thesis available at the end of the introduction. In the second case, we studied the qualitative dynamics of a piecewise smooth system that models the intermittent treatment of HIV. We exhibit the existence of typical singularities and periodic orbits and explore the dynamics around these objects. In addition, we conclude that such a protocol is successful, since the trajectory that passes through any initial condition converges to one of these distinct orbits. Our results corroborate the observation of the real world, where the virus is not eliminated, but is controlled around a specific value. The results derived from this study are the contents of preprints III and IV from the list available at the end of this section.

Also in chapter two, we revisit a piecewise smooth vector field in $\mathbb{R}^3$ that was obtained recently by modeling the interaction between a predator and two prey in which the predator adjusts its feeding preference between a preferred prey and an alternative. Such a model proposed by Piltz et al. in [99] is given by

$$(\dot{x}, \dot{y}, \dot{z})^T = \begin{cases} X(x,y,z) = \begin{pmatrix} (r_1 - z)x \\ r_2 y \\ (eq_1 x - m)z \end{pmatrix} & h(x,y,z) \geq 0; \\ Y(x,y,z) = \begin{pmatrix} r_1 x \\ \left(r_2 - \dfrac{\beta_2}{\beta_1} z\right) y \\ \left(\dfrac{eq_2}{a_q} y - m\right) z \end{pmatrix} & h(x,y,z) \leq 0, \end{cases}$$

where $(x, y, z) \in \mathbb{R}^3_{\geq 0}$ and $h(x, y, z) = x - y$. In this model, the authors observed numerical evidences of chaotic behavior. We proved that in a codimension one submanifold of the parameter space such a system exhibits a Shilnikov connection (see Definition 15) and through this fact we conclude that the system is chaotic (see Theorem 9). This work resulted in preprint V of the list of papers derived from this thesis available at the end of this section.

The third chapter is dedicated to the study of piecewise smooth vector fields tangent to the bidimensional sphere. We show the existence of discontinuous vector fields in the two-dimensional sphere that do not present singularities, but presenting chaotic non-trivial minimal sets, following Filippov's conventions. In addition, we show the existence of a discontinuous vector field that has the entire sphere as a minimal set. As far as we know, the literature does not yet contemplate the study of piecewise smooth vector fields in the sphere via Filippov's conventions. Such studies resulted in paper VI and preprint VII of the list of papers.

In the fourth chapter, we perturb a discontinuous vector field tangent to a foliation composed by topological nested tori. Such vector field in cylindrical coordinates is given by

$$Z_0(r,\theta,z)=\begin{cases} X(r,\theta,z)=\left(r,\,0\,,\dfrac{4+17r^2-12r^4}{4r}\right) & z\geq 0,\\[2ex] Y(r,\theta,z)=\left(-r,\,0\,,\dfrac{4+17r^2-12r^4}{4r}\right) & z\leq 0.\end{cases}$$

In each half-plane $\Pi_{\theta_0}=\{(x,y,z)\in\mathbb{R}^3\,|\,x=r\cos(\theta_0),y=r\sin(\theta_0)\text{ where }r\geq 0\}$ the vector field Z_0 is invariant and behaves like a center. Through two uncoupled perturbations we consider a perturbation of Z_0 of the form

$$Z_\varepsilon(r,\theta,z)=\begin{cases} X_\varepsilon(r,\theta,z)=\left(r,\,0\,,\dfrac{4+17r^2-12r^4}{4r}+r\dfrac{\partial F_\varepsilon}{\partial r}(r)\right) & z\geq 0,\\[2ex] Y^\nu(r,\theta,z)=\left(-r,\,\nu(\theta)\,,\dfrac{4+17r^2-12r^4}{4r}\right) & z\leq 0,\end{cases}$$

in order to generate a finite, or infinite, number of invariant half-planes, with each of these half-planes having a finite, or infinite, number of limit cycles. The stability of such limit cycles is related to the derivatives of the perturbation functions involved, and we can also have multiple limit cycles. This study resulted in preprint VIII of the list of papers derived from this thesis.

Finally, in chapter five, we study a k parameters unfolding of the family of discontinuous vector fields containing an invisible fold-fold at the origin given by

$$\mathfrak{Z}_{b,k,\lambda}(x,y)=\begin{cases}\mathfrak{X}_{b,k}(x,y)=\left(1,-x+bx^{2k}\right) & y\geq 0\\ Y_\lambda(x,y)=(-1,-x+\lambda) & y\leq 0,\end{cases}$$

where λ is a small parameter, b a non-zero real number and $k=1,2,3,\ldots$. We show that, for each fixed k, there exists $\lambda\in\mathbb{R}$ sufficiently small and $a=(a_2,a_4,\ldots,a_{2k-2})$ such that the unfolding $Z_{a,k,\lambda}$ given by

$$Z_{a,k,\lambda}(x,y)=\begin{cases}X_{a,k}(x,y)=\left(1,-x+a_2x^2+\cdots+a_{2k-2}x^{2k-2}+x^{2k}\right) & y\geq 0;\\ Y_\lambda(x,y)=(-1,-x+\lambda) & y\leq 0,\end{cases}$$

has exactly k crossing limit cycles in a neighborhood of the origin, a number that is also maximum. We generalize the results found in [80] and [62] in which such a family was studied with one and two parameters, respectively, where one and two limit cycles were found and the bifurcation diagrams displayed. Given the similarity of such diagrams with classic Hopf bifurcations, we wondered if there could be any relationship between the Lyapunov coefficients of the family of discontinuous vector field and its regularization. The answer was positive and we showed the following result: For $\varepsilon > 0$ small enough, the Lyapunov coefficients of the discontinuous vector field $Z_{a,k,0}$ and the Lyapunov coefficients of its regularization Z_ε has the same sign. This work is the content of preprint IX of the list of papers derived from this thesis available at the end of this introduction.

Also in chapter five, we consider a piecewise smooth vector field of the form

$$\mathcal{Z}(x,y,\mu,\nu) = \begin{cases} \mathcal{X}(x,y,\mu,\nu), & y \geq 0; \\ \mathcal{Y}(x,y,\mu,\nu), & y \leq 0, \end{cases}$$

containing an invisible fold-fold at the origin where $\mathcal{X}$ and $\mathcal{Y}$ are Hamiltonian systems. We obtained explicit formulas, written in terms of the derivatives of the Hamiltonian functions associated with the vector fields $\mathcal{X}$ and $\mathcal{Y}$, for the calculation of the first five Lyapunov coefficients associated with a Hamiltonian piecewise smooth vector field with an invisible fold-fold at the origin (see Theorem 15 and Theorem 18). In addition, we study the bifurcation diagrams associated with such a discontinuous vector field when the second Lyapunov coefficient is nonzero or when the second Lyapunov coefficient is zero and the fourth is nonzero (see Theorems 16 e 19). In the last case, we give a general expression for the curve of non-hyperbolic periodic orbits that occurs in this diagram (see Proposition 42 and Remark 22). This study resulted in the paper X of the list below of published and submitted papers derived from this thesis.

Published and submitted papers derived from this Thesis

I. L. F. Gonçalves, D. S. Rodrigues, P. F. A. Mancera, and T. Carvalho. Sliding mode control in a mathematical model to chemoimmunotherapy: the occurrence of typical singularities. Applied Mathematics and Computation, 2019. doi: 10.1016/j.amc.2019.124782.

II. L. F. Gonçalves, D. S. Rodrigues, P. F. A. Mancera, and T. Carvalho. A mathematical model for chemoimmunotherapy of chronic lymphocytic leukemia. Applied Mathematics and Computation, 349: 118-133, 2019. doi: 10.1016/j.amc.2018.12.008

III. L. F. Gonçalves, D. C. Vicentin, P. F. A. Mancera, and T. Carvalho. Mathematical model of an antiretroviral therapy to HIV via Filippov theory. Preprint, 2019.

IV. L. F. Gonçalves, T. Carvalho, R. Cristiano, and D. J. Tonon. Global analysis of the dynamics of a mathematical model to intermittent HIV treatment using sliding mode control. Preprint, 2019.

V. L. F. Gonçalves, T. Carvalho, and D. D. Novaes. Sliding Shilnikov Connection in Prey Switching Model. Preprint, 2019. Available in http://arxiv.org/abs/1809.02060.

VI. L. F. Gonçalves and T. Carvalho. Combing the Hairy ball using a vector field without equilibria. Journal of Dynamical and Control Systems, volume online, 2019. doi: 10.1007/s10883-019-09446-5

VII. L. F. Gonçalves and T. Carvalho. A flow on S^2 presenting the ball as its minimal set. Preprint, 2019.

VIII. L. F. Gonçalves and T. Carvalho. Creation of limit cycles in piecewise smooth vector fields tangent to nested tori. Preprint, 2019.

IX. L. F. Gonçalves, D. C. Braga, A. F. Fonseca, and L. F. Mello. Limit cycles bifurcating from an invisible fold-fold in planar piecewise Hamiltonian systems. Preprint, 2019.

X. L. F. Gonçalves, D. C. Braga, A. F. Fonseca, and L. F. Mello. Lyapunov coeficients for an invisible fold-fold singularity in planar piecewise Hamiltonian systems. Journal of Mathematical Analysis and Applications, volume online, 2019. doi:10.1016/j.jmaa.2019.123692

Chapter 1

Preliminaries

In this chapter, we present basic concepts and results concerning piecewise smooth vector fields which is the main subject of this work. Also, we present a method to compute the Lyapunov coefficients for smooth systems.

1.1 Basic theory about piecewise smooth vector fields

Let us consider a codimension one manifold Σ of $\mathbb{R}^n$ given by $\Sigma = h^{-1}(0)$, where $h : \mathbb{R}^n \to \mathbb{R}$ is a smooth function having $0 \in \mathbb{R}$ as a regular value, that is, $\nabla h(p) \neq 0$, for any $p \in h^{-1}(0)$. We call Σ the *switching manifold* that is the separating boundary of the regions $\Sigma^+ = \{q \in \mathbb{R}^n \,|\, h(q) > 0\}$ and $\Sigma^- = \{q \in \mathbb{R}^n \,|\, h(q) < 0\}$.

Designate by χ the space of C^r-vector fields on $V \subset \mathbb{R}^n$ endowed with the C^r-topology, with $r \geq 1$ large enough for our purposes. Call Ω^r the space of piecewise smooth vector fields (PSVFs for short) $Z : V \subset \mathbb{R}^n \to \mathbb{R}^n$ such that

$$Z(q) = \begin{cases} X(q), & \text{if} \quad h(q) \geq 0, \\ Y(q), & \text{if} \quad h(q) \leq 0, \end{cases} \tag{1.1}$$

where $X = (X_1, \ldots, X_n), Y = (Y_1, \ldots, Y_n) \in \chi$. We endow Ω^r with the product topology. As usual, System (1.1) is denoted by $Z = (X, Y)$ and the trajectories of Z are solutions of $\dot{q} = Z(q)$. We notice that Z is considered multivalued at points of Σ.

In order to establish a definition for the trajectories of Z and investigate its behavior we need a criterion for the transition of the orbits between Σ^+ and Σ^- across Σ. The contact between the smooth vector field X and the switching manifold Σ is characterized by the expression $Xh(p) = \langle \nabla h(p), X(p) \rangle$ where $\langle .,. \rangle$ is the usual inner product in $\mathbb{R}^n$. Observe that $Xh(p)$ is the derivative of h in the direction of X, also known as the Lie derivative of h with respect to X. Analogously, we have

$$X^i h(p) = \left\langle \nabla X^{i-1} h(p), X(p) \right\rangle, \qquad \text{for } i \geq 2.$$

The basic results of differential equations in this context were stated by Filippov [47]. We can divide the switching manifold Σ in the following regions (see Figure 1.1):

- Crossing Region: $\Sigma^c = \{p \in \Sigma \,|\, Xh(p) \cdot Yh(p) > 0\}$.
- Sliding Region: $\Sigma^s = \{p \in \Sigma \,|\, Xh(p) < 0, Yh(p) > 0\}$.
- Escaping Region: $\Sigma^e = \{p \in \Sigma \,|\, Xh(p) > 0, Yh(p) < 0\}$.

Moreover, we denote the sets $\Sigma^{c+} = \{p \in \Sigma \,|\, Xh(p) > 0, Yh(p) > 0\}$ and $\Sigma^{c-} = \{p \in \Sigma \,|\, Xh(p) < 0, Yh(p) < 0\}$.

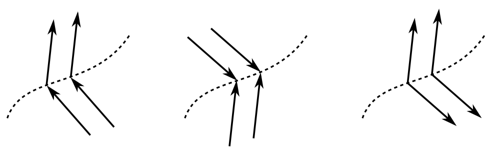

Figure 1.1: Crossing, sliding and escaping regions, respectively.

In the case $Xh(p) = 0$ the trajectories of X are tangent to Σ in p and we say that p is a *tangential singularity* of X. A tangential singularity $p \in \Sigma$ is a *fold point* of X if $Xh(p) = 0$ but $X^2h(p) \neq 0$. Moreover, $p \in \Sigma$ is a *visible* (respectively *invisible*) fold point of X if $Xh(p) = 0$ and $X^2h(p) > 0$ (respectively $X^2h(p) < 0$). When p is a fold point for both X and Y we say that p is a *fold-fold singularity* or *two-fold singularity.* When p is a cusp point for X ($Xh(p) = X^2h(p) = 0$ and $X^3h(p) \neq 0$) and a fold point for Y we say that p is a *cusp-fold singularity* (see Figure 1.2). These singularities are particularly relevant because in its neighborhood some of the key features of a piecewise smooth system are present: orbits that cross Σ, those that slide along it, among others. Generic 3D fold-fold and cusp-fold singularities are studied, for example, in [12, 30, 31, 38, 72] (two-fold) and [24, 26, 32] (cusp-fold).

In addition, a tangential singularity q is *singular* if q is an invisible tangency for both X and Y. On the other hand, a tangential singularity q is *regular* if it is not singular. Furthermore, given $Z = (X, Y) \in \Omega^r$ we say that an equilibrium point p of X (respectively, Y) is real for Z if $p \in \Sigma^+$ (respectively, Σ^-) and virtual if $p \in \Sigma^-$(respectively, Σ^+).

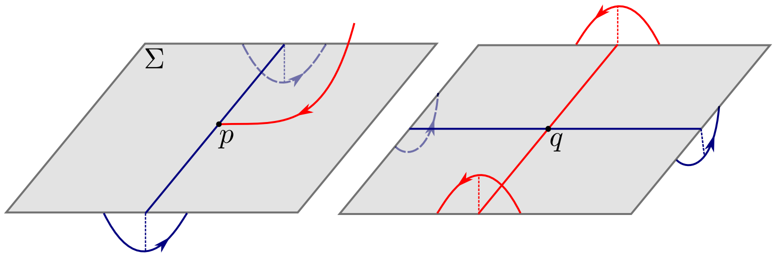

Figure 1.2: On the left, it appears a cusp-fold singularity and on the right a two-fold singularity.

In order to define the trajectories of a PSVF passing through a crossing point, since the vector fields X and Y point in the same direction, it is enough to concatenate the trajectories of X and Y by that point. However, in the sliding and escaping regions we need to define an auxiliary vector field. So, we consider the Filippov's convention in order to define a new vector field on $\Sigma^s \cup \Sigma^e$. This new vector field, called *sliding vector field*, is a convex linear combination of $X(p)$ and $Y(p)$ in a way that Z^s is tangent to Σ in the cone generated by $X(p)$ and $Y(p)$.

Definition 1. *Given a point $p \in \Sigma^s \cup \Sigma^e \subset \Sigma$, we define the **sliding vector field** at p as the vector field $Z^s(p) = m - p$ with m being the point of the segment joining $p + X(p)$ and $p + Y(p)$ such that $m - p$ is tangent to Σ. (see Figure 1.3).*

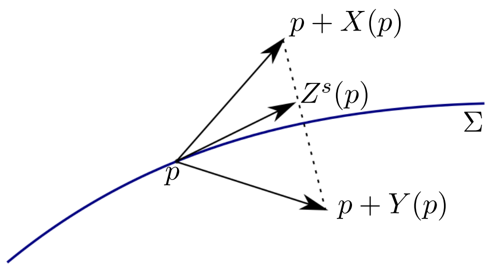

Figure 1.3: Sliding vector field.

The sliding vector field is given by the expression

$$Z^s(q) = \frac{Yh(q)X(q) - Xh(q)Y(q)}{Yh(q) - Xh(q)} \text{ for all } q \in \Sigma^s \cup \Sigma^e. \tag{1.2}$$

Moreover, when it is well defined (i.e., $\Sigma^s \cup \Sigma^e \neq \emptyset$), the sliding vector field can be extend to $\overline{\Sigma^e} \cup \overline{\Sigma^s}$. Any point $p \in \Sigma^s \cup \Sigma^e$ such that $Z^s(p) = 0$ is called a **pseudo equilibrium of** Z.

Let S_X (respectively, S_Y) be the set of all tangential singularities of X (respectively, Y). Next, we define a vector field at the tangential singularities when $\Sigma^s \cup \Sigma^e = \emptyset$.

Definition 2. *When $S_X = S_Y = S$ and the dimension of S is nonzero, we define a motion on S in the following way. Given a point $p \in S \subset \Sigma$, we define the **tangential sliding vector field***

at p as the vector field $Z^T(p) = m - p$ with m being the point of the segment joining $p + X(p)$ and $p + Y(p)$ such that $m - p$ is tangent to S (see Figure 1.4).

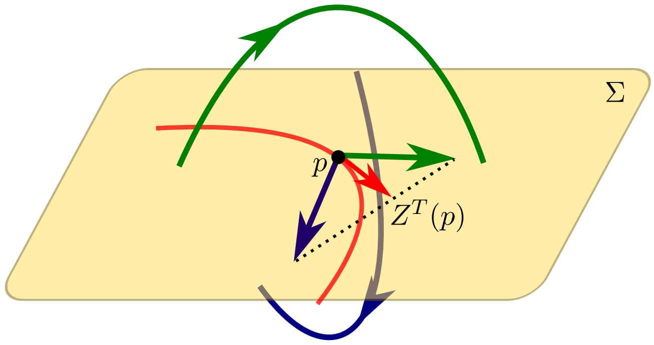

Figure 1.4: Tangential sliding vector field.

Remark 1. *Suppose that $S \subset \Sigma \subset \mathbb{R}^3$ is a curve depending on one variable, let us say $w(x)$. Then, the tangential sliding vector field Z^T in a point $p \in S$ is given by*

$$Z^T(p) = \frac{\big(Yw(p)\big)X(p) - \big(Xw(p)\big)Y(p)}{Yw(p) - Xw(p)},$$

where $Xw(p)$ is the Lie derivative of X restricted to the curve w given by $Xw(p) = X(p) \cdot W(x)$, with $W(x)$ a vector in the tangent space of Σ and normal to $w(x)$ at the point x.

We call a **tangential equilibrium** an equilibrium point of the tangential sliding vector field given in the Definition 2. In the next definitions, we establish the concepts of local and global trajectories of a PSVF.

Definition 3. *The **local trajectory (orbit)** $\phi_Z(t,p)$ of a PSVF given by (1.1) through $p \in V$ is defined as follows:*

(i) For $p \in \Sigma^+ \backslash \Sigma$ and $p \in \Sigma^- \backslash \Sigma$ the trajectory is given by $\phi_Z(t,p) = \phi_X(t,p)$ and $\phi_Z(t,p) = \phi_Y(t,p)$ respectively, where $t \in I$.

(ii) For $p \in \Sigma^{c+}$ and taking the origin of time at p, the trajectory is defined as $\phi_Z(t,p) = \phi_Y(t,p)$ for $t \in I \cap \{t \leq 0\}$ and $\phi_Z(t,p) = \phi_X(t,p)$ for $t \in I \cap \{t \geq 0\}$. For the case $p \in \Sigma^{c-}$ the definition is the same reversing time.

(iii) For $p \in \Sigma^e$ and taking the origin of time at p, the trajectory is defined as $\phi_Z(t,p) = \phi_{Z^s}(t,p)$ for $t \in I \cap \{t \leq 0\}$ and $\phi_Z(t,p)$ is either $\phi_X(t,p)$ or $\phi_Y(t,p)$ or $\phi_{Z^s}(t,p)$ for $t \in I \cap \{t \geq 0\}$. For $p \in \Sigma^s$ the definition is the same reversing time.

(iv) For p a regular tangency point and taking the origin of time at p, the trajectory is defined as $\phi_Z(t,p) = \phi_1(t,p)$ for $t \in I \cap \{t \le 0\}$ and $\phi_Z(t,p) = \phi_2(t,p)$ for $t \in I \cap \{t \ge 0\}$, where each ϕ_1, ϕ_2 is either ϕ_X, ϕ_Y, ϕ_{Z^s} or ϕ_{Z^T} .

(v) For p a singular tangency point in $\mathbb{R}^2$, $\phi_Z(t,p) = p$ for all $t \in \mathbb{R}$. In other cases, taking the origin of time at p, the trajectory is defined as $\phi_Z(t,p) = \phi_{Z^T}(t,p)$, for $t \in I$.

Definition 4. *The* ***global trajectory (orbit)*** *$\Gamma_Z(t,p_0)$ of Z passing through p_0 is a union*

$$\Gamma_Z(t,p_0) = \bigcup_{i \in \mathbb{Z}} \{\sigma_i(t,p_i) : t_i \le t \le t_{i+1}\}$$

of preserving-orientation local trajectories $\sigma_i(t,p_i)$ satisfying $\sigma_i(t_{i+1},p_i) = \sigma_{i+1}(t_{i+1},p_{i+1}) = p_{i+1}$.

Definition 5. *When the trajectory of X through $p \in \Sigma$ returns to Σ (by the first time) after a positive time $t_1(p)$, called* ***X-flight time****, we define the* ***half return map associated with*** *X by $\pi_X(p) = \phi_X(t_1(p),p) = p_1 \in \Sigma$. When the trajectory of Y through $p_1 \in \Sigma$ returns to Σ (by the first time) after a positive time $t_2(p_1)$, called* ***Y-flight time****, we define the* ***half return map associated with*** *Y by $\pi_Y(p_1) = \phi_Y(t_2(p_1),p_1) \in \Sigma$. The* ***first return map*** *associated with $Z = (X,Y)$ is defined by the composition of these two involutions, that is,*

$$\pi_Z(p) = \pi_Y \circ \pi_X(p) = \phi_Y(t_2(p_1), \phi_X(t_1(p),p)) \tag{1.3}$$

or in the reverse order, applying first the flow of Y and after the flow of X.

See Figure 1.5 and [119] for more details.

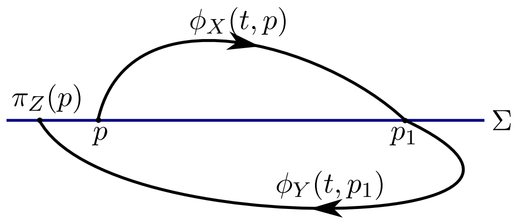

Figure 1.5: First return map for a PSVF.

When the vector fields X and Y associated with $Z = (X,Y)$ are Hamiltonian, the solution curves of the respective differential equations are contained in the level sets of the Hamiltonian functions. In this scenario, the first return map can be handily computed by seeking for points in Σ that are on the same level curves of these Hamiltonian functions. In this case, we avoid working with flight times.

Now we introduce some concepts about α-limit and ω-limit sets of a global trajectory of a PSVF. In order to define it we need to consider each trajectory passing through a given point since we do not have the uniqueness of solutions.

Definition 6. *Given $\Gamma_Z(t, p_0)$ a global trajectory passing through p_0, the set*

$$\omega\left(\Gamma_Z(t, p_0)\right) = \{q \in V : \exists (t_n) \text{ satisfying } \Gamma_Z(t_n, p_0) \to q \text{ when } t \to +\infty\}$$

*is called ω-**limit set** of $\Gamma_Z(t, p_0)$. In a similar way, we can define the α-**limit set** of $\Gamma_Z(t, p_0)$ as the set*

$$\alpha\left(\Gamma_Z(t, p_0)\right) = \{q \in V : \exists (t_n) \text{ satisfying } \Gamma_Z(t_n, p_0) \to q \text{ when } t \to -\infty\}.$$

The ω-limit (respectively, α-limit) set of a point p is the union of the ω-limit (respectively, α-limit) sets of all global trajectories passing through p.

We can notice that for single-valued trajectories the definition above coincides with the classical one. In what follows, we bring some results concerning understand the role that trajectories play in non-smooth vector fields with sliding motion.

Remark 2. *In general, the ω-limit set is not connected. In fact, since the global orbit through a given point may not be unique, the positive global trajectory can follow distinct paths. In Figure 1.6 the trajectory through p can follow three paths, namely, Γ_1, Γ_2 e Γ_3. Notice that the ω-limit of Γ_i, for $i = 1, 2, 3$ is, respectively, a focus, a pseudo equilibrium and a limit cycle. So, the ω-limit set of p, that is the union of these objects, is not connected. Nonetheless, in this example, the α-limit set of p is a connected set composed by a pseudo equilibrium.*

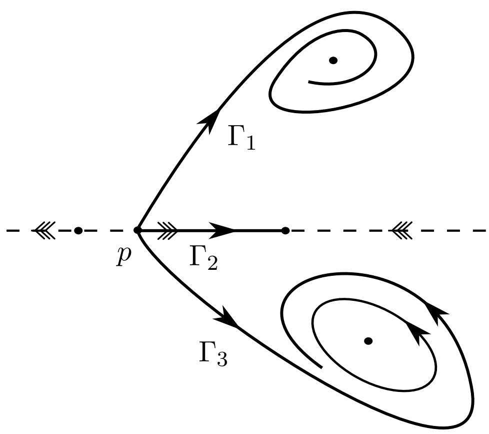

Figure 1.6: The ω-limit of p is disconnected.

In the opposite direction from what happened in Remark 2, the next proposition has an analogous in the classic theory for smooth vector fields, with similar proof which we include for sake of completeness.

Proposition 1. *The α and ω-limit sets of a trajectory Γ of a PSVF are closed subsets of $\mathbb{R}^n$. In particular, if Γ is contained in a compact subset of $\mathbb{R}^n$ then the α and ω-limit sets are non-empty compact subsets of $\mathbb{R}^n$.*

Proof. In fact, let p_n be a sequence of points in $\omega(\Gamma)$ with $p_n \to p$. Given $x_0 \in \Gamma$ since $p_n \in \omega(\Gamma)$, for each $n = 1, 2, \ldots$, there is a sequence $t_k^{(n)} \to \infty$ as $k \to \infty$ such that $\lim_{k\to\infty} \Gamma(t_k^{(n)}, x_0) = p_n$. We may assume $t_k^{(n+1)} > t_k^{(n)}$ since otherwise we can choose a subsequence of $t_k^{(n)}$. So, for all $n \geq 2$, there is a sequence of integers $K(n) > K(n+1)$ such that for $k > K(n)$,

$$|\Gamma(t_k^{(n)}, x_0) - p_n| < \frac{1}{n}.$$

Let $t_n = t_{K(n)}^{(n)}$. Then $t_n \to \infty$ and

$$|\Gamma(t_k^{(n)}, x_0) - p| \leq |\Gamma(t_k^{(n)}, x_0) - p_n| + |p_n - p| \leq \frac{1}{n} + |p_n - p| \to 0$$

as $n \to \infty$. Thus, $p \in \omega(\Gamma)$. If $\Gamma \subset K$, a compact subset of $\mathbb{R}^n$, and $\Gamma(t_n, x_0) \to p \in \omega(\Gamma)$ then $p \in K$. Thus, $\omega(\Gamma) \subset K$ and therefore $\omega(\Gamma)$ is compact since it is a closed subset of a compact set. Furthermore, $\omega(\Gamma) \neq \emptyset$ since the sequence of points $\Gamma(t_n, x_0)$ contains a convergent subsequence which converges to a point in $\omega(\Gamma) \subset K$. $\square$

Now we established the concept of periodic trajectories for PSVFs. Actually, it is analogous to the definition of periodic trajectory for smooth systems and it will be necessary to the following definitions that concern about chaos and minimal sets.

Definition 7. *Let $\Gamma_Z(t, q)$ a global trajectory of the PSVF* (1.1). *We say that Γ_Z is periodic if Γ_Z is periodic in the variable t, that is, if there exist $T > 0$ such that $\Gamma_Z(t + T, q) = \Gamma_Z(t, q)$, for all $t \in \mathbb{R}$.*

Finding limit sets of trajectories is one of the most important goals of the qualitative theory of dynamical systems. In the literature, there are recent papers (see [19], [20], [62]) where the authors exhibit the phase portrait of non-smooth vector fields. In what follows, we introduce the idea of minimality and non-deterministic chaos in non-smooth systems.

Definition 8. *A set $M \subset \mathbb{R}^n$ is invariant for $Z \in \Omega^r$ if for each $p \in M$ and all global trajectory $\Gamma_Z(t, p)$ passing through p it holds $\Gamma_Z(t, p) \subset M$.*

Definition 9. *Consider $Z \in \Omega^r$. A set $M \subset \mathbb{R}^n$ is minimal for Z if:*

(a) $M \neq \emptyset$;

(b) M is compact;

(c) M is invariant for Z;

(d) M does not contain proper subset satisfying (a)-(c).

The definition of non-deterministic chaos for PSVFs was first introduced in [31], where the authors adapt the classical definition (see, for example, [89]) to this context. Certainly, the definition should contemplate topological transitivity and sensibility to initial conditions. This leads us to the following definitions.

Definition 10. *System* (1.1) *is topologically transitive on an invariant set W if for every pair of non-empty, open sets U and V in W, there exist $p \in U$, $\Gamma_Z^+(t_0, p)$ a positive global trajectory and $t_0 > 0$ such that $\Gamma_Z^+(t_0, p) \in V$.*

Definition 11. *System* (1.1) *exhibits sensitive dependence on a compact invariant set W if there is a fixed $r > 0$ satisfying $r < diam(W)$ such that for each $x \in W$ and $\varepsilon > 0$ there exist $y \in B_\varepsilon(x) \cap W$ and positive global trajectories $\Gamma^+(x)$ and $\Gamma^+(y)$ passing through x and y, respectively, satisfying*

$$d_H(\Gamma^+(x), \Gamma^+(y)) = \sup_{a \in \Gamma^+(x), b \in \Gamma^+(y)} d(a, b) > r$$

where $diam(W)$ is the diameter of W and d is the Euclidean distance.

We remark that the two previous definitions make a natural extension since they coincide with those used for smooth systems when the flow is single-valued. In this way, we can define chaos in this context.

Definition 12. *System* (1.1) *is chaotic on a compact invariant set W if it is topologically transitive and exhibits sensitive dependence on W.*

1.2 Lyapunov coefficients for smooth systems

In this section, we present an efficient algebraic approach that allows us to compute what we will call *Lyapunov coefficients*, a recursive method that permits us to determine the stability of an equilibrium point whose linearization is a center.

Define $\mathcal{H}^n$ to be the vector space of all homogeneous polynomials of degree n in the variables x and y and consider the system

$$\begin{cases} \dot{x} = -y + P(x,y); \\ \dot{y} = x + Q(x,y), \end{cases} \tag{1.4}$$

where

$$P(x,y) = \sum_{j=2}^{\infty} P_j(x,y)$$

and

$$Q(x,y) = \sum_{j=2}^{\infty} Q_j(x,y)$$

with P_j and Q_j homogeneous polynomials of degree j for each $j \geq 2$, in other words, P_j,$Q_j \in \mathcal{H}^j$ for all $j \geq 2$. Let $X(x,y) = (-y + P(x,y), x + Q(x,y))$ denote the vector field associated with system (1.4). We notice that the origin $(x,y) = (0,0)$ is an equilibrium point of system (1.4) whose linearization is of center type. The main task is to show if the origin is indeed a center or a focus.

Definition 13. *Let p be an equilibrium point of system* (1.4)*. A function $V \colon U \longrightarrow \mathbb{R}$ defined in a neighborhood of p is called a Lyapunov function for system* (1.4) *at p if $V(p) = 0$, $V(x,y) > 0$ for all $x \neq p$ and $\dot{V}(x,y) \leq 0$, where*

$$\dot{V}(x,y) = \frac{d}{dt} V\left(\phi_t(x,y)\right)\big|_{t=0} = \nabla V(x,y) \cdot X(x,y)$$

is the derivative of V in the direction of the vector field X and ϕ_t denotes the flow of X.

In what follows we define stability in the sense of Lyapunov. See [27] for more details. Consider a system

$$\dot{x} = f(t,x) \tag{1.5}$$

where $f \colon U \longrightarrow \mathbb{R}^n$ is a continuous function and $U \subset \mathbb{R} \times \mathbb{R}^n$ an open set.

Definition 14. *Let $\phi(t)$ be the flow associated with system* (1.5) *defined for all $t \geq 0$. We say that $\phi(t)$ is stable if for all $\varepsilon > 0$ there exist $\delta > 0$ such that if $\psi(t)$ is a solution of system* (1.5) *and $|\psi(0) - \phi(0)| < \delta$ then $\psi(t)$ is defined for all $t \geq 0$ and $|\psi(t) - \phi(t)| < \varepsilon$ for all $t \geq 0$. Moreover, if there exists δ_1 such that*

$$|\psi(0) - \phi(0)| < \delta_1 \Longrightarrow \lim_{t \to \infty} |\psi(t) - \phi(t)| = 0$$

then we say that $\phi(t)$ is asymptotically stable.

The next result, due to Lyapunov, establish a criterion that allow us to analyze the stability of the origin of system (1.4). The proof can be found in [27].

Theorem 1. *If V is a Lyapunov function at $(x, y) = (0, 0)$ for the system (1.4) in a neighborhood of the origin then the equilibrium point is stable. If also holds $\dot{V}(x, y) < 0$ for each point (x, y) in the neighborhood of the origin, then the origin is asymptotically stable.*

In order to determine the stability of the origin of system (1.4) we will seek for a Lyapunov function represented formally as the series

$$V(x, y) = \frac{1}{2}\left(x^2 + y^2\right) + \sum_{j=3}^{\infty} V_j(x, y) \tag{1.6}$$

where each V_j is a homogeneous polynomial of degree j. So, the derivative of V in the direction of the vector field X is given by

$$\dot{V} = \nabla V(x, y) \cdot X(x, y) = \Big(x + V_{3x} + V_{4x} + \cdots, y + V_{3y} + V_{4y} + \cdots\Big) \cdot \Big(-y + P(x, y), x + Q(x, y)\Big)$$

where the subscripts x and y denote partial derivatives. Moreover, if we collect terms on the right hand side of this identity according to their degrees, we get

$$\begin{aligned} \dot{V} &= \Big[-xy + xy\Big] + \Big[-yV_{3x} + xV_{3y} + xP_2 + yQ_2\Big] + \\ &\quad + \Big[-yV_{4x} + xV_{4y} + xP_3 + yQ_3 + V_{3x}P_2 + V_{3y}Q_2\Big] + \cdots \end{aligned} \tag{1.7}$$

Observe that the terms of degree two in Equation (1.7) cancel. We will show that we can choose V_3 so that the terms of degree three vanish. However, the terms of degree four do not vanish in general. Consider the linear transformation

$$\begin{aligned} T_n\colon \quad \mathcal{H}^n &\longrightarrow \mathcal{H}^n \\ p(x, y) &\longmapsto T_n(p(x, y)) = -y\frac{\partial p}{\partial x}(x, y) + x\frac{\partial p}{\partial y}(x, y). \end{aligned}$$

Accordingly, Equation (1.7) can be write as follow

$$\dot{V} = \Big[T_3(V_3) + xP_2 + yQ_2\Big] + \Big[T_4(V_4) + xP_3 + yQ_3 + V_{3x}P_2 + V_{3y}Q_2\Big] + \cdots$$

The proof of the next result can be found in [69].

Theorem 2. *If n is odd, T_n is an isomorphism. If n is even, T_n has a one-dimensional kernel generated by $\left(x^2+y^2\right)^{\frac{n}{2}}$.*

In such manner, by Theorem 2 there exists $V_3 \in \mathcal{H}^3$ such that

$$T_3\left(V_3(x,y)\right) = -\Big(xP_2(x,y) + yQ_2(x,y)\Big)$$

and with this choice of V_3 we get

$$\dot{V} \quad = \quad \Big[T_4\left(V_4\right) + xP_3 + yQ_3 + V_{3x}P_2 + V_{3y}Q_2\Big] + \cdots$$

By Theorem 2 the linear transformation T_4 is not an isomorphism, but since it's kernel is generated by $\left(x^2+y^2\right)^2$ there exists $V_4 \in \mathcal{H}^4$ such that

$$T_4\left(V_4\right) = -\Big(xP_3 + yQ_3 + V_{3x}P_2 + V_{3y}Q_2\Big) + \eta_4\left(x^2+y^2\right)^2.$$

Therefore, with this choice of the function V we obtain

$$\dot{V} \quad = \quad \eta_4\left(x^2+y^2\right)^2 + \cdots$$

where η_4 is a constant with respect to the variables x and y. If $\eta_4 \neq 0$ the function

$$V(x,y) = \frac{1}{2}\left(x^2+y^2\right) + V_3(x,y) + V_4(x,y)$$

determines the stability of the equilibrium point at the origin. More precisely, if $\eta_4 < 0$, then V is a Lyapunov function in some sufficiently small neighborhood of the origin and the equilibrium point is a stable weak focus. If $\eta_4 > 0$, then the origin is an unstable weak focus. Repeating the same procedure we can produce a function V such that

$$\dot{V} = \eta_4\left(x^2+y^2\right)^2 + \eta_6\left(x^2+y^2\right)^3 + \cdots + \eta_{2n}\left(x^2+y^2\right)^n + \cdots.$$

Theorem 3. *If $\eta_{2n} = 0$, for $n = 2, ..., N$, but $\eta_{2N+2} \neq 0$, then the stability of the equilibrium point at the origin is determined: If $\eta_{2N+2} < 0$, then the origin is stable. If $\eta_{2N+2} > 0$, then the origin is unstable.*

As η_{2n} is relevant only if $\eta_{2l} = 0$ for $l < n$, we put $\eta_2 = \eta_4 = \cdots = \eta_{2j-2} = 0$ in the expression of η_{2n}. The quantities obtained in this way are called Lyapunov constants or Lyapunov coefficients and are denoted by

$$L_j = \eta_{2j+2}, \qquad j = 0, 1, 2, ..., n.$$

By convention, nonzero multiplicative factors can be omitted from the expressions given by the Lyapunov constants if we are interested only in knowing its sign. The question about what happens if all the Lyapunov coefficients vanish was answered by Lyapunov center theorem stated below. See [83] for details.

Theorem 4. *If the vector field X is analytic and $\eta_{2n} = 0$ for each integer $n \geq 2$, then the origin is a center. Moreover, the formal series for V is convergent in a neighborhood of the origin and it represents a function whose level sets are orbits of the differential equation corresponding to X.*

Another important tool in the analysis of bifurcation and stability of periodic orbits is the Poincaré map also called the first return map. This concept was established by Poincaré (see [100]) who brought a considerable development to the theory of differential equations.

Let $\phi(t, p)$ be the flow associated with system (1.5) and suppose that an $(n-1)$-dimensional submanifold S is transverse to the flow $\phi(t, p)$. If p is in S, then the curve $\phi(t, p)$ passes through S as t passes through $t = 0$. Suppose that there is an open subset $\Sigma \subset S$ such that each point of Σ returns to S. Then Σ is called a Poincaré section or a transversal section. In this way, we can define the Poincaré map by

$$\begin{array}{rccl} \pi: & \Sigma & \longrightarrow & S \\ & p & \longmapsto & \pi(p) = \phi\left(T(p), p\right) \end{array}$$

where $T(p) > 0$ is the time of the first return to S by the trajectories. See Figure 1.7.

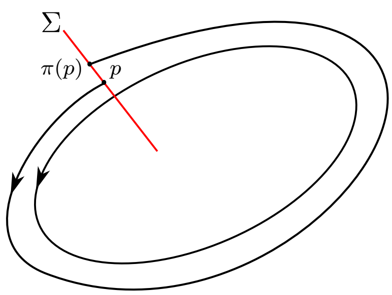

Figure 1.7: A Poincaré map for smooth systems.

Proposition 2. *Let X be a vector field of class C^r, $r \geq 1$ or analytic. Then the Poincaré map associated with a periodic orbit of X is a diffeomorphism of class C^r onto its image.*

Instead of studying the fixed points of the Poincaré map, sometimes it is more convenient to study the zeros of the corresponding displacement function defined by

$$\delta(p) = \pi(p) - p.$$

The Lyapunov coefficients can also be given by the Taylor coefficients of the series expansion of the displacement function. In [27, p. 518] it is established the relationship between the Taylor coefficients of the displacement function and the Lyapunov coefficients.

Theorem 5. *Suppose that $\xi \mapsto \delta(\xi)$ is the displacement function for the system* (1.4)*, and η_{2n} for $n \geq 2$, are the corresponding Lyapunov coefficients. If k is a positive integer and $\eta_{2j} = 0$ for the integers $j = 1, \dots, k-1$, then*

$$\frac{\partial^{2k-1}\delta}{\partial\xi^{2k-1}}(0) = (2k-1)!\, 2\pi\, \eta_{2k}.$$

Chapter 2

Discontinuous vector fields in applied models

In this chapter, we explore some applications of discontinuous vector fields in applied science. In Sections 2.1 and 2.2 we study intermittent treatment models of the Human Immunodeficiency Virus and Cancer and analyze its qualitative dynamical features. In Section 2.3 we revisit a prey switching model and prove the existence of a Shilnikov sliding connection which assures that the model behaves chaotically.

2.1 An application of piecewise smooth vector fields in a cancer model

The application of sliding mode control and piecewise smooth vector fields in cancer is an incipient research area. Here we propose a piecewise dynamics to explore chemoimmunotherapeutic strategies. We investigate the dynamic behavior of the discontinuous mathematical model and we observe the occurrence of typical singularities. The on-off treatment strategies are defined in terms of a time-dependent variable such as the number of cancer or immune cells. Concerning this section, the results can be found in [57, 58].

In the field of cancer, the application of piecewise smooth vector fields can be also valuable, since oncological therapies are usually administered in an on-off style. However, its use in oncology sciences remains almost unexplored until the present, with few papers published in applied areas such as discrete-continuous hybrid systems [66, 112], but not using Filippov's vector fields. These cited papers illustrate how "on-off" ordinary differential equations systems can shed light on the use of intermittent androgen suppression for treating prostate cancer.

The biological scenario that motivates our mathematical model is the use of chemoimmunotherapeutic protocols for the treatment of chronic lymphocytic leukemia. We consider the interplay between neoplastic B-lymphocytes and "healthy" T-lymphocytes under chemotherapy and immunotherapy. A detailed discussion of these intervening treatments is postponed until the presentation of the model, but for the moment we emphasize that an infusion of T-lymphocytes in time is considered for modeling adoptive cellular immunotherapy. Other blood cells such as erythrocytes are not taken into account in the model, but we consider that chemotherapy does negatively affect the immune cells. Cancer cells (as well as immune cells) are assumed to be identical within their niche and then modeled as a single compartment. For the sake of simplicity, we neglect the dynamics of natural killer cells since there is some evidence that their natural cytotoxic capacity may be weak in neoplastic B-lymphocytes (see [64, 70] for details). Finally, the other assumptions that complete the model are:

- Cancer cells grow according to the logistic law;
- Immune cells are naturally provided at a constant rate by the host (even in the absence of cancer), but they also die naturally (exponentially);
- Cancer cells stimulate the production of new immune cells, with a recruitment rate that saturates after a certain number of cancer cells;
- The interaction between cancer and immune cells has a negative impact on each other, whose rate is proportional to the number of encounters between them;
- The pharmacodynamics of the chemotherapeutic drug follows the log-kill hypothesis, but with a Michaelis-Menten drug saturation response;
- The drug is eliminated according to first-order kinetics.

Denoting the number of cancer cells by N (neoplastic B-lymphocytes), the number of immune cells by I ("healthy" T-lymphocytes) and the amount (or mass) of chemotherapeutic agent in the bloodstream by Q, based on de Pillis & Radunskaya (see [34]) we propose the following model:

$$\begin{cases} \dfrac{dN}{dt} = r\,N\left(1-\dfrac{N}{k}\right) - c_1\,N\,I - \dfrac{\mu\,N\,Q}{a+Q} \\[2ex] \dfrac{dI}{dt} = s(t) + s_0 - d\,I + \dfrac{\rho\,N\,I}{\gamma+N} - c_2\,N\,I - \dfrac{\delta\,I\,Q}{b+Q} \\[2ex] \dfrac{dQ}{dt} = q(t) - \lambda\,Q. \end{cases} \tag{2.1}$$

All parameters of the model are non-negative: $k > 0$, the cancer cells carrying capacity; r, the cancer cell growth rate; c_1 and c_2, the interaction coefficients between cancer and immune cells, respectively affecting cancer and immune populations; s_0, the natural influx of immune cells to the place of interaction; d, the natural death rate of immune cells; ρ, the production rate of immune cells estimulated by the cancer; γ, the number of cancer cells by which the immune system response is the half of its maximum; μ and δ, the mortalities rates due to the action of the chemotherapeutic drug on cancer and immune cells, respectively; a and b, the drug amount for which such effects are the half of its maximum in each cell population; and λ, the washout rate of a given cycle-nonspecific chemotherapeutic drug

$$\lambda \doteq \frac{\ln 2}{t_{1/2}}, \tag{2.2}$$

where $t_{1/2}$ is the drug elimination half-life (see [85]). Also, the time-dependent functions s and q are source terms respectively standing for immunotherapy and chemotherapy. To the simplest scenario, they are constants.

The first term in the equation for dN/dt describes the classical logistic cancer growth (see [10]), and the c_i term models the interspecific interaction between cancer and immune cells on each population ($i = \{1, 2\}$, respectively). Also, the immune system is represented by $s_0 - dI$, as discussed in [35].

The third equation in (2.1) describes the first order pharmacokinetics of a chemotherapeutic drug with an external source (see [9]). As for pharmacodynamics, the last term of the first and second equations of (2.1) represent the log-kill hypothesis (see [106]), with a Michaelis-Menten drug saturation response (see [6]) as it appears in the denominators of $\mu\, N\, Q/(a + Q)$ and $\delta\, I\, Q/(b + Q)$. An analogous functional response with positive sign is taken for bounding the production of immune cells stimulated by the cancer, i.e., $\rho\, N\, I/(\gamma + N)$.

With respect to the chemotherapeutic or immunotherapeutic infusion fluxes given by the functions q and s, there are two basic ways of therapy delivery. In terms of a generic function f they are:

1. Constant administration: f is a constant function everywhere,

$$f(t) \;=\; f_\infty \;\geq\; 0. \tag{2.3}$$

2. Periodic administration: f is defined by

$$f(t) \;=\; \begin{cases} f_{\mathrm{p}} > 0, \;\; n \leq t < n + \tau, \\ \\ 0, \;\; n + \tau \leq t < n + T, \end{cases} \tag{2.4}$$

where τ is the time taken for administration, T is the administration period and $n = \{0, T, 2T, \ldots, mT\}$, with $m+1$ being the number of administrations of chemotherapy or immunotherapy.

Constant administration is a more theoretical way of therapy delivery, but still important to understand thresholds of chemotherapy and immunotherapy infusion fluxes that lead to cancer cure. Periodic administration, on the other hand, is more practical in oncology and is the main point of our discussion.

The PSVF theory allow us to examine the system (2.1) when chemotherapy and/or immunotherapy suddenly starts or stops depending on a previously established threshold value of N, I or Q. To this end, we consider the functions $s(t)$ and $q(t)$ as being discontinuous. Moreover, the discontinuity occurs when a control function $f(N, I, Q)$ is equal to zero, as follows:

$$s(t) = \begin{cases} s_\infty, & f(N,I,Q) > 0 \\ \\ 0, & f(N,I,Q) \leq 0 \end{cases}, \quad \text{and} \quad q(t) = \begin{cases} q_\infty, & f(N,I,Q) > 0 \\ \\ 0, & f(N,I,Q) \leq 0 \end{cases}. \tag{2.5}$$

As a consequence, one gets a PSVF of the form:

$$\mathcal{Z}(N,I,Q) = \begin{cases} X(N,I,Q) & \text{if} \quad f(N,I,Q) \leq 0 \\ Y(N,I,Q) & \text{if} \quad f(N,I,Q) \geq 0 \end{cases}, \tag{2.6}$$

where

$$\begin{aligned} X(N,I,Q) &= \left(rN\left(1 - \frac{N}{k}\right) - c_1 NI - \frac{\mu NQ}{a+Q}, \;\; s_0 - dI + \frac{\rho NI}{\gamma + N} - c_2 NI - \frac{\delta IQ}{b+Q}, \;\; -\lambda Q \right) \\ &= \Big(X_1(N,I,Q), X_2(N,I,Q), X_3(N,I,Q) \Big), \end{aligned} \tag{2.7}$$

and

$$\begin{aligned} Y(N,I,Q) &= \left(rN\left(1 - \tfrac{N}{k}\right) - c_1 NI - \tfrac{\mu NQ}{a+Q}, \;\; s_\infty + s_0 - dI + \tfrac{\rho NI}{\gamma+N} - c_2 NI - \tfrac{\delta IQ}{b+Q}, \;\; q_\infty - \lambda Q \right) \\ &= \Big(Y_1(N,I,Q), \;\; Y_2(N,I,Q), \;\; Y_3(N,I,Q) \Big), \end{aligned} \tag{2.8}$$

which are multi-valuated in the switching manifold, chosen according to some control strategy imposed on the system. We observe that the first coordinates of the vector field X and Y are equals. The second (resp. third) one may be equal if we consider the case $s_\infty \equiv 0$ (resp. $q_\infty \equiv 0$). In such a case, s (resp. q) is continuous.

In practice, the values of the variables $N = N(t)$, $I = I(t)$ and $Q = Q(t)$ only make sense when they are non-negative. In a mathematical point of view, however, it is possible to admit negative values for them. Let us call the *positive octant* $\mathcal{O}^+$ being the octant in the domain $N \times I \times Q$ where these three coordinates are positive, i.e., $\mathcal{O}^+ = \{(N, I, Q) \in \mathbb{R}^3 : N \geq 0, I \geq 0, Q \geq 0\}$.

Generically, the behavior outside $\mathcal{O}^+$ could have an effect on $\mathcal{O}^+$. For example, an asymptotically stable equilibrium outside $\mathcal{O}^+$ could attract trajectories which initial conditions placed on $\mathcal{O}^+$. As consequence, there are points of these trajectories where exactly one of the variables N, I or Q vanishes and then the model must be analyzed considering the interaction modeled by the other two remaining variables. Now, we would like to understand the behavior of the model (2.1) in the border of $\mathcal{O}^+$.

Initially, let us analyze the plane $NQ = \{(N, I, Q) \in \mathbb{R}^3 : I = 0\}$. If $I = 0$, then it follows that $dI/dt = s(\cdot) + s_0 > 0$ since s_0 is positive and $s(\cdot) \geq 0$. Therefore, I is an increasing function for initial conditions on the plane NQ. Let us also consider the plane $IQ = \{(N, I, Q) \in \mathbb{R}^3 : N = 0\}$. In this case, $dN/dt = 0$ and any initial condition remains in the plane IQ, i.e., IQ is an invariant plane. Finally, the plane $NI = \{(N, I, Q) \in \mathbb{R}^3 : Q = 0\}$. If $Q = 0$, then $dQ/dt = q(\cdot) \geq 0$. If $q(t) > 0\ \forall t$, then Q is an increasing function and if $q(t) \equiv 0$ then NI is an invariant plane.

An immediate consequence is that $\mathcal{O}^+$ is invariant under the model and we can restrict our analysis to this region. A summary of the aforementioned planes is presented in Figure 2.1, either with or without chemotherapy and respective trajectories.

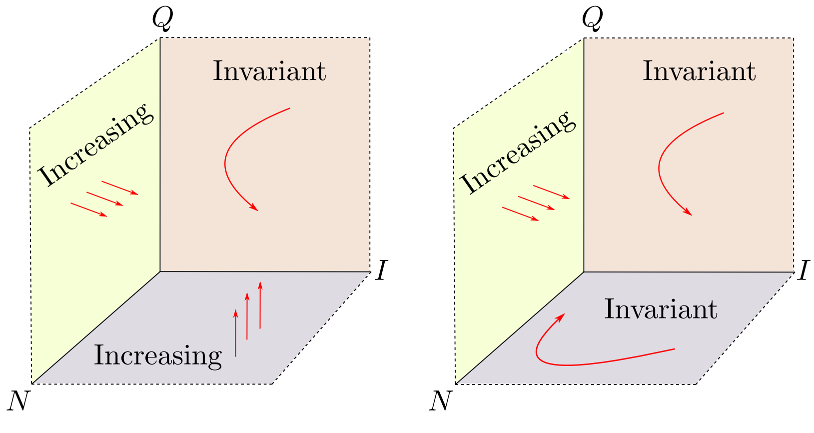

Figure 2.1: Trajectories over the planes NQ, IQ and NI respectively either with or without a chemotherapeutic agent.

Further, we can study the behavior of the system (2.1) on the axes. Let us consider the axis $I = \{(N, I, Q) \in \mathbb{R}^3 : N = 0, Q = 0\}$ over which then $dI/dt = s_\infty + s_0 + dI$. By assuming that $s(t) = s_\infty$, when $I = (s_\infty + s_0)/d \doteq I_0$ implies $dI/dt = 0$ so that I is a constant function for these values. On the other hand, the coordinate I is increasing for $0 < I < I_0$

and decreasing for $I > I_0$. If $q(t) \equiv 0$ we observe that the axis I is invariant. Besides, on the axis $N = \{(N, I, Q) \in \mathbb{R}^3 : I = 0, Q = 0\}$, follows that $dN/dt = rN(1 - N/k)$ and then N is an increasing function when $0 < N < k$ and decreasing for $N > k$. Lastly, considering $q(t) = q_\infty \ \forall t$, $dQ/dt = q(t) - \lambda Q$ and then Q is increasing if $0 < Q < q_\infty/\lambda$ and decreasing if $Q > q_\infty/\lambda$.

Let us analyze the vector fields X and Y given by Equations (2.7) and (2.8), respectively. Firstly, let us consider the vector field X. We have that $X_3(N, I, Q) = 0$ just when $Q = 0$. So, the equilibria of X is in the invariant plane NI. Supposing $Q = 0$ we get that $X_1(N, I, Q) = 0$ when $N = 0$ or $N = (-c_1kI + kr)/r$. Therefore, if $N = Q = 0$, then we have that $X_2 = 0$ when $I = s_0/d$. Therefore $(N, I, Q) = (0, s_0/d, 0)$ is an equilibrium point of X. Considering the Jacobian matrix of the vector field X we conclude that the equilibrium above has at least two negatives eigenvalues given by $-d$ and $-\lambda$. So the equilibrium $(0, s_0/d, 0)$ can be an attractor of the trajectories of X depending on the parameters values, more specifically when $r < c_1s_0/d$. The second case of N can give at most three real equilibria also depending on the parameters values.

Secondly, let us analyze the vector field Y. We have that $Y_3(N, I, Q) = 0$ just when $Q = q_\infty/\lambda$. So, the equilibria of Y is in the invariant plane $\mathcal{Q} = \{(N, I, Q) \in \mathbb{R}^3 : Q = q_\infty/\lambda\}$. So, Y_1 restricted to $Q = q_\infty/\lambda$ is null when $N = 0$ or

$$N = \frac{-c_1kIq_\infty + kq_\infty r - ac_1kI\lambda + akr\lambda - kq_\infty\mu}{r(q_\infty + a\lambda)}.$$

So, $Y_2(0, I, q_\infty/\lambda) = 0$ leads to

$$\tilde{I} = \frac{(s + s0)(q_\infty + b\lambda)}{dq_\infty + q_\infty\delta + bd\lambda}$$

and therefore $(0, \tilde{I}, q_\infty/\lambda)$ is an equilibrium point of Y. The analysis of the Jacobian matrix shows that this equilibrium has at least two negatives eigenvalues for all positive values of the parameters. The second case of N can give at most three real equilibria also depending on the parameters values.

The analyses that follows are performed using the parameter values summarized in Table 2.1.

Table 2.1: Parameters of the model.

Parameter	Value	Unity	Reference
r	10^{-2}	day^{-1}	[110]
k	10^{12}	cell	[124]
c_1	5×10^{-11}	cell^{-1}day^{-1}	-
c_2	1×10^{-13}	cell^{-1}day^{-1}	-
s_0	3×10^{5}	cell day^{-1}	-
d	10^{-3}	day^{-1}	-
ρ	10^{-12}	day^{-1}	-
γ	10^{2}	cell	-
μ	8	day^{-1}	-
δ	10^{4}	day^{-1}	-
a	2×10^{3}	mg	-
b	5×10^{6}	mg	-
λ	4.16	day^{-1}	[41]

Now we analyze the following system

$$\begin{cases} \dfrac{dN}{dt} & = & rN\left(1-\dfrac{N}{k}\right) - c_1NI - \dfrac{\mu NQ}{a+Q} \\ \\ \dfrac{dI}{dt} & = & s_0 - dI + \dfrac{\rho NI}{\gamma + N} - c_2NI - \dfrac{\delta IQ}{b+Q} \\ \\ \dfrac{dQ}{dt} & = & -\lambda Q \end{cases}, \tag{2.9}$$

which is related to the vector field X given by Equation (2.7). In this case, we guarantee the existence of three equilibria on the octant $\mathcal{O}^+$:

$$\begin{cases} p_1 & = & \left(0, 3\times 10^8, 0\right); \\ p_2 & = & \left(5.07654\times 10^9, 1.98985\times 10^8, 0\right); \\ p_3 & = & \left(9.84923\times 10^{11}, 3.01531\times 10^6, 0\right). \end{cases}$$

Analyzing the Jacobian matrix of the system (2.9) we can conclude that the equilibria p_1 and p_3 are attractors for the trajectories of X while the equilibrium p_2 has one positive and two negatives eigenvalues, that is, p_2 is of the saddle type (see Figure 2.2).

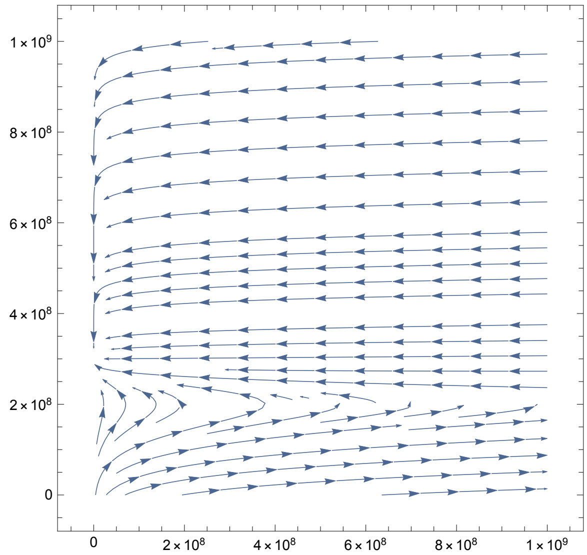

Figure 2.2: Behavior of the vector field given by (2.9) in a neighborhood of the attractor equilibrium p_1 on the invariant plane NI for parameters values taken from Table 2.1.

Furthermore, let us analyze the system

$$\begin{cases} \dfrac{dN}{dt} &= rN\left(1-\dfrac{N}{k}\right) - c_1 NI - \dfrac{\mu NQ}{a+Q}; \\[2ex] \dfrac{dI}{dt} &= s_0 - dI + \dfrac{\rho NI}{\gamma+N} - c_2 NI - \dfrac{\delta IQ}{b+Q}; \\[2ex] \dfrac{dQ}{dt} &= q_\infty - \lambda Q, \end{cases} \tag{2.10}$$

that is related to the vector field Y given by Equation (2.8) with $s_\infty = 0$ and $q_\infty = 300$. System (2.10) has a unique equilibria $p_4 = \big(0, 2.0657 \times 10^6, 72.1154\big)$ on the octant $\mathcal{O}^+$. The analysis of the Jacobian matrix of system (2.10) shows that p_4 is an attractor (see Figure 2.3).

The case with non-zero constant immunotherapy s_∞ is similar, but with a shifted equilibrium.

2.1.1 A change in the control strategy according to the number of cancer cells

Firstly, let us analyze the following PSVF:

$$Z(N,I,Q) = \begin{cases} X(N,I,Q) & \text{if} \quad N \le N_0; \\ Y(N,I,Q) & \text{if} \quad N \ge N_0, \end{cases} \tag{2.11}$$

where N_0 is a threshold value of cancer cells above which chemotherapy or immunotherapy is set to start. In this case, we observe that the switching manifold is characterized by $\Sigma = f^{-1}(0) = \{(N,I,Q) \in \mathbb{R}^3 : N = N_0\}$ where $f(N,I,Q) = N - N_0$ (see Figure 2.4).

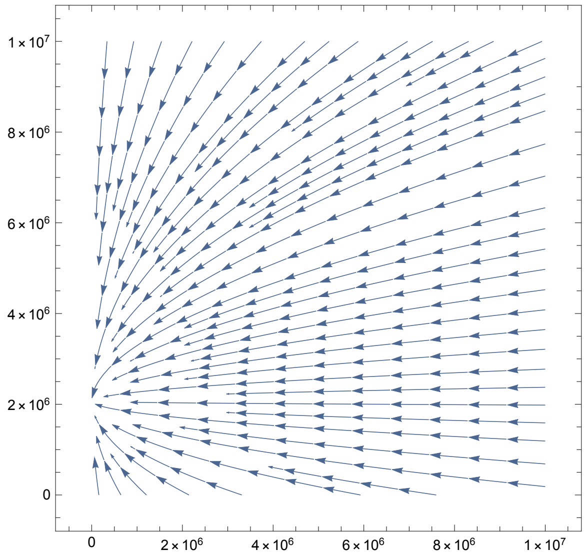

Figure 2.3: Behavior of the vector field given by (2.10) on the invariant plane $\mathcal{Q}$ without immunotherapy and with chemotherapy, for parameters values taken from Table 2.1 and $q_\infty = 300$ mg/day.

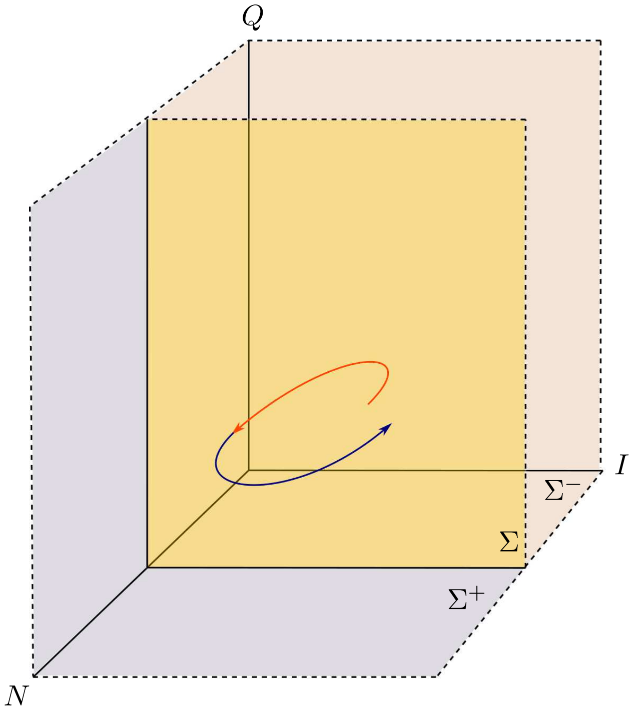

Figure 2.4: The switching manifold restricted to the octant $\mathcal{O}^+$.

Now we address the contact between the vector fields X and Y with Σ. Let us suppose that $N_0 > 0$ is less than the cancer cells carrying capacity k, which is biologically reasonable.

Proposition 3. *System* (2.11) *has only crossing regions and tangential singularities.*

Proof. By a straightforward calculation,

$$Xf(N,I,Q) = Yf(N,I,Q) = \frac{dN}{dt}.$$

So, we assure that $\Big(Xf(N,I,Q)\Big)\Big(Yf(N,I,Q)\Big) = (dN/dt)^2 \geq 0$ and the system (2.11) has only crossing regions and tangential singularities. $\square$

In addition, we get a curve of tangential singularities in Σ.

Proposition 4. *The tangential singularities of X and Y with $\Sigma = \{N = N_0\}$ is given by the curve*

$$Q(I) = \frac{-ac_1kI + akr - aN_0r}{c_1kI - kr + N_0r + k\mu} \subset \Sigma \cap \mathcal{O}^+.$$

Proof. Indeed, $Xf(N,I,Q)$ restricted to $N = N_0$ has the form

$$Xf(N_0,I,Q) = N_0\left(-c_1I + r - \frac{N_0r}{k} - \frac{Q\mu}{a+Q}\right).$$

So, $Xf(N_0,I,Q) = 0$ give us

$$Q = Q(I) = \frac{-ac_1kI + akr - aN_0r}{c_1kI - kr + N_0r + k\mu}.$$

Thus, we get a curve $\psi = \{(N,I,Q) \in \mathbb{R}^3 : N = N_0, Q = Q(I)\}$ in $\Sigma \cap \mathcal{O}^+$ that intersects the plane NQ at the point $\left(N_0, 0, \frac{a(-k+N_0)r}{-N_0r+k(r-\mu)}\right)$ and the plane NI at the point $\left(N_0, \frac{(k-N_0)r}{c_1k}, 0\right)$. We note that $Yf(N,I,Q) = Xf(N,I,Q)$, which completes the proof. $\square$

We observe that the points of the curve ψ can be visible or invisible for X or Y depending on the sign of $X^2f(N_0,I,Q)$ and $Y^2f(N_0,I,Q)$. See Figure 2.5.

It is crucial to understand the contact of the vector field Y with the plane $N_k = \{(N,I,Q) \in \mathbb{R}^3 : N = k\}$, remembering that k is the cancer cells carrying capacity. The derivative dN/dt restricted to $N = k$ is equal to $-c_1kI - (kQ\mu)/(a+Q)$. The vector field Y is then tangent to the plane N_k when $-c_1kI - (kQ\mu)/(a+Q) = 0$, with the curve of tangential singularities of Y in N_k given by $\nu(I) = -(ac_1I)/(c_1I + \mu)$. The curve ν passes through the point $(0,0)$ and its derivative is negative for $I > 0$. In fact,

$$\frac{d\nu(I)}{dI} = \frac{ac_1^2I}{(c_1I+\mu)^2} - \frac{ac_1}{c_1I+\mu},$$

so that, for $I > 0$,

$$\frac{d\nu(I)}{dI} < 0 \Longleftrightarrow \frac{c_1I}{c_1I+\mu} < 1.$$

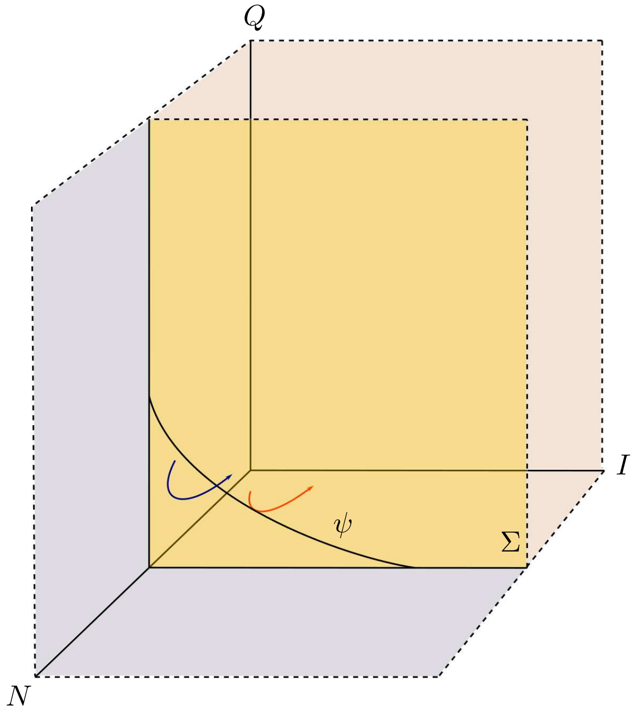

Figure 2.5: The curve ψ in the octant $\mathcal{O}^+$.

Since $\mu > 0$, we assure that all the trajectories of Y on the octant $\mathcal{O}^+$ are pointing to the same direction in N_k. Since dN/dt is negative for values of the form $(k, I, 0)$, with $I > 0$, we can conclude that the orbits of Y are entering N_k, following from $N > N_k$ to $N < N_k$. Therefore, the treatment may recede the cancer (see Figure 2.6).

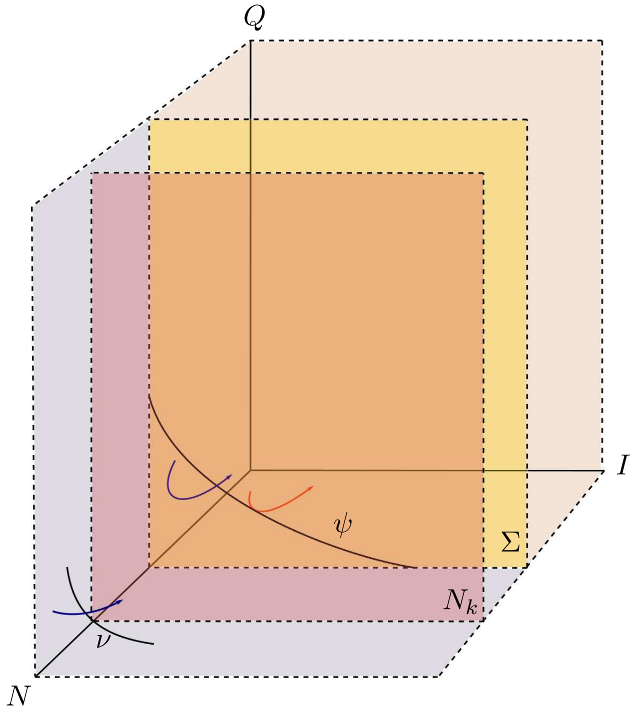

Figure 2.6: The curve ν in the plane N_k.

The analysis that follows is illustrated using the parameter values summarized in Table 2.1. Some studies show that the number of cancer cells $N = 10^{10}$ is detectable by standard medical techniques (see [124]). Thus, let us consider the system Z given by (2.11) with $N_0 = 10^{10}$ which defines the switching manifold $\Sigma = \{N = 10^{10}\}$ where the vector fields X and Y are given by Equations (2.7) and (2.8) with $s_\infty = 0$ and $q_\infty = 300$. As we have seen, the vector field X has three equilibria on the octant $\mathcal{O}^+$. We observe that only the attractor equilibrium p_1 and the saddle point p_2 occur in the region $\mathcal{O}^+ \cap \{N \leq 10^{10}\}$, where X is defined while p_3 is a virtual equilibria for Z. Moreover, the attractor equilibrium p_4 of the vector field Y is also a virtual equilibria for the PSVF Z.

Lemma 1. *The tangential singularities of X and Y with Σ are given by the curve*

$$Q_0(I) = -\frac{2000(-198000000 + I)}{159802000000 + I} \subset \Sigma \cap \mathcal{O}^+.$$

Proof. The proof follows from Proposition 4 using $f(N, I, Q) = N - 10^{10}$. □

We can observe that the curve Q_0 intersects the plane NQ at the point $\big(10^{10}, 0, 2.4780\big)$ and the plane NI at the point $\big(10^{10}, 1.98 \times 10^8, 0\big)$.

Proposition 5. *The tangential singularities of Lemma 1 are singular, that is, invisible fold points for both X and Y.*

Proof. In fact, we need to show that $X^2 f(p) > 0$ and $Y^2 f(p) < 0$ for all tangential singularity $p = (10^{10}, I, Q_0(I)) \in \Sigma \cap \mathcal{O}^+$. We have that

$$\begin{aligned} X^2 f(p) &= \langle X(p), \nabla X f(p)\rangle \\ &= \Big(X_1(p), X_2(p), X_3(p)\Big) \cdot \left(\tfrac{\partial X_1(p)}{\partial N}, \tfrac{\partial X_1(p)}{\partial I}, \tfrac{\partial X_1(p)}{\partial Q}\right) \\ &= \tfrac{6.57338\times 10^{19} - 3.30731\times 10^{11} I - 6.15291 I^2 - 1.3\times 10^{-11} I^3 - 7.10827\times 10^{-38} I^4 + 2.58597\times 10^{-49} I^5}{1.59866\times 10^{11} + 1.I}. \end{aligned}$$

So, since the function above does not have roots between zero and 1.98×10^8 and it is positive for $I = 0$ we can conclude that $X^2 f(p)$ is positive for $I \in \big[0, 1.98 \times 10^8\big]$. Moreover,

$$\begin{aligned} Y^2 f(p) &= \langle Y(p), \nabla Y f(p)\rangle \\ &= \Big(Y_1(p), Y_2(p), Y_3(p)\Big) \cdot \left(\tfrac{\partial Y_1(p)}{\partial N}, \tfrac{\partial Y_1(p)}{\partial I}, \tfrac{\partial Y_1(p)}{\partial Q}\right) \\ &= \tfrac{-1.84791\times 10^{21} - 3.66652\times 10^{11} I - 6.37766 I^2 - 1.34687\times 10^{-11} I^3 - 7.10827\times 10^{-38} I^4 + 2.58597\times 10^{-49} I^5}{1.59866\times 10^{11} + 1.I}. \end{aligned}$$

Therefore, since $Y^2 f(p)$ does not have roots in the interval $\big[-10, 1.98 \times 10^8\big]$ and it is negative for $I = 0$ we can conclude that $Y^2 f(p)$ is negative for $I \in \big[0, 1.98 \times 10^8\big]$. □

Since the tangential singularities of X and Y are the same, we can compute the tangential sliding vector field given by Definition 2. In order to study the contact between the vector field X and Y with the curve Q_0 let us consider a normal vector to Q_0 at I given by $v_0(I) = (0, -Q_0'(I), 1)$. In this way, the first Lie derivative of the vector field X restricted to the curve Q_0 is given by

$$\begin{aligned} XQ_0(I) &= X\left(10^{10}, I, Q_0(I)\right) \cdot (0, -Q_0'(I), 1) \\ &= -Q_0'(I)X_2\left(10^{10}, I, Q_0(I)\right) + X_3\left(10^{10}, I, Q_0(I)\right). \end{aligned}$$

Similarly,

$$YQ_0(I) = -Q_0'(I)Y_2\left(10^{10}, I, Q_0(I)\right) + Y_3\left(10^{10}, I, Q_0(I)\right).$$

So, the tangential sliding vector field Z^T on the curve of tangential singularities is given by the expression

$$\begin{aligned} Z^T(I) &= \frac{(YQ_0(I))\, X\left(10^{10}, I, Q_0(I)\right) - (XQ_0(I))\, Y\left(10^{10}, I, Q_0(I)\right)}{YQ_0(I) - XQ_0(I)} \\ &= \Big(0, X_2\left(10^{10}, I, Q_0(I)\right), Q_0'(I)X_2\left(10^{10}, I, Q_0(I)\right)\Big). \end{aligned} \tag{2.12}$$

Since Q_0' does not vanish, the singular points of the sliding vector field Z^T are the zeros of $X_2\left(10^{10}, I, Q_0(I)\right)$. So, for $I \in \left(0, 1.98 \times 10^8\right)$ the unique singularity of Z^T occurs for $I^* = 5.3396 \times 10^7$. The second coordinate of Z^T is positive for $I \in (0, I^*)$ and negative for $I \in \left(I^*, 1.98 \times 10^8\right)$. Therefore, this singularity behaves like an attractor for the tangential sliding vector field Z^T (see Figure 2.7).

Remark 3. *It is a significant achievement the comprehension of the trajectories of the vector field* (2.11) *in the neighborhood of the singular point of the sliding vector field Z^T. It is possible the existence of limit cycles and even a chaotic behavior.*

Another interesting behavior appears if one changes the switching manifold of the system studied above. In the sequel, we show the existence of a cusp-fold singularity, that is, a simultaneous occurrence of a cusp singularity for one vector field and a fold singularity for the other one.

Remark 4. *Since the tangential curves of X and Y coincide, this non-generic scenario was not studied in the literature until now. In fact, in the papers [24, 26, 32]) the tangential curves of X and Y are transversal at the cusp-fold singularity (also, bifurcations are considered).*

Let us consider the system Z given by (2.11) with $g(N, I, Q) = N - 10^9$. Consequently, the switching manifold is $\Sigma_1 = g^{-1}(0) = \{(N, I, Q) \in \mathbb{R}^3 : N = 10^9\}$ and we have the following

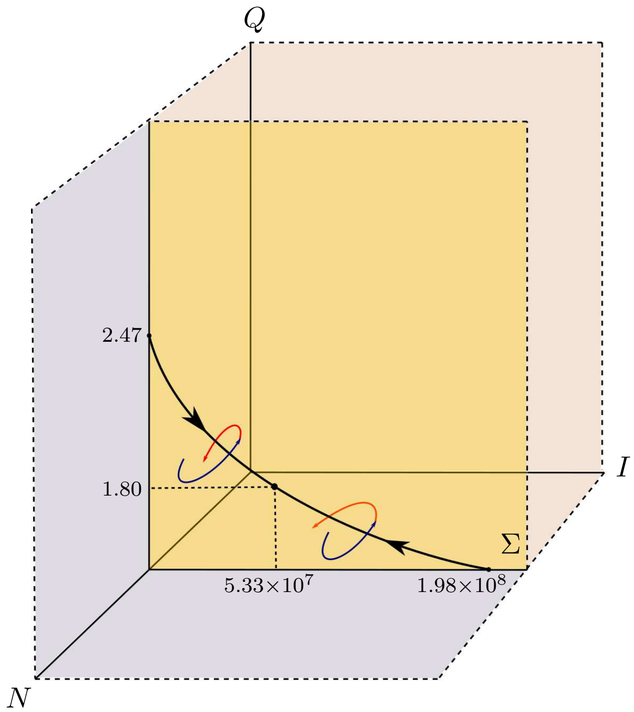

Figure 2.7: The sliding vector field Z^T.

system:

$$Z_1(N,I,Q) = \begin{cases} X(N,I,Q) & \text{if} \quad N \le 10^9; \\ Y(N,I,Q) & \text{if} \quad N \ge 10^9, \end{cases} \tag{2.13}$$

where X and Y are given by equations (2.7) and (2.8), respectively, with $s_\infty = 0$ and $q_\infty = 300$.

We observe that, in this case, the saddle point p_2 is also a virtual equilibria for Z_1, affecting the contact between the vector field X and Σ_1 so that generate a cusp-fold singularity. Thus, we have that p_1 is the only real equilibria for Z_1.

Lemma 2. *The tangential singularities of X and Y with Σ_1 are given by the curve*

$$Q_1(I) = -\frac{2000(-199800000 + I)}{159800200000 + I} \subset \Sigma \cap \mathcal{O}^+.$$

Proof. The proof follows from Proposition 4 using $g(N,I,Q) = N - 10^9$. □

We can notice that the curve Q_1 intersects the plane NQ at the point $\big(10^9, 0, 2.5006\big)$ and the plane NI at the point $\big(10^9, 1.998 \times 10^8, 0\big)$.

Proposition 6. *The tangential singularities of Lemma 2 are invisible fold points for the vector field Y.*

Proof. In fact, the contact between Y and Σ_1 at a tangential singularity $p = \big(10^9, I, Q_1(I)\big)$ is given by

$$\begin{aligned} Y^2g(p) &= \langle Y(p), \nabla Yg(p)\rangle \\ &= \Big(Y_1(p), Y_2(p), Y_3(p)\Big) \cdot \left(\tfrac{\partial Y_1(p)}{\partial N}, \tfrac{\partial Y_1(p)}{\partial I}, \tfrac{\partial Y_1(p)}{\partial Q}\right) \\ &= \tfrac{-1.84725\times 10^{20} - 3.66704\times 10^{10} I - 0.637804 I^2 - 1.34688\times 10^{-12} I^3 - 1.36479\times 10^{-45} I^4 + 2.58597\times 10^{-50} I^5}{1.59864\times 10^{11} + 1.I}. \end{aligned}$$

Therefore, since $Y^2g(p)$ does not have roots in the interval $\left[0, 1.998\times 10^8\right]$ and it is negative for $I=0$ we can conclude that $Y^2g(p)$ is negative for $I \in \left[0, 1.998\times 10^8\right]$. □

The next Proposition guarantees the existence of a cusp point in the contact between the vector field X and Σ_1.

Proposition 7. *There exists* $I_0 \in \left(0, 1.998\times 10^8\right)$ *such that* $X^2g\left(10^9, I_0, Q_1(I_0)\right) = 0$. *Moreover, the tangential singularities of* X *with* Σ_1 *are invisible for* $I \in (0, I_0)$ *and visible for* $I \in \left(I_0, 1.998\times 10^8\right)$.

Proof. Indeed, the contact between X and Σ_1 at a tangential singularity $p = \left(10^9, I, Q_1(I)\right)$ is given by the expression

$$\begin{aligned} X^2g(p) &= \langle X(p), \nabla Xg(p)\rangle \\ &= \Big(X_1(p), X_2(p), X_3(p)\Big) \cdot \left(\tfrac{\partial X_1(p)}{\partial N}, \tfrac{\partial X_1(p)}{\partial I}, \tfrac{\partial X_1(p)}{\partial Q}\right) \\ &= \tfrac{6.63301\times 10^{18} - 3.30785\times 10^{10} I - 0.615329 I^2 - 1.3\times 10^{-12} I^3 - 1.36479\times 10^{-45} I^4 + 2.58597\times 10^{-50} I^5}{1.59864\times 10^{11} + 1.I}. \end{aligned}$$

We observe that $X^2g(p)$ has a zero at the point $I_0 = 1.9978\times 10^8$, it is positive for $I \in [0, I_0)$ and negative for $I \in \left(I_0, 1.998\times 10^8\right]$. In order to guarantee the cubic contact, we get that $X^3g\left(10^9, I_0, Q_1(I_0)\right) = -16685.8 < 0$. □

Corollary 1. *The piecewise smooth vector field* Z_1 *has a cusp-fold singularity.*

Proof. The proof follows from Propositions 6 and 7. □

Let us analyze the tangential sliding vector field. The first Lie derivative of the vector field X restricted to the curve Q_1 is given by

$$\begin{aligned} XQ_1(I) &= X\left(10^9, I, Q_1(I)\right) \cdot (0, -Q_1'(I), 1) \\ &= -Q_1'(I) X_2\left(10^9, I, Q_1(I)\right) + X_3\left(10^9, I, Q_1(I)\right). \end{aligned}$$

Similarly,

$$YQ_1(I) = -Q_1'(I) Y_2\left(10^9, I, Q_1(I)\right) + Y_3\left(10^9, I, Q_1(I)\right).$$

So, the tangential sliding vector field Z_1^T on the curve of tangential singularities is given by the expression

$$\begin{aligned} Z_1^T(I) &= \frac{(YQ_1(I))\,X\left(10^9, I, Q_1(I)\right) - (XQ_1(I))\,Y\left(10^9, I, Q_1(I)\right)}{YQ_1(I) - XQ_1(I)} \\ &= \Big(0, X_2\left(10^9, I, Q_1(I)\right), Q_1'(I)X_2\left(10^9, I, Q_1(I)\right)\Big). \end{aligned} \tag{2.14}$$

Since Q_1' is a non-zero function, the singular points of the sliding vector field Z_1^T are the zeros of $X_2\left(10^9, I, Q_1(I)\right)$. So, for I in the interval of definition of Q_1, which is $\left(0, 1.998 \times 10^8\right)$, the zeros are $\bar{I} = 6.8355 \times 10^7$ and $\bar{\bar{I}} = 1.7538 \times 10^8$. The second coordinate of Z_1^T is positive for $I \in \left(0, \bar{I}\right)$, negative for $I \in \left(\bar{I}, \bar{\bar{I}}\right)$ and positive again for $I \in \left(\bar{\bar{I}}, 1.99 \times 10^8\right)$. Therefore, the singularity for $\bar{I}$ behaves like an attractor for the tangential sliding vector field Z_1^T while the singularity for $\bar{\bar{I}}$ like a repulsor (see Figure 2.8).

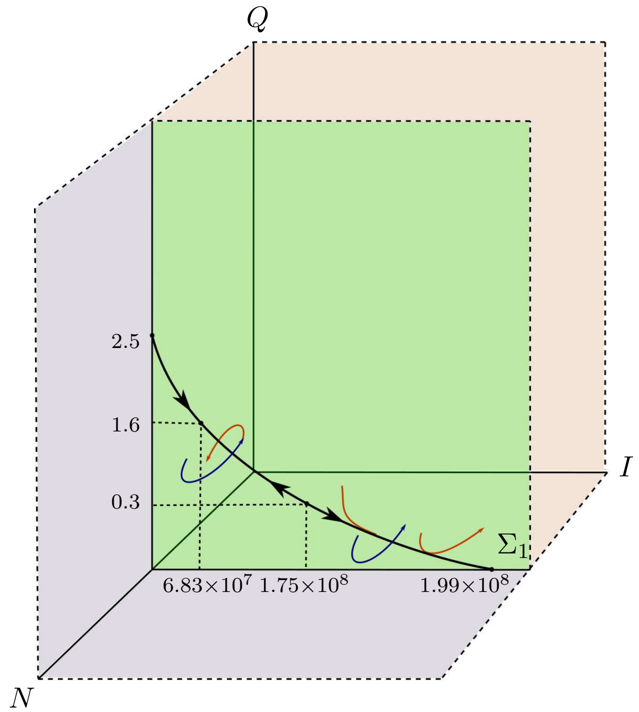

Figure 2.8: The cusp-fold singularity of Z_1 and the tangential sliding vector field Z_1^T.

We may observe that the tangential singularities that occur at the right side of the cusp-fold singularity, that is, for $I \in \left(1.9978 \times 10^8, 1.998 \times 10^8\right)$, are regular since they are invisible for the vector field Y while they are visible for X. So the trajectories of the tangential sliding vector field in a tangential singularity may escape for the trajectories of X. In this case, the trajectory in a tangential singularity may converge to the attractor equilibrium p_1.

2.1.2 A change on the control strategy according to the number of immune cells

Another way to analyze the effects of the treatment is by the analysis of the evolution of immune cells. In what follows we analyze the system

$$Z_2(N,I,Q) = \begin{cases} X(N,I,Q) & \text{if} \quad I \leq 10^7; \\ Y(N,I,Q) & \text{if} \quad I \geq 10^7, \end{cases} \tag{2.15}$$

where X and Y are given by equations (2.7) and (2.8), respectively, for $s_\infty = 0$ and $q_\infty = 300$. We can observe that the switching manifold is given by $\Sigma_2 = h^{-1}(0) = \{(N,I,Q) \in \mathbb{R}^3 : I = 10^7\}$ where $h(N,I,Q) = I - 10^7$. We note that the only real equilibria for Z_2 is the attractor p_3. We also have a cusp-fold singularity as we present in the sequel.

Proposition 8. *The tangential singularities of X and Y with Σ_2 is given by the curve*

$$Q_2(N) = -\frac{5000000\left(29000000000000 + 289999999910N - N^2\right)}{9999971000000000000 + 99999710000000090N + N^2} \subset \Sigma_2 \cap \mathcal{O}^+. \tag{2.16}$$

Proof. Indeed, $Xh(N,I,Q)$ restricted to $I = 10^7$ has the expression

$$Xh(10^7, I, Q) = X_2\big|_{I=10^7} = -\frac{N\,(90+N)}{1000000\,(100+N)} + 10000\left(29 - \frac{10000000Q}{5000000+Q}\right).$$

So, $Xh(10^7, I, Q) = 0$ give us $Q = Q_2(N)$ of Equation (2.16). Since we are studying the case without immunotherapy, $X_2 = Y_2$ and therefore $Xh(N,I,Q) = Yh(N,I,Q)$. $\square$

Proposition 9. *The tangential singularities of Proposition 8 are invisible fold points for the vector field Y. Moreover, there exists a cusp point in the contact between X and Σ_2.*

Proof. Given $p = \left(N, 10^7, Q_2(N)\right)$ by a straightforward calculation we get that $Y^2h(p)$ is negative for $N \in \left[0, 2.9\times 10^{11}\right]$. Furthermore, $X^2h(p)$ has a zero for $N^* = 2.8 \times 10^{11}$, it is positive for $N \in [0, N^*)$ and negative for $N \in \left(N^*, 2.9 \times 10^{11}\right]$. $\square$

Therefore, we get a curve Q_2 in $\Sigma_2 \cap \mathcal{O}^+$ that intersects the plane IQ at the point $\left(0, 10^7, 14.5\right)$ and the plane NI at the point $\left(2.9 \times 10^{11}, 10^7, 0\right)$ containing a cusp-fold singularity for Z_2. We can analyze the tangential sliding vector field associated with Z_2. The first Lie derivative of the vector field X restricted to the curve Q_2 is given by

$$\begin{aligned} XQ_2(I) &= X\left(N, 10^7, Q_2(N)\right) \cdot \left(-Q_2'(N), 0, 1\right) \\ &= -Q_2'(N) X_2\left(N, 10^7, Q_2(N)\right) + X_3\left(N, 10^7, Q_2(N)\right). \end{aligned}$$

Similarly,

$$YQ_2(N) \quad = \quad -Q_2'(N)Y_2\left(N, 10^7, Q_2(N)\right) + Y_3\left(N, 10^7, Q_2(N)\right).$$

So, the tangential sliding vector field Z_2^T on the curve of tangential singularities is given by the expression

$$\begin{aligned} Z_2^T(N) &= \frac{(YQ_2(N))\, X\left(N, 10^7, Q_2(N)\right) - (XQ_2(N))\, Y\left(N, 10^7, Q_2(N)\right)}{YQ_2(N) - XQ_2(N)} \\ &= \Big(X_1\left(N, 10^7, Q_2(N)\right), 0, Q_2'(N)X_1\left(N, 10^7, Q_2(N)\right)\Big). \end{aligned} \tag{2.17}$$

The equilibria of Z_2^T in the interval $\left[0, 2.9\times 10^{11}\right]$ of definition of Q_2 are given by $\bar{N} = 0$ and $\bar{\bar{N}} = 2.552\times 10^{11}$. The first coordinate of Z_2^T is negative for $N \in \left(0, \bar{\bar{N}}\right)$ and positive for $N \in \left(\bar{\bar{N}}, 2.9\times 10^{11}\right)$. Therefore, the singularity for $\bar{\bar{N}}$ behaves like a repulsor for the tangential sliding vector field Z_2^T (see Figure 2.9).

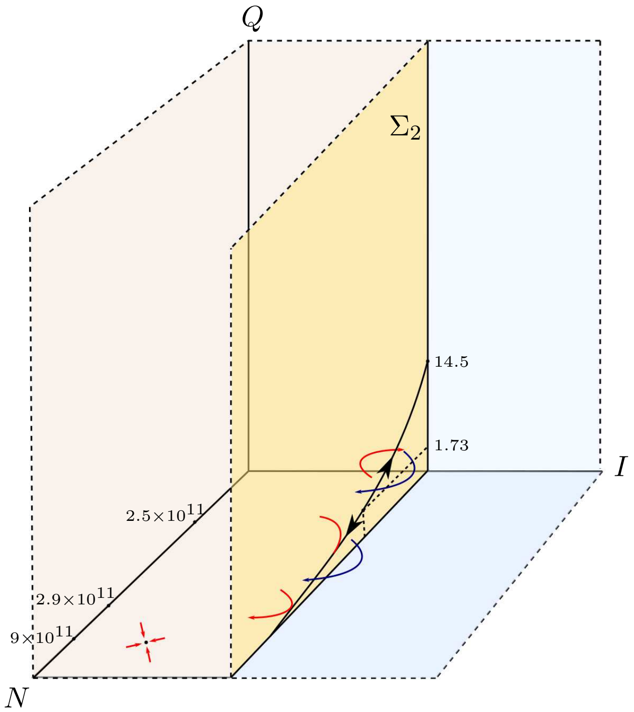

Figure 2.9: Behavior of the PSVF Z_2.

We can notice that the tangential singularities that occur for $N \in \left(2.8\times 10^{11}, 2.9\times 10^{11}\right)$ are regular since they are visible for X. In this way, the trajectories of the tangential sliding vector field in a tangential singularity may departure for the trajectories of X. In this case, the trajectory in a tangential singularity may converge to the attractor equilibrium p_3.

In what follows, we analyze the model with immunotherapy $s_\infty = 4\times 10^5$ where the switching manifold is given by Σ_2 and $q_\infty = 300$. Let us consider the system

$$Z_3(N,I,Q) = \begin{cases} X(N,I,Q) & \text{if} \quad I \leq 10^7; \\ Y(N,I,Q) & \text{if} \quad I \geq 10^7, \end{cases} \tag{2.18}$$

where X and Y are given by equations (2.7) and (2.8), respectively, for $s_\infty = 4 \times 10^5$ and $q_\infty = 300$. The equilibrium point of the vector field Y is given by $p_5 = \big(0, 4.81 \times 10^6, 72.11\big)$ which is an attractor and a virtual equilibria for Z_3.

Considering the PSVF Z_3, the sets of tangential singularities of X and Y are distinct and therefore one does not have just crossing regions. Indeed, Z_3 contains an escaping region. We can notice that the tangential singularities of X with Σ_2 are given by the curve Q_2 in (2.16) and they have the same behavior obtained in Proposition 8.

Proposition 10. *The tangential singularities of Y with Σ_2 is given by the curve*

$$Q_3(N) = -\frac{5000000\left(69000000000000 + 689999999910N - N^2\right)}{999993100000000000 + 99999310000000090N + N^2} \subset \Sigma_2 \cap \mathcal{O}^+. \tag{2.19}$$

Moreover, they are invisible fold points.

Proof. Indeed, $Yh(N,I,Q)$ restricted to $I = 10^7$ has the expression

$$Yh(10^7, I, Q) = Y_2\big|_{I=10^7} = -\frac{N\,(90+N)}{1000000\,(100+N)} + 10000\left(69 - \frac{10000000Q}{5000000+Q}\right).$$

So, $Yh(10^7, I, Q) = 0$ give $Q = Q_3(N)$, according to Equation (2.19). Furthermore, $Y^2h(p)$ is negative for $N \in \big[0, 6.9 \times 10^{11}\big]$. $\square$

The curve Q_2 of tangential singularities of X and Q_3 of tangential singularities of Y do not intercept each other on the octant $\mathcal{O}^+$ and they define a region $R \subset \mathcal{O}^+$ between them. Given $p \in R$, it follows that $Xh(p) < 0$ and $Yh(p) > 0$. Therefore, we conclude that R is an escaping region (see Figure 2.10).

Now we are able to calculate the sliding vector field given by Definition 1 which is defined in the region R.

Proposition 11. *The sliding vector field Z_3^s is given by $Z_3^s(N,Q) = (F_1(N,Q), F2(N,Q))$ where*

$$F_1(N,Q) = -\frac{N^2}{10^{14}} + N\left(\frac{19}{2000} - \frac{8Q}{2000+Q}\right)$$

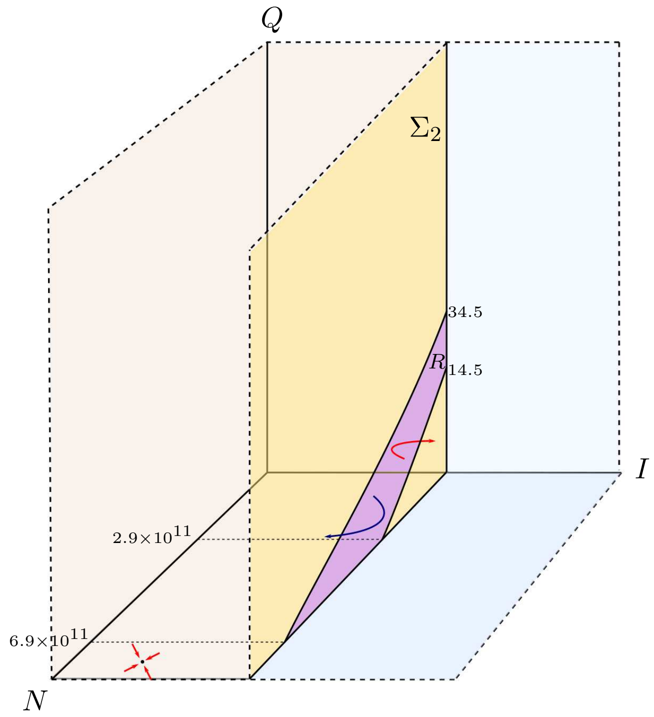

Figure 2.10: Behavior of the PSVF Z_3 in the escaping region R.

and $F_2(N,Q)$ *is equal to*

$$\frac{-1.0875\times10^{11}+N^2\left(0.00375+7.5\times10^{-10}Q\right)+5.41998\times10^{9}Q-416.Q^2+N\left(-1.0875\times10^{9}+5.41998\times10^{7}Q-4.16Q^2\right)}{(100.+N)(5.\times10^{6}+Q)}.$$

Proof. The proof is a computation of Equation (1.2). □

The sliding vector field Z_3^s has two equilibria in the region R given by $(N,Q)=(0,20.0647)$ and $(N,Q)=(2.65236\times10^{11},1.71338)$. By means of the analysis of the Jacobian matrix of the vector field Z_3^s we can conclude that the first equilibria is a saddle point attracting in the variable N and repelling in the variable Q while the second one is a repulsor equilibrium (see Figure 2.11).

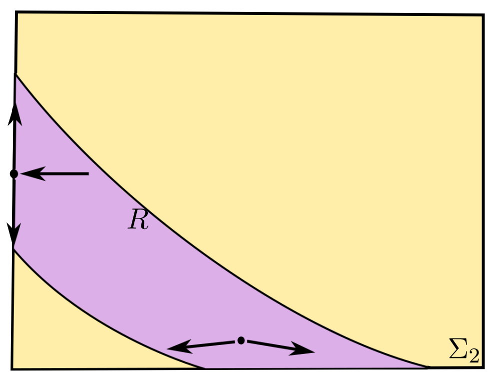

Figure 2.11: Behavior of the vector field Z_3^s.

2.1.3 A control strategy according to chemotherapeutic agent quantities

For sake of completeness we can consider the system

$$Z_4(N,I,Q) = \begin{cases} Y(N,I,Q) & \text{if} \quad Q \leq Q_\infty; \\ X(N,I,Q) & \text{if} \quad Q \geq Q_\infty, \end{cases} \tag{2.20}$$

where X and Y are given by equations (2.7) and (2.8), respectively, and $j(N,I,Q) = Q - Q_\infty$ where $\Sigma_3 = j^{-1}(0)$ with $Q_\infty > q_\infty/\lambda$. In this case, we have that both Lie derivatives Xj and Yj are strictly negative on Σ_3 and therefore we have no tangential singularities, that is, the third coordinate of the vector fields X and Y are negative on Σ_3 and we have just crossing regions on it. Moreover, the vector field Y has

$$p = \left(0, \frac{(s_\infty + s_0)(q_\infty + b\lambda)}{dq_\infty + q_\infty\delta + bd\lambda}, \frac{q_\infty}{\lambda}\right)$$

as an equilibrium on the octant $\mathcal{O}^+$ which is a real equilibrium for Z_4 and it has at least two negatives eigenvalues for positive values of the parameters. In the case where $s_\infty = 4 \times 10^5$, $q_\infty = 300$ and following the values of Table 2.1 we have that $p = p_5$ given above is the unique equilibrium of Y on the octant $\mathcal{O}^+$, which is the unique real equilibria for Z_4 and therefore globally asymptotically stable for Z_4 (see Figure 2.12).

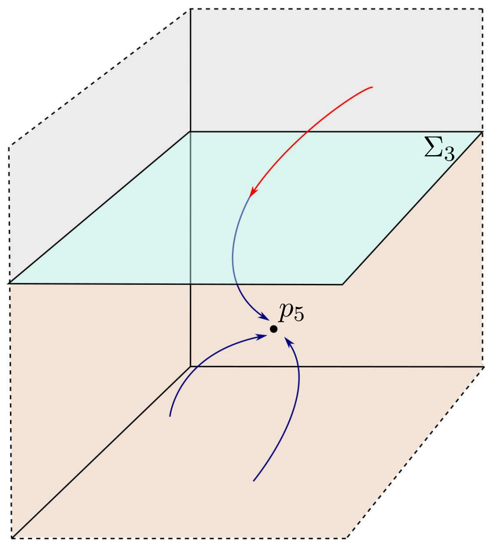

Figure 2.12: Behavior of the PSVF Z_4.

2.2 Analysis of the dynamics of a mathematical model to intermittent HIV treatment using sliding mode control

The aim of this section is to study the qualitative dynamics of a piecewise smooth system modeling the intermittent treatment of the Human Immunodeficiency Virus (HIV). Typical singularities and closed orbits are observable and we quantitatively explore the dynamic around those singularities and closed orbits. Moreover, we conclude that this protocol always will be successful since the trajectory passing through any initial condition converges to one of these distinguished orbits. Our results corroborate the real world observation, where the virus is not eliminated, but it is controlled around a specific value, namely critical value. The content of this section can be found in [55, 59].

The Human Immunodeficiency Virus (HIV) affects people around all over the world. According to World Health Organization (WHO), there are 37.9 million people in the world living with HIV in 2018 (about 25.7 million in Africa) being 1.7 million people newly infected with HIV in the last year (see [129]).

The immune function is regularly measured by CD4 cell count. As the virus impairs immune cells, infected individuals become immunodeficient which results in susceptibility to a wide range of infections. The virus infects $CD4^+$ T helper cells which results in strong viral response and virus replication, see [96] for more details. The advanced stage of HIV infection is Acquired Immunodeficiency Syndrome (AIDS) which inhibit the immune system of the body and can take many years to develop depending on the individual.

Several significant developments have occurred in the HIV field in the last years and more efficacious antiretroviral drugs are becoming available. Strong evidence shows that using antiretroviral treatment (ART) earlier increases the survival time for patients. In 2018, approximately 62% of people living with HIV were receiving antiretroviral treatment, which reduces the risk of transmitting the virus to their uninfected sexual partner until about 96% (see [128, 129]).

In the literature, many mathematical models have been proposed to describe the dynamics of HIV. The models can be deterministic or stochastic and usually describe the kinetics of the HIV infection and its therapies. See [44, 46, 60, 73, 95, 96] and references therein.

In the last years, strategies of scheduled treatment interruptions of antiretroviral therapies have been proposed for clinical management of HIV infected patients (see [3, 114, 115]). In this regimen, the patients continued their antiretroviral therapy until the studied cell counts went over to a fixed number, and then stopped the treatment until they dropped back. In this way, we get a piecewise smooth dynamic model of the HIV that allows us to investigate the scheduled treatment interruptions strategies. A formal cost-effectiveness analysis is not available, but it is explicit that a therapy based on intermittent treatment enables cost savings as well as reducing patient side effects (see [68, 87]).

In this context, we explore qualitative features of a piecewise smooth system modeling the dynamic of Human Immunodeficiency Virus. Of course, the purpose of any treatment is to provide a cure for the disease. However, in some cases, the treatment also affects healthy cells and as it kills diseased cells, it also kills healthy cells. In the end, the patient may become so weakened that he/she will eventually die. In order to avoid this situation, the protocol that we are investigating, predicts a drug-on stage suddenly interrupted by a drug-off stage, giving rise to an intermittent (and not necessary periodic in time) treatment. Thus, during the drug-off stage, the patient's immune system recovers before a new dose of drugs is given. So, there exists a mathematical model governed by ordinary differential equations for the drug-on stage and a similar one for the drug-off stage.

Usually, effective antiretroviral therapy is based on two classes of antiretroviral drugs: reverse transcriptase inhibitors (RTIs) and protease inhibitors (PIs). The protease inhibitors avoid HIV protease from divide the HIV polyprotein into functional units, inducing infected cells to produce immature virus particles that are non-infectious. At the same time, the RTIs block RT's enzymatic function and help to prevent the completion of the synthesis of the viral DNA from HIV-1 RNA.

A model of viral dynamics generally consists of a system of differential equations describing the interactions between infected cells, susceptible cells and the infective form of a virus. Let us denote by $T^*(t)$ the infected CD4$^+$ T helper cell population size at the time t, $T(t)$ the uninfected CD4$^+$ T cell population size at the time t, $V_I(t)$ concentration of infectious virus particles, η_{RT} and η_{PI} the effects of RTIs and PIs. In the scheduled treatment interruptions in HIV treatment considered by [3], the patients continued their antiretroviral therapy until T CD4$^+$ cell counts went over to 350 cells/μl, and then stopped the treatment until they dropped back to 350 cells/μl. Assume that there is a threshold value C_T which antiretroviral therapy will be triggered below this value and which the therapy will be stopped above this value. Based on the works of [3, 96, 115] the HIV dynamics models for drug-off and drug-on states can be written respectively as

$$\begin{cases} \dfrac{dT}{dt} &= s - d\,T - k\,V_I\,T \\ \dfrac{dT^*}{dt} &= k\,V_I\,T - \delta\,T^*, \qquad\qquad \text{if} \quad T + T^* > C_T, \\ \dfrac{dV_I}{dt} &= \lambda\,T^* - c\,V_I \end{cases} \tag{2.21}$$

and

$$\begin{cases} \dfrac{dT}{dt} &= s - d\,T - (1-\eta_{RT})\,k\,V_I\,T \\ \dfrac{dT^*}{dt} &= (1-\eta_{RT})\,k\,V_I\,T - \delta\,T^* \qquad \text{if} \quad T + T^* < C_T. \\ \dfrac{dV_I}{dt} &= (1-\eta_{PI})\,\lambda\,T^* - c\,V_I \end{cases} \tag{2.22}$$

The parameter d means the death rate of uninfected cells while s is the rate at which uninfected cells are generated from a source. Moreover, the parameter δ is the death rate of infected cells, λ is the rate of production of virus by infected cells, k is the infectivity rate and c is the clearance rate of free virus. The numerical analyses in this work are performed using the parameter values summarized in Table 2.2.

Table 2.2: Parameters for the HIV model (see [114]).

Parameter and description		Values
s	Generation rate for uninfected CD4$^+$ T cell	$15\,\mu\text{l}^{-1}\text{day}^{-1}$
d	Death rate of uninfected CD4$^+$ T cells	$0.01\,\text{day}^{-1}$
k	Infection rate for CD4$^+$ T cells by virus	$2.4 \times 10^{-6}\mu\text{l}^{-1}\text{day}^{-1}$
δ	Death rate of infected CD4$^+$ cells	$0.35\,\text{day}^{-1}$
λ	Number of free virus produced by lysing a CD4$^+$ cell	$3000\,\text{day}^{-1}$
c	Death or clearance rate of free virus	$3\,\text{day}^{-1}$
η_{RT}	RTI drug efficacy	$0.5-1$
η_{PI}	PI drug efficacy	$0.5-1$

In our approach, we consider the reproductive ratios (also called *basic numbers of reproduction*)

$$R_0 = \frac{ks\lambda}{cd\delta}$$

and

$$R_c = R_0(1-\eta_{PI})(1-\eta_{RT}).$$

In order to define the piecewise smooth vector field associated to the systems (2.21) and (2.22), following the theory of discontinuous vector fields and Filippov conventions, let us consider the function $f(p) = T + T^* - C_T$, where $p = (T, T^*, V_I)$ and C_T is the threshold value of T CD4$^+$ cells. Denoting the vector fields associated to the drug-off and drug-on state respectively by

$$X(T,T^*,V_I) = (s - dT - kV_IT, kV_IT - \delta T^*, \lambda T^* - cV_I)\,, \tag{2.23}$$

and

$$Y(T,T^*,V_I) = (s - dT - (1-\eta_{RT})kV_IT, (1-\eta_{RT})kV_IT - \delta T^*, (1-\eta_{PI})\lambda T^* - cV_I)\,, \tag{2.24}$$

the piecewise smooth vector field Z associated to the systems (2.21) and (2.22) is given by

$$Z(T,T^*,V_I) = \begin{cases} X(T,T^*,V_I), & \text{if} \quad T+T^* > C_T \\ Y(T,T^*,V_I), & \text{if} \quad T+T^* < C_T \end{cases}. \tag{2.25}$$

Observe that $\Sigma^+ = \{p \in \mathbb{R}^3_+ : f(p) > 0\}$, $\Sigma^- = \{p \in \mathbb{R}^3_+ : f(p) < 0\}$ and the switching manifold is given by the angled plane $\Sigma = \{p \in \mathbb{R}^3_+ : f(p) = 0\}$.

A direct inspection shows that the vector field X given by (2.23) has two equilibria, namely

$$p^0_+ = \left(\frac{s}{d}, 0, 0\right) \text{ and } p^1_+ = \left(\frac{c\delta}{k\lambda}, \frac{-cd\delta + ks\lambda}{k\delta\lambda}, \frac{-cd\delta + ks\lambda}{ck\delta}\right)$$

and the vector field Y given by (2.24) also has two equilibria, namely

$$p^0_- = p^0_+ \text{ and } p^1_- = \left(\frac{c\delta}{k(-1+\eta_{RT})\lambda(-1+\eta_{PI})}, \frac{-cd\delta + ks\lambda - ks\lambda\eta_{RT} - ks\lambda\eta_{PI} + ks\lambda\eta_{RT}\eta_{PI}}{k\delta(-1+\eta_{RT})\lambda(-1+\eta_{PI})},\right.$$
$$\left.\frac{cd\delta - ks\lambda + ks\lambda\eta_{RT} + ks\lambda\eta_{PI} - ks\lambda\eta_{RT}\eta_{PI}}{ck\delta(-1+\eta_{RT})}\right).$$

The parameter δ is the rate at which uninfected cells are generated and d is the death rate of uninfected cells, so by hypothesis (that is natural) we get:

$$d < \delta. \tag{2.26}$$

In order to determine the global dynamics of the piecewise smooth vector field $Z = (X,Y)$ we will explore the results of [81]. In fact, Theorem 2.1, item 1, of [81] ensures that, if $R_0 < 1$ in (2.23) (Drug-off), then p^1_+ is not placed at the positive octant of $\mathbb{R}^3$ and the disease-free state p^0_+ is globally attracting and the virus is cleared. Moreover, Lemma 3.1 of [81] establishes that the positive octant is positively invariant and there exists $M > 0$ such that $T(t), T^*(t), V_I(t) < M$ for some t large enough. For this reason, a treatment is not necessary and the protocol that we are planning to study is obsolete. So, it is natural to assume another important hypothesis:

$$R_0 = \frac{ks\lambda}{cd\delta} > 1. \tag{2.27}$$

Remark 5. *According to Theorem 2.1, item 2, of [81], we obtain that* p_+^1 *is globally asymptotically stable and* p_+^0 *is unstable for* (2.21)*. We also emphasize that Corollary 2.2 of [81] states that* p_-^0 *is globally attracting when* $R_c < 1$ *and it is unstable when* $R_c > 1$*. Now, Theorem 1.1 of [75] states that* p_-^1 *is globally attracting when* $R_c > 1$*.*

The position of the equilibria $p_+^0 = p_-^0$, p_+^1 and p_-^1 comparing to Σ will be very important for the dynamics of the PSVF Z given by (2.25). For this, consider the parameters

$$\widehat{C}_T^0 = \frac{s}{d}, \tag{2.28}$$

$$\widehat{C}_T^+ = \frac{s}{d}\left[1 - \left(1 - \frac{d}{\delta}\right)\left(1 - \frac{1}{R_0}\right)\right] = \frac{s}{\delta} + \frac{c(-d+\delta)}{k\lambda}, \tag{2.29}$$

$$\widehat{C}_T^- = \frac{s}{d}\left[1 - \left(1 - \frac{d}{\delta}\right)\left(1 - \frac{1}{R_c}\right)\right] = \frac{s}{\delta} + \frac{c(-d+\delta)}{k(-1+\eta_{RT})\lambda(-1+\eta_{PI})}, \tag{2.30}$$

that are the sum of the two first coordinates of the equilibria $p_+^0 = p_-^0$, p_+^1 and p_-^1, respectively.

Since $0 < \eta_{RT}, \eta_{PI} < 1$ we conclude that $\widehat{C}_T^- > \widehat{C}_T^+$. Moreover, $\widehat{C}_T^- < s/d$ if $R_c > 1$, $\widehat{C}_T^- > s/d$ if $R_c < 1$ and $\widehat{C}_T^- = s/d$ if $R_c = 1$. It is also important to note that $s/\delta < \widehat{C}_T^+ < s/d$. By hypothesis on the system parameters of (2.23)-(2.25), we then consider:

$$\widehat{C}_T^+ < C_T < \min\left[\widehat{C}_T^-, \widehat{C}_T^0\right]. \tag{2.31}$$

The first Lie derivatives of (2.23) and (2.24) coincide and are given by

$$Xf(T, T^*, V_I) = Yf(T, T^*, V_I) = s - dT - T^*\delta.$$

So, those first Lie derivatives of X and Y vanish just in the set

$$\left\{(T, T^*, V_I) \,|\, T = \frac{s - \delta T^*}{d}\right\}.$$

When restricted to Σ we obtain that the tangency lines of (2.23) and (2.24) coincide and are given by

$$S = \left\{(T, T^*, V_I) \in \Sigma \,|\, T = \frac{s - \delta T^*}{d}\right\} = \left\{(T, T^*, V_I) = \left(\frac{s - C_T\delta}{d - \delta}, \frac{-C_T d + s}{-d + \delta}, V\right)\right\}.$$

The second Lie derivatives of (2.23) and (2.24), respectively, restricted to Σ are

$$SL_X = \delta(s - dC_T) + k(s - \delta C_T)V_I \text{ and } SL_Y = \delta(s - dC_T) - k(s - \delta C_T)V_I(\eta RT - 1).$$

So, the vector field X given by (2.23) has a cusp point at

$$C_X = \left(\frac{s - \delta C_T}{d - \delta}, \frac{-s + dC_T}{d - \delta}, \frac{\delta(-s + dC_T)}{k(s - \delta C_T)}\right)$$

and the vector field Y given by (2.24) has a cusp point at

$$C_Y = \left(\frac{s - \delta C_T}{d - \delta}, \frac{-s + dC_T}{d - \delta}, \frac{\delta(-s + dC_T)}{k(s - \delta C_T)(1 - \eta_{RT})}\right).$$

We can notice that the third coordinate $C_{Y,3}$ of C_Y is bigger than that one $C_{X,3}$ for C_X. The cusp point C_X divides S in two semi-straight lines. A semi-straight line

$$r_X^V = \{(T, T^*, V_I) \in S \,|\, V_I < C_{X,3}\}$$

filled by visible fold points and a semi-straight line $r_X^I = \{(T, T^*, V_I) \in S \,|\, V_I > C_{X,3}\}$ filled by invisible fold points. On the other side, the cusp point C_Y divides S in two semi-straight lines. A semi-straight line $r_Y^V = \{(T, T^*, V_I) \in S \,|\, V_I > C_{Y,3}\}$ filled by visible fold points and a semi-straight line $r_Y^I = \{(T, T^*, V_I) \in S \,|\, V_I < C_{Y,3}\}$ filled by invisible fold points. See Figure 2.13.

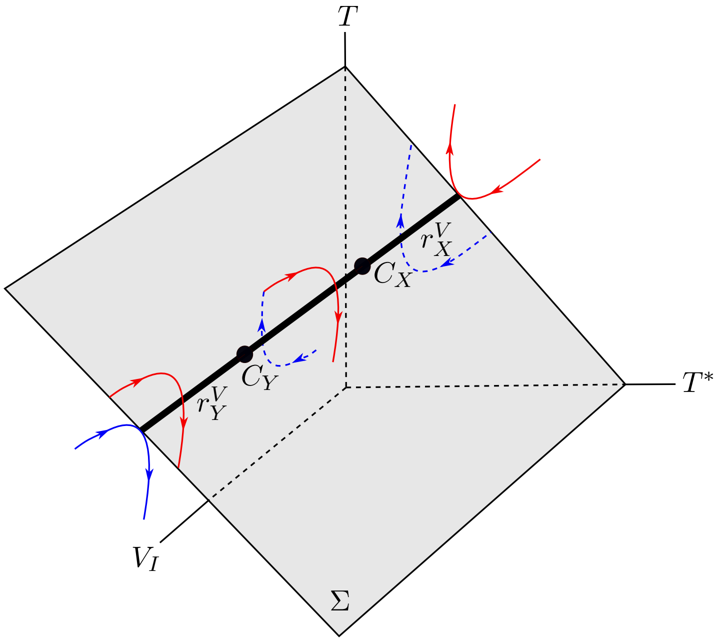

Figure 2.13: The dynamic near the tangencial singularities

Moreover, we can define the tangential sliding vector field Z^T on S (see Definition 2) given by

$$Z^T(T,T^*,V_I) = \Bigg(0,0,\frac{1}{k\eta_{RT}V_I(d-\delta)(\delta C_T-s)}\Big(ck\eta_{RT}V_I^2(d-\delta)(-\delta C_T+s)$$
$$+(dC_T-s)\lambda(-kV_I(\eta_{RT}-\eta_{PI})(s-\delta C_T)+(-dC_T+s)\delta\eta_{PI})\Big)\Bigg). \tag{2.32}$$

A direct calculation show that Z^T has just one equilibrium at the first octant. In fact, the denominator of the third coordinate of (2.32) is null only when $V_I=0$ and the numerator of the third coordinate is null when

$$V_I = \frac{\lambda k(dC_T-s)(\eta_{RT}-\eta_{PI})(s-\delta C_T) \pm \sqrt{(\lambda k(dC_T-s)(\eta_{RT}-\eta_{PI})(s-\delta C_T))^2-4\overline{a}\,\overline{c}}}{2\overline{a}} \tag{2.33}$$

where $\overline{a}=ck\eta_{RT}(d-\delta)(-\delta C_T+s)$ and $\overline{c}=-\lambda\delta\eta_{PI}(dC_T-s)^2$.

Therefore, we obtain that:

- p^1_+ is placed below Σ and p^1_- and $p^0_- = p^0_+$ are placed above Σ. That is, the equilibrium point p^0_+ is the unique real equilibrium for the PSVF Z given by (2.25).
- In (2.33), $\overline{a}\,\overline{c}<0$ and so, there is just one tangential equilibrium p_e placed at the first octant.
- Both cusp points C_X and C_Y are placed at the first octant.
- There is an invisible fold-fold line segment $TF \subset S$ between the cusp points. Moreover, $p_e \in TF$.

We have seen that the cusp point C_X divides S in the semi-straight lines $r^V_X=\{(T,T^*,V_I)\in S\,|\,V_I<C_{X,3}\}$ filled by visible fold points and $r^I_X=\{(T,T^*,V_I)\in S\,|\,V_I>C_{X,3}\}$ filled by invisible fold points. We would like to consider the saturation of the semi-straight lines of visible fold points involving a cusp singularity. See illustrated in Figure 2.14.

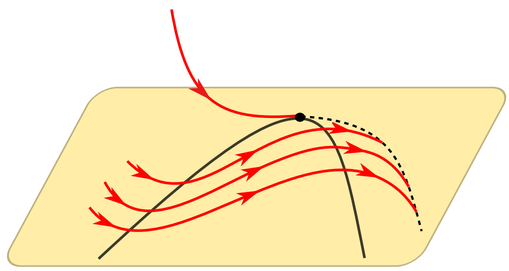

Figure 2.14: The cusp singularity.

Let $\phi_X\left(r_X^V\right)$ be the saturation of r_X^V through the flow of the vector field X given by (2.21). Since p_+^1 is an equilibrium globally attractor placed below Σ, it is well defined the curve $S\left(r_X^V\right) = \phi_X\left(r_X^V\right) \cap \Sigma$. Note that Closure $\left(S\left(r_X^V\right)\right) \cap$ Closure $\left(r_X^V\right) = \{C_X\}$. Call $\mathcal{A} \subset \Sigma$ the region bounded by $S(r_X^V) \cup \{C_X\} \cup r_X^I$. Besides, the cusp point C_Y divides S in the semi-straight lines $r_Y^V = \{(T, T^*, V_I) \in S \,|\, V_I > C_{Y,3}\}$ filled by visible fold points and $r_Y^I = \{(T, T^*, V_I) \in S \,|\, V_I < C_{Y,3}\}$ filled by invisible fold points. Let $\phi_Y\left(r_Y^V\right)$ be the saturation of r_Y^V through the flow of the vector field Y given by (2.22). Since p_-^0 is an equilibrium globally attractor placed above Σ, it is well defined the curve $S\left(r_Y^V\right) = \phi_Y\left(r_Y^V\right) \cap \Sigma$. Note that Closure $\left(S\left(r_Y^V\right)\right) \cap$ Closure $\left(r_Y^V\right) = \{C_Y\}$. Call $\mathcal{B} \subset \Sigma$ the region bounded by $S\left(r_Y^V\right) \cup \{C_Y\} \cup r_Y^I$. See Figure 2.15.

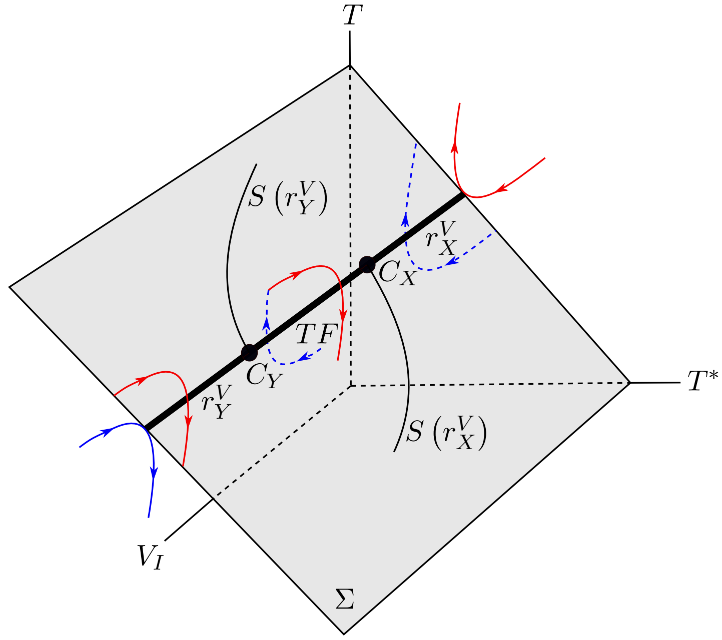

Figure 2.15: The global dynamic of Z.

In the following, we present the first result of this section that treats the global dynamics of the piecewise smooth dynamical system Z given by (2.25) which establishes a set, that contains the tangential singularities of X and Y, that is a global attractor.

Theorem 6. *If $d < \delta, R_0 > 1$ and $\widehat{C}_T^+ < C_T < min\left[\widehat{C}_T^-, \widehat{C}_T^0\right]$ then $\mathcal{A} \cup \mathcal{B} \subset \Sigma$ is a globally asymptotically stable set for* (2.25).

The proof of Theorem 6 follows from the next lemma.

Lemma 3. *Let us consider an arbitrary initial condition x_0 at the first octant. The trajectory of Z passing through x_0 hits Σ in a sequence of points $(s_i)_{i\in\mathbb{N}}$ such that $s_i \in \mathcal{A} \cup \mathcal{B}$ if $i \geq 2$.*

Proof. (Case 1) If x_0 is placed above Σ, the trajectory of X passing through x_0 tends to p_+^1 and then, it has to hit Σ in a point s_1 (it is possible that $s_1 \in \mathcal{A}$ or not). Now, the trajectory

$\phi_Y(s_1)$ of Y passing through s_1 tends to p_-^0 and then, it has to hit Σ in a point s_2. Moreover, $s_2 \in \mathcal{B}$ since, otherwise, $\phi_Y(s_1) \cap \phi_Y\left(r_Y^V\right) \neq \emptyset$ resulting in an absurd due to the uniqueness of trajectories of Y passing through a point. After that, due to the uniqueness of trajectories of X passing through a point, $\phi_X(s_2) \cap \phi_X\left(r_X^V\right) = \emptyset$ and the trajectory of X passing through s_2 returns to Σ at $s_3 \in \mathcal{A}$. Repeating the argument, we conclude the proof for this case.

(Case 2) If x_0 is placed below Σ, the trajectory of Y passing through x_0 tends to p_-^0 and then, it has to hit Σ in a point s_1 (it is possible that $s_1 \in \mathcal{B}$ or not). Now, the trajectory $\phi_X(s_1)$ of X passing through s_1 tends to p_+^1 and then, it has to hit Σ in a point s_2. Moreover, $s_2 \in \mathcal{A}$ since, otherwise, $\phi_X(s_1) \cap \phi_X\left(r_X^V\right) \neq \emptyset$ resulting in an absurd due to the uniqueness of trajectories of X passing through a point. After that, due to the uniqueness of trajectories of Y passing through a point, $\phi_Y(s_2) \cap \phi_Y\left(r_Y^V\right) = \emptyset$ and the trajectory of Y passing through s_2 returns to Σ at $s_3 \in \mathcal{B}$. Repeating the argument we conclude the proof for this case.

If $x_0 \in \Sigma$, then $x_0 \in \Sigma^{c,+} \cup \Sigma^{c,-} \cup \{C_X\} \cup \{C_Y\} \cup r_X^V \cup r_Y^V \cup TF$. When $x_0 \in \Sigma^{c,-} \cup \{C_Y\} \cup r_Y^V$ it is enough take $x_0 = s_1$ in Case 1. When $x_0 \in \Sigma^{c,+} \cup \{C_X\} \cup r_X^V$ it is enough take $x_0 = s_1$ in Case 2. When $x_0 \in TF$, the trajectory passing through x_0 is given by the tangential sliding vector field (2.32) and it is confined to the intersection of $\mathcal{A}$ and $\mathcal{B}$. □

Proof of the Theorem 6. The proof of the Theorem 6 when $R_c < 1$ follows direct from Lemma 3. For the case $R_c \geq 1$, it is enough to repeat the previous argumentation changing p_-^0 by p_-^1 at the proof of Lemma 3 (remember Remark 5, that ensures that p_-^1 is globally asymptotically stable for Y). □

In the sequel, we present a example that illustrates the global dynamics of the model where we observe the existence of a limit cycle. Next, the local dynamics around the curve of two-folds is studied and we prove the occurrence of a Hopf-Like bifurcation.

Example 1. *We consider the parameter values from Table 2.2, taking* $\eta_{RT} = \eta_{PI} = 0.6$ *and* $C_T = 400$. *In this case the phase portrait of system Z given by* (2.25) *presents a stable crossing limit cycle, as shown in Figure 2.16.*

Now we would like to analyze the local dynamics near the equilibrium of the tangential sliding vector field. In the previous calculations, we identified the existence of a tangential equilibrium point (equilibrium of the *tangential sliding vector field* Z^T given explicitly in (2.32)) belonging to the straight line of fold-fold singularities in Σ, that is, a point of Σ where the vector fields X and Y are tangent and become anti-collinear. This point is an admissible tangential equilibrium of (2.25) if the quadratic tangencies are invisible to X and Y.

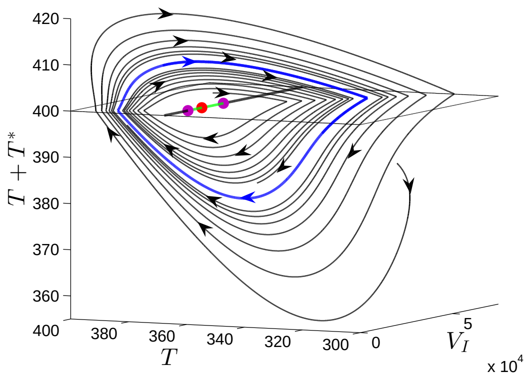

Figure 2.16: Simulations pf system Z given by (2.25) by taking the parameter values from Table 2.2 and considering $\eta_{RT} = \eta_{PI} = 0.6$ and $C_T = 400$. We visualize a stable limit cycle (blue color). Moreover, the line segment in green color represents the invisible fold-fold segment, the dots in red and purple colors indicate the tangential equilibrium point and cusp points, respectively.

We will describe the dynamic behavior of the trajectories of system Z given by (2.25) in a neighborhood of this tangential equilibrium point. In what follows, we will study the crossing dynamics using the standard tools for analysis of Poincaré return maps (see [33, 79]), and we will present the conditions on the system parameters that ensure local asymptotic stability at the tangential equilibrium point. In addition, we will prove the occurrence of bifurcations at the tangential equilibrium involving the change of its stability and the birth of a crossing limit cycle, similar to the supercritical and subcritical Hopf bifurcations (we call Hopf-Like bifurcations). These bifurcations are typical of non-smooth dynamical systems and have motivated several works in recent years (see [105] and references therein).

In order to simplify the study, we apply to system (2.25) the coordinate change given by

$$\begin{cases} T = x, \\ T^* = z - x, \\ V_I = y/k, \end{cases} \tag{2.34}$$

and we define a new state space domain $\mathcal{M} = \{\mathbf{x} = (x, y, z) \in \mathbb{R}^3_+ : z \geq x\}$ such that $\mathcal{M} = \Sigma^- \cup \Sigma \cup \Sigma^+$ with $\Sigma^- = \{\mathbf{x} \in \mathcal{M} : \ h(\mathbf{x}) < 0\}$, $\Sigma^+ = \{\mathbf{x} \in \mathcal{M} : \ h(\mathbf{x}) > 0\}$ and $\Sigma = \{\mathbf{x} \in \mathcal{M} : h(\mathbf{x}) = z - C_T = 0\}$ being the switching boundary in the new coordinates. So, we get the system

$$\dot{\mathbf{x}} = \begin{cases} \mathbf{F}_-(\mathbf{x}), & \text{if } \mathbf{x} \in \Sigma^- \\ \mathbf{F}_+(\mathbf{x}), & \text{if } \mathbf{x} \in \Sigma^+, \end{cases} \tag{2.35}$$

composed by the two vector fields

$$\mathbf{F}_+(\mathbf{x}) = \begin{bmatrix} s-(d+y)x \\ -cy+a(z-x) \\ s+(\delta-d)x-\delta z \end{bmatrix} \quad \text{and} \quad \mathbf{F}_-(\mathbf{x}) = \begin{bmatrix} s-(d+N_{RT}y)x \\ -cy+N_{PI}a(z-x) \\ s+(\delta-d)x-\delta z \end{bmatrix}, \tag{2.36}$$

where $a = k\lambda$, $N_{PI} = 1-\eta_{PI}$ and $N_{RT} = 1-\eta_{RT}$.

Figure 2.17 illustrates the configuration of the vector fields $\mathbf{F}_\pm$ at the switching boundary Σ and shows some of the involved elements as:

(i) The two-fold tangency line $L = \{(x, y, C_T) \in \Sigma : x = \bar{x}_t\}$ with

$$\bar{x}_t = \frac{C_T\delta - s}{\delta - d},$$

which divides Σ into two crossing regions, $\Sigma^{c,+} = \{(x, y, z) \in \Sigma : x > \bar{x}_t\}$ (where the trajectories pass from Σ^- to Σ^+) and $\Sigma^{c,-} = \{(x, y, z) \in \Sigma : x < \bar{x}_t\}$ (where the trajectories pass from Σ^+ to Σ^-);

(ii) The cusp points $\mathbf{q}^\pm = (\bar{x}_t, \bar{y}_q^\pm, C_T) \in L$ with

$$\bar{y}_q^- = \frac{(s-dC_T)\delta}{(\delta C_T - s)N_{RT}} \quad \text{and} \quad \bar{y}_q^+ = N_{RT}\bar{y}_q^- < \bar{y}_q^-;$$

(iii) The line segment

$$L_I = \left\{(\bar{x}_t, y, C_T) \in L : \bar{y}_q^+ < y < \bar{y}_q^-\right\}, \tag{2.37}$$

bounded by the cusp points and formed by invisible two-fold points;

(iv) The admissible tangential equilibrium point $\mathbf{p} \in \Sigma$ namely

$$\mathbf{p} = (\bar{x}_t, \bar{y}_p, C_T) \tag{2.38}$$

with

$$\bar{y}_p = \bar{y}_q^+ \left(\frac{a\bar{x}_t(\eta_{RT}-\eta_{PI}) + \sqrt{a\bar{x}_t\left[a\bar{x}_t(\eta_{RT}-\eta_{PI})^2 + 4c\delta\eta_{PI}\eta_{RT}\right]}}{2c\delta\eta_{RT}}\right) \tag{2.39}$$

We can observe that the hypothesis given by (2.31) ensures that $\bar{y}_q^+ < \bar{y}_p < \bar{y}_q^-$.

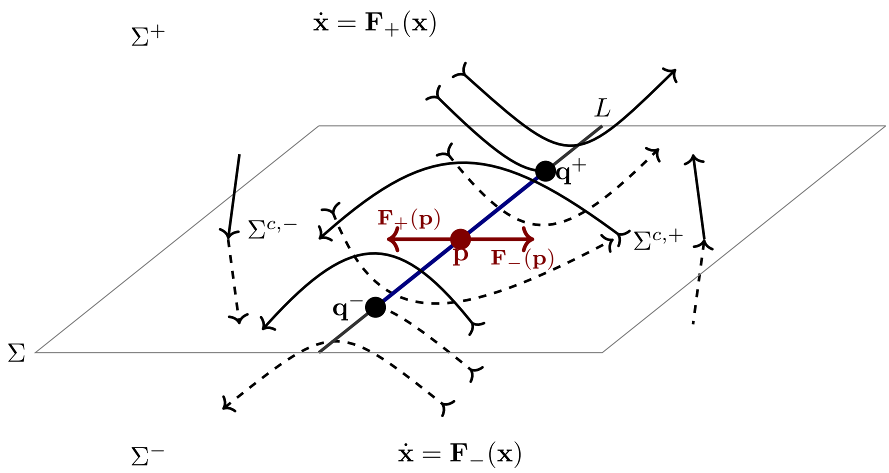

Figure 2.17: Configuration of $\mathbf{F}_\pm$ at the switching manifold Σ.

The second result analyses the local dynamics around the equilibrium of the tangential sliding vector field. We characterize the local stability of the equilibrium according system parameters and the birth of a crossing limit cycle, like a Hopf bifurcation. These results are dependent on two critical parameters, namely

$$\mu = \frac{\delta \bar{y}_p^2 + \left(\frac{c+d+\delta}{N_{RT}} - \bar{y}_q^-\right)\delta \bar{y}_p - \left[a\bar{x}_t N_{PI} N_{RT} + \delta(d+\delta)\right]\frac{\bar{y}_q^-}{N_{RT}}}{(\bar{y}_q^- - \bar{y}_p)^2} + \\ + \frac{\left[a\bar{x}_t + \delta(d+\delta)\right]\bar{y}_q^+ - \left(c+d+\delta - \bar{y}_q^+\right)\delta\bar{y}_p - \delta\bar{y}_p^2}{(\bar{y}_q^+ - \bar{y}_p)^2}, \tag{2.40}$$

with $N_{RT} = 1 - \eta_{RT}$, $N_{PI} = 1 - \eta_{PI}$, $a = k\lambda$, $\bar{y}_q^\pm$ and $\bar{y}_p$ given above; and

$$\kappa = \begin{bmatrix} 1 & -\frac{v_{20}}{v_{11}} \end{bmatrix} \left(M - \frac{p_{21}}{v_{11}} N\right) \begin{bmatrix} 1 \\ -\frac{v_{20}}{v_{11}} \end{bmatrix}, \tag{2.41}$$

where $p_{21} = p_{21}^- - p_{21}^+$, $v_{20} = v_{20}^+ - v_{20}^-$, $v_{11} = v_{11}^+ - v_{11}^- < 0$,

$$M = \begin{bmatrix} p_{40}^- - p_{40}^+ & p_{31}^- - p_{31}^+ \\ 0 & p_{22}^- - p_{22}^+ \end{bmatrix} \quad \text{and} \quad N = \begin{bmatrix} v_{30}^+ - v_{30}^- & v_{21}^+ - v_{21}^- \\ 0 & v_{12}^+ - v_{12}^- \end{bmatrix}, \tag{2.42}$$

with p_{ij}^+, v_{ij}^+ given in (2.55)-(2.57) and p_{ij}^-, v_{ij}^- given in (2.60)-(2.62). Both critical parameters are written as functions of all system parameters, but κ-parameter is considered constant and calculated for $\mu = 0$.

Theorem 7. *Assume in the discontinuous system* (2.35) *the hypotheses* (2.26) *and* (2.31)*. Consider* L_I*,* $\mathbf{p}$*,* μ *and* κ *defined in* (2.37)*,* (2.38)*,* (2.40) *and* (2.41)*, respectively. The following statements hold.*

(a) If $\mu < 0$ *then* $\mathbf{p} \in L_I$ *is an admissible tangential equilibrium locally asymptotically stable. If* $\mu > 0$ *it is unstable.*

(b) Assume $\kappa \neq 0$ *and* $\mu \in (-\varepsilon, \varepsilon)$ *for* $\varepsilon > 0$ *arbitrary and small. Then, for* $\mu = 0$*, a bifurcation occurs at* $\mathbf{p}$ *and a crossing limit cycle arises for* $\mu\kappa < 0$*. In addition, if* $\kappa < 0$ *(resp.* $\kappa > 0$*) this limit cycle is locally asymptotically stable (resp. unstable).*

Proof. Assume the hypotheses (2.26) and (2.31). Then, the tangential equilibrium $\mathbf{p}$ is an asymptotically stable equilibrium of the tangential sliding vector field defined in L_I. In fact, the eigenvalue associated with the sliding vector field (one-dimensional), in original coordinates (see equation (2.32)), is

$$-c - \frac{(s - dC_T)^2 \delta \lambda \eta_{PI}}{(\delta - d)(\delta C_T - s) k \eta_{RT} V_I^2} < 0$$

for any $V_I > 0$. Moreover, $\mathbf{p}$ is the only equilibrium in L_I and therefore for any initial condition in L_I the system (2.35) evolves to $\mathbf{p}$.

Let us now determine the local dynamics at $\mathbf{p}$ from the analysis of the first return map defined in $\Sigma^{c,+} \cup \{\mathbf{p}\}$, in a neighborhood of $\mathbf{p}$. For more details on the construction and properties of first return maps in systems that exhibit fold-fold singularities such as (2.35), see references [33, 118]. We consider a linear version of system (2.35) at $\mathbf{p}$ and, in order to facilitate calculations, we take $\mathbf{p}$ at the origin of a new state space with domain $\widetilde{\mathcal{M}} = \{(\widetilde{x}, \widetilde{y}, \widetilde{z}) \in \mathbb{R}^3 : \widetilde{x}^2 + \widetilde{y}^2 + \widetilde{z}^2 < \varepsilon^2\}$ for ε^2 arbitrarily small. From this change the L_I-set of invisible two-fold points is shifted to $(0, \widetilde{y}, 0)$ and the crossing region $\Sigma^{c,+}$ becomes definite for all $(\widetilde{x}, \widetilde{y}, 0) \in \widetilde{\mathcal{M}}$ with $\widetilde{x} > 0$.

Suppose a system trajectory started at $(\widetilde{x}_0, \widetilde{y}_0, 0) \in \widetilde{\mathcal{M}}$ with $\widetilde{x}_0 > 0$. First return point $(\widetilde{x}_2, \widetilde{y}_2, 0) \in \widetilde{\mathcal{M}}$ of the trajectory to the plane $\widetilde{z} = 0$ in the part $\widetilde{x} > 0$, is obtained by the composition of half-return maps P_+ and P_- (calculated below), given by the expansions (2.53)-(2.54) and (2.58)-(2.59), respectively. Then we define the first return map by $(\widetilde{x}_2, \widetilde{y}_2) = P(\widetilde{x}_0, \widetilde{y}_0) = P_- \circ P_+(\widetilde{x}_0, \widetilde{y}_0)$, such that

$$\widetilde{x}_2 = \widetilde{x}_0 + \frac{2\mu}{3\delta \bar{x}_t} \widetilde{x}_0^2 + \widetilde{x}_0^2 \cdot \mathcal{O}(1), \tag{2.43}$$

$$\widetilde{y}_2 = \widetilde{y}_0 + v_{11} \widetilde{x}_0 \widetilde{y}_0 + v_{20}^* \widetilde{x}_0^2 + \widetilde{x}_0 \cdot \mathcal{O}(2), \tag{2.44}$$

where

$$v_{11} = -\frac{2\bar{y}_q^+}{\bar{x}_t \delta} \left[\frac{a\bar{x}_t - c\delta}{(\bar{y}_q^+ - \bar{y}_p)^2} + \frac{c\delta - a\bar{x}_t N_{PI} N_{RT}}{(\bar{y}_q^+ - N_{RT} \bar{y}_p)^2} \right] < 0, \tag{2.45}$$

since (2.26), (2.31) ensures that $\frac{c\delta}{a} < \bar{x}_t < \frac{c\delta}{aN_{PI}N_{RT}}$, and v_{20}^* are coefficients dependent on all system parameters. Note that (2.45) is calculated by $v_{11} = v_{11}^+ - v_{11}^-$ with $v_{11}^\pm$ given in (2.55) and (2.60). We do not explicit the coefficient v_{20}^* since it does not interfere in the conclusions.

In order to prove item (a) of Theorem 7, it is sufficient to consider the map (2.43)-(2.44) truncated in quadratic terms. Note from equation (2.43) that $\widetilde{x} = 0$ is attractor for $\mu < 0$ and repeller for $\mu > 0$, since $\text{sign}\,[\widetilde{x}_2 - \widetilde{x}_0] = \text{sign}\,[\mu]$. Moreover, for a given initial condition $(\widetilde{x}_0, \widetilde{y}_0, 0) \in \widetilde{\mathcal{M}}$ with $\widetilde{x}_0 > 0$, from equation (2.44) we can ensure $\text{sign}\,[\widetilde{y}_2 - \widetilde{y}_0] = \text{sign}\,[v_{11}\widetilde{y}_0]$. In this case, $\widetilde{y}_2 > \widetilde{y}_0$ if $\widetilde{y}_0 < 0$ and $\widetilde{y}_2 < \widetilde{y}_0$ if $\widetilde{y}_0 > 0$. Therefore, $\widetilde{y} = 0$ is attractor. With this we conclude that the trivial fixed point $(0,0)$ is locally asymptotically stable for $\mu < 0$, with monotonic convergence, and unstable for $\mu > 0$. This stability result is directly extended to the tangential equilibrium $\mathbf{p}$.

In order to prove item (b) of Theorem 7 we consider the half-return maps P_+ and P_-, given respectively in (2.53)-(2.54) and (2.58)-(2.59). In looking for bifurcating crossing limit cycles from $(0,0)$, we must compose the two half-return maps P_+ and P_- by forcing the equality $(P_- \circ P_+)(\widetilde{x}_0, \widetilde{y}_0) = (\widetilde{x}_0, \widetilde{y}_0)$, that is $(\widetilde{x}_2, \widetilde{y}_2) = (\widetilde{x}_0, \widetilde{y}_0)$. However, it is more direct to write the condition

$$P_+(\widetilde{x}_0, \widetilde{y}_0) = P_-^{-1}(\widetilde{x}_0, \widetilde{y}_0) = P_-(\widetilde{x}_0, \widetilde{y}_0),$$

where the second equality comes from the involution property of P_-. Thus, suppressing the subscript 0 for coordinates, rearranging terms and eliminating the trivial solutions, we obtain the equations

$$0 = \frac{2\mu}{3\delta\bar{x}_t} + p_{30}\widetilde{x}_0 + p_{21}\widetilde{y} + \begin{bmatrix}\widetilde{x} & \widetilde{y}\end{bmatrix} M \begin{bmatrix}\widetilde{x} \\ \widetilde{y}\end{bmatrix} + \mathcal{O}(3), \tag{2.46}$$

$$0 = v_{20}\widetilde{x} + v_{11}\widetilde{y} + \begin{bmatrix}\widetilde{x} & \widetilde{y}\end{bmatrix} N \begin{bmatrix}\widetilde{x} \\ \widetilde{y}\end{bmatrix} + \mathcal{O}(3), \tag{2.47}$$

where $v_{11} < 0$ is given in (2.45), matrices M and N are defined in (2.42), and other coefficients p_{ij}, v_{ij} are given in (2.55)-(2.57) and (2.60)-(2.62).

We start by considering (2.47). A standard application of the Implicit Function Theorem allows to assure the existence of a smooth function $\rho(\widetilde{x})$ such that $\widetilde{y} = \widetilde{x}\cdot\rho(\widetilde{x})$, with $\rho(0) = -\frac{v_{20}}{v_{11}}$. In this case,

$$\rho(\widetilde{x}) = -\frac{v_{20}}{v_{11}} - \frac{1}{v_{11}}\begin{bmatrix}1 & -\frac{v_{20}}{v_{11}}\end{bmatrix} N \begin{bmatrix}1 \\ -\frac{v_{20}}{v_{11}}\end{bmatrix} \widetilde{x} + \mathcal{O}(2).$$

After substituting this expression for $\widetilde{y}$ in (2.46) we get

$$0 = \frac{2\mu}{3\delta\bar{x}_t} + \theta\widetilde{x} + \kappa\widetilde{x}^2 + \mathcal{O}(3), \tag{2.48}$$

where $\theta = p_{30} - \frac{p_{21}v_{20}}{v_{11}}$ and κ is given in (2.41). In equation (2.48) all coefficients can be dependent on the μ-parameter. In particular, we have $\theta = \theta(\mu)$ such that $\theta(0) = 0$, and $\kappa = \kappa(\mu)$ such that $\kappa(0) \neq 0$. Taking this into account, we can apply the Implicit Function Theorem at $(\widetilde{x}, \mu) = (0, 0)$ to solve for μ getting that for the emanating branch we have the expansion

$$\mu = -\frac{3\delta\bar{x}_t}{2}\kappa(0)\widetilde{x}^2 + \mathcal{O}(3).$$

In short, depending on the sign of κ we have a subcritical or supercritical bifurcation of non-trivial fixed points. We are focussing our attention in the non-trivial fixed point with $\widetilde{x} > 0$, but clearly there is another one with $\widetilde{x} < 0$. Figure 2.18 shows phase portraits of the first return maps P and P^{-1}, associated with the crossing dynamics in Σ of system (2.35). We observe the occurrence of a supercritical ($\kappa < 0$) bifurcation at $\mathbf{p}$ (equivalent to the trivial fixed point in $\widetilde{\mathcal{M}}$) for $\mu = 0$.

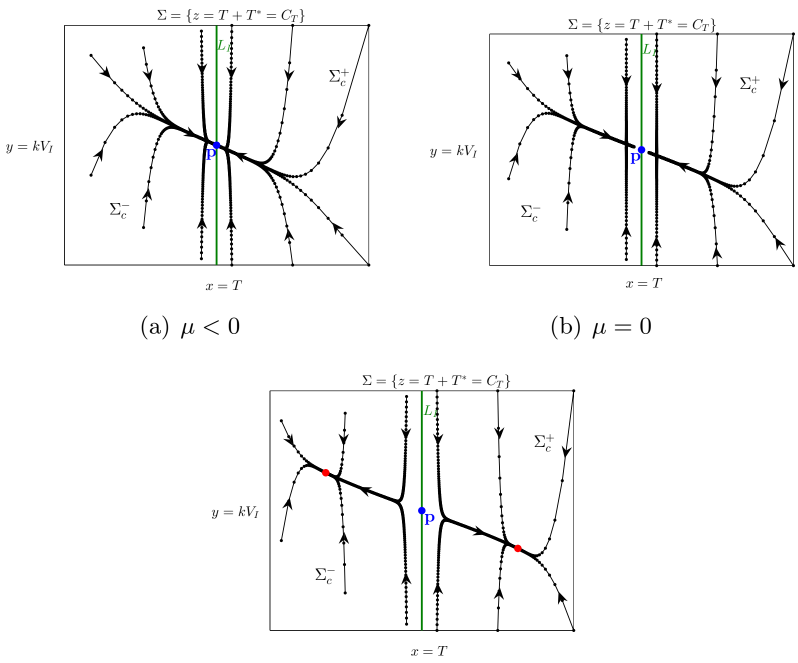

(a) $\mu < 0$ (b) $\mu = 0$

(c) $\mu > 0$

Figure 2.18: Crossing dynamics of system (2.35) in the neighborhood of the tangential equilibrium $\mathbf{p}$, supposing $\kappa < 0$.

To characterize the topological type of the non-trivial fixed point and its stability, we must compute the derivatives of the half-return maps, and evaluate them at the branch of non-trivial fixed points. Computing $DP(\widetilde{x}) = D\left(P_- \circ P_+\right)(\widetilde{x}, \widetilde{y}(\widetilde{x}))$, we get that the expansions for its determinant and trace share the coefficient of the terms of first, second and third degree, namely

$$\begin{aligned} \det DP(\widetilde{x}) &= 1 + v_{11}\widetilde{x} + d_2\widetilde{x}^2 + d_3\widetilde{x}^3 + d_4\widetilde{x}^4 + O(5), \\ \operatorname{trace} DP(\widetilde{x}) &= 2 + v_{11}\widetilde{x} + d_2\widetilde{x}^2 + d_3\widetilde{x}^3 + t_4\widetilde{x}^4 + O(5). \end{aligned} \tag{2.49}$$

Furthermore, it turns out that $t_4 - d_4 = -3\delta\bar{x}_t v_{11}\kappa$. Recall that given linear two dimensional discrete system, if the spectral radius, that is, the largest absolute value of its eigenvalues, is less than one then the fixed point is asymptotically stable (see [45, 126]). So, the standard stability conditions for fixed points of maps in $\mathbb{R}^2$ are

(i) $|\det DP| < 1$, and

(ii) $|\operatorname{trace} DP| < \det DP + 1$

at the fixed point. Since $v_{11} < 0$ and $\widetilde{x} > 0$, from (2.49) it is proved that (i) is satisfied. In order to check item (ii), we get

$$1 + (t_4 - d_4)\widetilde{x}^4 + O(5) = 1 - 3\delta\bar{x}_t v_{11}\kappa\widetilde{x}^4 + O(5) < 1,$$

which requires $\kappa < 0$. Therefore, we conclude that the non-trivial fixed point is locally asymptotically stable if $\kappa < 0$, with monotonic convergence (since $(\operatorname{trace} DP)^2 - 4(\det DP) \approx v_{11}^2\widetilde{x}^2 > 0$), and unstable if $\kappa > 0$. This stability result is directly extended to the limit cycle that crosses Σ at the non-trivial fixed points, as shown in Figure 2.19.

□

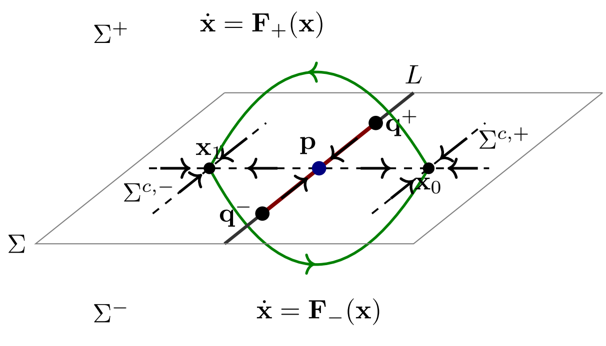

Figure 2.19: If $\kappa < 0$ then a stable crossing limit cycle appears along with unstable tangential equilibrium ($\mathbf{p}$) for $\mu > 0$. Points $\mathbf{x}_0$ and $\mathbf{x}_1$ represent the non-trivial fixed points of map P defined in $\Sigma^{c,+} \cup \{\mathbf{p}\}$ and P^{-1} defined in $\Sigma^{c,-} \cup \{\mathbf{p}\}$, respectively. The tangential equilibrium $\mathbf{p}$ is a trivial fixed point of both maps P and P^{-1}.

In order to compute the half-return maps used in the proof of Theorem 7, we consider a trajectory of system (2.35) initiated at the point $\mathbf{x}_0 = (x_0, y_0, 0) \in \Sigma^{c,+}$ such that for $t =$

$t_1 > 0$ this trajectory transversally returns to Σ at the point $\mathbf{x}_1 = (x_1, y_1, 0) \in \Sigma^{c,-}$. And its continuation from the point $\mathbf{x}_1$ such that for $t = t_2 > 0$ this trajectory transversally returns to Σ at the point $\mathbf{x}_2 = (x_2, y_2, 0) \in \Sigma^{c,+}$. See illustration in Figure 2.20. Then we define the half-return maps $(x_1, y_1) = P_+(x_0, y_0)$ and $(x_2, y_2) = P_-(x_1, y_1)$.

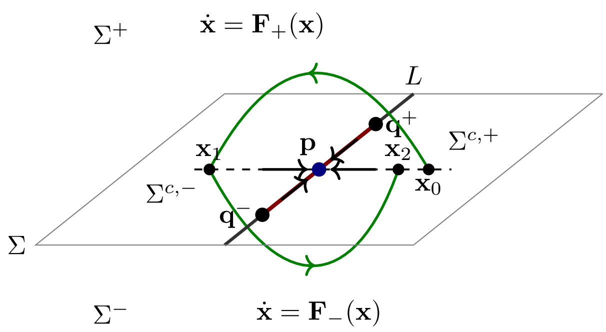

Figure 2.20: First return application in $\Sigma^{c,+}$.

In order to find the explicit expressions for the coefficients of each half-return map, we must determine the solution of system (2.35) for $\widetilde{z} = z - C_T \geq 0$ and for $\widetilde{z} = z - C_T \leq 0$. Such solution for $\widetilde{z} \geq 0$ can be obtained from the variation of constants formula

$$\widetilde{\mathbf{x}}(t) = e^{A^+ t}\widetilde{\mathbf{x}}_0 + \int_0^t e^{A^+(t-s)}\mathbf{v}^+ ds = e^{A^+ t}\widetilde{\mathbf{x}}_0 + \left(\int_0^t e^{A^+ s} ds\right)\mathbf{v}^+, \tag{2.50}$$

where

$$A^+ = \begin{bmatrix} -d - \bar{y}_p & -\bar{x}_t & 0 \\ -a & -c & a \\ \delta - d & 0 & -\delta \end{bmatrix}, \quad \widetilde{\mathbf{x}}_0 = \begin{bmatrix} \widetilde{x}_0 \\ \widetilde{y}_0 \\ 0 \end{bmatrix}, \quad \mathbf{v}^+ = \begin{bmatrix} \bar{x}_t(\bar{y}_q^+ - \bar{y}_p) \\ \frac{a\bar{x}_t\bar{y}_q^+}{\delta} - c\bar{y}_p \\ 0 \end{bmatrix},$$

and

$$\widetilde{\mathbf{x}}(t) = \begin{bmatrix} \widetilde{x}(t) \\ \widetilde{y}(t) \\ \widetilde{z}(t) \end{bmatrix} = \begin{bmatrix} x(t) - \bar{x}_t \\ y(t) - \bar{y}_p \\ z(t) - C_T \end{bmatrix},$$

being $\widetilde{x}_0 \geq 0$, $A^+ = D\mathbf{F}_+(\bar{x}_t, \bar{y}_p, C_T)$, $\mathbf{v}^+ = \mathbf{F}_+(\bar{x}_t, \bar{y}_p, C_T)$. For simplicity we take $C_T = \frac{\bar{x}_t\bar{y}_q^+}{\delta} + \bar{x}_t$ and $s = \bar{x}_t\left(d + \bar{y}_q^+\right)$. It will suffice to have the Taylor's series approximation until the sixth order terms for (2.50), namely

$$\widetilde{\mathbf{x}}(t) = \widetilde{\mathbf{x}}_0 + \left(tI + \frac{t^2}{2}A^+ + \frac{t^3}{6}(A^+)^2 + \frac{t^4}{24}(A^+)^3 + \frac{t^5}{5!}(A^+)^4 + \frac{t^6}{6!}(A^+)^5\right)M + O\left(t^7\right), \tag{2.51}$$

where $M = A^+\widetilde{\mathbf{x}}_0 + \mathbf{v}^+$ and I is the identity matrix of order 3.

Remark 6. *Note that solution* (2.51) *refers to system* (2.35) *linearized at the tangential equilibrium point* $\mathbf{p}$ *(given in* (2.38)*) with* $\mathbf{p}$ *moved to the origin of a new state space* $\widetilde{\mathcal{M}} = \{(\widetilde{x}, \widetilde{y}, \widetilde{z}) \in \mathbb{R}^3 : \widetilde{x}^2 + \widetilde{y}^2 + \widetilde{z}^2 < \varepsilon^2\}$ *for* ε^2 *arbitrarily small. With this change the set* L_I *of invisible two-folds is moved to* $(0, \widetilde{y}, 0)$ *and the crossing regions* $\Sigma^{c,+}$ *and* $\Sigma^{c,-}$ *are redefined for all* $(\widetilde{x}, \widetilde{y}, 0)$ *with* $\widetilde{x} > 0$ *and* $\widetilde{x} < 0$*, respectively.*

From the third component of (2.51) we can determine an expression for the half-return time $t_+ = t_+(\widetilde{x}_0, \widetilde{y}_0)$, which depends on $(\widetilde{x}_0, \widetilde{y}_0)$ and such that $\widetilde{z}(t_+) = 0$. The polynomial approximation for the time t_+ is given by

$$t_+(\widetilde{x}_0, \widetilde{y}_0) = \widetilde{x}_0 \cdot \Phi(\widetilde{x}_0, \widetilde{y}_0), \tag{2.52}$$

where $\Phi(0,0) = \frac{2}{\bar{x}_t(\bar{y}_p - \bar{y}_q^+)} > 0$. For our purpose, we must compute all the coefficients of the polynomial $\Phi(\widetilde{x}_0, \widetilde{y}_0)$ up to the fourth order terms. Some of these coefficients are very large expressions and therefore we do not make them explicit.

Now, substituting (2.52) in the first and the second component of (2.51), the half-return map $(\widetilde{x}_1, \widetilde{y}_1) = P_+(\widetilde{x}_0, \widetilde{y}_0)$ satisfies

$$\widetilde{x}_1 = -\widetilde{x}_0 + p_{20}^+\widetilde{x}_0^2 + p_{30}^+\widetilde{x}_0^3 + p_{21}^+\widetilde{x}_0^2\widetilde{y}_0 + p_{40}^+\widetilde{x}_0^4 + p_{31}^+\widetilde{x}_0^3\widetilde{y}_0 + p_{22}^+\widetilde{x}_0^2\widetilde{y}_0^2 + \widetilde{x}_0^2 \cdot O(3), \tag{2.53}$$

$$\widetilde{y}_1 = v_{10}^+\widetilde{x}_0 + \widetilde{y}_0 + v_{11}^+\widetilde{x}_0\widetilde{y}_0 + v_{20}^+\widetilde{x}_0^2 + v_{30}^+\widetilde{x}_0^3 + v_{21}^+\widetilde{x}_0^2\widetilde{y}_0 + v_{12}^+\widetilde{x}_0\widetilde{y}_0^2 + \widetilde{x}_0 \cdot O(3), \tag{2.54}$$

with coefficients of the quadratic terms given by

$$\begin{aligned}
p_{20}^+ &= \frac{\delta\left[c\bar{y}_p + (\bar{y}_p - \bar{y}_q^+)(d + \delta + \bar{y}_p)\right] - a\bar{x}_t\bar{y}_q^+}{3/2\bar{x}_t\delta(\bar{y}_q^+ - \bar{y}_p)^2}, \\
v_{10}^+ &= \frac{2(a\bar{x}_t\bar{y}_q^+ - c\delta\bar{y}_p)}{\bar{x}_t\delta(\bar{y}_p - \bar{y}_q^+)}, \\
v_{11}^+ &= \frac{2\bar{y}_q^+(c\delta - a\bar{x}_t)}{\bar{x}_t\delta(\bar{y}_p - \bar{y}_q^+)^2}, \\
v_{20}^+ &= \frac{2(a\bar{x}_t\bar{y}_q^+ - c\delta\bar{y}_p)(2a\bar{x}_t\bar{y}_q^+ + \delta[c(\bar{y}_p - 3\bar{y}_q^+) + (\bar{y}_p - \bar{y}_q^+)(d + \delta + \bar{y}_p)])}{3\bar{x}_t^2\delta^2(\bar{y}_q^+ - \bar{y}_p)^3},
\end{aligned} \tag{2.55}$$

the coefficients of the cubic terms given by

$$
\begin{aligned}
p_{21}^{+} &= \frac{\delta\left[c(\bar{y}_p+\bar{y}_q^{+})+(\bar{y}_p-\bar{y}_q^{+})(d+\delta+\bar{y}_p)\right]-2a\bar{x}_t\bar{y}_q^{+}}{3/2\bar{x}_t\delta(\bar{y}_q^{+}-\bar{y}_p)^3},\\
p_{30}^{+} &= \frac{2}{9\delta^2\bar{x}_t^2(\bar{y}_q^{+}-\bar{y}_p)^4}\left(4a^2\bar{x}_t^2(\bar{y}_q^{+})^2-a\delta\bar{x}_t\bar{y}_q^{+}\left[c(3\bar{y}_q^{+}+5\bar{y}_p)+(\bar{y}_q^{+}-\bar{y}_p)(d+\delta+\bar{y}_p)\right]+\right.\\
&\quad -\delta^2\left[c^2(-\bar{y}_p)(3\bar{y}_q^{+}+\bar{y}_p)+d(\bar{y}_q^{+}-\bar{y}_p)(4(\bar{y}_q^{+}-\bar{y}_p)(\delta+\bar{y}_p)-c\bar{y}_p)-c\bar{y}_p(\bar{y}_q^{+}-\bar{y}_p)(\delta+\bar{y}_p)+\right.\\
&\quad \left.\left.+2d^2(\bar{y}_q^{+}-\bar{y}_p)^2+2(\bar{y}_q^{+}-\bar{y}_p)^2(\delta+\bar{y}_p)^2\right]\right),\\
v_{30}^{+} &= \frac{-2}{9\delta^3\bar{x}_t^3(\bar{y}_q^{+}-\bar{y}_p)^5}\left(8a^3\bar{x}_t^3(\bar{y}_q^{+})^3-a^2\delta\bar{x}_t^2\bar{y}_q^{+}(3c\bar{y}_q^{+}(5\bar{y}_q^{+}+3\bar{y}_p)+(\bar{y}_q^{+}-\bar{y}_p)(5\bar{y}_q^{+}(d+\bar{y}_p)+\right.\\
&\quad +\delta(2\bar{y}_q^{+}+3\bar{y}_p)))+a\delta^2\bar{x}_t\left(6c^2(\bar{y}_q^{+})^2(\bar{y}_q^{+}+3\bar{y}_p)+c\bar{y}_q^{+}(\bar{y}_q^{+}-\bar{y}_p)(2(d+\bar{y}_p)(3\bar{y}_q^{+}+2\bar{y}_p)+\right.\\
&\quad \left.+\delta(3\bar{y}_q^{+}+7\bar{y}_p))+(\bar{y}_q^{+}-\bar{y}_p)^2\left(\delta(4d\bar{y}_q^{+}-3d\bar{y}_p+\bar{y}_q^{+}\bar{y}_p)+2\bar{y}_q^{+}(d+\bar{y}_p)^2+2\delta^2\bar{y}_q^{+}\right)\right)+\\
&\quad +c\delta^3\bar{y}_p\left(c^2\left(-6(\bar{y}_q^{+})^2-3\bar{y}_q^{+}\bar{y}_p+\bar{y}_p^2\right)-c\left(6(\bar{y}_q^{+})^2-7\bar{y}_q^{+}\bar{y}_p+\bar{y}_p^2\right)(d+\delta+\bar{y}_p)+\right.\\
&\quad \left.\left.-(\bar{y}_q^{+}-\bar{y}_p)^2\left(2\delta^2+\delta(d+\bar{y}_p)+2(d+\bar{y}_p)^2\right)\right)\right),\\
v_{21}^{+} &= \frac{2}{3\delta^2\bar{x}_t^2(\bar{y}_q^{+}-\bar{y}_p)^4}\left(6a^2\bar{x}_t^2(\bar{y}_q^{+})^2-2a\delta\bar{x}_t\bar{y}_q^{+}\left[c(5\bar{y}_q^{+}+\bar{y}_p)+(\bar{y}_q^{+}-\bar{y}_p)(d+\delta+\bar{y}_p)\right]+\right.\\
&\quad \left.+c\delta^2\left[c\left(3(\bar{y}_q^{+})^2+4\bar{y}_q^{+}\bar{y}_p-\bar{y}_p^2\right)+((\bar{y}_q^{+})^2-\bar{y}_p^2)(d+\delta+\bar{y}_p)\right]\right),\\
v_{12}^{+} &= \frac{2\bar{y}_q^{+}(c\delta-a\bar{x}_t)}{\delta\bar{x}_t(\bar{y}_q^{+}-\bar{y}_p)^3},
\end{aligned}
\tag{2.56}
$$

and the coefficients of the fourth order terms of the first equation are given by

$$
\begin{aligned}
p_{31}^{+} = {} & \frac{2}{9\delta^2\bar{x}_t^2(\bar{y}_q^+-\bar{y}_p)^5}\left(16a^2\bar{x}_t^2(\bar{y}_q^+)^2 - a\delta\bar{x}_t\bar{y}_q^+\left[c(17\bar{y}_q^+ + 15\bar{y}_p) + 3(\bar{y}_q^+-\bar{y}_p)(d+\delta+\bar{y}_p)\right] + \right. \\
& + \delta^2\left[c^2\left(3(\bar{y}_q^+)^2 + 11\bar{y}_q^+\bar{y}_p + 2\bar{y}_p^2\right) + c(\bar{y}_q^+-\bar{y}_p)(\bar{y}_q^+ + 2\bar{y}_p)(d+\delta+\bar{y}_p) - \right. \\
& \left.\left. -4(\bar{y}_q^+-\bar{y}_p)^2(d+\delta+\bar{y}_p)^2\right]\right), \\
p_{22}^{+} = {} & \frac{\delta\left[c(2\bar{y}_q^+ + \bar{y}_p) - (\bar{y}_q^+-\bar{y}_p)(d+\delta+\bar{y}_p)\right] - 3a\bar{x}_t\bar{y}_q^+}{3/2\delta\bar{x}_t(\bar{y}_q^+-\bar{y}_p)^4}, \\
p_{40}^{+} = {} & \frac{-2}{135\delta^3\bar{x}_t^3(\bar{y}_q^+-\bar{y}_p)^6}\left(100a^3\bar{x}_t^3(\bar{y}_q^+)^3 - 3a^2\delta\bar{x}_t^2\bar{y}_q^+(20c\bar{y}_q^+(2\bar{y}_q^+ + 3\bar{y}_p) + (\bar{y}_q^+-\bar{y}_p)\cdot\right. \\
& \cdot(20\bar{y}_q^+(d+\bar{y}_p) + \delta(11\bar{y}_q^+ + 9\bar{y}_p))) + 3a\delta^2\bar{x}_t(c^2\bar{y}_q^+\left(9(\bar{y}_q^+)^2 + 62\bar{y}_q^+\bar{y}_p + 29\bar{y}_p^2\right) + \\
& + c(\bar{y}_q^+-\bar{y}_p)(2\bar{y}_q^+(d+\bar{y}_p)(7\bar{y}_q^+ + 13\bar{y}_p) + \delta(8(\bar{y}_q^+)^2 + 29\bar{y}_q^+\bar{y}_p + 3\bar{y}_p^2)) - \\
& -(\bar{y}_q^+-\bar{y}_p)^2(\delta(2d\bar{y}_q^+ + 9d\bar{y}_p + 8\bar{y}_q^+\bar{y}_p + 3\bar{y}_p^2) + \bar{y}_q^+(d+\bar{y}_p)^2 + \delta^2(3\bar{y}_p - 2\bar{y}_q^+))) + \\
& + \delta^3(c^3(-\bar{y}_p)(9\bar{y}_q^+ + \bar{y}_p)(3\bar{y}_q^+ + 7\bar{y}_p) + 3d(\bar{y}_q^+-\bar{y}_p)(-2c^2\bar{y}_p(7\bar{y}_q^+ + 3\bar{y}_p) + \\
& + c\bar{y}_p(\bar{y}_q^+-\bar{y}_p)(11\delta + 2\bar{y}_p) + (\bar{y}_q^+-\bar{y}_p)^2(19\delta^2 + 22\bar{y}_p^2 + 38\delta\bar{y}_p)) - \\
& -6c^2\bar{y}_p(\bar{y}_q^+-\bar{y}_p)(7\bar{y}_q^+ + 3\bar{y}_p)(\delta+\bar{y}_p) + 3d^2(\bar{y}_q^+-\bar{y}_p)^2(c\bar{y}_p + (\bar{y}_q^+-\bar{y}_p)(19\delta + 22\bar{y}_p)) + \\
& + 3c\bar{y}_p(\bar{y}_q^+-\bar{y}_p)^2(\delta^2 + \bar{y}_p^2 + 11\delta\bar{y}_p) + 22d^3(\bar{y}_q^+-\bar{y}_p)^3 \\
& \left. + (\bar{y}_q^+-\bar{y}_p)^3(\delta+\bar{y}_p)(22\delta^2 + 22\bar{y}_p^2 + 35\delta\bar{y}_p))\right).
\end{aligned}
\tag{2.57}
$$

The computations for the map P_- are totally similar. We use again the formula given in (2.50), this time with

$$
A^- = \begin{bmatrix} -d - N_{RT}\bar{y}_p & -N_{RT}\bar{x}_t & 0 \\ -N_{PI}a & -c & N_{PI}a \\ \delta - d & 0 & -\delta \end{bmatrix}, \quad \widetilde{\mathbf{x}}_1 = \begin{bmatrix} \widetilde{x}_1 \\ \widetilde{y}_1 \\ 0 \end{bmatrix}, \quad \mathbf{v}^- = \begin{bmatrix} \bar{x}_t(\bar{y}_q^+ - N_{RT}\bar{y}_p) \\ \frac{a\bar{x}_t\bar{y}_q^+N_{PI}}{\delta} - c\bar{y}_p \\ 0 \end{bmatrix},
$$

being $\widetilde{x}_1 \leq 0$, $A^- = D\mathbf{F}_-(\bar{x}_t, \bar{y}_p, C_T)$ and $\mathbf{v}^- = \mathbf{F}_-(\bar{x}_t, \bar{y}_p, C_T)$. We compute the approximation up to fifth order of the half-return time $t_- = t_-(\widetilde{x}_1, \widetilde{y}_1)$. This is done by solving the equation $\widetilde{z}(t_-) = 0$ so that, after the evaluation at such a time for the other two coordinates of the solution, we determine the image of the half-return map $(\widetilde{x}_2, \widetilde{y}_2) = P_{-}(\widetilde{x}_1, \widetilde{y}_1)$, namely

$$\widetilde{x}_2 = -\widetilde{x}_1 + p_{20}^{-}\widetilde{x}_1^2 + p_{30}^{-}\widetilde{x}_1^3 + p_{21}^{-}\widetilde{x}_1^2\widetilde{y}_1 + p_{40}^{-}\widetilde{x}_1^4 + p_{31}^{-}\widetilde{x}_1^3\widetilde{y}_1 + p_{22}^{-}\widetilde{x}_1^2\widetilde{y}_1^2 + \widetilde{x}_1^2 \cdot O(3), \tag{2.58}$$

$$\widetilde{y}_2 = v_{10}^{-}\widetilde{x}_1 + \widetilde{y}_1 + v_{11}^{-}\widetilde{x}_1\widetilde{y}_1 + v_{20}^{-}\widetilde{x}_1^2 + v_{30}^{-}\widetilde{x}_1^3 + v_{21}^{-}\widetilde{x}_1^2\widetilde{y}_1 + v_{12}^{-}\widetilde{x}_1\widetilde{y}_1^2 + \widetilde{x}_1 \cdot O(3), \tag{2.59}$$

with coefficients of the quadratic terms given by

$$\begin{aligned}
p_{20}^{-} &= \frac{\delta\left[c\bar{y}_p + (\bar{y}_p - \bar{y}_q^{-})(d + \delta + N_{RT}\bar{y}_p)\right] - a\bar{x}_t\bar{y}_q^{-}N_{PI}N_{RT}}{3/2\bar{x}_t\delta(\bar{y}_q^{-} - \bar{y}_p)^2N_{RT}},\\
v_{10}^{-} &= \frac{2\left(\frac{c\delta}{N_{RT}}\bar{y}_p - a\bar{x}_t\bar{y}_q^{-}N_{PI}\right)}{\bar{x}_t\delta(\bar{y}_q^{-} - \bar{y}_p)},\\
v_{11}^{-} &= \frac{2\bar{y}_q^{-}(c\delta - a\bar{x}_tN_{PI}N_{RT})}{\bar{x}_t\delta(\bar{y}_q^{-} - \bar{y}_p)^2N_{RT}},\\
v_{20}^{-} &= \frac{2(aN_{PI}N_{RT}\bar{x}_t\bar{y}_q^{-} - c\delta\bar{y}_p)(2aN_{PI}N_{RT}\bar{x}_t\bar{y}_q^{-} + \delta[c(\bar{y}_p - 3\bar{y}_q^{-}) + (\bar{y}_p - \bar{y}_q^{-})(d + \delta + N_{RT}\bar{y}_p)])}{3\bar{x}_t^2\delta^2(\bar{y}_q^{-} - \bar{y}_p)^3N_{RT}^2}
\end{aligned} \tag{2.60}$$

and coefficients of the cubic terms given by

$$\begin{aligned}
p_{21}^{-} &= \frac{\delta\left[c(\bar{y}_p + \bar{y}_q^{-}) + (\bar{y}_p - \bar{y}_q^{-})(d + \delta + N_{RT}\bar{y}_p)\right] - 2a\bar{x}_t\bar{y}_q^{-}N_{PI}}{3/2\bar{x}_t\delta(\bar{y}_q^{-} - \bar{y}_p)^3N_{RT}},\\
p_{30}^{-} &= \frac{2}{9\delta^2N_{RT}^2\bar{x}_t^2(\bar{y}_q^{-} - \bar{y}_p)^4}\left(4a^2N_{PI}^2N_{RT}^2\bar{x}_t^2(\bar{y}_q^{-})^2 - a\delta N_{PI}N_{RT}\bar{x}_t\bar{y}_q^{-}(c(3\bar{y}_q^{-} + 5\bar{y}_p)+\right.\\
&\quad +(\bar{y}_q^{-} - \bar{y}_p)(d + \delta + N_{RT}\bar{y}_p)) - \delta^2\left(-c^2\bar{y}_p(3\bar{y}_q^{-} + \bar{y}_p) + d(\bar{y}_p - \bar{y}_q^{-})(c\bar{y}_p - 4(\bar{y}_q^{-} - \bar{y}_p)\right.\\
&\quad \left.\left.(\delta + N_{RT}\bar{y}_p)) + c\bar{y}_p(\bar{y}_p - \bar{y}_q^{-})(\delta + N_{RT}\bar{y}_p) + 2d^2(\bar{y}_q^{-} - \bar{y}_p)^2 + 2(\bar{y}_q^{-} - \bar{y}_p)^2(\delta + N_{RT}\bar{y}_p)^2\right)\right),\\
v_{30}^{-} &= \frac{-2}{9\delta^3N_{RT}^3\bar{x}_t^3(\bar{y}_q^{-} - \bar{y}_p)^5}\left(8a^3N_{PI}^3N_{RT}^3\bar{x}_t^3(\bar{y}_q^{-})^3 - a^2\delta N_{PI}^2N_{RT}^2\bar{x}_t^2\bar{y}_q^{-}(3c\bar{y}_q^{-}(5\bar{y}_q^{-} + 3\bar{y}_p)+\right.\\
&\quad +(\bar{y}_q^{-} - \bar{y}_p)(5d\bar{y}_q^{-} + 5N_{RT}\bar{y}_q^{-}\bar{y}_p + 2\delta\bar{y}_q^{-} + 3\delta\bar{y}_p)) + a\delta^2N_{PI}N_{RT}\bar{x}_t\left(6c^2(\bar{y}_q^{-})^2(\bar{y}_q^{-} + 3\bar{y}_p)+\right.\\
&\quad +c\bar{y}_q^{-}(\bar{y}_q^{-} - \bar{y}_p)(2(3\bar{y}_q^{-} + 2\bar{y}_p)(d + N_{RT}\bar{y}_p) + \delta(3\bar{y}_q^{-} + 7\bar{y}_p)) + (\bar{y}_q^{-} - \bar{y}_p)^2\left(\delta(4d\bar{y}_q^{-}-\right.\\
&\quad \left.\left.-3d\bar{y}_p + N_{RT}\bar{y}_q^{-}\bar{y}_p) + 2\bar{y}_q^{-}(d + N_{RT}\bar{y}_p)^2 + 2\delta^2\bar{y}_q^{-}\right)\right) + c\delta^3\bar{y}_p\left(c^2\left(-6(\bar{y}_q^{-})^2 - 3\bar{y}_q^{-}\bar{y}_p + \bar{y}_p^2\right)+\right.\\
&\quad -c\left(6(\bar{y}_q^{-})^2 - 7\bar{y}_q^{-}\bar{y}_p + \bar{y}_p^2\right)(d + \delta + N_{RT}\bar{y}_p)-\\
&\quad \left.\left.-(\bar{y}_q^{-} - \bar{y}_p)^2\left(2\delta^2 + \delta(d + N_{RT}\bar{y}_p) + 2(d + N_{RT}\bar{y}_p)^2\right)\right)\right),
\end{aligned} \tag{2.61}$$

$$v_{21}^{-} = \frac{2}{3\delta^2 N_{RT}^2 \bar{x}_t^2 (\bar{y}_q^- - \bar{y}_p)^4} \left(6a^2 N_{PI}^2 N_{RT}^2 \bar{x}_t^2 (\bar{y}_q^-)^2 - 2a\delta N_{PI} N_{RT} \bar{x}_t \bar{y}_q^- (c(5\bar{y}_q^- + \bar{y}_p) + (\bar{y}_q^- - \bar{y}_p)\cdot\right.$$

$$\left.\cdot(d+\delta+N_{RT}\bar{y}_p)) + c\delta^2 \left(c\left(3(\bar{y}_q^-)^2 + 4\bar{y}_q^-\bar{y}_p - \bar{y}_p^2\right) + (\bar{y}_q^- - \bar{y}_p)(\bar{y}_q^- + \bar{y}_p)(d+\delta+N_{RT}\bar{y}_p)\right)\right),$$

$$v_{12}^{-} = \frac{2\bar{y}_q^-(c\delta - aN_{PI}N_{RT}\bar{x}_t)}{\delta N_{RT}\bar{x}_t(\bar{y}_q^- - \bar{y}_p)^3}.$$

Also, the coefficients of the fourth order terms of the first equation are given by

$$p_{31}^{-} = \frac{2}{9\delta^2 N_{RT}^2 \bar{x}_t^2 (\bar{y}_q^- - \bar{y}_p)^5} \left(16a^2 N_{PI}^2 N_{RT}^2 \bar{x}_t^2 (\bar{y}_q^-)^2 - a\delta N_{PI} N_{RT} \bar{x}_t \bar{y}_q^- (c(17\bar{y}_q^- + 15\bar{y}_p) + \right.$$

$$+3(\bar{y}_q^- - \bar{y}_p)(d+\delta+N_{RT}\bar{y}_p)) + \delta^2 \left(c^2\left(3(\bar{y}_q^-)^2 + 11\bar{y}_q^-\bar{y}_p + 2\bar{y}_p^2\right) + \right.$$

$$\left.\left. + c(\bar{y}_q^- - \bar{y}_p)(\bar{y}_q^- + 2\bar{y}_p)(d+\delta+N_{RT}\bar{y}_p) - 4(\bar{y}_q^- - \bar{y}_p)^2(d+\delta+N_{RT}\bar{y}_p)^2\right)\right),$$

$$p_{22}^{-} = \frac{\delta\left[c(2\bar{y}_q^- + \bar{y}_p) - (\bar{y}_q^- - \bar{y}_p)(d+\delta+N_{RT}\bar{y}_p)\right] - 3aN_{PI}N_{RT}\bar{x}_t\bar{y}_q^-}{3/2\delta N_{RT}\bar{x}_t(\bar{y}_q^- - \bar{y}_p)^4},$$

$$p_{40}^{-} = \frac{-2}{135\delta^3 N_{RT}^3 \bar{x}_t^3 (\bar{y}_q^- - \bar{y}_p)^6} \left(100a^3 N_{PI}^3 N_{RT}^3 \bar{x}_t^3 (\bar{y}_q^-)^3 - 3a^2\delta N_{PI}^2 N_{RT}^2 \bar{x}_t^2 \bar{y}_q^- (20c\bar{y}_q^-(2\bar{y}_q^- + 3\bar{y}_p) + \right.$$

$$+(\bar{y}_q^- - \bar{y}_p)(20\bar{y}_q^-(d+N_{RT}\bar{y}_p) + \delta(11\bar{y}_q^- + 9\bar{y}_p)))$$

$$-3a\delta^2 N_{PI} N_{RT} \bar{x}_t \left(-c^2\bar{y}_q^-\left(9(\bar{y}_q^-)^2 + 62\bar{y}_q^-\bar{y}_p + 29\bar{y}_p^2\right) + \right.$$

$$+c(-(\bar{y}_q^- - \bar{y}_p))\left(2\bar{y}_q^-(7\bar{y}_q^- + 13\bar{y}_p)(d+N_{RT}\bar{y}_p) + \delta\left(8(\bar{y}_q^-)^2 + 29\bar{y}_q^-\bar{y}_p + 3\bar{y}_p^2\right)\right) +$$

$$\left. +(\bar{y}_q^- - \bar{y}_p)^2\left(\delta(d(2\bar{y}_q^- + 9\bar{y}_p) + N_{RT}\bar{y}_p(8\bar{y}_q^- + 3\bar{y}_p)) + \bar{y}_q^-(d+N_{RT}\bar{y}_p)^2 + \delta^2(3\bar{y}_p - 2\bar{y}_q^-)\right)\right) +$$

$$+\delta^3\left(c^3(-\bar{y}_p)(9\bar{y}_q^- + \bar{y}_p)(3\bar{y}_q^- + 7\bar{y}_p) + 3d(\bar{y}_q^- - \bar{y}_p)\left(-2c^2\bar{y}_p(7\bar{y}_q^- + 3\bar{y}_p) + \right.\right.$$

$$\left. +c\bar{y}_p(\bar{y}_q^- - \bar{y}_p)(11\delta + 2N_{RT}\bar{y}_p) + (\bar{y}_q^- - \bar{y}_p)^2\left(19\delta^2 + 22N_{RT}^2\bar{y}_p^2 + 38\delta N_{RT}\bar{y}_p\right)\right) +$$

$$-6c^2\bar{y}_p(\bar{y}_q^- - \bar{y}_p)(7\bar{y}_q^- + 3\bar{y}_p)(\delta + N_{RT}\bar{y}_p) + 3d^2(\bar{y}_q^- - \bar{y}_p)^2(c\bar{y}_p + (\bar{y}_q^- - \bar{y}_p)(19\delta + 22N_{RT}\bar{y}_p))$$

$$+3c\bar{y}_p(\bar{y}_q^- - \bar{y}_p)^2\left(\delta^2 + N_{RT}^2\bar{y}_p^2 + 11\delta N_{RT}\bar{y}_p\right) +$$

$$\left.\left. +22d^3(\bar{y}_q^- - \bar{y}_p)^3 + (\bar{y}_q^- - \bar{y}_p)^3(\delta + N_{RT}\bar{y}_p)\left(22\delta^2 + 22N_{RT}^2\bar{y}_p^2 + 35\delta N_{RT}\bar{y}_p\right)\right)\right). \tag{2.62}$$

Remark 7. *Substituting* (2.39) *in* v_{10}^{-} *and* v_{10}^{+}*, we prove that* $v_{10}^{-} = v_{10}^{+}$*. Although in the half-return maps* P_- *and* P_+ *we have not given the coefficients of the fifth order terms of the first equation and the fourth and fifth order terms of the second equation, such coefficients can be calculated since it appear in terms of the third and fourth order of the determinant and trace* *given in* (2.49). *We prefer not to show such coefficients since they are not necessary for the conclusion of this study.*

2.3 Shilnikov orbit and chaos in prey switching model

Recently, a piecewise smooth system was derived as a model of a 1 predator-2 prey interaction where the predator feeds adaptively on its preferred prey and an alternative prey. In such a model, strong evidence of chaotic behavior was numerically found. Here, we revisit this model and prove the existence of a Shilnikov sliding connection when the parameters are taken in a codimension one submanifold of the parameter space. As a consequence of this connection, we conclude that the model behaves chaotically for an open region of the parameter space. The content of this chapter can be found in [56].

2.3.1 The prey switching model

In ecology, prey switching refers to a predator's adaptive change of habitat or diet in response to prey abundance and has been observed in many predator species [2, 49, 61, 123]. Roughly speaking, a predator is said to be switching between prey species if the number of attacks upon a species is disproportionately large when the species is abundant relative to other prey, and disproportionately small when the species is relatively rare [91, 123]. Switching in predators is often related to stabilizing mechanisms of prey populations and is a possible explanation for coexistence [1, 78]. Intuitively, predators tend to feed most heavily upon the most abundant prey species. As this prey species declines the predator "switches" the major fraction of its attacks to another prey, which has become the most abundant. In this way, no prey population is drastically reduced nor becomes very abundant [91].

Using the principle of optimal foraging [111], Piltz et al. in the work [99] have modeled a 1 predator-2 prey interaction as a piecewise dynamical system. It is assumed that the predator instantaneously switches its food preference according to the availability of preys in the environment. This sudden change in the food preference of the predator induces discontinuities in the mathematical model used to describe such behavior.

Piltz et al. [99] found evidence that for a given choice of parameters their model exhibits chaotic behavior. Roughly speaking, chaotic behavior can be understood as the existence of an invariant set for which the dynamics is topologically transitive, sensitive to initial conditions, and have dense periodic points (see Definition 12). For the biological model in question, chaotic behavior means that for a given initial condition of population density of the species involved one cannot estimate even vaguely its long-term evolution. Hence, knowledge of chaotic behavior in a specific ecological model is of major importance, particularly, for experimentalists who need to be aware of potential implications of chaos for long-term predictions.

For smooth dynamical systems, chaotic behavior may be tracked by studying the existence of objects previously known as being chaotic. This is the case of a *Shilnikov homoclinic orbit*, which is a trajectory connecting a hyperbolic saddle-focus equilibrium to itself, bi-asymptotically (see, for instance, [103, 104, 122]).

In the Filippov context, pseudo-equilibria are special points on the discontinuous manifold that must be distinguished and treated as typical singularities (see [47, 62]). These singularities give rise to the definition of the *sliding Shilnikov orbit* (see Definition 15), which is a trajectory in the Filippov sense connecting a hyperbolic pseudo saddle-focus to itself in an infinity time at least by one side, forward or backward. This object has been first considered in [94], where some of their properties were studied. In particular, it was proved the existence of infinitely many sliding periodic solutions near a sliding Shilnikov orbit.

If $\mathbf{x}^* \in \Sigma^s$ (resp. $\mathbf{x}^* \in \Sigma^e$) is an unstable (resp. stable) hyperbolic focus of the sliding vector field then we call $\mathbf{x}^*$ a *hyperbolic saddle-focus pseudo-equilibrium* or just *hyperbolic pseudo saddle-focus*.

Definition 15. *Let $Z = (X, Y)$ be a piecewise smooth vector field having a hyperbolic pseudo saddle-focus $p \in \Sigma^s$ (resp. $p \in \Sigma^e$), and let $q \in \partial\Sigma^s$ (resp. $q \in \partial\Sigma^e$) be a visible fold point of the vector field X such that*

(j) *the orbit passing through q following the sliding vector field Z^s converges to p backward in time (resp. forward in time);*

(jj) *the orbit starting at q and following the vector field X spends a time $t_0 > 0$ (resp. $t_0 < 0$) to reach p.*

So, through p and q a sliding loop Γ is easily characterized. We call Γ a **sliding Shilnikov orbit** (*see Figure 2.21*).

In [93], using the well known theory of Bernoulli shifts, it was provided a full topological and ergodic description of the dynamics of Filippov systems near a sliding Shilnikov orbit Γ. In particular, it was established the existence of a set $\Lambda \subset \partial M^s$ such that the restriction to Λ of the first return map π, defined near Γ, is topologically conjugate to a Bernoulli shift with infinite topological entropy. This ensures π, consequently the flow, to be chaotic. In particular, given any natural number $m \geq 1$ one can find infinitely many periodic points of the first return map with period m and, consequently, infinitely many closed orbits near Γ. The next theorem

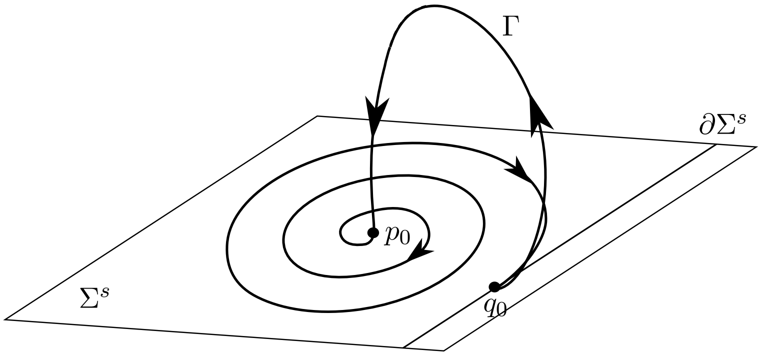

Figure 2.21: The point $p_0 \in \Sigma^s$ is a hyperbolic pseudo saddle-focus. The trajectory Γ, called Shilnikov sliding orbit, connects p_0 to itself passing through the point $q_0 \in \partial\Sigma^s$. Notice that the flow leaving q_0 reaches the point p_0 in a finite positive time, and approaches backward to p_0, asymptotically.

ensures that a PSVF presenting a sliding Shilnikov connection is chaotic. The proof of Theorem 8 is performed in [93].

Theorem 8. *Let $Z = (X, Y)$ be given by* (1.1)*. Assume that Z admits a sliding Shilnikov orbit. Then, there exists a neighborhood $\mathcal{U} \subset \chi^r$ of Z such that each $\widetilde{Z} \in \mathcal{U}$ admits an invariant compact set $\Lambda_{\widetilde{Z}}$ on which $\widetilde{Z}$ is chaotic.*

Ciliates are eukaryotic single cells that belong to the protist kingdom and dislocate themselves using an undulation movement generated by small hair-like protuberances (called cilia) that cover the cell body. They occur in aquatic environment and feed on small phytoplankton, constituting a relevant link between levels of marine and freshwater food webs (see [120]). Coexistence of species in a shared environment, as exhibited in Lake Constance data, may arise from ecological trade-offs (see [74]), which appear in many situations in ecology, for example, due to limited resources, an organism that invest energy in feeding strategies of one preferred prey cannot spend as much energy in specialize feeding another kind of prey. Lake Constance is a freshwater lake situated on the German-Swiss-Austrian border that has been under scientific investigation for decades and a substantial amount of data on the biomass of several phytoplankton and zooplankton species is available (see [8, 120, 121]). Based on the available data, Piltz et al. [99] derive the following piecewise smooth model for a 1 predator-2 prey interaction where the predator feeds adaptively on its preferred prey and an alternative prey:

$$\left(\dot{p}_1, \dot{p}_2, \dot{P}\right)^T = \begin{cases} \begin{pmatrix} (r_1 - \beta_1 P)p_1 \\ r_2 p_2 \\ (e\, q_1 \beta_1 p_1 - m)P \end{pmatrix} & \text{if} \quad H(p_1, p_2, P) \geq 0, \\ \begin{pmatrix} r_1 p_1 \\ (r_2 - \beta_2 P)p_2 \\ (e\, q_2 \beta_2 p_2 - m)P \end{pmatrix} & \text{if} \quad H(p_1, p_2, P) \leq 0, \end{cases} \tag{2.63}$$

where $(p_1, p_2, P) \in \mathbb{R}^3_{\geq 0}$ and $H(p_1, p_2, P) = \beta_1 p_1 - a_q \beta_2 p_2$. The plane $S = H^{-1}(0)$ is the discontinuous manifold for system (2.63). The variables of the model (2.63), P, p_1, and p_2, represent the density of the predator population, preferred prey, and alternative prey, respectively. Regarding the parameters, $q_1 \geq 0$ represents the desire to consume the preferred prey, $a_q > 0$ is the slope of the preference trade-off, and $q_2 \geq 0$ is the desire to consume the alternative prey. It is assumed that the intercept of the preference trade-off $b_q = q_2 - a_q q_1$ satisfies $b_q \geq 0$. In addition, $e > 0$ is the proportion of predation that goes into predator growth, $\beta_1 > 0$ and $\beta_2 > 0$ are, respectively, the death rates of the preferred and alternative prey due to predation. Finally, $m > 0$ is the predator per capita death rate per day and $r_1 > r_2 > 0$ are the per capita growth rates of the preferred and alternative prey, respectively.

The above constraints imply that the parameters of the differential system (2.63) lie in a subset of the Euclidean space $\mathbb{R}^9$, namely $\eta = (r_1, r_2, a_q, q_1, q_2, \beta_1, \beta_2, m, e) \in \mathcal{M} = R \times Q \times \mathbb{R}^4_{>0} \subset \mathbb{R}^9$, where $R = \{(r_1, r_2) \in \mathbb{R}^2_{>0} : r_1 > r_2\}$ and $Q = \{(a_q, q_1, q_2) \in \mathbb{R}_{>0} \times \mathbb{R}^2_{\geq 0} : q_2 \geq a_q q_1\}$. The set $\mathcal{M}$ is called *space of parameters* which is a 9-dimensional submanifold of $\mathbb{R}^9$ with boundary and corner.

In what follows, we state the main result of this chapter.

Theorem 9. *There exists a codimension one submanifold $\mathcal{N}$ of $\mathcal{M}$ such that the differential system* (2.63) *possesses a sliding Shilnikov orbit whenever $\eta \in \mathcal{N}$. Moreover, there exists a neighborhood $\mathcal{U} \subset \mathcal{M}$ of $\mathcal{N}$ such that the differential system* (2.63) *behaves chaotically whenever $\eta \in \mathcal{U}$.*

2.3.2 Qualitative dynamic of the model

Consider the differential system (2.63). In order to eliminate the dependence of the switching manifold on the parameters, let us consider the change of variables $x = p_1/\beta_1$, $y = p_2/(a_q \beta_2)$ and $z = P/\beta_1$. In these new variables, system (2.63) reads

$$
(\dot{x}, \dot{y}, \dot{z})^T = \begin{cases} X(x,y,z) = \begin{pmatrix} (r_1 - z)x \\ r_2 y \\ (eq_1 x - m)z \end{pmatrix} & \text{if} \quad h(x,y,z) \geq 0; \\ Y(x,y,z) = \begin{pmatrix} r_1 x \\ \left(r_2 - \dfrac{\beta_2}{\beta_1} z\right) y \\ \left(\dfrac{eq_2}{a_q} y - m\right) z \end{pmatrix} & \text{if} \quad h(x,y,z) \leq 0, \end{cases} \tag{2.64}
$$

where $(x,y,z) \in \mathbb{R}^3_{\geq 0}$ and $h(x,y,z) = x - y$. In these variables the switching manifold is given by $\Sigma = h^{-1}(0) = \{(x,x,z) : x \geq 0, \, z \geq 0\}$. Notice that the plane $\Pi_y = \{y = 0\}$ is invariant through the flow of X. The restriction of X onto the plane Π_y reads

$$
\overline{X}(x,z) = \begin{pmatrix} (r_1 - z)x \\ (eq_1 x - m)z \end{pmatrix}. \tag{2.65}
$$

Moreover, the projection of each orbit of X into the plane Π_y coincides with an orbit of $\overline{X}$. Indeed, the subsystems $(\dot{x}, \dot{z})$ and $\dot{y}$ are uncoupled.

The equilibria of $\overline{X}$ are $E_1 = (0,0)$ and $E_2 = (m/(eq_1), r_1)$. The equilibrium E_1 is a saddle with eigenvectors $(1,0)$ and $(0,1)$ associated with the eigenvalues r_1 and $-m$, respectively. The equilibrium E_2 has pure imaginary eigenvalues, namely $\pm i\sqrt{mr_1}$. Furthermore, $\overline{X}$ is a Lotka-Volterra system which has the following first integral:

$$
F(x,z) = -m - r_1 + eq_1 x + z - m \log\left(\frac{eq_1\, x}{m}\right) - r_1 \log\left(\frac{z}{r_1}\right). \tag{2.66}
$$

It implies that the equilibrium E_2 is a center (see Figure 2.22). Furthermore, since

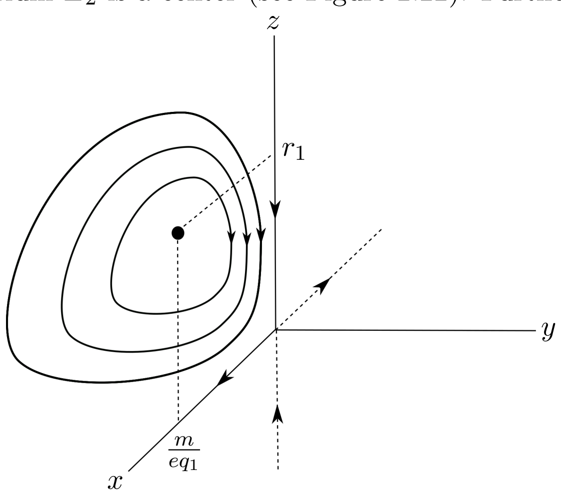

Figure 2.22: Projection of X into the plane Π_y.

$$y(t) = y_0 \exp(r_2 t), \tag{2.67}$$

the dynamics on the y-direction is unbounded increasing and the X-trajectories spiral from Π_y toward Σ, crossing Σ. The trajectories of X, on the domain $\mathbb{R}^3_{\geq 0}$, lie on cylinders around the straight line $\ell = \{(m/(eq_1), y, r_1) \,|\, y \geq 0\}$. See Figure 2.23.

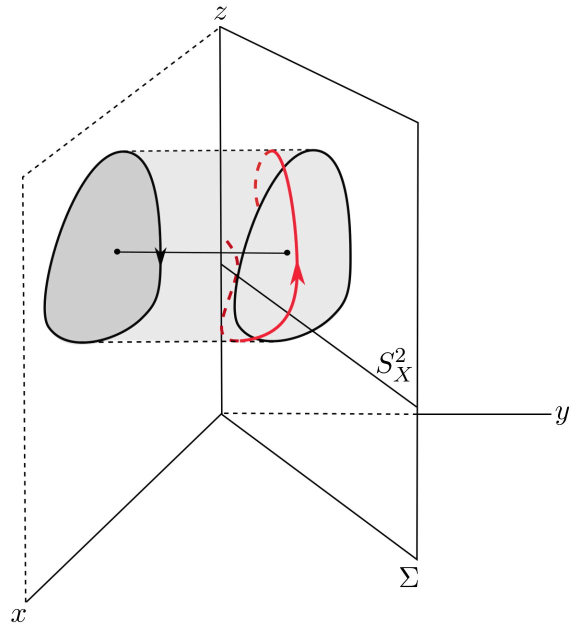

Figure 2.23: Invariant cylinder of X.

The next step is to study the contacts of the vectors fields X and Y with the switching manifold Σ. Let $p = (x, x, z) \in \Sigma$, computing the Lie derivatives $Xh(p)$ and $Yh(p)$ we get:

$$Xh(p) = (r_1 - r_2 - z)x \quad \text{and} \quad Yh(p) = \left(r_1 - r_2 + \frac{\beta_2 z}{\beta_1}\right) x.$$

Solving the equation $Xh(p) = 0$ we conclude that the contacts between the vector field X and the switching manifold Σ occur at $S_X = S_X^1 \cup S_X^2$, where $S_X^1 = \{(0,0,z) : z \geq 0\}$ and $S_X^2 = \{(x, x, r_1 - r_2) : x \geq 0\}$. Analogously, solving the equation $Yh(p) = 0$, we conclude that the contacts between Y and Σ occurs at $S_Y = S_Y^1 \cup S_Y^2$ where $S_Y^1 = S_X^1$ and $S_Y^2 = \{(x, x, -r_1 + r_2)\}$. The switching manifold Σ is then partitioned in two open regions, namely *sliding region* $\Sigma^s = \{(x, x, z) \in \Sigma \,|\, z > r_1 - r_2\}$ and *crossing region* $\Sigma^c = \{(x, x, z) \in \Sigma \,|\, 0 < z < r_1 - r_2\}$.

Notice that the tangency line S_X^2 is the boundary of the sliding region Σ^s. From Definition (15), S_X^2 will play an important role in finding a sliding Shilnikov orbit. In order to determine the kind of contact between X and Σ occurring on S_X^2, we compute the second Lie derivative $X^2 h$. Accordingly, let $\overline{p} = (x, x, r_1 - r_2) \in S_X^2$, so

$$X^2 h(\overline{p}) = (r_1 - r_2)(m - eq_1 x)x.$$

Solving the equation, $X^2h(\overline{p}) = 0$, we obtain two solutions, namely

$$\overline{p} = \overline{p}_1 = \big(0, 0, r_1 - r_2\big) \quad \text{and} \quad \overline{p} = c = \left(\frac{m}{eq_1}, \frac{m}{eq_1}, r_1 - r_2\right).$$

Moreover, we have that $X^2h(x, x, r_1 - r_2) > 0$ for $0 < x < m/(eq_1)$. So, the set

$$S_X^v = \{(x, x, r_1 - r_2) \in S_X^2 \; : \; 0 < x < m/(eq_1)\}$$

is a segment of *visible fold points* of X and, therefore, the local trajectories of X remain at the region where X is defined (i.e. $h(x, y, z) \geq 0$), before and after the tangential contact with S_X^v. It is worthwhile to mention that $c \in \mathbb{R}^3_{\geq 0}$ is a contact of cusp type.

In order to state the main result of this subsection (Lemma 4), we introduce the following new parameters

$$\phi = r_1 - r_2 \quad \text{and} \quad \tau = \frac{m}{e\, q_1}. \tag{2.68}$$

Solving the above relations for r_1 and m we get $S_X^2 = \{(x, x, \phi) \in S_X^2 \mid x \geq 0\}$ and $c = (\tau, \tau, \phi)$.

Lemma 4. *For each $x_0 \in (0, \tau)$, the forward trajectory of X passing through $(x_0, x_0, r_1 - r_2)$ intersects transversally the switching manifold Σ at a point called $\mu(x_0) = (u(x_0), u(x_0), v(x_0))$. In other words, the saturation of S_X^v through the forward flow of X intersects Σ transversally in the curve $\{\mu(x_0) : 0 < x_0 < \tau\}$. Moreover, the following statements hold:*

i) for $x_0 < \tau$ sufficiently close to τ we have

$$\begin{aligned} u(x_0) &= \tau - 2(x_0 - \tau) + \mathcal{O}(x_0 - \tau)^2, \\ v(x_0) &= r_1 - r_2 + \mathcal{O}(x_0 - \tau)^2; \end{aligned} \tag{2.69}$$

ii) and given $x_0 \in (0, \tau)$, for $r_2 > 0$ sufficiently small we have

$$\begin{aligned} u(x_0) &= x_0 + \mathcal{O}(r_2), \\ v(x_0) &= r_1 + \sqrt{2r_1T(x_0)(m - eq_1x_0)}\sqrt{r_2} + \mathcal{O}(r_2^{3/2}), \end{aligned} \tag{2.70}$$

where $T(x_0)$ is the period of the solution $\big(x(t, x_0; r_2), z(t, x_0; r_2)\big)$ for $r_2 = 0$.

Proof. Take $(x_0, x_0, \phi) \in S_x^v$, such that $0 < x_0 < \tau$. The parameter r_2 will play an important role in this proof, so we shall make it explicit in what follows. Let us consider $\psi(t, x_0; r_2) = (x(t, x_0; r_2), y(t, x_0; r_2), z(t, x_0; r_2))$ the solution of X such that $\psi(0, x_0; r_2) = (x_0, x_0, \phi)$. Notice that

$$\frac{\partial x}{\partial t}(0, x_0; r_2) = r_2 x_0, \quad \frac{\partial^2 x}{\partial t^2}(0, x_0; r_2) = r_2^2 x_0 + e q_1 x_0 (\tau - x_0)\phi,$$
$$\frac{\partial y}{\partial t}(0, x_0; r_2) = r_2 x_0, \quad \text{and} \quad \frac{\partial^2 y}{\partial t^2}(0, x_0; r_2) = r_2^2 x_0.$$

Since

$$x(0, x_0; r_2) = y(0, x_0; r_2) = x_0, \quad \frac{\partial x}{\partial t}(0, x_0; r_2) = \frac{\partial y}{\partial t}(0, x_0; r_2), \quad \text{and}$$
$$\frac{\partial^2 x}{\partial t^2}(0, x_0; r_2) > \frac{\partial^2 y}{\partial t^2}(0, x_0; r_2),$$

we conclude that $y(t, x_0; r_2) < x(t, x_0; r_2)$ for $t > 0$ sufficiently small. However, $x(t, x_0; r_2)$ is bounded and $y(t, x_0; r_2)$ is unbounded increasing, therefore there exists a first positive time $t_1(x_0; r_2) > 0$ such that

$$x(t_1(x_0; r_2), x_0; r_2) = y(t_1(x_0; r_2), x_0; r_2) = x_0 \exp(r_2 t_1(x_0; r_2)). \tag{2.71}$$

It means that the trajectory of X passing tangentially by each $(x_0, x_0, \phi) \in S_x^v$, for $0 < x_0 < \tau$, reaches transversally the switching manifold Σ at $\psi(t_1(x_0; r_2), x_0; r_2)$. Accordingly, for $0 < x_0 < \tau$, we define $\mu(x_0) = \psi(t_1(x_0; r_2), x_0; r_2)$,

$$\begin{aligned} u(x_0) &= x(t_1(x_0; r_2), x_0; r_2) = x_0 \exp(r_2 t_1(x_0; r_2)), \text{ and} \\ v(x_0) &= z(t_1(x_0; r_2), x_0; r_2). \end{aligned} \tag{2.72}$$

This concludes the proof of the first part of the lemma. Now, let us prove that the Taylor series of $u(x_0)$ around $x_0 = \tau$ reads

$$u(x_0) = \tau - 2(x_0 - \tau) + \mathcal{O}(x_0 - \tau)^2. \tag{2.73}$$

Notice that the difference $x(t, x_0; r_2) - x_0 \exp(r_2 t)$ around $t = 0$ reads

$$x(t, x_0; r_2) - x_0 \exp(r_2 t) = -\frac{e q_1 \phi x_0 (x_0 - \tau)}{2} t^2 - \frac{e q_1 \phi x_0 (r_2 (4x_0 - 3\tau) + e q_1 (x_0 - \tau)^2)}{6} t^3 + \mathcal{O}(t^4).$$

Therefore, the function

$$\Delta(t, x_0) := \frac{x(t, x_0; r_2) - x_0 \exp(r_2 t)}{t^2}$$

is well defined and, around $t = 0$, reads

$$\Delta(t, x_0) = -\frac{e q_1 \phi x_0 (x_0 - \tau)}{2} - \frac{e q_1 \phi x_0 (r_2 (4x_0 - 3\tau) + e q_1 (x_0 - \tau)^2)}{6} t + \mathcal{O}(t^2).$$

In order to apply the Implicit Function Theorem, we compute

$$\Delta(0,\tau)=0, \quad \frac{\partial \Delta}{\partial t}(0,\tau)=-\frac{eq_1r_2\tau^2\phi}{6}\neq 0, \quad \text{and} \quad \frac{\partial \Delta}{\partial x_0}(0,\tau)=-\frac{eq_1\tau\phi}{2}.$$

Therefore, we find a unique function $t_2(x_0)$ such that

$$t_2(\tau)=0, \quad t_2'(\tau)=-\frac{\dfrac{\partial \Delta}{\partial x_0}(0,\tau)}{\dfrac{\partial \Delta}{\partial t}(0,\tau)}=-\frac{3}{r_2\tau}. \tag{2.74}$$

From the uniqueness of t_2 we conclude that, for x_0 sufficiently close to τ, $t_1(x_0;r_2)=t_2(x_0)$. So, using (2.74), $u(x_0)=x_0\exp(r_2t_1(x_0))$ can be expanded around $x_0=\tau$ in order to get (2.73). Finally, we shall prove that given $x_0^*\in(0,\tau)$ there exists a neighborhood $\mathcal{U}$ of x_0^* and $r_2^*>0$ such that $u(x_0)<\tau$ and $v(x_0)>r_1$ for every $(x_0,r_2)\in\mathcal{U}\times(0,r_2^*]$. Indeed, consider the function

$$\delta(t,r_2)=x(t,x_0;r_2)-y(t,x_0;r_2)=x(t,x_0;r_2)-x_0e^{r_2t}.$$

We know that $\big(x(t,x_0;r_2),z(t,x_0;r_2)\big)$ is periodic in the variable t (see Figure 2.22). In fact, this is the solution of the Lotka-Volterra system (2.65) with initial condition (x_0,r_1-r_2) and, therefore, satisfies

$$F\left(x(t,x_0;r_2),z(t,x_0;r_2)\right)=F(x_0,r_1-r_2), \tag{2.75}$$

for every $r_1>r_2>0$, $0<x_0<\tau$, and t on its interval of definition. For the value $r_2=0$, denote by $T(x_0)>0$ the period of the solution $\big(x(t,x_0;0),z(t,x_0;0)\big)$, that is, $\big(x(T(x_0),x_0;0),z(T(x_0),x_0;0)\big)=(x_0,r_1)$. Consequently, $\delta(T(x_0),0)=0$. We shall see that there is a saddle-node bifurcation occurring at $t=T(x_0)$ for the critical value of the parameter $r_2=0$. Computing the derivative in the variable r_2 of (2.75) at $t=T(x_0)$ and $r_2=0$ we get

$$\frac{\partial x}{\partial r_2}(T(x_0),x_0,0)=0.$$

So, we get

$$\frac{\partial \delta}{\partial t}(T(x_0),0)=0, \quad \frac{\partial^2 \delta}{\partial t^2}(t(x_0),0)=r_1(m-eq_1x_0)x_0>0,$$

and

$$\frac{\partial \delta}{\partial r_2}(T(x_0),0)=-x_0T(x_0)<0. \tag{2.76}$$

This implies the existence of a saddle-node bifurcation. In order to conclude this proof, we shall explicitly compute the solutions bifurcating from $t=T(x_0)$. From (2.76), applying the

Implicit Function Theorem, we get the existence of neighborhoods I_1 and V_1 of $T(x_0)$ and 0, respectively, and a unique differentiable function $\rho\colon I_1 \to V_1$ such that $\delta(t,\rho(t)) = 0$ for every $t \in I_1$. Moreover,

$$\rho(T(x_0)) = \rho'(T(x_0)) = 0 \text{ and } \rho''(T(x_0)) = \frac{r_1(m - eq_1x_0)}{2T(x_0)}.$$

Notice that we are taking

$$r_2 = \rho(t) = \frac{r_1(m - eq_1x_0)}{2T(x_0)}(t - T(x_0))^2 + \mathcal{O}(t - T(x_0))^3. \tag{2.77}$$

Proceeding with the change $s = (t - T(x_0))^2$, equation (2.77) is equivalent to

$$r_2 = \frac{r_1(m - eq_1x_0)}{2T(x_0)}s + \mathcal{O}(|s|^{3/2}).$$

The above equation can be inverted using the Inverse Function Theorem, so that, we get the existence of neighborhoods U_2 and I_2 of 0, and a unique differentiable function $\sigma\colon U_2 \to I_2$ such that

$$s = \sigma(r_2), \quad \sigma(0) = 0, \quad \sigma'(0) = \frac{2T(x_0)}{r_1(m - eq_1x_0)} > 0.$$

Going back through the change $s = (t - T(x_0))^2$ we get two distinct positive times $t = T(x_0) \pm \sqrt{\sigma(r_2)}$ bifurcating from $t = T(x_0)$. Since $t_1(x_0; r_2)$ is the first return time we conclude that

$$t_1(x_0; r_2) = T(x_0) - \sqrt{\sigma(r_2)} = T(x_0) + \sqrt{\frac{2T(x_0)}{r_1(m - eq_1x_0)}}\sqrt{r_2} + \mathcal{O}(r_2^{3/2}).$$

Finally, from (2.72) we compute

$$\begin{aligned} u(x_0) &= x_0 + \mathcal{O}(r_2), \\ v(x_0) &= r_1 + \sqrt{2r_1T(x_0)(m - eq_1x_0)}\sqrt{r_2} + \mathcal{O}(r_2^{3/2}). \end{aligned} \tag{2.78}$$

This concludes the proof. See Figure 2.24. $\square$

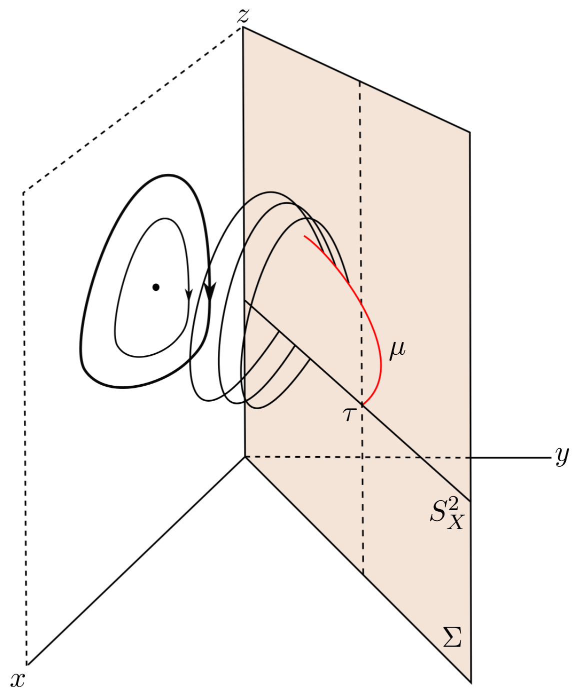

Figure 2.24: Saturation of the curve μ.

Lemma 5. *There exist $a, b, c,$ and d, with $0 < a < b < \tau$ and $0 < c < d$, such that $0 < u(x_0) < \tau$ and $v(x_0) > r_1$ for every $(x_0, r_2) \in [a, b] \times [c, d]$. Moreover, for $r_2 \in [c, d]$, $\mu(x_0)$ is differentiable on $[a, b]$ and $u'(x_0)^2 + v'(x_0)^2 \neq 0$ for every $(x_0, r_2) \in [a, b] \times [c, d]$.*

Proof. From (2.73) we have that $u(x_0) > \tau$ for x_0 sufficiently close to τ, and from (2.78) we have that for a fixed $x_0 \in (0, \tau)$ there exists $r_2^* > 0$ such that $u(x_0) < \tau$ for every $r_2 \in (0, r_2^*]$. Therefore, for $r_2 = r_{2*} < r_2^*$ there exists $x_1^* \in (0, \tau)$ such that $u(x_1^*) = \tau$ and $u(x_0) < \tau$ for $x_0 < x_1^*$ sufficiently close to x_1^*. Moreover, $v(x_1^*) > r_1$ and, consequently, $v(x_0) > r_1$ for $x_0 < x_1^*$ sufficiently close to x_1^* because (τ, r_1) is a critical point for the first integral (2.66). Hence, take $x_{1*} < x_1^*$ such that $v(x_{1*}) > r_1$ and $u(x_{1*}) < \tau$. So, from the continuous dependence of the solutions on the initial conditions and parameters, we first get the existence of $a, b, c,$ and d, with $0 < a < x_{1*} < b < \tau$ and $0 < c < r_{2*} < d$ such that $0 < u(x_0) < \tau$ and $v(x_0) > r_1$ for every $(x_0, r_2) \in [a, b] \times [c, d]$. Now, in order to get the differentiability of μ, define

$$\Gamma(t, x_0, r_2) = x(t, x_0; r_2) - x_0 \exp(r_2 t).$$

From the proof of Lemma 4, for each $(\overline{x_0}, \overline{r_2}) \in [a, b] \times [c, d]$ we got the existence of $t_1(\overline{x_0}; \overline{r_2}) > 0$ such that $\Gamma(t_1(\overline{x_0}; \overline{r_2}), \overline{x_0}, \overline{r_2}) = 0$. Since

$$\frac{\partial \Gamma}{\partial t}(t_1(\overline{x_0}; \overline{r_2}), \overline{x_0}, \overline{r_2}) = (r_1 - r_2 - v(\overline{x_0}))u(\overline{x_0}) \neq 0,$$

we obtain, from the Implicit Function Theorem, the existence of a unique differentiable function $t_2(x_0, r_0)$, defined in a neighborhood of $(\overline{x_0}, \overline{r_2})$, such that $t_2(\overline{x_0}, \overline{r_2}) = t_1(\overline{x_0}; \overline{r_2})$ and $\Gamma(t_2(x_0, r_2), x_0, r_2) = 0$ for every (x_0, r_2) in this neighborhood. From the uniqueness property it follows that $t_1 = t_2$, which implies the differentiability of t_1 at $(\overline{x_0}; \overline{r_2})$ and, consequently, the differentiability of μ at $x_0 = \overline{x_0}$ for $r_2 = \overline{r_2}$. Since $(\overline{x_0}, \overline{r_2})$ was taken arbitrary in the compact set $[a, b] \times [c, d]$, we conclude the differentiability of μ for every $(x_0, r_2) \in [a, b] \times [c, d]$. Finally, notice that $F(u(x_0), v(x_0)) = F(x_0, r_1 - r_2)$ since they are at the same level set. Assuming that $u'(x_0) = v'(x_0) = 0$ and computing the derivative of the last identity in the variable x_0 we get that $x_0 = \tau$. Hence, we conclude that $u'(x_0)^2 + v'(x_0)^2 \neq 0$ for every $(x_0, r_2) \in [a, b] \times [c, d]$. $\square$

Now we are going to look more closely at the sliding vector field. Firstly, consider system (2.64) in the variables $(x, w, z) = (x, x - y, z)$, $(x, w, z) \in \mathbb{R}_{\geq 0} \times \mathbb{R} \times \mathbb{R}_{\geq 0}$. So, $(\dot{x}, \dot{w}, \dot{z})^T = Z(x, w, z)$, where

$$Z(x,w,z) = \begin{cases} \begin{pmatrix} (r_1 - z)x \\ r_2 w + x(r_1 - r_2 - z) \\ (eq_1 x - m)z \end{pmatrix} & \text{if} \quad w > 0, \\ \begin{pmatrix} r_1 x \\ r_1 x - (x - w)\left(r_2 - \dfrac{\beta_2}{\beta_1} z\right) \\ \left(\dfrac{eq_2}{a_q}(x - w) - m\right) z \end{pmatrix} & \text{if} \quad w < 0. \end{cases} \tag{2.79}$$

The switching manifold is now given by $\{(x, 0, z) : x \geq 0, z \geq 0\}$ and the associated sliding vector field reads:

$$Z^s(x,z) = \begin{pmatrix} \dfrac{\beta_1 r_2 + \beta_2 r_1}{\beta_1 + \beta_2} x - \dfrac{\beta_2}{\beta_1 + \beta_2} x\, z \\ \dfrac{e(a_q q_1 - q_2)(r_1 - r_2)\beta_1}{a_q(\beta_1 + \beta_2)} x - m\, z + \dfrac{e(\beta_1 q_2 + a_q \beta_2 q_1)}{a_q(\beta_1 + \beta_2)} x\, z \end{pmatrix}. \tag{2.80}$$

The vector field (2.80) admits two equilibria, namely $(0, 0)$ and

$$(x_c, z_c) = \left(\frac{a_q m(\beta_1 r_2 + \beta_2 r_1)}{e(\beta_1 q_2 r_2 + a_q \beta_2 q_1 r_1)}, r_1 + \frac{\beta_1}{\beta_2} r_2 \right) \tag{2.81}$$

Notice that, from the original condition $\eta \in \mathcal{M}$, $0 < x_c < \tau$ and $z_c > r_1 = \phi - r_2$.

The next lemma is very important in the sequel.

Lemma 6. *Let $\eta \in \mathcal{M}$ and assume that*

$$m < \frac{4(\beta_1+\beta_2)(r_2\beta_1+r_1\beta_2)(q_2r_2\beta_1+a_qq_1r_1\beta_2)^2}{(q_2-a_qq_1)^2(r_1-r_2)^2\beta_1^2\beta_2^2}. \tag{2.82}$$

Then, the following statements hold:

(i) the equilibrium (x_c, z_c) is a repulsive focus;

(ii) there exists $x^* \in [0,\tau)$ such that the backward orbit of Z^s of any point of the straight segment $L = \{(x,\phi) : x^* < x \leq \tau\} \subset S_X^v$ is contained in Σ^s and converges asymptotically to the equilibrium (x_c, z_c).

Proof. Denote by $\alpha \pm ib$ the eigenvalues of the jacobian matrix of the vector field Z^s at (x_c, z_c). It is straightforward to see that (2.82) implies that $b \neq 0$. In this case

$$\alpha = \frac{m(q_2-a_qq_1)(r_1-r_2)\beta_1\beta_2}{2(\beta_1+\beta_2)(a_qq_1r_1\beta_2+q_2r_2\beta_1)} > 0.$$

Hence, (x_c, z_c) is a repulsive focus. This concludes the proof of statement (i). In order to prove statement (ii), we first claim that the sliding vector field $Z^s(x,z) = (Z_1^s(x,z), Z_2^s(x,z))$ given by equation (2.80) does not admit limit cycles contained in the region $\{(x,z) \in \mathbb{R}^2 : x > 0, z > 0\}$. Indeed,

$$\frac{\partial}{\partial x}\left(\frac{Z_1^s(x,z)}{x\,z}\right) + \frac{\partial}{\partial z}\left(\frac{Z_2^s(x,z)}{x\,z}\right) = \frac{e(q_2-a_qq_1)(r_1-r_2)\beta_1}{a_q(\beta_1+\beta_2)z^2} > 0,$$

for $x, z > 0$. Since the function $(x,z) \mapsto \dfrac{1}{xz}$ is C^1 in the region $\{(x,z) \in \mathbb{R}^2 : x > 0, z > 0\}$, the claim follows by the Bendixson-Dulac criterion (see [43]).

We may observe that the sliding vector field writes

$$Z^s(x,z) = Z_{LV}(x,z) + \left(0, \frac{e(a_qq_1-q_2)(r_1-r_2)\beta_1}{a_q(\beta_1+\beta_2)}\,x\right),$$

where Z_{LV} is a Lotka-Volterra vector field. We know that Z_{LV} admits the following first integral

$$\begin{aligned} H(x,z) = \quad & -m - \frac{r_2\beta_1+r_1\beta_2}{\beta_1+\beta_2} + \frac{e(a_qq_1\beta_2+q_2\beta_1)}{a_q(\beta_1+\beta_2)}x + \frac{\beta_2}{\beta_1+\beta_2}z \\ & -m\log\left(\frac{e(a_qq_1\beta_2+q_2\beta_1)}{a_qm(\beta_1+\beta_2)}\right) - \frac{r_2\beta_1+r_1\beta_2}{\beta_1+\beta_2}\log\left(\frac{\beta_2}{r_2\beta_1+r_1\beta_2}z\right), \end{aligned}$$

that is, $\langle \nabla H(x,z), Z_{LV}(x,z)\rangle = 0$. Now, let

$$a = \frac{(\beta_1+\beta_2)(q_2r_2\beta_1+a_qq_1r_1\beta_2)}{(q_2\beta_1+a_qq_1\beta_2)(r_2\beta_1+r_1\beta_2)} > 0.$$

Since

$$\langle \nabla H(ax,z), Z^s(x,y)\rangle = \frac{(q_2 - a_q q_1)(r_1 - r_2)\beta_1(r_2\beta_1 + (r_1 - z)\beta_2)^2}{r_2\beta_1 + r_1\beta_2} > 0,$$

for every $x, z > 0$ and $z \neq z_c$, we get that the level curves of $H(ax,z)$ are negatively invariant. Since Z^s has no limit cycles, the focus (x_c, z_c) must attract, backward in time, the orbits of every point in the positive quadrant. Finally, consider $\psi^s(t)$ the trajectory of Z^s passing through (ϕ, τ). If there exists $t_s > 0$ such that $\psi^s(t_s) \in S^2_X$, then take $x^* = \psi^s(t_s)$. Otherwise take $x^* = 0$. It is easy to see that, in this case, $x^* < \tau$. Indeed, $x^* \neq \tau$, otherwise there would exist a periodic solution passing through $(\tau, r_1 - r_2)$, and $\pi_2 Z^s(x, r_1 - r_2) = (r_1 - r_2)(eq_1 x - m) > 0$ for every $x > \tau$. Hence, the proof of statement (ii) follows. $\square$

Remark 8. *If we consider the following change on the parameters*

$$e = \frac{a_q m z_c}{(a_q q_1 r_1 + q_2(z_c - r_1))x_c} \quad \text{and} \quad \beta_2 = \frac{r_2\beta_1}{z_c - r_1},$$

then the inequality (2.82) *becomes*

$$m < \frac{4r_2 z_c(z_c - \phi)(a_q q_1 r_1 + q_2(z_c - r_1))^2}{\phi^2(q_2 - a_q q_1)^2(z_c - r_1)^2}.$$

2.3.3 The Shilnikov sliding connection

Let us guarantee the existence of a *Sliding Shilnikov Connection* according to Definition 15. Lemma 4 ensures that the saturation of S^v_X through the forward flow of X intersects transversally the switching manifold Σ in a curve $\mu(x_0) = (u(x_0), u(x_0), v(x_0))$, $0 < x_0 < \tau$. Moreover, from Lemma 5 there exist a, b, c, and d, with $0 < a < b < \tau$ and $0 < c < d$, such that the curve $0 < u(x_0) < \tau$ and $v(x_0) > r_1$ for every $(x_0, r_2) \in [a,b] \times [c,d]$. Accordingly, for some $x_0 \in [a,b]$, take $(x_c, z_c) = (u(x_0), v(x_0))$ and assume

$$c < r_2 < d \quad \text{and} \quad m < \frac{4r_2 v(x_0)(v(x_0) - \phi)(a_q q_1 r_1 + q_2(v(x_0) - r_1))^2}{\phi^2(q_2 - a_q q_1)^2(v(x_0) - r_1)^2}.$$

From Lemma 6 and Remark 8 we have that $(x_c, z_c) \in \Sigma^s \subset \Sigma$ is a repulsive focus of Z^s and there exists $x^* \in [0, \tau)$ such that the backward orbit of any point in the straight segment $L = \{(x, \phi) : x^* < x \leq \tau\} \subset S^v_X$ is contained in Σ^s and converges asymptotically to p.

If $x^* = 0$, then from Lemma 6 we have characterized a sliding Shilnikov connection through the fold-regular point (x_0, x_0, ϕ) and the pseudo-equilibrium $(u(x_0), u(x_0), v(x_0))$. Now, assume that $x^* \neq 0$. It remains to prove $(x_c, z_c) = (u(x_0), v(x_0))$ implies that $x^* < x_0$. Notice that, in this case, the points (x_c, z_c) and (x_0, ϕ) lie in the same level set of F. Recall that F is the first integral (2.66) of the Lotka-Volterra system (2.65). Denote $C = F^{-1}(F(x_c, z_c))$. Firstly, we shall study the behavior of Z^s on C, which is equivalent to analyze the sign of the product

$$\langle \nabla F(x,z), Z^s(x,z)\rangle = \frac{(r_1 - r_2 - z)(eq_2x(r_1 - z) + a_q(-eq_1r_1x + mz)\beta_1}{a_qz(\beta_1 + \beta_2)}.$$

for $(x, z) \in C$. Since $a_qz(\beta_1 + \beta_2) > 0$ and $r_1 - r_2 - z \le 0$ for $z \ge r_1 - r_2$, it is sufficient to analyze the sign of $eq_2x(r_1 - z) + a_q(-eq_1r_1x + mz)$ on C. Notice that the equation

$$eq_2x(r_1 - z) + a_q(-eq_1r_1x + mz) = 0 \tag{2.83}$$

describes a hyperbole containing the points $(0, 0)$ and (x_c, z_c). Indeed, (2.83) is a quadratic equation of the form $\mathcal{A}x^2 + \mathcal{B}xz + \mathcal{C}z^2 + \mathcal{D}x + \mathcal{E}z + \mathcal{F} = 0$, where $\mathcal{B} = -eq_2$, $\mathcal{D} = r_1e(q_2 - a_qq_1)$, $\mathcal{E} = a_qm$, $\mathcal{A} = \mathcal{C} = \mathcal{F} = 0$, and so $\mathcal{B}^2 - 4\mathcal{A}\mathcal{C} = \mathcal{B}^2 > 0$. From convexity, each connected component of the hyperbola (2.83) intersects C at most in two points. Solving (2.83), we get

$$z = z_h(x) = \frac{e(q_2 - a_qq_1)r_1x}{eq_2x - a_qm}.$$

Define

$$F_c(x) = F(x, z_h(x)) - F(x_c, z_c).$$

Notice that $F_c(x) > 0$, $F_c(x) = 0$, and $F_c(x) < 0$ imply $(x, z_h(x)) \in \text{ext}(C)$, $(x, z_h(x)) \in C$, and $(x, z_h(x)) \in \text{int}(C)$, respectively. Clearly, $F_c(x_c) = 0$. Moreover,

$$F_c'(x_c) = -\frac{eq_1r_1(\tau - x_c)^2 + \tau(r_1 - x_c)^2}{r_1(\tau - x_c)x_c} < 0.$$

This implies that $F_c(x) > 0$ for every $x \in (0, x_c)$. Consequently, $eq_2x(r_1-z)+a_q(-eq_1r_1x+mz) < 0$ and $\langle \nabla F(x,z), Z^s(x,z)\rangle > 0$ for every $(x, z) \in C$ such that $x \in (0, x_c)$. It means that the vector field Z^s points outwards C provided that $(x, z) \in C$ and $x \in (0, x_c)$.

Finally, consider $\psi^s(t)$ the trajectory of Z^s passing through (τ, ϕ). Since $x^* = \pi_x\psi^s(t_s)$ for some $t_s > 0$ and $\psi^s(t_s) \in S_X^v$, there exists $t_s' \in (0, t_s)$ such that $\pi_x\psi^s(t_s') = x_c$. Moreover, $\psi^s(t_s') \in \text{ext}(C)$ because (x_c, z_c) is a repulsive focus lying on C. From the previous comments, the trajectory $\psi^s(t)$ remains in the exterior of C for every $t \in [t_s', t_s]$. Hence, $\psi^s(t_s) \in \text{ext}(C)$ implying that $x^* < x_0$. Then, applying Lemma 6 we have characterized a sliding Shilnikov connection through the fold-regular point (x_0, x_0, ϕ) and the pseudo-equilibrium $(u(x_0), u(x_0), v(x_0))$.

Now, define $\widetilde{\mathcal{N}}$ as the set of parameter vectors $\eta = (r_1, r_2, a_q, q_1, q_2,\ \beta_1, \beta_2,\ e, m) \in \mathcal{M}$

satisfying the inequalities

$$
\begin{aligned}
&a \leq x_0 \leq b, \quad c \leq r_2 \leq d, \qquad \text{and} \\
&m < M(x_0, r_2) := \frac{4r_2 v(x_0)(v(x_0)-\phi)(a_q q_1 r_1 + q_2(v(x_0)-r_1))^2}{\phi^2 (q_2 - a_q q_1)^2 (v(x_0)-r_1)^2},
\end{aligned} \tag{2.84}
$$

and the identities

$$
e = E(x_0) := \frac{a_q m v(x_0)}{(a_q q_1 r_1 + q_2(v(x_0)-r_1))u(x_0)} \quad \text{and} \quad \beta_2 = B(x_0) := \frac{r_2 \beta_1}{v(x_0) - r_1}, \tag{2.85}
$$

The identities (2.85) come from assuming $(x_c, z_c) = (u(x_0), v(x_0))$ (see Remark 8). From the construction above, the differential system (2.63) possesses a sliding Shilnikov orbit whenever $\eta \in \widetilde{\mathcal{N}}$.

In what follows, we shall identify a codimension one submanifold $\mathcal{N} \subset \widetilde{\mathcal{N}}$ of $\mathcal{M}$. Firstly, notice that M is a positive continuous function and, therefore, assumes a minimum $M_0 > 0$ on the compact set $[a, b] \times [c, d]$. Moreover, $E'(x_0)^2 + B'(x_0)^2 \neq 0$ for every $\tau \in (0, \tau)$. Indeed, it is easy to see that $E'(x_0)^2 + B'(x_0)^2 = 0$ if, and only if, $u'(x_0)^2 + v'(x_0)^2 = 0$, which would contradict Lemma 5. Without loss of generality, assume that for some $x_0 \in (a, b)$, $B'(x_0) \neq 0$. From the Inverse Function Theorem, the function B can be locally inverted, that is, there exists a neighborhood $\mathcal{B}$ of $B(x_0)$ and a unique function $B^{-1} : \mathcal{B} \to (a, b)$ such that $B \circ B^{-1}(\beta_2) = \beta_2$ whenever $\beta_2 \in \mathcal{B}$. Hence, taking

$$
c \leq r_2 \leq d, \quad m \leq M_0, \quad \beta_2 \in \mathcal{B} \quad \text{and} \quad e = E \circ B^{-1}(\beta_2),
$$

the inequalities (2.84) and the identities (2.85) are fulfilled. So, for $\eta = (r_1, r_2, a_q, q_1, q_2, \beta_1, \beta_2, e, m) \in \mathcal{M}$, define

$$
\mathcal{N} = \{\eta \in \mathcal{M} : c < r_2 < d, \, m < M_0, \, \beta_2 \in \mathcal{B} \text{ and } e = E \circ B^{-1}(\beta_2)\} \subset \widetilde{\mathcal{N}}.
$$

Notice that $\mathcal{N}$ is a graph defined in an open domain. Therefore, $\mathcal{N}$ is a codimension one submanifold of $\mathcal{M}$. Finally, the existence of the neighborhood $\mathcal{U} \subset \mathcal{M}$ of $\mathcal{N}$, satisfying that the differential system (2.63) behaves chaotically whenever $\eta \in \mathcal{U}$, follows directly form Theorem 8.

2.3.4 Numerical Simulations

In order to illustrate our results, we perform a numerical simulation that puts in evidence the existence of the Shilnikov sliding connection obtained in Subsection 2.3.3. We were able to find parameter values for which the repulsive focus (x_c, z_c) of the sliding vector field Z_s changes its position crossing the curve μ. Recall that the curve μ, given by Lemma 4, is the saturation of S_X^v through the flow of X intersected with Σ. The simulation rely on computer algebra and numerical evaluations carried out with the software MATHEMATICA (see [127]).

Notice that the vector field X given by (2.64) does not depend on the parameter β_1. So, the repulsive focus (x_c, z_c) can be moved by varying the parameter β_1 keeping the trajectories of X unchanged. Accordingly, we shall fix all the parameter values but β_1 (see Table 2.3).

Parameter	Value
m	0,790
r_1	0,836
e	0,948
q_1	0,772
a_q	0,660
q_2	1,084
β_2	0,896
r_2	0,126

Table 2.3: Parameters for the numerical simulation of the Shilnikov sliding connection.

Taking either $\beta_1 = 6$ or $\beta_1 = 10$ and considering the parameter values given by Table 2.3 we see that the conditions of Lemma 6 are satisfied, that is, (x_c, z_c) is a repulsive focus. For $\beta_1 = 6$, the numerical simulation indicates that (x_c, z_c) is below the curve μ (see Figure 2.25(a)). For $\beta_1 = 10$, the numerical simulation indicates that (x_c, z_c) is above the curve μ (see Figure 2.25(c)).

Finally, from the continuous dependence on the parameter β_1, there exists β_1^*, with $6 < \beta_1^* < 10$, such that for $\beta_1 = \beta_1^*$ the repulsive focus (x_c, z_c) belongs to the curve μ. This gives rise to a Shilnikov sliding connection (see Figure 2.25(b)). We mention that the return x^* of the sliding vector field through the point (τ, ϕ) on S_X^v satisfies $x^* < a$ where $0 < a < \tau$ is the x-coordinate of the fold point which is connected to the repulsive focus through an orbit of X. In other words, a belongs to the segment L given by Lemma 6.

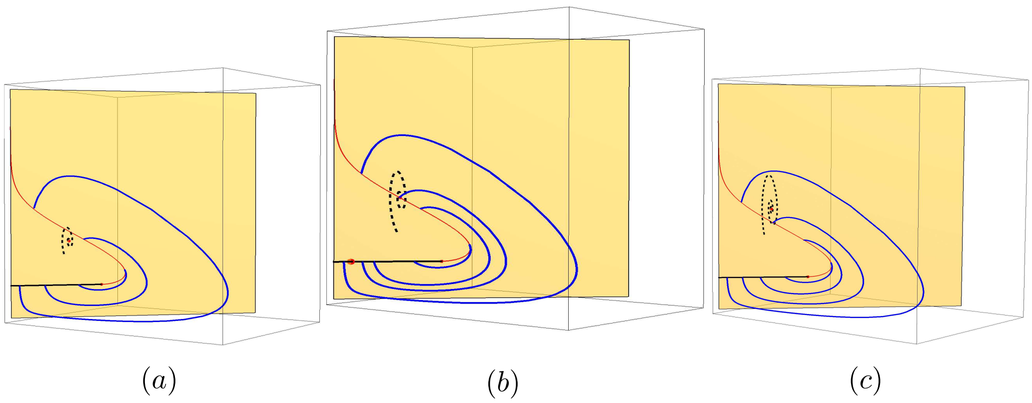

Figure 2.25: Relative position between the curve μ and the repulsive pseudo-focus (x_c, z_c). In (a) and (c) we are taking $\beta_1 = 6$ and $\beta_1 = 10$, respectively. In (b) there exists β_1^* such that $(x_c, z_c) \in \mu$.

Chapter

3

Combing the ball

This chapter is devoted to exhibiting two 3D vector fields tangent to the sphere S^2. In the first one, we present a piecewise smooth vector field tangent to S^2 without equilibrium points. Moreover, we show that this vector field contains a chaotic non-trivial minimal set. In the second one, we present a piecewise smooth vector field tangent to the unit sphere S^2 such that S^2 itself is a minimal set. The content of this chapter can be found in [52, 54].

Questions concerning the structure and characterization of minimal sets are of great relevance in the theory of dynamical systems. Let $M \subset \mathbb{R}^n$ be a manifold and consider the flow $\phi\colon \mathbb{R}\times M \to M$. Associated with ϕ there exists a vector field X given by $X = \frac{d}{dt}\phi$ which carries a point $p \in M$ to a vector in T_pM the tangent space to M at p. When M is a two dimensional manifold, a **trivial minimal set** Λ of ϕ (or X) is either an equilibrium point or a closed trajectory or else the whole manifold M, provide that $\Lambda = M$ is the torus and ϕ is (topologically equivalent to) an irrational flow. The following result characterizes minimal sets, according to the differentiability of the two-dimensional flow.

Smoothing Theorem:(see [63]) Let $\phi\colon \mathbb{R}\times M \to M$ be a continuous flow on a compact C^∞ two dimensional manifold M. Then there exists a C^1 flow ψ on M which is topologically equivalent to ϕ. Furthermore, the following conditions are equivalent:

(a) any minimal set of ϕ is trivial;

(b) ϕ is topologically equivalent to a C^2 flow;

(c) ϕ is topologically equivalent to a C^∞ flow.

The assertion that (b) implies (a) is the celebrated *Denjoy-Schwartz Theorem* (see [36, 101]), that generalizes to closed two-dimensional manifolds the planar, and even more celebrated, *Poincaré-Bendixson Theorem* (see [97]). We stress that the existence of C^1 flows which are not topologically equivalent to C^2 flows is given in [36] (see also [102]).

This subject is also related to the so called **Hairy Ball Theorem**. Worth speaking, this theorem says that:

A continuous vector field on a spherical surface has at least one equilibrium point.

The theorem was proved by several (great) authors independently. Since it can be seen as a corollary of the *Poincaré-Hopf Index Theorem*, Poincaré is quoted as the first to prove it in 1885. However, the version of the theorem presented above was first proved in [17], in 1908. In his proof, Brouwer uses concepts of algebraic topology, like homotopy. Another author that proves this theorem was Milnor. In 1978 (see [90]) he uses concepts of differentiability and gave an analytic proof of it. A good survey about this subject is found in [42].

The Hairy Ball Theorem has intriguing consequences. For example, we are able to conclude that in some place of the earth the vector field modeling the wind has "horizontal" component null. Of course, the theorem is valid in any surface *homotopic* to S^2. In order to obtain a vector field that *comb* the sphere, it must not be continuous.

Despite of being theoretical in some sense, the example that we show here, is more related to the kind of discontinuous vector fields that can be found in real world applications since *a Filippov's vector field provide an average between the smooth vector fields at the discontinuity set.* Moreover, we not know any other work combing the hairy ball where the discontinuity set is not composed by isolated points. In fact, few paper can be found in the literature concerning Filippov's vector fields tangent to S^2. See, for instance, [98].

3.1 Stereographic and central projections

In order to establish a correspondence between a trajectory associated with a vector field in $\mathbb{R}^2$ and a trajectory in the sphere $S^2 = \{(x, y, z) : x^2 + y^2 + z^2 = 1\}$ we are going to use stereographic and central projections. Given a point $p = (x, y, 0)$ in the plane $z = 0$ we can consider the straight line between p and the north pole $N = (0, 0, 1)$, whose expression is given by $\lambda(t) = tp + (1 - t)N$ (see Figure 3.1).

This line will intercept S^2 if, and only if, $t = 2/(x^2 + y^2 + 1)$. Therefore, we can define the function $\pi_N \colon \mathbb{R}^2 \longrightarrow S^2 \setminus \{N\}$ whose expression is given by

$$\pi_N(x, y) = \left(\frac{2x}{x^2 + y^2 + 1}, \frac{2y}{x^2 + y^2 + 1}, \frac{x^2 + y^2 - 1}{x^2 + y^2 + 1} \right). \tag{3.1}$$

By a straightforward calculation, we can notice that the inverse function of π_N is given by

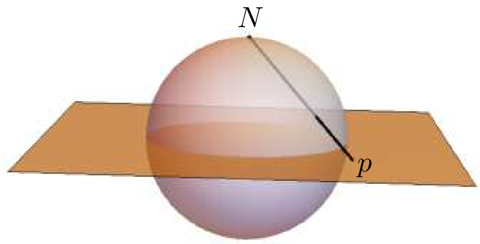

Figure 3.1: Projection π_N.

$$\begin{array}{rccl} \pi_N^{-1}\colon & S^2 & \longrightarrow & \mathbb{R}^2 \\ & (x,y,z) & \longmapsto & \pi_N^{-1}(x,y,z) = \left(\dfrac{x}{1-z}, \dfrac{y}{1-z}\right). \end{array} \tag{3.2}$$

In a similar way, it is possible to find the stereographic projection related to the south pole $S = (0,0,-1)$ considering the straight line $r(t) = tp + (1-t)S$ (see Figure 3.2). This line will

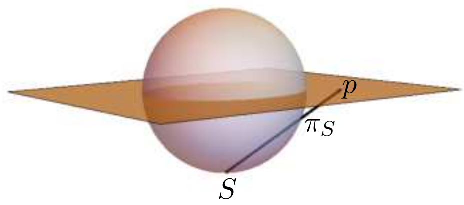

Figure 3.2: Projection π_S.

intercept S^2 if, and only if, $t = 2/(x^2+y^2+1)$ and, consequently, we can determine the function $\pi_S\colon \mathbb{R}^2 \longrightarrow S^2 \setminus \{S\}$ whose expression is given by

$$\pi_S(x,y) = \left(\frac{2x}{x^2+y^2+1}, \frac{2y}{x^2+y^2+1}, \frac{1-x^2-y^2}{x^2+y^2+1}\right). \tag{3.3}$$

and whose inverse is the function

$$\begin{array}{rccl} \pi_S^{-1}\colon & S^2 & \longrightarrow & \mathbb{R}^2 \\ & (x,y,z) & \longmapsto & \pi_S^{-1}(x,y,z) = \left(\dfrac{x}{1+z}, \dfrac{y}{1+z}\right). \end{array} \tag{3.4}$$

Another kind of projection that will be very helpful in this work is the central projection. Let us consider the plane $P = \{(x,y,z) : y = 1\}$ and the straight line α between the origin O and $q \in S^2 \cap H_1$, where $H_1 = \{(x,y,z) \in S^2 : y > 0\}$. See Figure 3.3. So the line $\alpha(t) = (tx, ty, tz)$ belongs to P if $t = 1/y$. Therefore, the central projection $\pi_c\colon S^2 \cap H_1 \longrightarrow \mathbb{R}^2$ is given by

$$\pi_c(x,y,z) = \left(\frac{x}{y}, \frac{z}{y}\right). \tag{3.5}$$

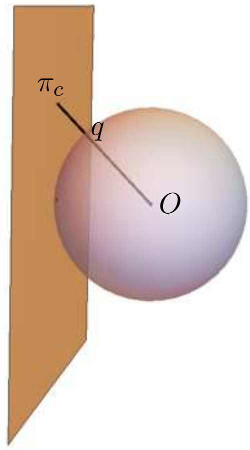

Figure 3.3: Central projection.

It is easy to see that the inverse function of the central projection is given by

$$\begin{array}{rccl} \pi_c^{-1}: & \mathbb{R}^2 & \longrightarrow & S^2 \cap H_1 \\ & (u,v) & \longmapsto & \pi_c^{-1}(u,v) = \left(\dfrac{u}{\sqrt{u^2+v^2+1}}, \dfrac{1}{\sqrt{u^2+v^2+1}}, \dfrac{v}{\sqrt{u^2+v^2+1}}\right). \end{array} \tag{3.6}$$

An analogous of the central projection can be defined in the rear hemisphere $H_2 = \{(x,y,z) \in S^2 : y < 0\}$ of S^2. We will call it rear projection and it is given by

$$\pi_r(x,y,z) = \left(\frac{-x}{y}, \frac{-z}{y}\right). \tag{3.7}$$

We may observe that the inverse of the function π_r is described by

$$\begin{array}{rccl} \pi_r^{-1}: & \mathbb{R}^2 & \longrightarrow & S^2 \cap H_2 \\ & (u,v) & \longmapsto & \pi_r^{-1}(u,v) = \left(\dfrac{u}{\sqrt{u^2+v^2+1}}, \dfrac{-1}{\sqrt{u^2+v^2+1}}, \dfrac{v}{\sqrt{u^2+v^2+1}}\right). \end{array} \tag{3.8}$$

Those projections will be handy in the changeover between the systems in the plane and in the sphere.

3.2 Obtainment of a PSVF in S^2 without equilibria and containing a chaotic minimal set

Firstly, we describe some important features of the vector fields that we are considering. Particularly, we analyze the behavior of their trajectories and their projections on the unit sphere in order to create a flow in S^2 without equilibria and with a non-trivial minimal set. In this way, let us consider the planar vector field given by

$$\begin{cases} \dot{x} &= 2; \\ \dot{y} &= y\left(x^3 - 3x\right), \end{cases} \tag{3.9}$$

where the overhead dot means the derivative with respect to time t. The phase portrait of the vector field $X(x,y) = \big(2, y(x^3 - 3x)\big)$ is given in Figure 3.4.

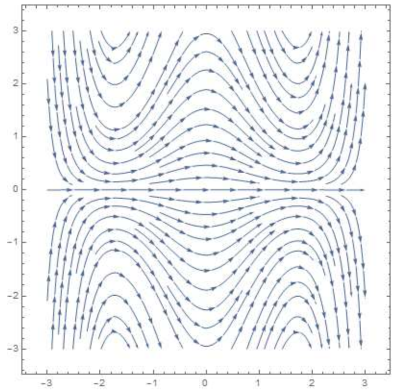

Figure 3.4: Vector field X.

The vector field X is tangent to $S^1 = \big\{(x,y) \in \mathbb{R}^2 : x^2 + y^2 = 1\big\}$ if, and only if, the scalar product between $X(x,y)$ and $(x,y) \in S^1$ is zero, that is, $2x + \big(1 - x^2\big)\left(x^3 - 3x\right) = 0$. So, for positive values of y, the vector field X is tangent to S^1 at the points $p_0 = (0,1)$, $p_1 = (\sqrt{2-\sqrt{3}}, \sqrt{-1+\sqrt{3}})$ and $p_2 = (-\sqrt{2-\sqrt{3}}, \sqrt{-1+\sqrt{3}})$. Since $\dot{x} = dx/dt = 2$ we have that $dy/dx = y(x^3 - 3x)/2$. Therefore

$$y_1(x) = y_0 e^{\frac{x^4}{8} - \frac{3x^2}{4}}$$

and every integral curve of (3.9) can be described by $y_1(x)$. We may also observe that $y_1(x) = y_1(-x)$ which means the function y_1 is symmetric with respect to axis y.

In what follows, we project the trajectories of (3.9) in the south hemisphere $V = \big\{(x,y,z) \in S^2 : z \leq 0\big\}$ of S^2. Let us consider the set $W = \big\{(x,y) \in \mathbb{R}^2 : x^2 + y^2 \leq 1\big\}$. Given a point $(x, y_1(x)) \in W$ we have that

$$\pi_N(x, y_1(x)) = \left(\frac{2x}{x^2 + y_1^2(x) + 1}, \frac{2y_1(x)}{x^2 + y_1^2(x) + 1}, \frac{x^2 + y_1^2(x) - 1}{x^2 + y_1^2(x) + 1}\right) \tag{3.10}$$

is a point of V. Then, we have projected the trajectories of X in the south hemisphere of S^2 as we can see illustrated in Figure 3.5. We can notice that, as the projection π_N is the identity in S^1, we have the points p_0, p_1 and p_2 are still the tangency points between π_N and $S^1 \subset S^2$.

In a similar way, we can project another vector field in the north hemisphere $U =$

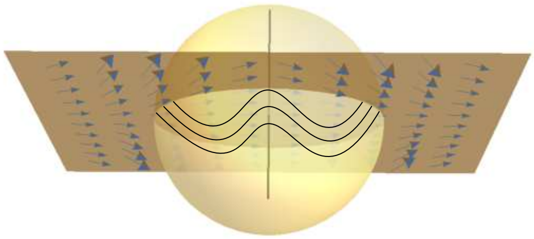

Figure 3.5: Projection of the trajectories of X on S^2 by π_N.

$\{(x, y, z) \in S^2 : z \geq 0\}$ of S^2 using the south stereographic projection π_S. Indeed, consider the following vector field

$$\begin{cases} \dot{x} &= -1; \\ \dot{y} &= 0. \end{cases} \tag{3.11}$$

The phase portrait of the vector field $Y(x, y) = (-1, 0)$ is given in Figure 3.6.

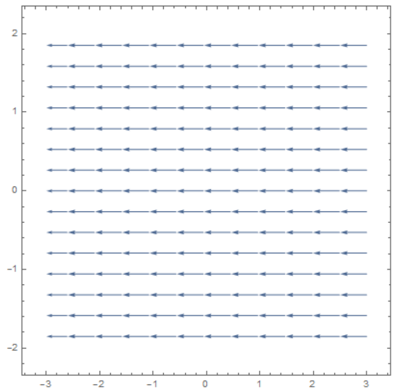

Figure 3.6: Vector field Y.

The vector field Y is tangent to S^1 if, and only if, $x = 0$. So, Y is tangent to S^1 at the points $p_3 = (0, 1)$ and $p_4 = (0, -1)$. Since $dx = -dt$ we have $dy/dx = 0$ and therefore $y_2(x) = c$, where $c \in \mathbb{R}$, describe the trajectories of (3.11). We observe that this function is also symmetric with respect to axis y. Considering the projection π_S we have that

$$\pi_S(x, y_2(x)) = \left(\frac{2x}{x^2 + c^2 + 1}, \frac{2c}{x^2 + c^2 + 1}, \frac{1 - x^2 - c^2}{x^2 + c^2 + 1} \right) \tag{3.12}$$

where $(x, y_2(x)) \in W$ and, consequently, $\pi_S(x, y_2(x)) \in U$. See Figure 3.7.

Attaching those two distinct flows given by Equations (3.10) and (3.12) we have accomplished piecewise smooth trajectories in S^2 whose switching manifold is S^1. See Figure 3.8.

In order to exhibit some properties of the vector field Z associated with the trajectories in S^2, we move towards the projection of those orbits in a plane using the central projection. Since

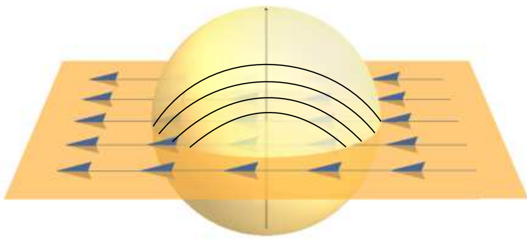

Figure 3.7: Projection of the trajectories of Y in S^2 by π_S.

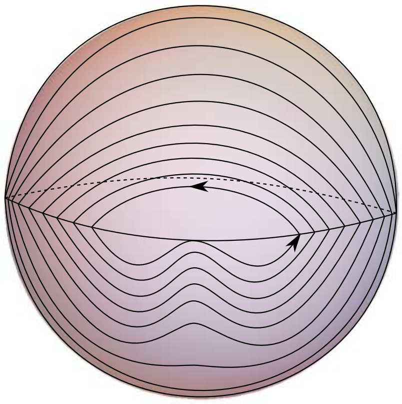

Figure 3.8: Trajectories in S^2.

we have a bijection between a hemisphere of the sphere and $W \subset \mathbb{R}^2$, the properties of these two systems will be related. In this way, let us consider the central projection given by Equation (3.5). Applying the central projection in the hemisphere $H_1 = \{(x, y, z) \in S^2 : y > 0\}$ of S^2 we get the trajectories in $\mathbb{R}^2$ are modelled by $\pi_c\left(\pi_N(x, y_1(x))\right)$ and $\pi_c\left(\pi_S(x, y_2(x))\right)$ where

$$\pi_c\left(\pi_N(x, y_1(x))\right) = \left(\frac{x}{y_1(x)}, \frac{x^2 + y_1^2(x) - 1}{2y_1(x)}\right) \tag{3.13}$$

and

$$\pi_c\left(\pi_S(x, y_2(x))\right) = \left(\frac{x}{c}, \frac{1 - x^2 - c^2}{2c}\right). \tag{3.14}$$

We must notice that $\pi_c \circ \pi_N$ and $\pi_c \circ \pi_S$ provide us a change of variables in $\mathbb{R}^2$. In fact, doing $\pi_N^{-1}\left(\pi_c^{-1}(u, v)\right) = (x, y_1(x))$ we obtain the change of variables

$$\begin{cases} x &= \dfrac{u}{\sqrt{u^2 + v^2 + 1} - v}; \\[2ex] y_1(x) &= \dfrac{1}{\sqrt{u^2 + v^2 + 1} - v}. \end{cases} \tag{3.15}$$

Similarly, doing $\pi_S^{-1}\left(\pi_c^{-1}(u,v)\right) = (x, y_2(x))$ we have the change of variables

$$\begin{cases} x &=& \dfrac{u}{\sqrt{u^2+v^2+1}+v}; \\ y_2(x) &=& \dfrac{1}{\sqrt{u^2+v^2+1}+v}. \end{cases} \tag{3.16}$$

By (3.15), we have

$$\begin{array}{rcl} \dfrac{du}{dt} &=& \dfrac{du}{dx} \\ &=& \dfrac{d}{dx}\left(\dfrac{x}{y_1(x)}\right) \\ &=& \dfrac{2-x^4+3x^2}{y_1(x)} \\ &=& (\sqrt{u^2+v^2+1}-v)\left(2-\dfrac{u^4}{(\sqrt{u^2+v^2+1}-v)^4}+\dfrac{3u^2}{(\sqrt{u^2+v^2+1}-v)^2}\right) \\ &:=& G_1(u,v) \end{array}$$

and

$$\begin{array}{rcl} \dfrac{dv}{dt} &=& \dfrac{dv}{dx} \\ &=& \dfrac{d}{dx}\left(\dfrac{x^2+y_1^2(x)-1}{2y_1(x)}\right) \\ &=& \dfrac{x+4x^3-x^5+y_1^2(x)(x^3-3x)}{2y_1(x)} \\ &=& \dfrac{u\left(-1+2u^4+v^2+4v^4+v\sqrt{u^2+v^2+1}-4v^3\sqrt{u^2+v^2+1}+u^2\left(2+8v^2-6v\sqrt{u^2+v^2+1}\right)\right)}{(v-\sqrt{u^2+v^2+1})^4} \\ &:=& G_2(u,v) \end{array}$$

Then, the system in the plane uv, for $v<0$, associated with the trajectories of the vector field X is given by

$$\begin{cases} \dot{u} &=& G_1(u,v); \\ \dot{v} &=& G_2(u,v). \end{cases} \tag{3.17}$$

In the same way, by (3.16), we have

$$\begin{array}{rcl} \dfrac{du}{dt} &=& -\dfrac{du}{dx} \\ &=& -\dfrac{d}{dx}\left(\dfrac{x}{y_2(x)}\right) \\ &=& -\dfrac{1}{c} \\ &:=& F_1(u,v) \end{array}$$

and

$$\begin{aligned}\tfrac{dv}{dt} &= -\frac{dv}{dx} \\ &= -\frac{d}{dx}\left(\frac{1-x^2-y_2^2(x)}{2y_2(x)}\right) \\ &= \frac{x}{c} \\ &= \frac{u}{c(v+\sqrt{u^2+v^2+1})} \\ &:= F_2(u,v)\end{aligned}$$

Thus, the system in the plane uv, for $v>0$, associated with the trajectories of the vector field Y is given by

$$\left\{\begin{aligned}\dot{u} &= F_1(u,v); \\ \dot{v} &= F_2(u,v).\end{aligned}\right. \tag{3.18}$$

Therefore, we obtain the piecewise smooth vector field

$$Z_1(u,v) = \begin{cases} F(u,v) = (F_1(u,v), F_2(u,v)) & \text{if } v \geq 0; \\ G(u,v) = (G_1(u,v), G_2(u,v)) & \text{if } v \leq 0, \end{cases} \tag{3.19}$$

where the switching manifold is given by $\Sigma = f^{-1}(0)$ with $f(u,v) = v$. See Figure 3.9.

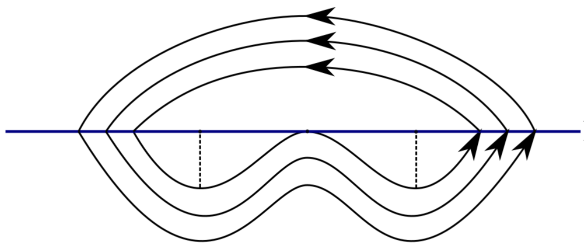

Figure 3.9: Trajectories of the vector field Z_1.

The next result will bring some properties of the vector field Z_1.

Proposition 12. *Let Z_1 be given by (3.19). Then, the fold points of the vector field G are $q_0 = (0,0)$, $q_1 = \left(\frac{\sqrt{2-\sqrt{3}}}{\sqrt{-1+\sqrt{3}}}, 0\right)$ and $q_2 = \left(-\frac{\sqrt{2-\sqrt{3}}}{\sqrt{-1+\sqrt{3}}}, 0\right)$. Moreover, q_0 is a visible fold point while q_1 and q_2 are invisible fold points.*

Proof. In fact, by a straightforward calculation we get

$$\begin{aligned}Gf(u,v) &= \langle G(u,v), \nabla f(u,v)\rangle \\ &= G(u,v)\cdot(0,1) \\ &= G_2(u,v).\end{aligned}$$

Then $Gf(u,0)=0$ if, and only if,

$$G_2(u,0)=\frac{u(-1+2u^2+2u^4)}{(1+u^2)^2}=0$$

which nulls at zero, $\frac{\sqrt{2-\sqrt{3}}}{\sqrt{-1+\sqrt{3}}}$ or $-\frac{\sqrt{2-\sqrt{3}}}{\sqrt{-1+\sqrt{3}}}$. Also, we have

$$G^2f(u,v)=\langle G(u,v),\nabla Gf(u,v)\rangle=(G_1(u,v),G_2(u,v))\cdot\left(\frac{\partial G_2(u,v)}{\partial u},\frac{\partial G_2(u,v)}{\partial v}\right).$$

Since

$$G^2f(u,0)=\frac{2\left(-1+10u^2+6u^4\right)}{(1+u^2)^{\frac{3}{2}}}$$

we obtain $G^2f(q_0)=-2<0$ and $G^2f(q_1)=G^2f(q_2)=\frac{8\sqrt{6}}{(1+\sqrt{3})^{\frac{3}{2}}}>0$. □

Remark 9. *We can observe that the fold points of the vector field G are images of the points p_0, p_1 and p_2 by the function composition $\pi_c\circ\pi_N$.*

Proposition 13. *Let Z_1 be given by* (3.19)*. Then, the unique fold point of the vector field F is $q_0=(0,0)$ which is an invisible fold point.*

Proof. Indeed, we have $Ff(u,v)=\langle F(u,v),\nabla f(u,v)\rangle=F_2(u,v)$. Since

$$F_2(u,0)=\frac{u}{c\sqrt{1+u^2}},$$

then the equation $Ff(u,0)=F_2(u,0)=0$ has $u=0$ as unique real root. Furthermore,

$$F^2f(u,v)=\frac{-1}{c^2(v+\sqrt{1+u^2+v^2})}.$$

Therefore, $F^2f(0,0)=-1/c^2<0$ and we conclude that q_0 is an invisible fold point. □

We may observe that the vector field Z_1 given by (3.19) has a sliding region Σ^s given by the interval $\left(-\frac{\sqrt{2-\sqrt{3}}}{\sqrt{-1+\sqrt{3}}},0\right)\subset\Sigma$ and it has an escaping region Σ^e given by the interval $\left(0,\frac{\sqrt{2-\sqrt{3}}}{\sqrt{-1+\sqrt{3}}}\right)\subset\Sigma$ where we can define the sliding vector field associated with the vector field Z_1 given by Definition 1.

Proposition 14. *The sliding vector field associated to the vector field Z_1 does not have equilibria.*

Proof. Let Z_1^s be the sliding vector field associated with Z_1. By Equation (1.2) we have that

$$Z_1^s(u,v)=\frac{Gf(u,v)F(u,v)-Ff(u,v)G(u,v)}{Gf(u,v)-Ff(u,v)}.$$

Then, by a straightforward calculation we get

$$Z_1^s(u,0) = \frac{1+9u^2+6u^4}{(1+u^2)^{\frac{3}{2}} + c(1-2(u^2+u^4))}. \tag{3.20}$$

So, it is easy to see that Z_1^s does not have equilibria in its domain $\Sigma^s \cup \Sigma^e$. Moreover, since the sliding vector field can be extend to its closure we need to verify that $\lim_{u\to a} Z_1^s(u,0)$ is non-zero for all $a \in \overline{\Sigma^e} \cup \overline{\Sigma^s}$. Since $\lim_{u\to 0} Z_1^s(u,0) > 0$ and

$$\lim_{u\to q_1} Z_1^s(u,0) = \lim_{u\to q_2} Z_1^s(u,0) = \frac{\sqrt{2}(5+3\sqrt{3})}{(-1+\sqrt{3})^{\frac{3}{2}}},$$

we can conclude that Z_1^s does not have equilibria. □

An analogous of the central projection can be applied in the hemisphere $H_2 = \{(x,y,z) \in S^2 : y < 0\}$ of S^2 and we can obtain a planar piecewise smooth vector field Z_2 with similar properties of system Z_1 given by (3.19).

In order to exhibit a chaotic non-trivial minimal set associated with the trajectories in S^2 we are going to use the planar piecewise smooth vector field Z_1 and then relate this new piecewise system to the one found by the authors in [19] and [18], where it was proved containing a chaotic non-trivial minimal set.

Consider $Z_3 = (X_3, Y_3) \in \Omega^r$, where $X_3(x,y) = (1,-2x)$, $Y_3(x,y) = (-2, 4x^3 - 2x)$ and $\Sigma_3 = \{(x,y) \in \mathbb{R}^2 : y = 0\}$ is the switching manifold. The parametric equation for the integral curves of X and Y with initial conditions $(x(0), y(0)) = (0, k_+)$ and $(x(0), y(0)) = (0, k_-)$, respectively, are known and its algebraic expressions are given by $y = -x^2 + k_+$ and $y = x^4/2 - x^2/2 + k_-$, respectively. It is easy to see that $(0,0)$ is an invisible tangency point of X and a visible one of Y. Moreover the points $(\pm\sqrt{2}/2, 0)$ are both invisible tangency points of Y. Note that there exists an escaping and sliding regions between those points. Consider now the particular trajectories of X and Y for the cases when $k_+ = 1$ and $k_- = 0$, respectively. These particular curves delimit a bounded region of plane that we call Λ_3. See Figure 3.10.

The next result is very important in the sequel and the proof can be found in [19] and [18].

Proposition 15. *Consider $Z_3 = (X_3, Y_3) \in \Omega^r$, where $X_3(x,y) = (1,-2x)$, $Y_3(x,y) = (-2, 4x^3 - 2x)$ and $\Sigma_3 = \{(x,y) \in \mathbb{R}^2 : y = 0\}$ is the switching manifold. The set Λ_3 is a minimal set for Z_3. Moreover, the planar piecewise smooth vector field Z_3 is chaotic on the compact invariant set Λ_3.*

By Proposition 15, we will conclude that the piecewise smooth vector field Z_1 given by (3.19) has the same properties of the vector field Z_3 in a related set. Let us consider the particular

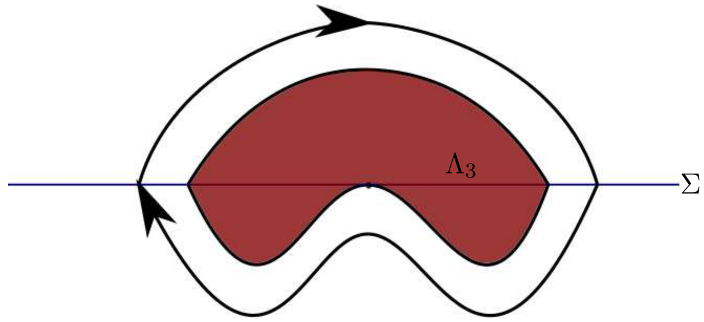

Figure 3.10: Piecewise smooth vector field Z_3 and region Λ_3.

trajectory $\phi_G(q_0)$ of the vector field G passing through q_0. Let a be the point of intersection between $\phi_G(q_0)$ and $\Sigma\cap\{u>0\}$ and consider $\phi_F(a)$. Let us call Λ the bounded region delimited by these trajectories. See Figure 3.11.

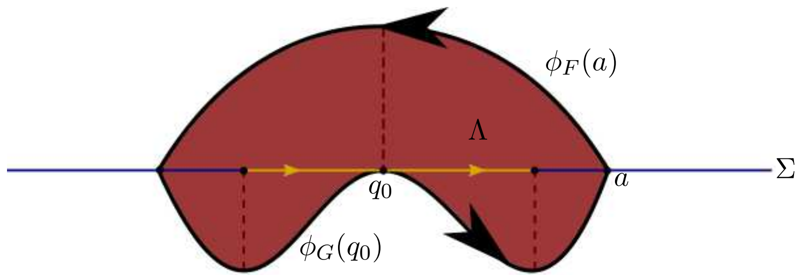

Figure 3.11: Piecewise smooth vector field Z_1 and region Λ.

Definition 16. *Two piecewise smooth vector fields Z and $\bar{Z}$ defined in open sets U, $\bar{U}$ and with switching manifolds $\Sigma \subset U$ and $\bar{\Sigma} \subset \bar{U}$, respectively, are Σ-equivalent if there exists an orientation preserving homeomorphism $h\colon U \longrightarrow \bar{U}$ which sends Σ to $\bar{\Sigma}$ and sends orbits of Z to orbits of $\bar{Z}$.*

Proposition 16. *Consider the piecewise smooth vector field Z_1 given by* (3.19). *Then Λ is a minimal set for Z_1. Moreover, Z_1 is chaotic on Λ.*

Proof. It it enough to see that Z_3 is Σ-equivalent to $-Z_1$. Therefore, the piecewise smooth vector field Z_1 has the same properties of Z_3. □

We observe that the trajectories given by Equations (3.10) and (3.12) defined in the sphere S^2 generate a PSVF Z tangent to S^2. Since we have a bijection between the trajectories of the planar piecewise smooth vector fields Z_1 and the trajectories defined in the hemisphere H_1 of S^2 we have a respective behavior in the trajectories of Z. Therefore, $\pi_c^{-1}(\Lambda)$ is a minimal chaotic set for the vector field Z defined in S^2. Similarly, there is a bijection between the trajectories of the planar piecewise smooth vector field Z_2 and the trajectories defined in the hemisphere H_2 of S^2. These trajectories will generate a minimal chaotic set similar to Λ. Therefore we can conclude the following result:

Theorem 10. *There exists a piecewise smooth vector field Z tangent to the sphere S^2 such that Z does not have equilibria. Moreover, the piecewise smooth vector field Z contain a chaotic non-trivial minimal set.*

3.3 Obtainment of a PSVF in S^2 where S^2 itself is a minimal set

Let us consider the projection of the trajectories of X given by (3.9) on S^2 by π_N studied in the above section. In a similar way, we can project another vector field in the north hemisphere $U = \{(x, y, z) \in S^2 : z \geq 0\}$ of S^2 using the south stereographic projection π_S. In fact, consider a new vector field given by

$$\begin{cases} \dot{x} &= -1; \\ \dot{y} &= x\left(\frac{x}{2} - y\right). \end{cases} \tag{3.21}$$

The phase portrait of the vector field $\overline{Y}(x, y) = (-1, x(x/2 - y))$ is given in Figure 3.12.

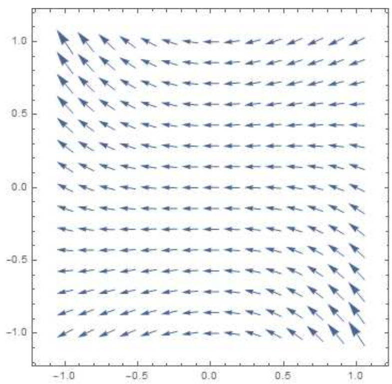

Figure 3.12: Vector field $\overline{Y}$.

The vector field $\overline{Y}$ is tangent to S^1 if, and only if, $x = 0$. So, $\overline{Y}$ is tangent to S^1 at the points $p_3 = (0, 1)$ and $p_4 = (0, -1)$. Since $dx = -dt$ we have

$$\frac{dy}{dx} = -\frac{x^2}{2} + xy$$

and therefore

$$y_2(x) = \frac{1}{4}\left(2x + 4e^{\frac{x^2}{2}}c_0 - e^{\frac{x^2}{2}}\sqrt{2\pi}\,\mathrm{Erf}\left(\frac{x}{\sqrt{2}}\right)\right),$$

with $y_2(0) = c_0$, describe the trajectories of (3.21). Here, Erf $(\cdot)$ is the Gauss error function (see [125]). Considering expression (3.3) we get

$$\pi_S(x, y_2(x)) = \left(\frac{2x}{x^2 + y_2^2(x) + 1}, \frac{2y_2(x)}{x^2 + y_2^2(x) + 1}, \frac{1 - x^2 - y_2^2(x)}{x^2 + y_2^2(x) + 1} \right) \tag{3.22}$$

where $(x, y_2(x)) \in W$ and, consequently, $\pi_S(x, y_2(x)) \in U$. See Figure 3.13.

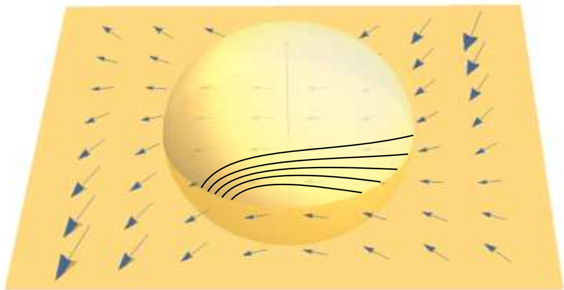

Figure 3.13: Projection of the trajectories of $\overline{Y}$ in S^2 by π_S.

Considering the two distinct flows given by Equations (3.10) and (3.22) we have piecewise smooth trajectories in S^2 as we see illustrated in Figure 3.14. Associated with this trajectories there exists a three dimensional piecewise smooth vector field Z whose switching manifold is S^1.

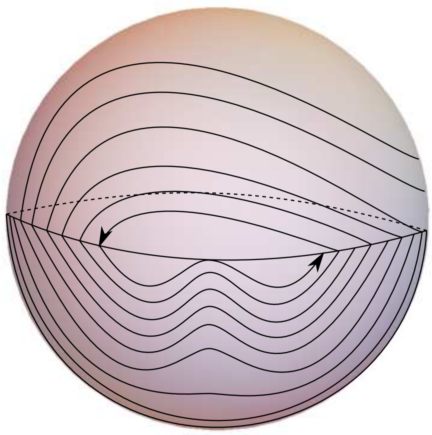

Figure 3.14: Trajectories in S^2.

We can notice that these trajectories will not configure periodic orbits since $\overline{Y}$ is asymmetric. In fact, let us consider the system $\overline{Y}$ given by (3.21). Considering an initial condition $\left(x_0, \sqrt{1-x_0^2}\right) \in S^1$, where $x_0 \in (0,1)$, and solving the initial value problem given by

$$\begin{cases} \dot{x} = -1; \\ \dot{y} = x\left(\frac{x}{2} - y\right); \\ x(0) = x_0; \\ y(0) = \sqrt{1-x_0^2}, \end{cases} \tag{3.23}$$

we can find an explicit solution $y(t) = y(-x+x_0)$ whose expression will be omitted. Let us consider the displacement function $P(x_0) = y(x_0) - y(-x_0)$. We can observe that the displacement function P allow us to analyze the y-coordinate of the trajectory passing through x_0 at the transversal section $\{x = -x_0\}$. See Figure 3.15. By a straightforward calculation we

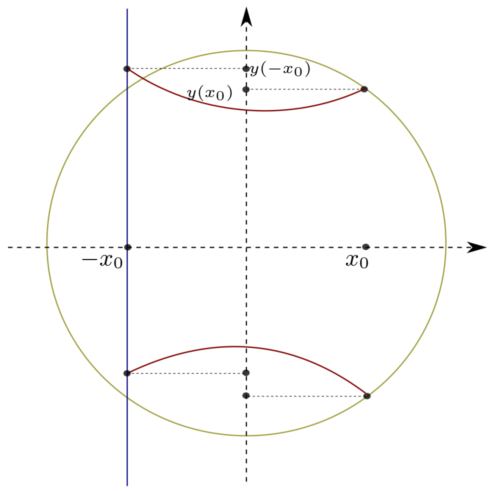

Figure 3.15: Displacement function.

have that $P(x_0)$ is given by

$$P(x_0) = x_0 - e^{\frac{x_0^2}{2}} \sqrt{\frac{\pi}{2}} \ \mathrm{Erf}\left(\frac{x_0}{\sqrt{2}}\right).$$

Since $P(0) = 0$ and the derivative of P is strictly negative for $x_0 \in (0,1)$ we can conclude that P does not have real roots for $x_0 \in (0,1)$. Therefore, we have that $y(x_0) < y(-x_0)$ for all $x_0 \in (0,1)$. Since the stereographic projection π_S is the identity in S^1, we will not have symmetry in the projected trajectories of $\overline{Y}$ in S^2.

Let us consider the central projection given by Equation (3.5). Applying the central projection in the hemisphere $H_1 = \{(x,y,z) \in S^2 : y > 0\}$ of S^2 we get the trajectories in

$\mathbb{R}^2$ are modeled by $\pi_c\left(\pi_N(x, y_1(x))\right)$ and $\pi_c\left(\pi_S(x, y_2(x))\right)$ where

$$\pi_c\left(\pi_N(x, y_1(x))\right) = \left(\frac{x}{y_1(x)}, \frac{x^2 + y_1^2(x) - 1}{2y_1(x)}\right) \tag{3.24}$$

and

$$\pi_c\left(\pi_S(x, y_2(x))\right) = \left(\frac{x}{y_2(x)}, \frac{1 - x^2 - y_2^2(x)}{2y_2(x)}\right). \tag{3.25}$$

We must notice that $\pi_c \circ \pi_N$ and $\pi_c \circ \pi_S$ provide us a change of variables in $\mathbb{R}^2$. In fact, doing $\pi_N^{-1}\left(\pi_c^{-1}(u, v)\right) = (x, y_1(x))$ we obtain the change of variables

$$\begin{cases} x & = \dfrac{u}{\sqrt{u^2 + v^2 + 1} - v}; \\ y_1(x) & = \dfrac{1}{\sqrt{u^2 + v^2 + 1} - v}. \end{cases}$$

given by Equation (3.15). Similarly, doing $\pi_S^{-1}\left(\pi_c^{-1}(u, v)\right) = (x, y_2(x))$ we have the change of variables

$$\begin{cases} x & = \dfrac{u}{\sqrt{u^2 + v^2 + 1} + v}; \\ y_2(x) & = \dfrac{1}{\sqrt{u^2 + v^2 + 1} + v}. \end{cases} \tag{3.26}$$

Due to these changes of variables, we can find the piecewise smooth vector field associated with these trajectories. Indeed, by (3.15) we have

$$\begin{cases} \dot{u} & = G_1(u, v); \\ \dot{v} & = G_2(u, v). \end{cases}$$

already given by (3.17). In the same way, by (3.26) we have

$$\begin{aligned} \frac{du}{dt} &= -\frac{du}{dx} \\ &= -\frac{d}{dx}\left(\frac{x}{y_2(x)}\right) \\ &= -\frac{2 + u^3 + 4v^2 + 4v\sqrt{1 + u^2 + v^2}}{2(v + \sqrt{1 + u^2 + v^2})} \\ &:= W_1(u, v) \end{aligned}$$

and

$$\begin{aligned}\frac{dv}{dt} &= -\frac{dv}{dx}\\ &= -\frac{d}{dx}\left(\frac{1-x^2-y_2^2(x)}{2y_2(x)}\right)\\ &= \frac{u(4+2u^2+6v^2+6v\sqrt{1+u^2+v^2}-u(1+v^2+v\sqrt{1+u^2+v^2}))}{2(v+\sqrt{1+u^2+v^2})^2}\\ &:= W_2(u,v)\end{aligned}$$

Thus the system in the plane uv, for $v>0$, associated with the trajectories of the vector field $\overline{Y}$ is given by

$$\begin{cases}\dot{u} = W_1(u,v);\\ \dot{v} = W_2(u,v).\end{cases} \tag{3.27}$$

Therefore, we obtain the piecewise smooth vector field

$$Z_3(u,v) = \begin{cases} W(u,v) = (W_1(u,v), W_2(u,v)) & \text{if } v \geq 0;\\ G(u,v) = (G_1(u,v), G_2(u,v)) & \text{if } v \leq 0,\end{cases} \tag{3.28}$$

where the switching manifold is given by $\Sigma = f^{-1}(0)$ with $f(u,v) = v$. See Figure 3.16.

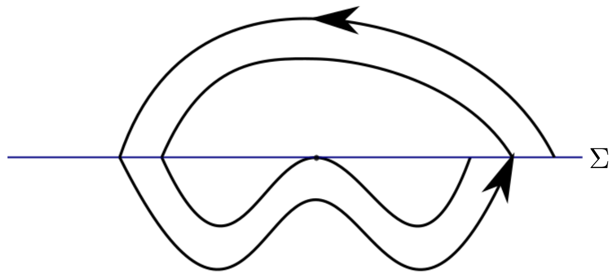

Figure 3.16: Trajectories of the vector field Z_1.

By Proposition 12 we have seen that the fold points of the vector field G are given by $q_0 = (0,0)$, $q_1 = \left(\frac{\sqrt{2-\sqrt{3}}}{\sqrt{-1+\sqrt{3}}}, 0\right)$ and $q_2 = \left(-\frac{\sqrt{2-\sqrt{3}}}{\sqrt{-1+\sqrt{3}}}, 0\right)$. Also, q_0 is a visible fold point while q_1 and q_2 are invisible fold points.

Proposition 17. *Let Z_3 be given by* (3.28)*. Then, the unique fold point of the vector field W is $q_0 = (0,0)$ which is an invisible fold point.*

Proof. Indeed, we have $Wf(u,v) = \langle W(u,v), \nabla f(u,v)\rangle = W_2(u,v)$. Since

$$W_2(u,0) = \frac{u(4-u+2u^2)}{2(1+u^2)},$$

then the equation $Wf(u,0) = W_2(u,0) = 0$ has $u = 0$ as unique real root. Furthermore,

$$W^2 f(u,v) = \frac{-8+4u-4u^2-2u^3+5u^4-4u^5}{4(1+u^2)^{\frac{3}{2}}}.$$

Therefore, $W^2 f(0,0) = -2 < 0$ and we conclude that q_0 is an invisible fold point. $\square$

We note that the vector field Z_3 given by (3.28) has the sliding region $\Sigma^s = \left(-\frac{\sqrt{2-\sqrt{3}}}{\sqrt{-1+\sqrt{3}}}, 0\right)$ and the escaping region $\Sigma^e = \left(0, \frac{\sqrt{2-\sqrt{3}}}{\sqrt{-1+\sqrt{3}}}\right)$ where we can define the sliding vector field.

Proposition 18. *The sliding vector field associated with the vector field Z_3 does not have equilibria.*

Proof. Let Z_3^s be the sliding vector field associated with Z_3. By Equation (1.2), we have that

$$Z_3^s(u,v) = \frac{Gf(u,v)W(u,v) - Wf(u,v)G(u,v)}{Gf(u,v) - Wf(u,v)}.$$

Then, by a straightforward calculation we get

$$Z_3^s(u,0) = -\frac{2(3-u+18u^2-4u^3+17u^4-u^5+4u^6+u^7)}{\sqrt{1+u^2}(-6+u-2u^2+u^3+2u^4)}. \tag{3.29}$$

So, we have that Z_3^s does not have equilibria in its domain $\Sigma^s \cup \Sigma^e$. Moreover, since the sliding vector field can be extended to its closure we need to verify that $\lim_{u\to a} Z_3^s(u,0)$ is non-zero for all $a \in \overline{\Sigma^e} \cup \overline{\Sigma^s}$. Since $\lim_{u\to 0} Z_3^s(u,0) = 1$ and

$$\lim_{u\to q_1} Z_3^s(u,0) = \lim_{u\to q_2} Z_3^s(u,0) = \frac{2}{(-1+\sqrt{3})^{\frac{3}{2}}},$$

we can conclude that Z_3^s does not have equilibria. $\square$

We can apply the central projection to the hemisphere $H_2 = \{(x,y,z) \in S^2 : y < 0\}$ of S^2 in order to obtain a planar piecewise smooth vector field Z_4 with similar properties of system Z_3 given by (3.28). Indeed, let us consider the projection π_r given by equation (3.7). Applying the function π_r in the hemisphere H_2 of S^2 we get the trajectories in $\mathbb{R}^2$ are modeled by $\pi_r(\pi_N(x,y_1(x)))$ and $\pi_r(\pi_S(x,y_2(x)))$ where

$$\pi_r(\pi_N(x,y_1(x))) = \left(\frac{-x}{y_1(x)}, \frac{1-x^2-y_1^2(x)}{2y_1(x)}\right) \tag{3.30}$$

and

$$\pi_r(\pi_S(x,y_2(x))) = \left(\frac{-x}{y_2(x)}, \frac{x^2+y_2^2(x)-1}{2y_2(x)}\right). \tag{3.31}$$

Proceeding in the same way used to find the vector field Z_3, applying the changes of variables provided by $\pi_S^{-1}\left(\pi_r^{-1}(u,v)\right) = (x, y_2(x))$ and $\pi_N^{-1}\left(\pi_r^{-1}(u,v)\right) = (x, y_1(x))$ we can obtain the piecewise smooth vector field

$$Z_4(u,v) = \begin{cases} Q(u,v) = (Q_1(u,v), Q_2(u,v)) & \text{if } v \geq 0; \\ G(u,v) = (G_1(u,v), G_2(u,v)) & \text{if } v \leq 0, \end{cases} \tag{3.32}$$

where the switching manifold is given by $\Sigma = f^{-1}(0)$ with $f(u,v) = v$,

$$Q_1(u,v) = \frac{-2 + u^3 - 4v^2 - 4v\sqrt{1+u^2+v^2}}{2\left(v + \sqrt{1+u^2+v^2}\right)}$$

and

$$Q_2(u,v) = \frac{u\left(4 + 2u^2 + 6v^2 + 6v\sqrt{1+u^2+v^2} + u\left(1 + v^2 + v\sqrt{1+u^2+v^2}\right)\right)}{2\left(v + \sqrt{1+u^2+v^2}\right)^2}.$$

See Figure 3.17.

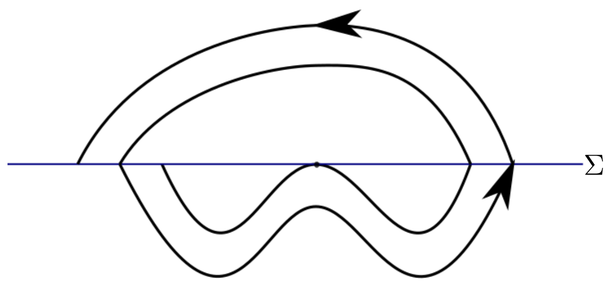

Figure 3.17: Trajectories of the vector field Z_4.

Proposition 19. *Let Z_4 be given by (3.32). Then, the unique fold point of the vector field Q is $q_0 = (0,0)$ which is an invisible fold point.*

Proof. Indeed, we have $Qf(u,v) = \langle Q(u,v), \nabla f(u,v)\rangle = Q_2(u,v)$. Since

$$Q_2(u,0) = \frac{u(4+u+2u^2)}{2(1+u^2)}$$

then the equation $Qf(u,0) = Q_2(u,0) = 0$ has $u = 0$ as unique real root. Furthermore,

$$Q^2 f(u,v) = \frac{-8 - 4u - 4u^2 + 2u^3 + 5u^4 + 4u^5}{4(1+u^2)^{\frac{3}{2}}}.$$

Therefore, $Q^2 f(0,0) = -2 < 0$ and we derive that q_0 is an invisible fold point. $\square$

We may notice that the vector field Z_4 given by (3.32) also has the sliding region Σ^s and the escaping one Σ^e. In this way, we can define the sliding vector field associated with the vector field Z_4.

Proposition 20. *The sliding vector field associated with the vector field Z_4 does not have equilibria.*

Proof. Let Z_4^s be the sliding vector field associated with Z_4. By Equation (1.2) we have that

$$Z_4^s(u,v) = \frac{Gf(u,v)Q(u,v) - Qf(u,v)G(u,v)}{Gf(u,v) - Qf(u,v)}.$$

Then, by a straightforward calculation we get

$$Z_4^s(u,0) = \frac{2\sqrt{1+u^2}(3+u+18u^2+4u^3+17u^4+u^5+4u^6-u^7)}{6+u+8u^2+2u^3+u^5-2u^6}. \tag{3.33}$$

So, it is easy to see that Z_4^s does not have equilibria in its domain. Moreover, since the sliding vector field can be extended to its closure we need to verify that $\lim_{u\to a} Z_4^s(u,0)$ is non-zero for all $a \in \overline{\Sigma^e} \cup \overline{\Sigma^s}$. Since $\lim_{u\to 0} Z_4^s(u,0) = 1$ and

$$\lim_{u\to q_1} Z_4^s(u,0) = \lim_{u\to q_2} Z_4^s(u,0) = \frac{2}{(-1+\sqrt{3})^{3/2}},$$

we can conclude that Z_4^s does not have equilibria.

□

In order to exhibit non-trivial minimal sets associated with the trajectories in S^2, we are going to use the planar piecewise smooth vector fields studied above. Since the orbit passing through a sliding or escaping region on the switching manifold can depart from it when the time goes to future or past, we can introduce some definitions concerning positive and negative invariance for global trajectories.

Definition 17. *A set $M \subset \mathbb{R}^n$ is positively invariant (respectively, negatively invariant) for $Z \in \Omega^r$ if for each $p \in M$ and all positive global trajectory $\Gamma_Z^+(t,p)$ (respectively, negative global trajectory $\Gamma_Z^-(t,p)$) passing through p it holds $\Gamma_Z^+(t,p) \subset M$ (respectively, $\Gamma_Z^-(t,p) \subset M$).*

Remark 10. *We may notice that a set is invariant if, and only if, it is positively invariant and negatively invariant.*

Let us consider the vector field Z_3 given by (3.28) and the particular trajectory $\phi_G(q_0)$ of the vector field G passing through q_0. Let a be the intersection point between $\phi_G(q_0)$ and $\Sigma \cap \{u > 0\}$

and consider $\phi_F(a)$. Furthermore, let us consider $c = \phi_F(a) \cap (\Sigma \cap \{u < 0\})$. These particular curves and the segment $I_1 = (-a, c)$ contained in Σ, delimit a bounded region of the plane that we call K_1. See Figure 3.18.

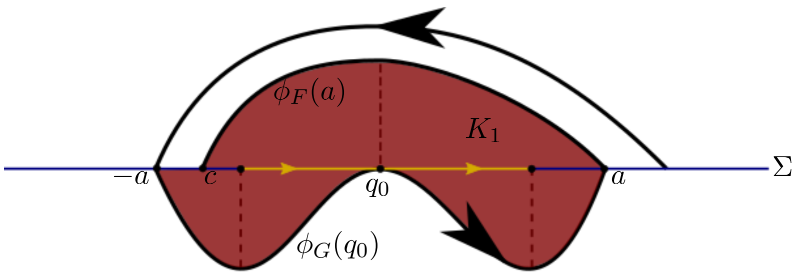

Figure 3.18: Piecewise smooth vector field Z_3 and region K_1.

Lemma 7. *For all $p \in K_1$, q_0 belongs to an orbit passing through p, where $q_0 = (0, 0)$ is a visible fold point for G and an invisible fold point for F.*

Proof. In fact, the positive global trajectory of $p \in K_1$ reaches the sliding region between q_2 and q_0 and slides to q_0 after some time t_p. □

Proposition 21. *Consider the PSVF Z_3 given by* (3.28)*. The set K_1 is positively invariant for Z_3.*

Proof. Indeed, by Lemma 7 a positive global trajectory of any point p in K_1 meets q_0 for some time t_p. Since q_0 is a visible tangency point for G and $q_0 \in \partial\Sigma^e \cap \partial\Sigma^s$ according to the fourth item of Definition 3 any trajectory passing through q_0 remains in K_1. Therefore, K_3 is Z_1-positively invariant. □

Remark 11. *We may observe that K_1 is not Z_3-negatively invariant.*

Let us consider the vector field Z_4 given by (3.32) and the particular trajectory $\phi_G(q_0)$ of the vector field G passing through q_0. Let $-a$ be the intersection point between $\phi_G(q_0)$ and $\Sigma \cap \{u < 0\}$ and consider $\phi_F(-a)$. Furthermore, let us consider $b = \phi_F(-a) \cap (\Sigma \cap \{u > 0\})$. These particular curves and the segment $I_2 = (b, a)$ contained in Σ, delimit a bounded region of plane that we call K_2. See Figure 3.19.

Lemma 8. *For all $p \in K_2$, q_0 belongs to an orbit passing through p, where $q_0 = (0, 0)$ is a visible fold point for G and an invisible fold point for Q.*

Proof. In fact, the negative global trajectory of $p \in K_2$ reaches the escaping region between q_0 and q_1 and slides to q_0 after some time t_p. □

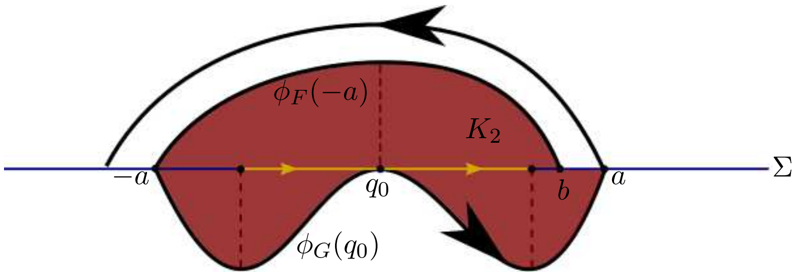

Figure 3.19: Piecewise smooth vector field Z_4 and region K_2.

The next result follows in a similar way from Proposition 21.

Proposition 22. *Consider the vector field Z_4 given by (3.32). The set K_2 is negatively invariant for Z_4. Moreover, K_2 is not positively invariant for Z_4.*

Since we have a bijection between the trajectories of the planar piecewise smooth vector field Z_3 in W and the trajectories defined in the hemisphere H_1 of S^2, we have a respective behavior in the trajectories given by Equations (3.10) and (3.22) defined in the sphere S^2. Similarly, there is a bijection between the trajectories of the planar piecewise smooth vector field Z_4 and the trajectories defined in the hemisphere H_2 of S^2. We can notice that the trajectories defined in the sphere S^2 by Equations (3.10) and (3.22) generate a piecewise smooth vector field Z^* tangent to S^2.

Proposition 23. *The ω-limit of every point of S^2 is contained in $\pi_c^{-1}(K_1)$.*

Proof. In fact, since $\pi_c^{-1}(K_1)$ is Z^*-positively invariant, given $p \in \pi_c^{-1}(K_1)$ we have $\omega(p) \in \pi_c^{-1}(K_1)$. Now, let us suppose $p = (-1, 0, 0)$. Since the vector field X is symmetric we have that the orbit passing through p goes to the point $q = (1, 0, 0)$. Solving the initial value problem given by (3.23) with $x_0 = 1$ we can conclude that the orbit passing through the point $(1, 0)$ in the xy-plane intersects S^1 in a point (x, y) with $y > 0$. So, the trajectory in S^2 passing through p will reach $\pi_c^{-1}(\Sigma)$ and goes to $\pi_c^{-1}(K_1)$ by Proposition 21. See Figure 3.20. For $p \in H_1 = \{(x, y, z) \in S^2 : y > 0\}$ we have that $\pi_c^{-1}(K_1)$ is an attractor of the trajectory through p. Since $\pi_r^{-1}(K_2)$ is a repeller, the orbit passing through $p \in H_2$ will reach H_1 and therefore goes to $\pi_c^{-1}(K_1)$.

□

The next result follows in a similar way from Proposition 23.

Proposition 24. *The α-limit of every point of S^2 is contained in $\pi_r^{-1}(K_2)$.*

In this context, we can prove the following result.

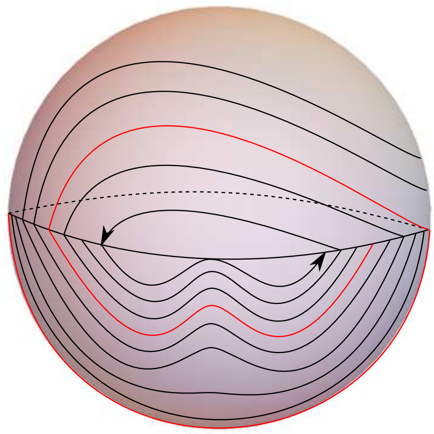

Figure 3.20: Trajectory in S^2 passing through $p = (-1, 0, 0)$.

Proposition 25. *S^2 is minimal for the vector field Z^* generated by the trajectories described by Equations* (3.10) *and* (3.22)*.*

Proof. Indeed, it is easy to see that S^2 is a non-empty compact set. Moreover, S^2 is Z^*-invariant. Now, let M be a Z^*-invariant proper subset of S^2. We have that the ω-limit of every point of S^2 is contained in $\pi_c^{-1}(K_1)$ and the α-limit is contained in $\pi_r^{-1}(K_2)$. So, by Lemma 7, given $p \in M$ we have that q_0 belongs to a positive trajectory of p. Since M is Z^*-invariant we conclude that $q_0 \in M$. Let us consider $q \notin M$. In a similar way, we can conclude that q_0 belongs to a positive trajectory of q. Therefore, since $q_0 \in M$ we have that $q \in M$. This is a contradiction. □

As the main result, we state that there exists a Filippov's vector field tangent to S^2 (a compact two dimensional C^∞ manifold) such that the minimal set is S^2 itself.

Theorem 11. *There exists a piecewise smooth vector field Z^* tangent to the unit sphere S^2 such that S^2 itself is a non-trivial minimal set.*

Proof. It follows from Proposition 25. □

In order to use the well established theory of smooth vector fields to provide properties of discontinuous vector fields, some papers (see [13, 107, 109]) take a discontinuous vector field and regularize it (see Definition 20), giving rise to a smooth vector field. However, this approach can fail in some cases. In fact, combining Theorem 11 and the Smoothing Theorem, we are able to conclude that:

Corollary 2. *None regularization process can establish a topological equivalence between the piecewise smooth vector field of Theorem 11 and a smooth vector field (both tangent to S^2).*

Proof. In fact, if the vector field of Theorem 11 could be regularized giving rise to a smooth vector field $\widetilde{X}$ topologically equivalent to it, then S^2 is a non-trivial minimal set of $\widetilde{X}$. This produces a contradiction, according to the Smoothing Theorem. $\square$

At this point, we are able to introduce a discussion about the density of orbits in minimal sets for PSVFs and about (non)wandering points for PSVFs. As defined in [23],

*a point p is a **nonwandering point** for a PSVF Z if each one of its neighborhoods meets arbitrarily large iterations of itself, for some global trajectory.*

When a point is not nonwandering then it is called wandering. Once a time, this definition coincides with the classical one when the PSVF is a smooth vector field (taking $X = Y$).

Consider the sets $\pi_c^{-1}(K_1)$ and $\pi_c^{-1}(K_2)$ described above. Given a point $q \in S^2$ such that $q \notin \left\{\pi_c^{-1}(K_1) \cup \pi_c^{-1}(K_2)\right\}$, every global trajectory passing through q converges to $\pi_c^{-1}(K_1)$ (see Proposition 23). Moreover, given a small neighborhood $V_q \subset S^2$ of q, none global trajectory passing through a point $\overline{q} \in V_q$ returns to V_q since it enters the positively invariant set $\pi_c^{-1}(K_1)$ (see Proposition 21). As consequence, q is a wandering point for Z and there is neither a dense nor periodic orbit passing through q.

However, it is easy to see that given a point $\widetilde{q} \in \left\{\pi_c^{-1}(K_1) \cup \pi_c^{-1}(K_2)\right\} \subset S^2$, then $\widetilde{q}$ is a nonwandering point for Z and there is not a dense orbit passing through $\widetilde{q}$. According to the choice on $\widetilde{q}$, it is possible the occurrence of a periodic orbit passing through $\widetilde{q}$.

Chapter

4

Creation of periodic orbits in piecewise smooth vector fields tangent to nested tori

The main point of this chapter is to present the interesting behavior generated by piecewise smooth vector fields tangent to foliations. In fact, we consider two smooth foliations $\mathcal{F}_1$ and $\mathcal{F}_2$ that are coupled in order to produce a foliation composed by nested topological tori. Moreover, a piecewise smooth vector field composed by periodic orbits and tangent to these tori is considered. After, we perturb the vector field (and, consequently, the foliations) and we observe the birth of (either finite or infinite many) limit cycles for the 3D piecewise smooth vector field. As consequence, a single trajectory of the piecewise smooth vector field visits infinitely many leaves of the foliations obtained as perturbations of $\mathcal{F}_1$ and $\mathcal{F}_2$ in the process of turning around the limit cycle. The results of this chapter can be found in [53].

A foliation is a decomposition of a smooth manifold M of class C^r (the coordinate charts h should be C^r*-diffeomorphisms*) into a disjoint union of immersed connected submanifolds, that are called leaves. So, such charts induce on each leaf a unique C^r*-smooth structure*, so that must be a C^r*-immersion*. See [21] for details. Just like it happens in the smooth case, some PSVFs are tangent to foliations. Actually, PSVFs are tangent to *piecewise foliations* obtained by the concatenation of smooth foliations. In this work, we consider two smooth foliations (formed as the revolution of parabolas around the z-axis) that are coupled in order to produce a new (piecewise) foliation composed by nested topological tori. Figure 4.1 illustrates this situation.

For $(x,y,x) \in \mathbb{R}^3 \backslash \{z\text{-axis}\}$, the smooth vector field

$$X(x,y,z) = \left(x, y, \frac{4 + \left(x^2+y^2\right)\left(17 - 12\left(x^2+y^2\right)\right)}{4\sqrt{x^2+y^2}} \right)$$

is tangent to the foliation $\mathcal{F}_1$ formed as the revolution of parabolas with concavity down, around the z-axis and

$$Y(x,y,z) = \left(-x, -y, \frac{4 + \left(x^2+y^2\right)\left(17 - 12\left(x^2+y^2\right)\right)}{4\sqrt{x^2+y^2}} \right)$$

is tangent to the foliation $\mathcal{F}_2$ formed as the revolution of parabolas with concavity up, around the z-axis.

In this way, we are able to couple $\mathcal{F}_1$ and $\mathcal{F}_2$ giving rise to a piecewise smooth foliation $\mathcal{F}$ formed by topological tori in such a way that the infinite codimension PSVF (see Corollary 4), defined in $\mathbb{R}^3 \backslash \{z\text{-axis}\}$, given by

$$Z_0(x,y,z) = \begin{cases} X(x,y,z) = \left(x, y, \dfrac{4 + \left(x^2+y^2\right)\left(17 - 12\left(x^2+y^2\right)\right)}{4\sqrt{x^2+y^2}} \right) & z \geq 0, \\ Y(x,y,z) = \left(-x, -y, \dfrac{4 + \left(x^2+y^2\right)\left(17 - 12\left(x^2+y^2\right)\right)}{4\sqrt{x^2+y^2}} \right) & z \leq 0, \end{cases} \tag{4.1}$$

is tangent to $\mathcal{F}$. Through all this chapter we assume that $\Sigma = f^{-1}(0)$, where $f(x,y,z) = z$.

As we prove in the sequel, each trajectory of Z_0 describes a topological circumference (periodic orbit) on the phase portrait and these circumferences take place along a central circumference $C_a = \{(x,y,0) \in \Sigma \,|\, x^2+y^2 = a^2\}$, with $a = \frac{1}{2}\sqrt{\frac{17+\sqrt{481}}{6}}$. Next, we perturb System (4.1) (consequently, the foliations) and the consequences are stated in our main results which concern about the birth of periodic orbits.

Remark 12. *We stress that the results in this chapter have a theoretical purpose and are a continuation/progress of those ones obtained in [25] in the sense that here, there are perturbations of Z_0 where none topological tori persists. In fact, in an opposite situation of that one observed in [25], limit cycles for the 3D PSVF are obtained and it is easy to see that a single trajectory of the PSVF Z_ε can visits infinitely many leaves of the perturbed smooth foliations $\mathcal{F}_1^\varepsilon$ and $\mathcal{F}_2^\varepsilon$ (obtained from $\mathcal{F}_1$ and $\mathcal{F}_2$, respectively) in the process of turning around the limit cycle. This fact is not observed for smooth vector fields, where each trajectory is confined to a single leaf.*

4.1 Properties of the vector field Z_0

This section has the purpose to describe some important features of the vector field Z_0 given by (4.1). In particular, we analyze the first return map associated with it and the behavior of invariant sets. In order to exhibit the first return map associated with $Z_0 = (X, Y)$ given by (4.1) we need the expressions of the half return maps associated with X and Y. A straightforward calculation shows that the trajectories ϕ_X and ϕ_Y are parameterized, respectively, by

$$\phi_X(t) = \left(k_1 e^t, k_2 e^t, \frac{-4 + e^{2t}\left(k_1^2 + k_2^2\right)\left(17 - 4e^{2t}\left(k_1^2 + k_2^2\right)\right)}{4\sqrt{e^{2t}\left(k_1^2 + k_2^2\right)}} + k_3 \right) \tag{4.2}$$

and

$$\phi_Y(t) = \left(l_1 e^{-t}, l_2 e^{-t}, \frac{4 + e^{-2t}\left(l_1^2 + l_2^2\right)\left(-17 + 4e^{-2t}\left(l_1^2 + l_2^2\right)\right)}{4\sqrt{e^{-2t}\left(l_1^2 + l_2^2\right)}} + l_3 \right), \tag{4.3}$$

with $k_1, k_2, k_3, l_1, l_2, l_3 \in \mathbb{R}$.

Although Equations (4.2) and (4.3) give explicit expressions of the flows of X and Y it will be useful the cylindrical coordinates $x(t) = r(t)\cos(\theta(t))$, $y(t) = r(t)\sin(\theta(t))$ and $z(t) = z(t)$. In this way, we may write Equations (4.1), (4.2) and (4.3), respectively, as follows:

$$Z_0(r, \theta, z) = \begin{cases} X(r, \theta, z) = \left(r, 0, \dfrac{4 + 17r^2 - 12r^4}{4r} \right) & \text{if } z \geq 0, \\ Y(r, \theta, z) = \left(-r, 0, \dfrac{4 + 17r^2 - 12r^4}{4r} \right) & \text{if } z \leq 0, \end{cases} \tag{4.4}$$

$$\phi_X(t) = \left(r_0 e^t, \theta_0, -\frac{e^{-t}}{r_0} + \frac{17 r_0 e^t}{4} - r_0^3 e^{3t} + m_0 \right) \tag{4.5}$$

and

$$\phi_Y(t) = \left(\widetilde{r}_0 e^{-t}, \widetilde{\theta}_0, \frac{e^t}{\widetilde{r}_0} - \frac{17\widetilde{r}_0 e^{-t}}{4} + \widetilde{r}_0^3 e^{-3t} + \widetilde{m}_0 \right), \tag{4.6}$$

with $r_0, \widetilde{r}_0 \geq 0$, $\theta_0, \widetilde{\theta}_0 \in [0, 2\pi)$ and $m_0, \widetilde{m}_0 \in \mathbb{R}$.

In the next auxiliary results, let us consider $a = \frac{1}{2}\sqrt{\frac{17+\sqrt{481}}{6}}$,

$$C_r = \{(x, y, 0) \in \mathbb{R}^3 \,|\, x = r\cos(\theta), y = r\sin(\theta) \text{ with } 2\pi > \theta \geq 0\}$$

and establish the half-planes

$$\Pi_{\theta_0} = \{(x, y, z) \in \mathbb{R}^3 \,|\, x = r\cos(\theta_0), y = r\sin(\theta_0) \text{ with } r \geq 0\}.$$

Proposition 26. *Given an arbitrary point* $(r_0, \theta_0, 0) \in \Sigma$ *with* $r_0 < a$ *we have that* $\phi_X(r_0, \theta_0, 0) = (r_0 e^{t_2}, \theta_0, 0)$. *Similarly, if* $(r_0, \theta_0, 0) \in \Sigma$ *with* $r_0 > a$ *then* $\phi_Y(r_0, \theta_0, 0) =$

$(r_0 e^{-t_2}, \theta_0, 0)$, *where the X-flight time (respectively, Y-flight time) $t_2 > 0$ is given by*

$$t_2 = \log\left(\frac{1}{24}\Big(-8 + \frac{4r_0^2(51-8r_0^2)}{M} + \frac{4}{r_0^4}M\Big)\right), \tag{4.7}$$

where

$$M = \left(r_0^8(108 - 153r_0^2 + 28r_0^4) + 3\sqrt{3}\sqrt[3]{r_0^{16}(432 - 6137r_0^2 + 3403r_0^4 - 680r_0^6 + 48r_0^8)}\right)^{1/3}.$$

Proof. Consider the polar expressions (4.5) and (4.6) with

$$m_0 = \widetilde{m}_0 = \frac{4 - 17r_0^2 + 4r_0^4}{4r_0},$$

since the third coordinates of both are equal to zero for $t = 0$. By a straightforward calculation we have that the third coordinates of (4.5) and (4.6) have a strictly positive root for $t = t_2$, given by (4.7). □

Proposition 27. *Let Z_0 be given by (4.1) and $\theta_0 \in [0, 2\pi)$ be fixed. Then each half-plane Π_{θ_0} is fulfilled with periodic orbits.*

Proof. The proof is based on expressions (4.5) and (4.6). Consider $0 < r_0 < a$ and $p_0 = (x_0, y_0, 0) = (r_0\cos(\theta_0), r_0\sin(\theta_0), 0) \in \Sigma \cap \Pi_{\theta_0}$. In polar coordinates, $p_0 = (r_0, \theta_0, 0)$. Using Proposition 26 and (4.5) we derive that the X-trajectory through p_0 returns to $\Sigma \cap \Pi_{\theta_0}$ at $p_1 = (r_0 e^{t_2}, \theta_0, 0)$, where $t_2 > 0$ is given by (4.7). Using Proposition 26 and (4.6) we deduce that the Y-trajectory through p_1 returns to $\Sigma \cap \Pi_{\theta_0}$ at $p_2 = ((r_0 e^{t_2})e^{-t_2}, \theta_0, 0) = p_0$. Therefore, each half-plane Π_{θ_0} is fulfilled with periodic orbits. □

By Proposition 27 we assure that through each cycle C_{r_0}, where $r_0 \in (0, +\infty) \setminus \{a\}$, passes an invariant topological torus T_{r_0}. In fact, given $p_0 = (x_0, y_0, z_0) = (r_0\cos(\theta_0), r_0\sin(\theta_0), 0) \in C_{r_0} \cap \Pi_{\theta_0}$, by Proposition 27 we deduce that there is a periodic orbit passing through p_0. When θ_0 varies on $[0, 2\pi]$ we get a branch of periodic orbits, that is, a topological torus, passing through C_{r_0}. See illustration in Figure 4.1.

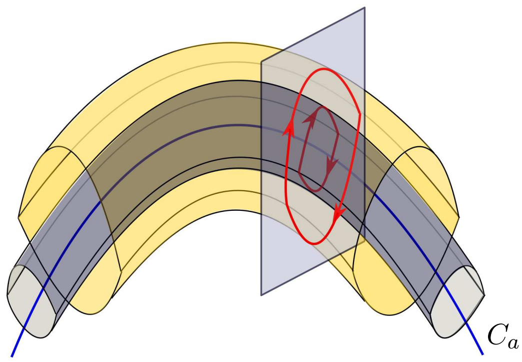

Figure 4.1: The half-planes are invariant and behave like a center for Z_0.

Proposition 28. *The central axis of each torus T_{r_0} is given by the circle $C_a = \{(x, y, 0) \in \Sigma \,|\, x^2 + y^2 = a^2\}$ which also corresponds to the tangential singularities of X and Y. Moreover, C_a is fulfilled with equilibria.*

Proof. Let $p = (x, y, 0) \in \Sigma$. The first Lie derivative of X and Y with Σ is given by

$$Xf(p) = Yf(p) = \frac{4 + (x^2 + y^2)(17 - 12(x^2 + y^2))}{4\sqrt{x^2 + y^2}}.$$

So, $Xf(p) = Yf(p) = 0$ for $p \in C_a$, and C_a correspond to the tangential singularities of X and Y. Note that $p \in \Sigma^{c+}$ for $x^2 + y^2 < a^2$, $p \in \Sigma^{c-}$ for $x^2 + y^2 > a^2$ and $\Sigma \setminus C_a$ is a crossing region where passes the invariant tori so that each half-plane Π_{θ_0} is fulfilled with periodic orbits, by Proposition 27. In addition, since the tangential singularities of X and Y coincide we can define the tangential sliding vector field given by Definition 1.4. Indeed, let us consider the vector $N = (x, y, 0)$ which is normal to C_a and is contained in tangent space of Σ. So, the tangential sliding vector field Z^T associated to Z_0 at $p = (x, y, 0) \in C_a$ is given by

$$Z^T(p) = \frac{(Y(p) \cdot N)\, X(p) - (X(p) \cdot N)\, Y(p)}{(Y(p) \cdot N) - (X(p) \cdot N)} = \frac{1}{2}\Big[\, (x, y, 0) + (-x, -y, 0) \,\Big],$$

that is, the tangential sliding vector field is null at every point of C_a. Therefore, each $p_0 \in C_a$ is a stationary point of Z_0.

□

By the previous calculations we get the following result.

Proposition 29. *Let Z_0 be given by (4.4). The half-planes Π_{θ_0} are Z_0-invariant, for all $\theta_0 \in [0, 2\pi)$.*

Proof. By either (4.4) or (4.5) and (4.6), we observe that there is no variation of the angle θ. Moreover, by Proposition 28 the tangential sliding vector field is null at every point of C_a. □

4.2 Properties of a rotational perturbation of Z_0

In this section, we exhibit some properties of a suitable perturbation of Z_0 given by

$$Z^\eta(r,\theta,z) = \begin{cases} X(r,\theta,z) = \left(r, 0, \dfrac{4+17r^2-12r^4}{4r}\right) & \text{if } z \geq 0, \\ Y^\eta(r,\theta,z) = \left(-r, g(\theta), \dfrac{4+17r^2-12r^4}{4r}\right) & \text{if } z \leq 0, \end{cases} \tag{4.8}$$

where

$$g(\theta) = \varepsilon \prod_{i=0}^{2\eta-1} (i\mu - \theta) \tag{4.9}$$

and $\mu = \pi/\eta$ with η a natural number.

In what follows, we will prove that this perturbation of the vector field Z_0 keeps exactly 2η invariant half-planes. It is worth to mention that the main property of (4.8) is that its trajectories turn around the circle C_a in such a way that its α-limit and ω-limit are centers in the invariant half-planes. This case is illustrated in Figure 4.2.

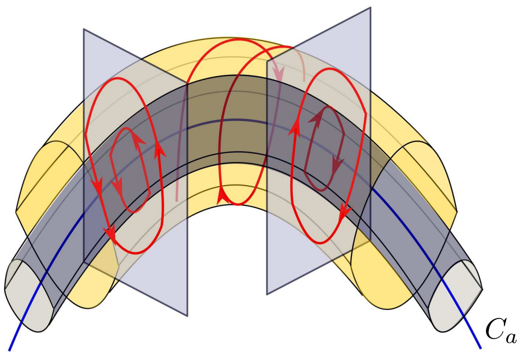

Figure 4.2: The perturbed system Z^η and the invariant nested tori.

By a straightforward calculation $\phi_{Y^\eta}(t)$ has the expression

$$\phi_{Y^\eta}(t) = \left(\widetilde{r}_0 e^{-t}, \psi_{\widetilde{\theta}_0}(t), \frac{e^t}{\widetilde{r}_0} - \frac{17\widetilde{r}_0 e^{-t}}{4} + \widetilde{r}_0^3 e^{-3t} + \widetilde{m}_0\right), \tag{4.10}$$

with $\widetilde{r}_0 \geq 0$, $\widetilde{\theta}_0 \in [0, 2\pi)$, $\widetilde{m}_0 \in \mathbb{R}$ and the expression of the solution $\psi_{\widetilde{\theta}_0}(t)$ comes from the integral of the function g.

Remark 13. *Observe that the flight times of both, Y and Y^η, coincide since the last coordinate of both is the same.*

Proposition 30. *Let Z^η be given by (4.8) and $p_0 = (r_0, \theta_0, 0) \in \Sigma$. Then the first return map* *associated with Z^η is given by*

$$\varphi_{Z^\eta}(p_0) = (r_0, \psi_{\theta_0}(t_2), 0) \tag{4.11}$$

where t_2 is given by (4.7).

Proof. From (4.5) we get $p_1 = \phi_X(t_2) = (r_0 e^{t_2}, \theta_0, 0)$. Using Remark 13 and (4.10) we conclude that

$$\varphi_{Z^\eta}(p_0) = \phi_{Y^\eta}(t_2, p_1) = \left(r_0 e^{t_2} e^{-t_2}, \psi_{\theta_0}(t_2), 0\right) = (r_0, \psi_{\theta_0}(t_2), 0)\,.$$

□

As an immediate consequence of Proposition 30 we obtain the next result.

Corollary 3. *The topological tori that pass through each cycle C_{r_0} are Z^η-invariant.*

The next result will be very useful in the sequel.

Proposition 31. *The half-planes $\Pi_i = \{(r, \theta, z) | \theta = i\mu\}$ with $i \in \{0, \ldots, 2\eta - 1\}$ are Z^η-invariant.*

Proof. Let i be fixed. If $\theta = i\mu$, then it follows that the second coordinate of the vector field Y^η is zero. It follows that the half-plane Π_i is Y^η-invariant. Besides, we can notice that all half-planes, with a fixed angle, are X-invariant. In addition, the tangential singularities of Y and Y^η coincide. So, C_a is still the set of tangential singularities of Z^η and we can define the tangential sliding vector field given by Definition 1.4 associated to the PSVF Z^η. Let us consider again the vector $N = (a\cos(\theta), a\sin(\theta), 0)$ which is normal to C_a and is contained in tangent space of Σ. So, the tangential sliding vector field Z^T_η associated to Z^η at $p = (a\cos(\theta), a\sin(\theta), 0) \in C_a$ is given by

$$\begin{aligned} Z^T_\eta(p) &= \frac{(Y^\eta(p)\cdot N)\,X(p) - (X(p)\cdot N)\,Y^\eta(p)}{(Y^\eta(p)\cdot N) - (X(p)\cdot N)} \\ &= \left(-\frac{ag(\theta)\sin(\theta)}{2a\cos(\theta) - g(\theta)\sin(\theta)}, \frac{ag(\theta)\cos(\theta)}{2a\cos(\theta) - g(\theta)\sin(\theta)}, 0\right). \end{aligned}$$

Since the sine and cosine functions are not null simultaneously the equilibrium points of Z^T_η are the zeroes of the function g, that is, $\theta = i\mu$ for $i \in \{0, 1, \ldots, 2\eta - 1\}$. Therefore, each half-plane Π_i is Z^η-invariant. □

Observe that the Jacobian of the vector field Z^T_η at $(r, \theta) = (a, j\mu)$, for $j \in \{0, 1, \ldots, 2\eta - 1\}$ has the expression

$$DZ^T_\eta(a, j\mu) = \begin{pmatrix} 0 & -\frac{1}{2}\tan(j\mu) g'(j\mu) \\ 0 & \frac{g'(j\mu)}{2} \end{pmatrix}.$$

So, the eigenvalues associated to the equilibrium points of the tangential sliding vector field are 0 and $g'(j\mu)/2$. Therefore, each half-plane Π_i, for $i \in \{0, \ldots, 2\eta - 1\}$ behaves like a stable or unstable center manifold depending on the sign of the derivative of the function g.

Proposition 32. *Let Z^η given by* (4.8) *and i fixed, with $i \in \{0, \dots, \eta-1\}$. Then each invariant half-plane Π_i is fulfilled with periodic orbits.*

Proof. It is an immediate consequence of Corollary 3 and Propositions 27 and 31 since Z^η and Z_0 coincide at the invariant half-planes Π_i. □

Lemma 9. *Consider the function g given by* (4.9)*. For $\varepsilon > 0$ the function g has 2η roots in $[0, 2\pi]$, these roots are $\theta = i\mu$, with $i \in \{0, \dots, 2\eta - 1\}$ and*

$$g'(j\mu) = \frac{\partial g}{\partial \theta}(j\mu) = \varepsilon \mu^{2\eta-1}(-1)^{j+1} j!(2\eta - (j+1))! \text{ for } j \in \{0, 1, \dots, 2\eta - 1\}.$$

It means that such derivative at $j\mu$ is positive for j odd and negative for j even and $j = 0$.

Proof. By a straightforward calculation we get $g(\theta) = 0$ if, and only if, $\theta = i\mu$, with $i \in \{0, \dots, 2\eta - 1\}$. Moreover,

$$\frac{\partial g}{\partial \theta}(\theta) = \frac{\partial}{\partial \theta}\Big((j\mu - \theta)H(\theta)\Big),$$

where $H(\theta) = g(\theta)/(j\mu - \theta)$. So, we obtain

$$\begin{aligned}
\frac{\partial g}{\partial \theta}(j\mu) &= -H(j\mu) \\
&= -\varepsilon(-j\mu)(\mu - j\mu)\dots((j-1)\mu - j\mu)((j+1)\mu - j\mu)\dots((2\eta-1)\mu - j\mu) \\
&= \varepsilon \mu^{2\eta-1}(-1)^{j+1}\Big(j(j-1)\dots(j-(j-1))\Big)\Big(((j+1)-j)\dots((2\eta-1)-j)\Big) \\
&= \varepsilon \mu^{2\eta-1}(-1)^{j+1} j!(2\eta - (j+1))!
\end{aligned}$$

□

Proposition 33. *The invariant half-planes Π_i given in Proposition 32 behave like an unstable (resp. stable) center manifold when i is odd (resp. even or zero), with $i \in \{0, \dots, 2\eta - 1\}$.*

Proof. From Proposition 30 we can notice that the behavior of the return map associated with Z^η is determined by the function ψ_θ, that is related to the function g whose derivative is given by Lemma 9. Therefore, since the derivative of g is positive for i odd (respectively, negative for i even or zero) each invariant half-plane Π_i behaves like an unstable (respectively, stable) center manifold. □

4.3 Properties of a radial perturbation of Z_0

Let us consider the function $h\colon (0, \infty) \to \mathbb{R}$ given by

$$h(r) = \begin{cases} 0, & \text{if } r \le a, \\ e^{-1/(r-a)}, & \text{if } r > a. \end{cases} \tag{4.12}$$

and define the functions $F_\varepsilon^\rho\colon (0,\infty)\to\mathbb{R}$, with either $\rho=f$, $\rho=i$ or $\rho=m$ where

$$F_\varepsilon^f(r)=\varepsilon h(r)((a+\varepsilon)-r)((a+2\varepsilon)-r)\dots((a+k\varepsilon)-r)\,, \tag{4.13}$$

$$F_\varepsilon^i(r)=\varepsilon^3 h(r)\sin(\pi\varepsilon^2/(-a+r)), \tag{4.14}$$

and

$$F_\varepsilon^m(r)=\varepsilon h(r)\,(r-(a+\varepsilon))^m \tag{4.15}$$

with $k,m\in\mathbb{N}$.

Lemma 10. *Consider the function $F_\varepsilon^f(r)$ given by* (4.13)*.*

(i) If $\varepsilon<0$ then F_ε^f does not have roots for $r>a$;

(ii) If $\varepsilon>0$ then F_ε^f has exactly k roots for $r>a$. These roots are $\{a+\varepsilon,a+2\varepsilon,\dots,a+k\varepsilon\}$;

(iii) $\dfrac{\partial F_\varepsilon^f}{\partial r}(a+j\varepsilon)=\varepsilon^k h(a+j\varepsilon)(-1)^j(k-j)!(j-1)!$, for $j\in\{1,2,\dots,k\}$. It means that such partial derivative at $a+j\varepsilon$ is positive for j even and negative for j odd.

Proof. By a straightforward calculation, if $r>a$ we get $F_\varepsilon^f(r)=0$ if, and only if,

$$((a+\varepsilon)-r)((a+2\varepsilon)-r)\dots((a+k\varepsilon)-r)=0.$$

Since (4.13) depends only on the variable r, the roots of it for $r>a$ and $\varepsilon>0$ are given by $r=a+\varepsilon,a+2\varepsilon,\dots,a+k\varepsilon$. Moreover,

$$\frac{\partial F_\varepsilon^f}{\partial r}(r)=\frac{\partial}{\partial r}\Big(((a+j\varepsilon)-r)H(r)\Big)$$

where $H(r)=F_\varepsilon^f(r)/(a+j\varepsilon-r)$. So, we obtain

$$\begin{aligned}\frac{\partial F_\varepsilon^f}{\partial r}(a+j\varepsilon) &= -H(a+j\varepsilon)\\ &= -\varepsilon^k h(a+j\varepsilon)(1-j)\dots((j-1)-j)((j+1)-j)\dots(k-j)\\ &= -\varepsilon^k h(a+j\varepsilon)(-1)^{j-1}\Big((j-1)\dots(j-(j-1))\Big)\Big(((j+1)-j)\dots(k-j)\Big)\\ &= \varepsilon^k h(a+j\varepsilon)(-1)^j(k-j)!(j-1)!\end{aligned}$$

This proves items (ii) and (iii). Item (i) is immediate. □

Lemma 11. *Consider the function F_ε^i given by* (4.14)*. For $\varepsilon>0$ and $r>a$ the function F_ε^i has infinitely many roots in $\big(a,a+\varepsilon^2\big]$, these roots are given by $\big\{a+\varepsilon^2,a+\varepsilon^2/2,a+\varepsilon^2/3,\dots\big\}$*

and

$$\frac{\partial F_\varepsilon^i}{\partial r}\left(a+\varepsilon^2/j\right) = \varepsilon\,\pi\,j^2\,h\left(a+\varepsilon^2/j\right)(-1)^{j+1} \quad \textit{for } j \in \{1,2,3,\dots\}.$$

It means that such derivative at $a+\varepsilon^2/j$ is positive for j odd and negative for j even.

Proof. If $r > a$, by a straightforward calculation we get that $F_\varepsilon^i(r) = 0$ if, and only if, $\sin(\pi\varepsilon^2/(-a+r)) = 0$. So, the roots of F_ε^i in $\left(a, a+\varepsilon^2\right]$ are $\left\{a+\varepsilon^2, a+\varepsilon^2/2, a+\varepsilon^2/3, \dots\right\}$. Moreover,

$$\frac{\partial F_\varepsilon^i}{\partial r}(r) = \varepsilon^3\frac{\partial h}{\partial r}(r)\sin\left(\frac{\pi\varepsilon^2}{r-a}\right) - \frac{\pi\,\varepsilon^5\,h(r)}{(r-a)^2}\cos\left(\frac{\pi\varepsilon^2}{(r-a)}\right).$$

Therefore,

$$\frac{\partial F_\varepsilon^i}{\partial r}\left(a+\varepsilon^2/j\right) = \varepsilon\,\pi\,j^2\,(-1)^{j+1}\,h\left(a+\varepsilon^2/j\right)\ \cdot$$

□

Lemma 12. *Consider the function F_ε^m given by (4.15). For $\varepsilon \neq 0$ and $r > a$ the unique zero of the function F_ε^m is $r = a+\varepsilon$. Moreover, this zero has multiplicity m.*

Proof. Suppose $\varepsilon \neq 0$ and $r > a$. It is immediate that $F_\varepsilon^m(r) = 0$ if, and only if, $r = a+\varepsilon$. By a straightforward calculation, we get that

$$\frac{\partial^j F_\varepsilon^m}{\partial r^j}(r) = \varepsilon\sum_{k=0}^{j}\left[r-(a+\varepsilon)\right]^{m-k}\binom{j}{k}\frac{\partial^{j-k}h(r)}{\partial r^{j-k}}\,m(m-1)\cdots(m-(k-1)).$$

Therefore,

$$F_\varepsilon^m(a+\varepsilon) = \frac{\partial F_\varepsilon^m}{\partial r}(a+\varepsilon) = \ldots = \frac{\partial^{m-1}F_\varepsilon^m}{\partial r^{m-1}}(a+\varepsilon) = 0 \quad \text{and} \quad \frac{\partial^m F_\varepsilon^m}{\partial r^m}(a+\varepsilon) = \varepsilon\,h(a+\varepsilon)\,m! \neq 0.$$

□

In this way, we can investigate some properties of a perturbation of Z_0 of the form

$$Z_\varepsilon^\rho(r,\theta,z) = \begin{cases} X_\varepsilon^\rho(r,\theta,z) = \left(r, 0, \dfrac{4+17r^2-12r^4}{4r} + r\dfrac{\partial F_\varepsilon^\rho}{\partial r}(r)\right) & \text{if } z \geq 0, \\ Y(r,\theta,z) = \left(-r, 0, \dfrac{4+17r^2-12r^4}{4r}\right) & \text{if } z \leq 0, \end{cases} \tag{4.16}$$

or equivalently, in xyz-coordinates,

$$Z_\varepsilon^\rho(x,y,z) = \begin{cases} \left(x, y, \dfrac{4+\left(x^2+y^2\right)\left(17-12\left(x^2+y^2\right)\right)}{4\sqrt{x^2+y^2}} + G(x,y)\right) & \text{if } z \geq 0, \\ \left(-x, -y, \dfrac{4+\left(x^2+y^2\right)\left(17-12\left(x^2+y^2\right)\right)}{4\sqrt{x^2+y^2}}\right) & \text{if } z \leq 0, \end{cases} \tag{4.17}$$

where $G(x,y)$ comes from the expression of $r\,\partial F_\varepsilon^\rho/\partial r$.

Remark 14. *It is easy to see that $Z_\varepsilon^\rho \to Z_0$ when $\varepsilon \to 0$, with $\rho = i, f, m$.*

The trajectory $\phi_{X_\varepsilon^\rho}$ of X_ε^ρ given in (4.16) is parameterized by

$$\phi_{X_\varepsilon^\rho}(t) = \left(r_0 e^t, \theta_0, -\frac{e^{-t}}{r_0} + \frac{17 r_0 e^t}{4} - r_0^3 e^{3t} + F(t) + m_0\right), \tag{4.18}$$

where $F(t)$ is obtained from the expression of $F_\varepsilon^\rho(r)$ replacing r by $r_0 e^t$.

Remark 15. *By Equations* (4.6) *and* (4.18) *we obtain that there is no variation in the angle θ. Therefore the half-planes Π_{θ_0} are Z_ε^ρ-invariant. Note that, in this case, the first Lie derivative $X_\varepsilon^\rho f$ of X_ε^ρ is the third component of X_ε^ρ. Since X_ε^ρ is a small perturbation of X, and the derivative of F_ε^ρ involves terms of the function h and its derivative, which are null at $r = a$, we get that C_a still corresponds to the tangential singularities of X_ε^ρ. So, the tangential singularities of X_ε^ρ and Y coincide, and proceeding in the same way as in Proposition 31 we obtain that the tangential sliding vector field is null at every point of C_a.*

Proposition 34. *Given an arbitrary point $(r_0, \theta_0, 0) \in \Sigma$, with $r_0 < a$, we have that*

$$\phi_{X_\varepsilon^\rho}(r_0, \theta_0, 0) = (r_0 e^{\bar{t}}, \theta_0, 0)$$

where the X_ε^ρ-flight time $\bar{t} > 0$ is given implicitly by

$$-\frac{e^{-\bar{t}}}{r_0} + \frac{17 r_0 e^{\bar{t}}}{4} - r_0^3 e^{3\bar{t}} + F(\bar{t}) - \left(-\frac{1}{r_0} + \frac{17 r_0}{4} - r_0^3\right) = 0. \tag{4.19}$$

Proof. Observe that $F(0) = 0$ since $h(r) = 0$ for $r < a$. Let $\bar{t} > 0$ be the first time such that

$$-\frac{e^{-t}}{r_0} + \frac{17 r_0 e^t}{4} - r_0^3 e^{3t} + F(t) - \left(-\frac{1}{r_0} + \frac{17 r_0}{4} - r_0^3\right) = 0.$$

Therefore, by Equation (4.18) we obtain $\phi_{X_\varepsilon^\rho}(r_0, \theta_0, 0) = (r_0 e^{\bar{t}}, \theta_0, 0)$. □

We are now able to ensure the existence of periodic orbits in the invariant half-planes Π_{θ_0} of Z_ε^ρ.

Proposition 35. *Let $\theta_0 \in [0, 2\pi)$ be fixed, $\varepsilon > 0$ and consider the PSVF Z_ε^ρ given by (4.16). Then*

(i) In each invariant half-plane Π_{θ_0} the PSVF Z_ε^f has exactly k nested periodic orbits;

(ii) In each invariant half-plane Π_{θ_0} the PSVF Z_ε^i has infinitely many nested periodic orbits;

(iii) In each invariant half-plane Π_{θ_0} the PSVF Z_ε^m has a unique periodic orbit of multiplicity m. Moreover, for all $m_0 < m$ there exists PSVF exhibiting a periodic orbit of multiplicity m_0 in a neighborhood of Z_ε^m.

Proof. Let $p_0 = (r_0, \theta_0, 0) \in \Sigma$. In order to get a periodic orbit, it must happen

$$\phi_{Z_\varepsilon^\rho}(r_0, \theta_0, 0) = \phi_Y \circ \phi_{X_\varepsilon^\rho}(r_0, \theta_0, 0) = (r_0 e^{\bar{t}} e^{-t_2}, \theta_0, 0) = (r_0, \theta_0, 0),$$

and therefore it must satisfies $r_0 e^{\bar{t}-t_2} = r_0$ where t_2 is given in (4.7). This means that periodic orbits appear just when $\bar{t} = t_2$. Substituting $\bar{t} = t_2$ in (4.19) we conclude that the periodic orbits appear just when $F(t_2) = 0$. By Lemmas 10 and 11 we have periodic orbits for $r = a + \varepsilon, a + 2\varepsilon, \dots, a + k\varepsilon$ if $\rho = f$ or for $r = a + \varepsilon^2, a + \varepsilon^2/2, a + \varepsilon^2/3, \dots$ if $\rho = i$. This proves items (i) and (ii). In the same way, if $\rho = m$, then a periodic orbit appears only for $r = a + \varepsilon$ which is, by Lemma 12, a root of multiplicity m of the function F_ε^m and, therefore, the periodic orbit has multiplicity m. Moreover, consider the function

$$F_\varepsilon^{m_0,m}(r) = \varepsilon h(r)\,(r - (a+\varepsilon))^{m_0} \left(r - \left(a + \frac{\varepsilon}{2}\right)\right) \cdots \left(r - \left(a + \frac{\varepsilon}{m - m_0 + 1}\right)\right).$$

Repeating the same argument above we obtain a PSVF with one periodic orbit of multiplicity m_0 and $m - m_0$ simple periodic orbits. This concludes the proof. □

Now, just varying the variable θ in the interval $[0, 2\pi)$ the following result is immediate.

Proposition 36. *Consider Z_ε^ρ given by (4.16), where $\rho = f, i$ or m. Then Z_ε^m has a unique topological tori, Z_ε^f has exactly k nested topological tori and Z_ε^i has infinitely many topological tori.*

Remark 16. *Since the tori of Proposition 36 are nested and isolated, We call the j^{th}-torus that one containing $(j-1)$ tori in the interior of the region bounded by it. If we consider $\varepsilon > 0$ and the expressions for the derivative of the functions F_ε^f and F_ε^i given by Lemmas 10 and 11 we obtain that the j^{th}-torus of Proposition 36 is an attractor for Z_ε^f if j is odd and it is a repeller for Z_ε^f if j is even. Similarly, the j^{th}-torus of Proposition 36 is a repeller for Z_ε^i if j is odd and it is an attractor for Z_ε^i if j is even.*

4.4 The main results

In this section, a new family of PSVFs is produced combining the two previous perturbations given in the Sections 4.2 and 4.3 in order to destroy all tori described in Section 4.3, but at the same time preserving some of the invariant half-planes. For this purpose, let us consider the following PSVF

$$Z_\varepsilon^{\eta,\rho}(r,\theta,z)=\begin{cases} X_\varepsilon^\rho(r,\theta,z)=\left(r,\,0\,,\dfrac{4+17r^2-12r^4}{4r}+r\dfrac{\partial F_\varepsilon^\rho}{\partial r}(r)\right) & \text{if } z\geq 0,\\ Y^\eta(r,\theta,z)=\left(-r,\,g(\theta)\,,\dfrac{4+17r^2-12r^4}{4r}\right) & \text{if } z\leq 0,\end{cases} \tag{4.20}$$

where $\rho=i$ or f and the function g is given by (4.9).

Remark 17. *We can notice that $Z_\varepsilon^{\eta,\rho}$, with $\rho=i,f$, converges to Z_0 when ε tends to zero.*

The flows of $X_\varepsilon^\rho(r,\theta,z)$ and $Y^\eta(r,\theta,z)$ are respectively given by (4.18) and (4.10). Accordingly, the X_ε^ρ-flight time $\bar{t}$ is given implicitly by (4.19) and the Y^η-flight time t_2 is given by (4.7). Therefore, the first return map associated with $Z_\varepsilon^{\eta,\rho}$ in a point $p_0=(r_0,\theta_0,0)$ is given by

$$\begin{aligned}\varphi_{Z_\varepsilon^{\eta,\rho}}(r_0,\theta_0,0) &= \varphi_{Y^\eta}\circ\varphi_{X_\varepsilon^\rho}(r_0,\theta_0,0)\\ &= \varphi_{Y^\eta}\left(r_0e^{\bar{t}},\theta_0,0\right)\\ &= \left(r_0e^{\bar{t}-t_2},\psi_{\theta_0}(t_2),0\right).\end{aligned} \tag{4.21}$$

We observe that the first coordinate of Equation (4.21) controls the occurrence of the limit cycles (including its stability) and his second coordinate controls the way that a given trajectory twist until converging to a limit cycle. Now, we use the previous results in order to prove the main result of this work.

Theorem 12. *Consider the piecewise smooth vector field Z_0 given by* (4.1) *and the half-planes $\Pi_i=\{(r,\theta,z)|\theta=i\mu\}$. For each pair k,η there exists a one-parameter family of PSVFs $Z_\varepsilon^{\rho,\eta}=Z_\varepsilon$ satisfying:*

(a) $Z_\varepsilon\to Z_0$ when $\varepsilon\to 0$;

(b) Z_ε can be chosen to have exactly 2η invariant half-planes Π_i;

(c) Z_ε can be chosen to have exactly k hyperbolic nested limit cycles in each invariant half-plane Π_i. The same holds for $k=\infty$. Moreover, the stability of these limit cycles are determined;

(d) Z_ε can be chosen to have exactly $2k\eta$ hyperbolic limit cycles.

Proof. Firstly, we notice that the perturbations considered are uncoupled. Item (a) follows from Remark 17. Item (b) follows from Proposition 31. Since the perturbations are uncoupled, by Propositions 31 and 35 we can generate k limit cycles in each invariant half-plane Π_i, where $i = 0, \dots, 2\eta - 1$. The same argument is valid for $k = \infty$ and the stability is given by the expressions for the derivative of the functions F_ε^f and F_ε^i given by Lemmas 10 and 11 as in Remark 16 and Lemma 9. Item (d) is immediate from (b) and (c). □

The purpose now is to create a PSVF with invariant half-planes containing a multiple limit cycle. In this way, we consider

$$Z_\varepsilon^{\eta,m}(r,\theta,z) = \begin{cases} X_\varepsilon^m(r,\theta,z) = \left(r,\, 0\,, \dfrac{4+17r^2-12r^4}{4r} + r\dfrac{\partial F_\varepsilon^m}{\partial r}(r)\right) & \text{if } z \geq 0, \\ Y^\eta(r,\theta,z) = \left(-r,\, g(\theta)\,, \dfrac{4+17r^2-12r^4}{4r}\right) & \text{if } z \leq 0, \end{cases} \tag{4.22}$$

where F_ε^m is given by (4.15) and the function g given by (4.9).

Remark 18. *We can notice that $Z_\varepsilon^{\eta,m}$ converges to Z_0 when ε tends to zero.*

Theorem 13. *Consider the piecewise smooth vector field Z_0 given by (4.1). For each η there exists a one-parameter family of PSVFs $Z_\varepsilon^{\eta,m}$ satisfying:*

(a) $Z_\varepsilon^{\eta,m} \to Z_0$ when $\varepsilon \to 0$;

(b) $Z_\varepsilon^{\eta,m}$ can be chosen to have exactly 2η invariant half-planes Π_i;

(c) $Z_\varepsilon^{\eta,m}$ has one multiple limit cycle of multiplicity m in each invariant half-plane Π_i;

(d) $Z_\varepsilon^{\eta,m}$ can be chosen to have exactly 2η multiple limit cycles.

Proof. Indeed, consider the PSVF $Z_\varepsilon^{\eta,m}$ given by (4.22). Item (a) follows from Remark 18. Item (b) follows from Proposition 31. Since the perturbations are uncoupled, by Proposition 35 we can generate one multiple limit cycle of multiplicity m in each invariant half-plane Π_i, where Π_i are given by item (b). Item (d) follows from (b) and (c). □

Instead of consider the function g given by (4.9) we can consider a function where it is possible to create a infinite number of invariant half-planes whose respective angles form a convergent sequence. For this purpose, we consider the continuously differentiable function

$$\begin{cases} f(\theta) = \theta^3 \cos\left(\dfrac{1}{\theta}\right), \\ f(0) = 0. \end{cases} \tag{4.23}$$

Lemma 13. *Consider the function f given by* (4.23)*. The function f has infinitely many roots in $[0, 2\pi)$, these roots are $\theta = 0$ or $\theta = 2/\pi(2n+1)$, where $n = 0, 1, 2, \ldots$ and*

$$\frac{\partial f}{\partial \theta}\left(\frac{2}{\pi(2n+1)}\right) = \frac{2(-1)^n}{\pi(2n+1)}.$$

It means that such derivative at $2/\pi(2n+1)$ is positive for n even and it is negative for n odd.

Proof. By definition we have that $f(0) = 0$. For $\theta \neq 0$, $f(\theta) = 0$ if, and only if, $\cos(1/\theta) = 0$ and, therefore, $\theta = 2/\pi(2n+1)$, where $n = 0, 1, 2, \ldots$. Moreover,

$$\frac{\partial f}{\partial \theta}\left(\frac{2}{\pi(2n+1)}\right) = \frac{2}{\pi(2n+1)} \sin\left(\frac{(2n+1)\pi}{2}\right) = \frac{2(-1)^n}{\pi(2n+1)}.$$

□

In this way, we can consider the PSVF Z^f given by

$$Z^f(r,\theta,z) = \begin{cases} X(r,\theta,z) = \left(r,\, 0\,, \dfrac{4+17r^2-12r^4}{4r}\right) & \text{if } z \geq 0, \\ Y^f(r,\theta,z) = \left(-r,\ f(\theta)\,, \dfrac{4+17r^2-12r^4}{4r}\right) & \text{if } z \leq 0. \end{cases} \tag{4.24}$$

Proposition 37. *Let Z^f given by* (4.24)*. The half-planes Π_θ, with $\theta = 0$ or $\theta = 2/\pi(2n+1)$, where $n = 0, 1, 2, \ldots$, are Z^f-invariant.*

Proof. It is analogous to Proposition 31. □

Proposition 38. *Let Z^f given by* (4.24) *and θ fixed, with $\theta = 0$ or $\theta = 2/\pi(2n+1)$, where $n = 0, 1, 2, \ldots$. Then each half-plane Π_θ is fulfilled with periodic orbits. Moreover, the half-planes Π_θ with $\theta = 2/\pi(2n+1)$ behaves like a center manifold whose stability is determined.*

Proof. The first statement is an immediate consequence of Proposition 37. Furthermore, the behavior of the first return map associated with Z^f is determined by the second coordinate of Y^f in a way that the stability of these invariant half-planes are determined by the sign of the derivative of the function f given by Lemma 13. □

Remark 19. *We can notice that the root $\theta = 0$ of the function f is not isolated. Therefore, it is not possible to determine the stability of the center manifold generated by it. See figure 4.3.*

Joining the perturbation described above with the perturbation described in Section 4.3 we

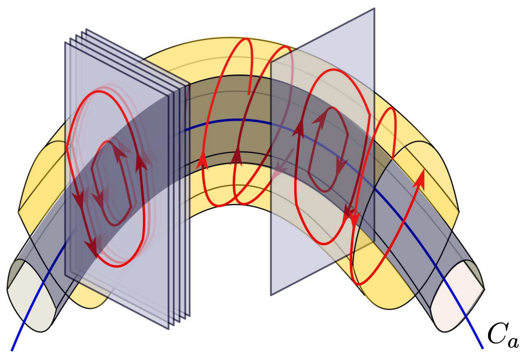

Figure 4.3: Behavior of the vector field Z^f.

have the following PSVF

$$Z_\varepsilon^{f,\rho}(r,\theta,z)=\begin{cases} X_\varepsilon^\rho(r,\theta,z)=\left(r,\,0\,,\dfrac{4+17r^2-12r^4}{4r}+r\dfrac{\partial F_\varepsilon^\rho}{\partial r}(r)\right) & \text{if } z\geq 0,\\ Y^f(r,\theta,z)=\left(-r,\,\varepsilon f(\theta)\,,\dfrac{4+17r^2-12r^4}{4r}\right) & \text{if } z\leq 0,\end{cases} \tag{4.25}$$

where $\rho=f$ or i and the function f given by (4.23).

Remark 20. *We can notice that $Z_\varepsilon^{f,\rho}$ converges to Z_0 when ε tends to zero.*

Theorem 14. *Let Z_0 be given by (4.1). For each positive integer k there exists a one-parameter family of PSVFs $Z_\varepsilon^{f,\rho}=Z_\varepsilon^2$ satisfying:*

(a) $Z_\varepsilon^2\to Z_0$ when $\varepsilon\to 0$;

(b) Z_ε^2 has infinitely many invariant half-planes Π_θ;

(c) Z_ε^2 can be chosen to have exactly k nested limit cycles in each invariant half-plane Π_θ of item (b). The same holds for $k=\infty$. Moreover, the stability of the limit cycles are determined for those contained in an invariant half-plane whose respective angle is an isolated root of f.

Proof. In fact, consider the PSVF $Z_\varepsilon^{f,\rho}$ given by (4.25). Item (a) follows from Remark 20. Item (b) is proved by Proposition 37. Since the perturbations are uncoupled, by Proposition 35 we can generate k limit cycles in each invariant half-plane Π_θ, where Π_θ are given by item (b). The same argument is valid for $k=\infty$. The last statement of the Theorem follows from Lemma 13 and Remark 19 since the behavior of the first return map associated with $Z_\varepsilon^{f,\rho}$ is determined by the sign of the derivative of the function f. □

A consequence of Theorem 12 is the following result.

Corollary 4. *The piecewise smooth vector field Z_0 given by Equation* (4.1) *has infinite codimension in the set Ω^r of all PSVFs with two zones in $\mathbb{R}^3$.*

In order to prove Corollary 4, let us define the classical notion of codimension of vector fields.

Definition 18. *Consider $\Theta(W)$ the set of all small unfoldings of a vector field W. We say that W has codimension k if it appears exactly k distinct topological types of vector fields in $\Theta(W)$.*

Proof of Corollary 4: Suppose that the codimension of the PSVF given by (4.1) is $m < \infty$. Therefore, in its neighborhood there exist PSVFs of, at most, m distinct topological types. This is a contradiction due to the Theorem 12. $\square$

Chapter 5

Limit cycles and Lyapunov coefficients in planar piecewise Hamiltonian vector fields with an invisible fold-fold singularity

In this chapter, we study Lyapunov coefficients and limit cycles for planar piecewise Hamiltonian vector fields presenting an invisible fold-fold singularity. In the first part of this work, we obtain the general expressions for the first five Lyapunov coefficients to general piecewise Hamiltonian vector fields presenting a crossing invisible fold-fold singularity. As a consequence, the bifurcation diagrams, illustrating the number, types and positions of the bifurcating small amplitude crossing limit cycles for these vector fields, are determined. Next, we study the existence of limit cycles in an unfolding of a family of piecewise smooth vector fields with an invisible fold–fold. More precisely, given a positive integer k, we prove that this family has exactly k hyperbolic crossing limit cycles in a suitable neighborhood of this singularity. Moreover, we provide a complete study relating the existence and stability of these crossing limit cycles with the limit cycles of the family of smooth vector fields obtained by the regularization method. This relationship is obtained by studying the equivalence between the signs of the Lyapunov coefficients of the family of piecewise smooth vector fields and the ones of its regularization. The content of this chapter can be found in [50, 51].

5.1 Lyapunov coefficients for piecewise Hamiltonian systems presenting a crossing invisible fold-fold singularity

The appearance of limit cycles in a family of smooth vector fields containing a focus type equilibrium can be associated with a Hopf bifurcation. A Hopf bifurcation occurs where a periodic orbit is created as the stability of the equilibrium point changes. So, in the smooth case, the stability of an equilibrium point with complex eigenvalues is reduced to the computation of the so-called Lyapunov coefficients. Remark that the Lyapunov coefficients for smooth systems are given by the coefficients of the series expansion of the displacement function (Theorem 5).

In the same way, we can obtain some kind of Lyapunov coefficients for piecewise smooth vector fields by the analysis of the displacement function associated with the first return map, when it is well defined, in the neighborhood of points that play the role of monodromic singular points for smooth systems, that is, points where there exists a neighborhood such that the solutions of the associated vector field turn around it either in forward or in backward time. In [29] the authors study the stability of some special points of planar discontinuous differential equations with a line of discontinuities by computing the first three Lyapunov coefficients. Inspired by the results of [29], we provide expressions for the first five Lyapunov coefficients as well as a complete study of the birth of crossing periodic orbits generated by the unfolding of the crossing invisible fold-fold singularity in a planar piecewise Hamiltonian vector field.

In this section all the functions and maps are assumed to be analytic. Consider the displacement function $\Delta(a) = \Pi_Z(a) - a$ associated with the first return map Π_Z of a PSVF Z in a neighborhood of a crossing invisible fold-fold singularity. In this way, it turns out that either $\Delta(a) = 0$ or there exists $k \in \mathbb{N}$ such that $\Delta(a) = L_k^* a^k + \mathcal{O}\left(a^{k+1}\right)$. In the first case, the invisible fold-singularity behaves like a center and, in the second one, the invisible fold-fold singularity behaves like a focus. In this case, we say that L_k^* is the k-th Lyapunov coefficient. An expression for L_k^* only makes sense when $L_1^* = L_2^* = \cdots = L_{k-1}^* = 0$. By convention, nonzero multiplicative factors can be omitted from the expressions given for the Lyapunov coefficients.

Consider a family of Hamiltonian PSVFs

$$\mathcal{Z}(x,y,\mu,\nu) = \begin{cases} \mathcal{X}(x,y,\mu,\nu) = \left(-H_y^+(x,y,\mu,\nu), H_x^+(x,y,\mu,\nu)\right), & y \geq 0, \\ \mathcal{Y}(x,y,\mu,\nu) = \left(-H_y^-(x,y,\mu,\nu), H_x^-(x,y,\mu,\nu)\right), & y \leq 0, \end{cases} \tag{5.1}$$

where $H_x^\pm$ and $H_y^\pm$ denote partial derivatives of $H^\pm \colon \mathbb{R}^2 \longrightarrow \mathbb{R}$ with respect to the state variables

x and y, respectively, $(\mu, \nu) \in I_\mu \times I_\nu$ are real parameters, being both I_μ and I_ν open intervals containing zero. The switching manifold is given by $\Sigma = f^{-1}(0)$ where $f(x, y) = y$.

Suppose that there exists an invisible fold singularity $\big(x_0^+(\mu), 0\big) \in \Sigma$ of $\mathcal{X}$, for all $\nu \in I_\nu$. By a translation we can suppose that this invisible fold singularity is at origin for $\mu = \mu_0 = 0$, that is, $x_0^+(0) = 0$. In a similar way, let us suppose that there exists an invisible fold-fold singularity $\big(x_0^-(\mu), 0\big) \subset \Sigma$ of $\mathcal{Y}$ such that $x_0^-(0) = 0$. Accordingly, we need study the quadratic contact between $\mathcal{X}$, $\mathcal{Y}$ and the switching manifold Σ. The derivative of f in the direction of the vector field $\mathcal{X}$ is given by

$$\mathcal{X}f(x, y, \mu, \nu) = \Big(- H_y^+(x, y, \mu, \nu), H_x^+(x, y, \mu, \nu)\Big) \cdot (0, 1) = H_x^+(x, y, \mu, \nu).$$

Therefore, for the purpose of obtaining a tangential singularity of $\mathcal{X}$ we must assume that

$$H_x^+ \left(x_0^+(\mu), 0, \mu, \nu\right) = 0. \tag{5.2}$$

Similarly, the tangential singularities of the vector field $\mathcal{Y}$ are given by

$$\mathcal{Y}f(x, y, \mu, \nu) = \Big(- H_y^-(x, y, \mu, \nu), H_x^-(x, y, \mu, \nu)\Big) \cdot (0, 1) = H_x^-(x, y, \mu, \nu)$$

and we assume that

$$H_x^- \left(x_0^-(\mu), 0, \mu, \nu\right) = 0. \tag{5.3}$$

Moreover,

$$\begin{aligned} \mathcal{X}^2 f(x, y, \mu, \nu) &= \mathcal{X}(x, y, \mu, \nu) \cdot \nabla \mathcal{X} f(x, y, \mu, \nu) \\ &= -H_y^+(x, y, \mu, \nu) H_{xx}^+(x, y, \mu, \nu) + H_x^+(x, y, \mu, \nu) H_{xy}^+(x, y, \mu, \nu). \end{aligned}$$

Therefore, an invisible fold point of $\mathcal{X}$ must satisfies

$$\mathcal{X}^2 f\left(x_0^+(\mu), 0, \mu, \nu\right) = -H_y^+\left(x_0^+(\mu), 0, \mu, \nu\right) H_{xx}^+\left(x_0^+(\mu), 0, \mu, \nu\right) < 0.$$

Analogously,

$$\mathcal{Y}^2 f\left(x_0^-(\mu), 0, \mu, \nu\right) = -H_y^-\left(x_0^-(\mu), 0, \mu, \nu\right) H_{xx}^-\left(x_0^-(\mu), 0, \mu, \nu\right) > 0.$$

In addition, with the purpose of getting a crossing region in a neighborhood of the invisible fold-fold point at the origin we assume $-H_y^+(0, 0, 0, \nu) > 0$ and $-H_y^-(0, 0, 0, \nu) < 0$. The previous calculations prove the next result.

Proposition 39. *Consider the family of PSVFs $\mathcal{Z}$ given in* (5.1)*. If the following assumptions are satisfied*

$$H_x^{\pm}(0,0,0,\nu)=0,\quad H_y^{+}(0,0,0,\nu)<0,\quad H_y^{-}(0,0,0,\nu)>0,\quad H_{xx}^{\pm}(0,0,0,\nu)<0, \tag{5.4}$$

then $\mathcal{Z}$ possesses a crossing invisible fold-fold singularity at the origin.

Consider the switching manifold Σ with the order inherited from the abscissa axis. In order to have a kind of "transversality", we will consider that the collision between the fold points occurs as follows: the abscissa $x_0^+(\mu)$ of the fold point of $\mathcal{X}$ is smaller (greater) than the abscissa $x_0^-(\mu)$ of the fold point of $\mathcal{Y}$ for negative values of μ. For $\mu=0$ the tangential singularities coincide and for $\mu>0$ the abscissa $x_0^+(\mu)$ of the fold point of $\mathcal{X}$ is greater (smaller) than the abscissa $x_0^-(\mu)$ of the fold point of $\mathcal{Y}$. In this way, we can define the function

$$\gamma(\mu)=x_0^+(\mu)-x_0^-(\mu),\quad \mu\in I_\mu. \tag{5.5}$$

Note that $\gamma(0)=0$. To satisfy the above description we consider $\gamma'(0)\neq 0$, that is, the graph of γ cross transversally the μ-axis and changes its sign in a neighborhood of the origin. Observe that

$$\gamma'(\mu)=\left(x_0^+\right)'(\mu)-\left(x_0^-\right)'(\mu).$$

From the derivative of Equations (5.2) and (5.3) with respect to μ we get

$$\left(x_0^{\pm}\right)'(\mu)=-\frac{H_{x\mu}^{\pm}\left(x_0^{\pm}(\mu),0,\mu,\nu\right)}{H_{xx}^{\pm}\left(x_0^{\pm}(\mu),0,\mu,\nu\right)}.$$

Therefore, to get $\gamma'(0)\neq 0$ we need to assume

$$\mathcal{T}=\frac{H_{x\mu}^{-}(0,0,0,\nu)}{H_{xx}^{-}(0,0,0,\nu)}-\frac{H_{x\mu}^{+}(0,0,0,\nu)}{H_{xx}^{+}(0,0,0,\nu)}\neq 0. \tag{5.6}$$

For positive values of $\gamma'(0)=\mathcal{T}$ we have that the function γ is increasing. So, we obtain the sliding set $\{(x,y)\in\mathbb{R}^2 : x_0^+(\mu)<x<x_0^-(\mu),\ y=0\}\subset\Sigma$, for $\mu<0$, while we get the escaping set $\{(x,y)\in\mathbb{R}^2 : x_0^-(\mu)<x<x_0^+(\mu),\ y=0\}\subset\Sigma$, for $\mu>0$. The reverse order holds for negative values of $\gamma'(0)$. In these sets, the sliding vector field Z^s given by equation (1.2) has pseudo equilibria. In fact, the sliding vector field Z^s has the expression

$$\mathcal{Z}^s(x,y,\mu,\nu)=\frac{H_x^+(x,y,\mu,\nu)H_y^-(x,y,\mu,\nu)-H_x^-(x,y,\mu,\nu)H_y^+(x,y,\mu,\nu)}{H_x^-(x,y,\mu,\nu)-H_x^+(x,y,\mu,\nu)}.$$

Note that the zeros of $\mathcal{Z}^s$ correspond to points where X and Y are linearly dependent, that is, when it holds

$$\xi(x,y,\mu,\nu) = H_x^+(x,y,\mu,\nu)H_y^-(x,y,\mu,\nu) - H_x^-(x,y,\mu,\nu)H_y^+(x,y,\mu,\nu) = 0.$$

By the hypothesis of Proposition 39 we have that $\xi(p_\nu) = 0$ and $\xi_x(p_\nu) = H_{xx}^+(p_\nu)H_y^-(p_\nu) - H_{xx}^-(p_\nu)H_y^+(p_\nu) < 0$. By the Implicit Function Theorem there exist an open interval I containing zero and a function $x\colon I \to \mathbb{R}$ such that $x(0) = 0$ and $\xi(x(\mu), 0, \mu, \nu) = 0$ for all $\mu \in I$. Therefore, for each $\mu \neq 0$ sufficiently small there exists $x(\mu)$ such that the point $(x(\mu), 0) \in \Sigma$ is a equilibrium of $\mathcal{Z}^s$ which behaves like an attractor on Σ since the derivative of ξ with respect to x at $(x(\mu), 0, \mu, \nu)$ is negative for μ sufficiently small.

In order to analyze if two points $(a, 0)$ and $(b, 0)$ of the switching manifold Σ are on the same level sets of the Hamiltonian functions $H^\pm$ associated with the vector fields $\mathcal{X}$ and $\mathcal{Y}$ we may define

$$F^\pm(a,b,\mu,\nu) = H^\pm(b,0,\mu,\nu) - H^\pm(a,0,\mu,\nu) \tag{5.7}$$

Since $F^\pm(a,a,\mu,\nu) = 0$ we can write

$$F^\pm(a,b,\mu,\nu) = (b-a)G^\pm(a,b,\mu,\nu). \tag{5.8}$$

In fact, it is enough to consider $b = a_0 + a$ and take the Taylor series of $F^\pm$ next to $a_0 = 0$. Observe that

$$\begin{aligned} F_b^\pm(a,b,\mu,\nu) &= \frac{\partial F^\pm}{\partial b}(a,b,\mu,\nu) \\ &= G^\pm(a,b,\mu,\nu) + (b-a)G_b^\pm(a,b,\mu,\nu) \\ &= H_x^\pm(b,0,\mu,\nu). \end{aligned}$$

Thus, $F_b^\pm(0,0,0,\nu) = H_x^\pm(0,0,0,\nu) = G^\pm(0,0,0,\nu) = 0$. Additionally,

$$\begin{aligned} F_{bb}^\pm(a,b,\mu,\nu) &= 2G_b^\pm(a,b,\mu,\nu) + (b-a)G_{bb}^\pm(a,b,\mu,\nu) \\ &= H_{xx}^\pm(b,0,\mu,\nu). \end{aligned}$$

Therefore, we have that $F_{bb}^\pm(0,0,0,\nu) = H_{xx}^\pm(0,0,0,\nu) = 2G_b^\pm(0,0,0,\nu) \neq 0$. Since $G^\pm(0,0,0,\nu) = 0$ and $G_b^\pm(0,0,0,\nu) \neq 0$, by Implicit Function Theorem there exist open sets

$A^{\pm} \subset \mathbb{R}^3$, $B^{\pm} \subset \mathbb{R}$ and $\varphi^{\pm}\colon A^{\pm} \longrightarrow \mathbb{R}$ such that $\varphi^{\pm}(0,0,\nu) = 0$ and

$$G^{\pm}(a, \varphi^{\pm}(a,\mu,\nu), \mu, \nu) = 0 \tag{5.9}$$

for all $(a,\mu,\nu) \in A^{\pm}$.

In short, given $(a,0) \in \Sigma$ we can define the half return map associated with the vector field $\mathcal{X}$ by $\varphi^{+}(a,\mu,\nu) = \phi_{\mathcal{X}}(t_{+}(a,0,\mu,\nu), a, 0, \mu, \nu)$, where $\varphi^{+}(0,0,\nu) = 0$, and the half return map associated with the vector field $\mathcal{Y}$ by $\varphi^{-}(a,\mu,\nu) = \phi_{\mathcal{Y}}(t_{-}(a,0,\mu,\nu), a, 0, \mu, \nu)$, where $\varphi^{-}(0,0,\nu) = 0$. Thus, the first return map associated with the vector field $\mathcal{Z}$ is given by (see Figure 5.1)

$$\Pi(a,\mu,\nu) = \varphi^{+}(\varphi^{-}(a,\mu,\nu), \mu, \nu). \tag{5.10}$$

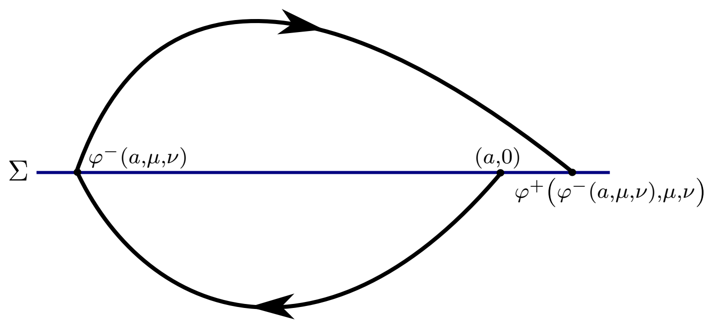

Figure 5.1: First return map associated with $\mathcal{Z}$.

Lemma 14. *Consider the functions $G^{\pm}$ given in* (5.8)*. It holds that*

$$G_a^{\pm}(0,0,0,\nu) = G_b^{\pm}(0,0,0,\nu).$$

Proof. Indeed, let us define

$$\vartheta(a,b,\mu,\nu) = H^{\pm}(b,0,\mu,\nu) - H^{\pm}(a,0,\mu,\nu) - (b-a)G^{\pm}(a,b,\mu,\nu).$$

Taking the Taylor series of ϑ about $(a,b,\mu) = (0,0,0)$ we get that the coefficient of the term $a^1b^1\mu^1$ is $G_a^{\pm}(0,0,0,\nu) - G_b^{\pm}(0,0,0,\nu)$. Since $\vartheta(0,0,0,\nu) = 0$ it follows that $G_a^{\pm}(0,0,0,\nu) = G_b^{\pm}(0,0,0,\nu)$. $\square$

Consider the first return map Π given by (5.10). The Taylor series of Π in a neighborhood of $(a,\mu)=(0,0)$ can be write as

$$\Pi(a,\mu,\nu)=c_{01}(\nu)\mu+c_{10}(\nu)a+c_{20}(\nu)a^2+c_{11}(\nu)a\mu+c_{02}(\nu)\mu^2+\cdots. \tag{5.11}$$

Proposition 40. *Consider the first return map* Π *given by* (5.11). *Then* $c_{10}(\nu)=1$.

Proof. Firstly, observe that $c_{10}(\nu)=\varphi_a^-(0,0,\nu)\varphi_a^+(0,0,\nu)$. Considering the Taylor series of $G^{\pm}(a,\varphi^{\pm}(a,\mu,\nu),\mu,\nu)$ in a neighborhood of $(a,\mu)=(0,0)$ we have that the coefficient of the term $a^1\mu^0$ is given by

$$\varphi_a^{\pm}(0,0,\nu)G_b^{\pm}(0,0,0,\nu)+G_a^{\pm}(0,0,0,\nu).$$

Therefore, by (5.9) and Lemma 14 we obtain that

$$\varphi_a^{\pm}(0,0,\nu)=-\frac{G_a^{\pm}(0,0,0,\nu)}{G_b^{\pm}(0,0,0,\nu)}=-1$$

and consequently $c_{10}(\nu)=1$. □

By Proposition 40 and Equation (5.11) we have that the displacement function Δ associated with $\mathcal{Z}$ has the expression

$$\Delta(a,\mu,\nu)=\Pi(a,\mu,\nu)-a=c_{01}(\nu)\mu+c_{20}(\nu)a^2+c_{11}(\nu)a\mu+c_{02}(\nu)\mu^2+\cdots \tag{5.12}$$

Proposition 41. *Consider the displacement function* Δ *given by* (5.12). *There exist open sets* $U\subset\mathbb{R}^2$, $V\subset\mathbb{R}$ *and a function* $\alpha\colon U\longrightarrow V$ *such that* $\alpha(0,\nu)=0$ *and* $\Delta(a,\alpha(a,\nu),\nu))=0$ *for all* $(a,\nu)\in U$.

Proof. Observe that $\Delta(0,0,\nu)=0$. Moreover, the derivative of Δ with respect to μ is given by

$$\Delta_\mu(0,0,\nu)=c_{01}(\nu)=\varphi_\mu^+(0,0,\nu)+\varphi_\mu^-(0,0,\nu)\varphi_a^+(0,0,\nu).$$

Considering the Taylor series of $G^{\pm}(a,\varphi^{\pm}(a,\mu,\nu),\mu,\nu)$ given by (5.9) in a neighborhood of $(a,\mu)=(0,0)$ and equaling their coefficients to zero we can obtain expressions for the derivatives of $\varphi^{\pm}$ in terms of $G^{\pm}$ and consequently in terms of $H^{\pm}$. In this way, we obtain

$$\Delta_\mu(0,0,\nu)=\frac{2H_{x\mu}^-(0,0,0,\nu)}{H_{xx}^-(0,0,0,\nu)}-\frac{2H_{x\mu}^+(0,0,0,\nu)}{H_{xx}^+(0,0,0,\nu)}.$$

By the transversality hypothesis given in (5.6), it follows that $\Delta_\mu(0,0,\nu)\neq 0$. Since $\Delta(0,0,\nu)=0$ and $\Delta_\mu(0,0,\nu)\neq 0$ by Implicit Function Theorem there exists open sets $U\subset\mathbb{R}^2$, $V\subset\mathbb{R}$ and a function $\alpha\colon U\longrightarrow V$ such that $\alpha(0,\nu)=0$ and $\Delta(a,\alpha(a,\nu),\nu)=0$, for all $(a,\nu)\in U$. □

By Proposition 41, we obtain the function $\mu = \alpha(a, \nu)$ giving the zeroes of the displacement function Δ, that is, by the fixed points of the Poincaré map Π. Expanding $\Delta(a, \alpha(a, \nu), \nu)$ in Taylor series around $a = 0$ and equaling their coefficients to zero we can conclude that

$$\alpha(a, \nu) = -\frac{c_{20}(\nu)}{c_{01}(\nu)} a^2 + \frac{c_{11}(\nu)c_{20}(\nu) - c_{01}(\nu)c_{30}(\nu)}{c_{01}(\nu)^2} a^3 + R_4(\nu)a^4 + \mathcal{O}\left(a^5\right), \tag{5.13}$$

where

$$R_4(\nu) = -\frac{c_{40}(\nu)c_{01}(\nu)^2 - c_{20}(\nu)c_{21}(\nu)c_{01}(\nu) - c_{11}(\nu)c_{30}(\nu)c_{01}(\nu) + c_{02}(\nu)c_{20}(\nu)^2 + c_{11}(\nu)^2 c_{20}(\nu)}{c_{01}(\nu)^3}.$$

It follows that the derivative of the Poincaré map Π with respect to the variable a and evaluated on $\mu = \alpha(a, \nu)$ has the expression

$$\Pi_a(a, \alpha(a, \nu), \nu) = 1 + 2c_{20}(\nu)a + \left(3c_{30}(\nu) - \frac{c_{11}(\nu)c_{20}(\nu)}{c_{01}(\nu)}\right) a^2 + C_3(\nu)a^3 + C_4(\nu)a^4 + \mathcal{O}(a^5), \tag{5.14}$$

where

$$C_3(\nu) = \frac{c_{11}(\nu)^2 c_{20}(\nu)}{c_{01}(\nu)^2} - \frac{2c_{20}(\nu)c_{21}(\nu) + c_{11}(\nu)c_{30}(\nu)}{c_{01}(\nu)} + 4c_{40}(\nu) \tag{5.15}$$

and

$$\begin{aligned} C_4(\nu) \;=\; & -\frac{c_{20}(\nu)c_{11}(\nu)^3}{c_{01}(\nu)^3} + \frac{c_{30}(\nu)c_{11}(\nu)^2}{c_{01}(\nu)^2} - \frac{c_{02}(\nu)c_{20}(\nu)^2 c_{11}(\nu)}{c_{01}(\nu)^3} + \frac{3c_{20}(\nu)c_{21}(\nu)c_{11}(\nu)}{c_{01}(\nu)^2} \\ & -\frac{c_{40}(\nu)c_{11}(\nu)}{c_{01}(\nu)} + \frac{c_{12}(\nu)c_{20}(\nu)^2}{c_{01}(\nu)^2} - \frac{2c_{21}(\nu)c_{30}(\nu)}{c_{01}(\nu)} - \frac{3c_{20}(\nu)c_{31}(\nu)}{c_{01}(\nu)} + 5c_{50}(\nu). \end{aligned} \tag{5.16}$$

Equivalently, we have

$$\Delta_a(a, \alpha(a, \nu), \nu) = 2c_{20}(\nu)a + \left(3c_{30}(\nu) - \frac{c_{11}(\nu)c_{20}(\nu)}{c_{01}(\nu)}\right) a^2 + C_3(\nu)a^3 + C_4(\nu)a^4 + \mathcal{O}(a^5). \tag{5.17}$$

In this way, we can identify the kth Lyapunov coefficient for the PSVF $\mathcal{Z}$ as the kth obstruction on the fixed point of the first return map to have derivative distinct to one, that is, the kth obstruction on the zero of the displacement function to be simple.

In agreement with these definition we have the following result.

Theorem 15. *Consider the family of PSVFs $\mathcal{Z}$ given in* (5.1) *satisfying the assumptions* (5.4)*, that is, there exists an invisible fold-fold singularity at the origin with a crossing region on its neighborhood. Suppose also that it satisfies the transversality hypothesis $\mathcal{T} \neq 0$ given in* (5.6)*.*

Then, the first Lyapunov coefficients of $\mathcal{Z}$ at $p_\nu = (0,0,0,\nu)$, $\nu \in I_\nu$, are given by

$$L_1^* = 0, \quad L_2^* = \frac{1}{3}\left(\frac{H^-_{xxx}(p_\nu)}{H^-_{xx}(p_\nu)} - \frac{H^+_{xxx}(p_\nu)}{H^+_{xx}(p_\nu)}\right), \quad L_3^* = 0. \tag{5.18}$$

Proof. By equation (5.17), we obtain that the displacement function Δ does not have the linear term and consequently $L_1^* = 0$. The next obstruction to the function Δ be zero is the coefficient $c_{20}(\nu)$. Considering the Taylor series of $G^\pm(a, \varphi^\pm(a,\mu,\nu), \mu, \nu)$ given by (5.9) around $(a,\mu) = (0,0)$ and equaling their coefficients to zero we can obtain expressions for the derivatives of $\varphi^\pm$ in terms of $G^\pm$ and consequently in terms of $H^\pm$. So, we get

$$L_2^* = c_{20}(\nu) = \frac{1}{3}\left(\frac{H^-_{xxx}(p_\nu)}{H^-_{xx}(p_\nu)} - \frac{H^+_{xxx}(p_\nu)}{H^+_{xx}(p_\nu)}\right).$$

Similarly, we get that the coefficient $c_{30}(\nu)$ is given by

$$\begin{aligned} c_{30}(\nu) &= \frac{1}{9}\left(\frac{H^-_{xxx}(p_\nu)^2}{H^-_{xx}(p_\nu)^2} - \frac{2H^-_{xxx}(p_\nu)H^+_{xxx}(p_\nu)}{H^-_{xx}(p_\nu)H^+_{xx}(p_\nu)} + \frac{H^+_{xxx}(p_\nu)^2}{H^+_{xx}(p_\nu)^2}\right) \\ &= \left[\frac{1}{3}\left(\frac{H^-_{xxx}(p_\nu)}{H^-_{xx}(p_\nu)} - \frac{H^+_{xxx}(p_\nu)}{H^+_{xx}(p_\nu)}\right)\right]^2 = (c_{20}(\nu))^2. \end{aligned} \tag{5.19}$$

So, if $c_{20}(\nu) = 0$ then $c_{30}(\nu) = 0$ and the coefficient of the quadratic term of Π_a vanishes. Therefore, $L_3^* = 0$ and the proof of Theorem 15 is complete.

□

Remark 21. *Equivalently, the second Lyapunov coefficient can be written as*

$$L_2^* = \frac{1}{3}\left(\frac{H^+_{xx}(p_\nu)H^-_{xxx}(p_\nu) - H^-_{xx}(p_\nu)H^+_{xxx}(p_\nu}{H^-_{xx}(p_\nu)H^+_{xx}(p_\nu)}\right).$$

By hypotheses (5.4) *the above denominator is positive and therefore the sign of L_2^* is given by its numerator.*

The following two theorems summarize the local bifurcations that occur in a neighborhood of an invisible fold-fold singularity when the second Lyapunov coefficient is nonzero.

Theorem 16. *Consider the family of PSVFs $\mathcal{Z}$ given in* (5.1) *satisfying the assumptions* (5.4) *and $\mathcal{T} > 0$. The following statements hold:*

1. *Type I: if $L_2^* > 0$ then there exists a repelling hyperbolic crossing limit cycle for $\mu < 0$ and none for $\mu > 0$. Moreover, the invisible fold-fold singularity is a repellor when $\mu = 0$. See Figure 5.2.*

2. *Type II: if $L_2^* < 0$ then there exists an attracting hyperbolic crossing limit cycle for $\mu > 0$ and none for $\mu < 0$. Moreover, the invisible fold-fold singularity is an attractor when $\mu = 0$.*

Proof. Note that, for $\mu = 0$, the displacement function is given by $\Delta(a, 0, \nu) = c_{20}(\nu)a^2 + \mathcal{O}(a^3)$. Therefore, the invisible fold-fold singularity is a repellor if $L_2^* = c_{20}(\nu) > 0$ and it is an attractor if $L_2^* = c_{20}(\nu) < 0$. If $L_2^* = c_{20}(\nu) > 0$ and $\mathcal{T} = \gamma'(0) = c_{01}(\nu)/2 > 0$, then, by equation (5.13), it follows that $\mu = \alpha(a, \nu) < 0$, for small a. Also, from equation (5.14), we obtain $\Pi_a(a, \alpha(a, \nu), \nu) > 1$ and therefore the crossing limit cycle is a repellor. This proves item 1 of Theorem 16. On the other hand, if $L_2^* = c_{20}(\nu) < 0$, then $\mu = \alpha(a, \nu) > 0$, for small a, and $\Pi_a(a, \alpha(a, \nu), \nu) < 1$. Therefore, there exists an attracting crossing limit cycle for $\mu > 0$ and none for $\mu < 0$ proving item 2 of Theorem 16.

□

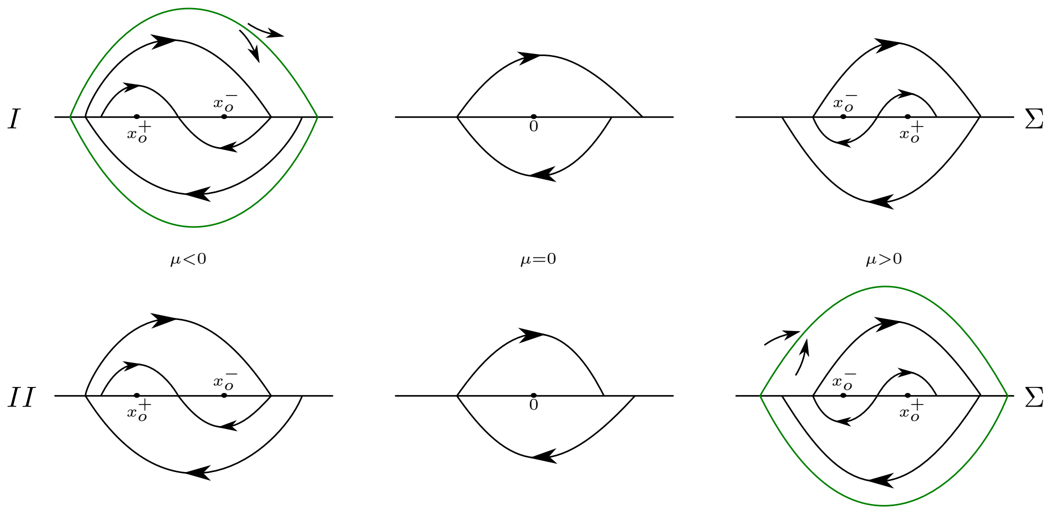

Figure 5.2: Bifurcation diagrams of an invisible fold-fold singularity for $L_2^* \neq 0$ and $\mathcal{T} > 0$.

An analogous of Theorem 16 can be obtained when $\mathcal{T} = \gamma'(0) < 0$.

Theorem 17. *Consider the family of PSVFs $\mathcal{Z}$ given in* (5.1) *satisfying the assumptions* (5.4) *and $\mathcal{T} < 0$. The following statements hold:*

1. *Type III: if $L_2^* > 0$ then there exists a repelling hyperbolic crossing limit cycle for $\mu > 0$ and none for $\mu < 0$. Moreover, the invisible fold-fold singularity is a repellor when $\mu = 0$. See Figure 5.3.*

2. *Type IV: if $L_2^* < 0$ then there exists an attracting hyperbolic crossing limit cycle for $\mu < 0$ and none for $\mu > 0$. Moreover, the invisible fold-fold singularity is an attractor when $\mu = 0$. See Figure 5.3.*

Proof. If $\mu = 0$, then the displacement function is given by $\Delta(a,0,\nu) = c_{20}(\nu)a^2 + \mathcal{O}\left(a^3\right)$. Therefore, the invisible fold-fold singularity is a repellor if $L_2^* = c_{20}(\nu) > 0$ and it is an attractor if $L_2^* = c_{20}(\nu) < 0$. If $L_2^* = c_{20}(\nu) > 0$ and $\mathcal{T} = \gamma'(0) = c_{01}(\nu)/2 < 0$, then, by equation (5.13), it follows that $\mu = \alpha(a,\nu) > 0$, for small a. From equation (5.14) we obtain $\Pi_a(a,\alpha(a,\nu),\nu) > 1$ and therefore the crossing limit cycle is a repellor. So, item 1 of Theorem 17 is proved. On the other hand, if $L_2^* = c_{20}(\nu) < 0$, then $\mu = \alpha(a,\nu) < 0$, for small a, and $\Pi_a(a,\alpha(a,\nu),\nu) < 1$. Therefore, there exists an attracting crossing limit cycle for $\mu < 0$ and none for $\mu > 0$ which proves item 2 of Theorem 17.

□

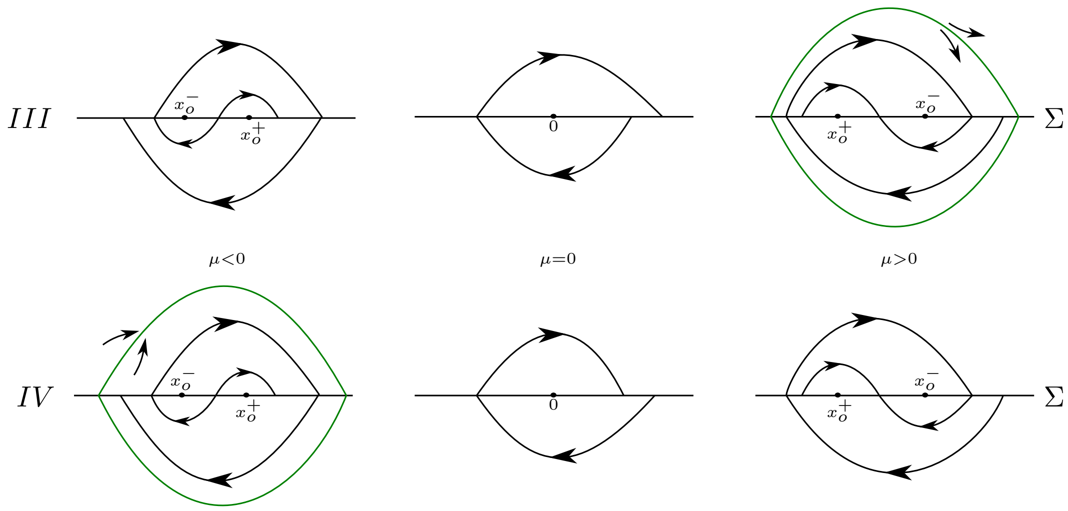

Figure 5.3: Bifurcation diagram of an invisible fold-fold singularity for $L_2^* \neq 0$ and $\mathcal{T} < 0$.

Next result gives a formula for the fourth Lyapunov coefficient associated with the vector field $\mathcal{Z}$.

Theorem 18. *Consider the family of PSVFs $\mathcal{Z}$ given in* (5.1) *satisfying the assumptions* (5.4) *and* (5.6)*. Then, the fourth and fifth Lyapunov coefficients of $\mathcal{Z}$ at $p_\nu = (0,0,0,\nu)$ are given by*

$$\begin{aligned} L_4 &= -\frac{H^+_{xxx}(p_\nu)H^-_{xxxx}(p_\nu)}{18H^-_{xx}(p_\nu)H^+_{xx}(p_\nu)} + \frac{H^+_{xxx}(p_\nu)H^+_{xxxx}(p_\nu)}{18H^+_{xx}(p_\nu)^2} + \frac{H^-_{xxxxx}(p_\nu)}{60H^-_{xx}(p_\nu)} - \frac{H^+_{xxxxx}(p_\nu)}{60H^+_{xx}(p_\nu)}, \\ L_5 &= 0. \end{aligned} \tag{5.20}$$

Proof. Recall that L_4^* must be computed just when $L_1^* = L_2^* = 0$, since this implies that $L_3^* = 0$. By equation (5.19), if $L_2^* = c_{20}(\nu) = 0$ then the coefficient of the quadratic term of equation (5.14) also vanishes and thus we have

$$\Pi_a(a,\alpha(a,\nu),\nu) = 4c_{40}(\nu)a^3 + \mathcal{O}(a^4).$$

Therefore, $L_4^* = c_{40}(\nu)$. Similarly to the approach used in the proof of Theorem 15, we obtain

$$\begin{aligned} L_4^* &= \frac{2H^-_{xxx}(p_\nu)^3}{27H^-_{xx}(p_\nu)^3} - \frac{H^-_{xxx}(p_\nu)^2 H^+_{xxx}(p_\nu)}{9H^-_{xx}(p_\nu)^2 H^+_{xx}(p_\nu)} + \frac{H^-_{xxx}(p_\nu) H^+_{xxx}(p_\nu)^2}{9H^-_{xx}(p_\nu) H^+_{xx}(p_\nu)^2} - \frac{2H^+_{xxx}(p_\nu)^3}{27H^+_{xx}(p_\nu)^3} \\ &\quad - \frac{H^-_{xxx}(p_\nu) H^-_{xxxx}(p_\nu)}{18H^-_{xx}(p_\nu)^2} + \frac{H^+_{xxx}(p_\nu) H^+_{xxxx}(p_\nu)}{18H^+_{xx}(p_\nu)^2} + \frac{H^-_{xxxxx}(p_\nu)}{60H^-_{xx}(p_\nu)} - \frac{H^+_{xxxxx}(p_\nu)}{60H^+_{xx}(p_\nu)}. \end{aligned}$$

Adding the hypothesis $L_2^* = 0$, we obtain that L_4^* can be written as in (5.20). When $L_2^* = L_4^* = 0$, the coefficient C_4 given by equation (5.16), that will determine the fifth Lyapunov coefficient, can be written as $C_4 = 5c_{50}(\nu)$. By definition we get that the fifth Lyapunov coefficient is given by

$$\begin{aligned} L_5^* &= c_{50}(\nu) \\ &= \frac{4H^-_{xxx}(p_\nu)^4}{81H^-_{xx}(p_\nu)^4} - \frac{2H^-_{xxx}(p_\nu)^3 H^+_{xxx}(p_\nu)}{27H^-_{xx}(p_\nu)^3 H^+_{xx}(p_\nu)} + \frac{2H^-_{xxx}(p_\nu)^2 H^+_{xxx}(p_\nu)^2}{27H^-_{xx}(p_\nu)^2 H^+_{xx}(p_\nu)^2} \\ &\quad - \frac{8H^-_{xxx}(p_\nu) H^+_{xxx}(p_\nu)^3}{81H^-_{xx}(p_\nu) H^+_{xx}(p_\nu)^3} + \frac{4H^+_{xxx}(p_\nu)^4}{81H^+_{xx}(p_\nu)^4} - \frac{H^-_{xxx}(p_\nu)^2 H^-_{xxxx}(p_\nu)}{18H^-_{xx}(p_\nu)^3} \\ &\quad + \frac{H^-_{xxx}(p_\nu) H^+_{xxx}(p_\nu) H^-_{xxxx}(p_\nu)}{27H^-_{xx}(p_\nu)^2 H^+_{xx}(p_\nu)} + \frac{2H^-_{xxx}(p_\nu) H^+_{xxx}(p_\nu) H^+_{xxxx}(p_\nu)}{27H^-_{xx}(p_\nu) H^+_{xx}(p_\nu)^2} \\ &\quad - \frac{H^+_{xxx}(p_\nu)^2 H^+_{xxxx}(p_\nu)}{18H^+_{xx}(p_\nu)^3} + \frac{H^-_{xxx}(p_\nu) H^-_{xxxxx}(p_\nu)}{60H^-_{xx}(p_\nu)^2} - \frac{H^+_{xxx}(p_\nu) H^-_{xxxxx}(p_\nu)}{90H^-_{xx}(p_\nu) H^+_{xx}(p_\nu)} \\ &\quad - \frac{H^-_{xxx}(p_\nu) H^+_{xxxxx}(p_\nu)}{45H^-_{xx}(p_\nu) H^+_{xx}(p_\nu)} + \frac{H^+_{xxx}(p_\nu) H^+_{xxxxx}(p_\nu)}{60H^+_{xx}(p_\nu)^2}. \end{aligned}$$

By a straightforward calculation we conclude that L_5^* vanishes when $L_2^* = L_4^* = 0$. □

Based on Theorems 15 and 18 and taking into account the smooth case (see [4, 27]) we state the following conjecture.

Conjecture 1. *Consider the family of PSVFs $\mathcal{Z}$ given in* (5.1) *satisfying the assumptions* (5.4) *and* (5.6)*. Let*

$$\Delta(a) = \sum_{k=1}^{\infty} L_k^* a^k$$

be the displacement function associated with $\mathcal{Z}$ in a neighborhood of the crossing invisible fold-fold singularity. If there exists $k \in \mathbb{N}$ such that $L_1^* = \ldots = L_{k-1}^* = 0$ and $L_k^* \neq 0$ then k is an even number.

By Proposition 41, we get the function $\alpha(a, \nu)$ such that $\Delta(a, \alpha(a, \nu), \nu) = 0$ for all $(a, \nu) \in U$ where

$$\alpha(a, \nu) = -\frac{c_{20}(\nu)}{c_{01}(\nu)} a^2 + \frac{c_{11}(\nu)c_{20}(\nu) - c_{01}(\nu)c_{30}(\nu)}{c_{01}(\nu)^2} a^3 + \mathcal{O}\left(a^4\right).$$

By equation (5.14), we write

$$\begin{aligned}\Delta_a(a,\alpha(a,\nu),\nu) &= 2c_{20}(\nu)a + \left(3c_{30}(\nu) - \frac{c_{11}(\nu)c_{20}(\nu)}{c_{01}(\nu)}\right)a^2 + \\ &+ \left(\frac{c_{11}(\nu)^2c_{20}(\nu)}{c_{01}(\nu)^2} - \frac{2c_{20}(\nu)c_{21}(\nu)+c_{11}(\nu)c_{30}(\nu)}{c_{01}(\nu)} + 4c_{40}(\nu)\right)a^3 + \mathcal{O}(a^4) \\ &= a\psi(a,\nu)\end{aligned} \tag{5.21}$$

where $\psi(a,\nu) = f_1(\nu) + f_2(\nu)a + f_3(\nu)a^2 + \mathcal{O}(a^3)$ with $f_1(\nu) = 2c_{20}$,

$$f_2(\nu) = 3c_{30}(\nu) - \frac{c_{11}(\nu)c_{20}(\nu)}{c_{01}(\nu)},$$

$$f_3(\nu) = \frac{c_{11}(\nu)^2c_{20}(\nu)}{c_{01}(\nu)^2} - \frac{2c_{20}(\nu)c_{21}(\nu)+c_{11}(\nu)c_{30}(\nu)}{c_{01}(\nu)} + 4c_{40}(\nu)$$

and so forth.

As already mentioned before, the periodic orbits of $\mathcal{Z}$ are given by the fixed points of the first return map Π that correspond to the zeros of the displacement function Δ. Thus, the bifurcation that leads to the disappearance of these periodic orbits corresponds to the existence of a double zero of Δ.

Let us suppose that $f_1(0) = 0$ and $f_1'(0) \neq 0$, that is, the second Lyapunov coefficient L_2^* is null and L_2^* is regular for $\nu = 0$. The last assumption, when written in terms of the Hamiltonian functions, has the expression

$$L_2^{*\prime}(0) = c_{20}'(0) = -\frac{H^-_{xx\nu}(p_0)H^-_{xxx}(p_0)}{3H^-_{xx}(p_0)^2} + \frac{H^+_{xx\nu}(p_0)H^+_{xxx}(p_0)}{3H^+_{xx}(p_0)^2} + \frac{H^-_{xxx\nu}(p_0)}{3H^-_{xx}(p_0)} - \frac{H^+_{xxx\nu}(p_0)}{3H^+_{xx}(p_0)},$$

where $p_0 = (0,0,0,0)$, and can be seen as a second transversality condition. Therefore, since $\psi(0,0) = 0$ and $\psi_\nu(0,0) = f_1'(0) \neq 0$, by Implicit Function Theorem there exists a function $\nu = \eta(a)$ such that $\eta(0) = 0$ and $\psi(a,\eta(a)) = 0$ in a neighborhood of $a = 0$. So, by Equation (5.21), we obtain

$$\Delta_a(a,\alpha(a,\eta(a)),\eta(a)) = 0. \tag{5.22}$$

Moreover, by equation 5.19 we have seen that if $f_1(0) = 0$ then $f_2(0) = 0$. So, from the derivatives of $\psi(a,\eta(a)) = 0$ with respect to the variable a, we can obtain

$$\begin{aligned}\eta(a) &= -\frac{f_3(0)}{f_1'(0)}a^2 - \frac{f_4(0)f_1'(0) - f_3(0)f_2'(0)}{f_1'(0)^2}a^3 + \\ &+ \frac{2f_4(0)f_1'(0)f_2'(0) - 2f_3(0)f_2'(0)^2 + 2f_3(0)f_1'(0)f_3'(0) - f_3(0)^2f_1''(0)}{2f_1'(0)^3}a^4 + \mathcal{O}(a^5).\end{aligned}$$

In other words,

$$\eta(a) = \left(-\frac{c_{20}(0)\left(c_{11}(0)^2 - 2c_{01}(0)c_{21}(0)\right) - c_{01}(0)c_{11}(0)c_{30}(0)}{2c_{01}(0)^2 c_{20}'(0)} - \frac{4c_{40}(0)}{2c_{20}'(0)} \right) a^2 + \mathcal{O}(a^3). \quad (5.23)$$

When $c_{20}(0) = c_{30}(0) = 0$, equation (5.23) can be written as

$$\eta(a) = -\frac{2c_{40}(0)}{c_{20}'(0)} a^2 + \mathcal{O}(a^3). \quad (5.24)$$

Furthermore, the Taylor series of α (see (5.13)) about $(a, \nu) = (0, 0)$, and considering equation (5.23), has the expression

$$\alpha(a, \eta(a)) = -\frac{c_{20}(0)}{c_{01}(0)} a^2 + \frac{c_{11}(0)c_{20}(0) - c_{01}(0)c_{30}(0)}{c_{01}(0)^2} a^3 + B_4 a^4 + \mathcal{O}(a^5).$$

where

$$\begin{aligned} B_4 &= \frac{-c_{20}(0)c_{11}(0)^2\big(c_{20}(0)c_{01}'(0)+c_{01}(0)c_{20}'(0)\big)+c_{01}(0)c_{30}(0)c_{11}(0)\big(c_{20}(0)c_{01}'(0)+c_{01}(0)c_{20}'(0)\big)}{2c_{01}(0)^4 c_{20}'(0)} \\ &+ \frac{2c_{01}(0)\big(c_{40}(0)c_{01}(0)^2c_{20}'(0)-2c_{20}(0)c_{40}(0)c_{01}(0)c_{01}'(0)+c_{20}(0)^2\big(c_{21}(0)c_{01}'(0)-c_{02}(0)c_{20}'(0)\big)\big)}{2c_{01}(0)^4 c_{20}'(0)}. \end{aligned}$$

Taking into account that $c_{20}(0) = c_{30}(0) = 0$, the above expression can be written as

$$\alpha(a, \eta(a)) = \frac{c_{40}(0)}{c_{01}(0)} a^4 + \mathcal{O}(a^5). \quad (5.25)$$

The earlier calculations will be useful in the following result.

Proposition 42. *If $c_{20}(0) = 0$, $c_{20}'(0) \neq 0$ and $c_{40}(0) \neq 0$ the curve of non-hyperbolic periodic orbits associated with the PSVF $\mathcal{Z}$ has the following representation*

$$a \longmapsto \left(\frac{c_{40}(0)}{c_{01}(0)} a^4 + \mathcal{O}\left(a^5\right), -\frac{2c_{40}(0)}{c_{20}'(0)} a^2 + \mathcal{O}\left(a^3\right) \right)$$

as a curve parameterized by a or locally as a graphic of a function

$$\mu = \frac{c_{20}'(0)^2}{4c_{01}(0)c_{40}(0)} \nu^2 + \mathcal{O}\left(\nu^3\right). \quad (5.26)$$

Moreover, saddle-node bifurcations of periodic orbits take place on this curve.

Proof. Suppose $c_{20}(0) = 0$, $c_{20}'(0) \neq 0$ and $c_{40}(0) \neq 0$. We are seeking for a double zero of the displacement function Δ. By Proposition 41, there exists $\alpha(a, \nu)$ such that $\Delta(a, \alpha(a, \nu), \nu) = 0$, for all $(a, \nu) \in U$. By Implicit Function Theorem there exists a function $\nu = \eta(a)$ such that

$\eta(0) = 0$ and $\psi(a, \eta(a)) = 0$, where ψ is given by Equation (5.21). So, by Equation (5.21) we get $\Delta_a(a, \alpha(a, \eta(a)), \eta(a)) = 0$. Therefore, $a \longmapsto (\alpha(a, \eta(a)), \eta(a))$ corresponds to the curve of non-hyperbolic periodic orbits of $\mathcal{Z}$. If

$(A1)$ $\Delta(a, \alpha(a, \eta(a)), \eta(a)) = 0$;

$(A2)$ $\Delta_a(a, \alpha(a, \eta(a)), \eta(a)) = 0$;

$(A3)$ $\Delta_{aa}(a, \alpha(a, \eta(a)), \eta(a)) \neq 0$;

$(A4)$ $\Delta_\mu(a, \alpha(a, \eta(a)), \eta(a)) \neq 0$.

then a saddle-node bifurcation of periodic orbits occurs. It remains to show items $(A3)$ and $(A4)$. The Taylor series of the second derivative of the displacement function Δ given by Equation (5.12) with respect to the variable a evaluated on $(a, \alpha(a, \eta(a), \eta(a))$ and taking into account that $c_{20}(0) = c_{30}(0) = 0$ is given by

$$\Delta_{aa}(a, \alpha(a, \eta(a)), \eta(a)) = 8c_{40}(0)a^4 + \mathcal{O}\left(a^5\right).$$

So, $\Delta_{aa}(a, \alpha(a, \eta(a)), \eta(a)) \neq 0$ for a sufficiently small. Item $(A3)$ is proved. Analogously, the Taylor series of the derivative of the displacement function Δ with respect to the variable μ is given by

$$\Delta_\mu(a, \alpha(a, \eta(a)), \eta(a)) = c_{01}(0) + c_{11}(0)a + \mathcal{O}\left(a^2\right),$$

which is nonzero, for a sufficiently small, by the transversality condition $\gamma'(0) = c_{01}(0)/2 \neq 0$ given in (5.6). This proves item $(A4)$ and guarantee the existence of a saddle-node bifurcation in the curve of non-hyperbolic periodic orbits. By Equation (5.24)

$$\nu = \eta(a) = -\frac{2c_{40}(0)}{c_{20}'(0)}a^2 + \mathcal{O}(a^3).$$

So, by the Implicit Function Theorem we obtain

$$a^2 = -\frac{c_{20}'(0)}{2c_{40}(0)}\nu + \mathcal{O}(\nu^2).$$

Therefore, we can write

$$\mu = \alpha(a, \eta(a)) = \frac{c_{40}(0)}{c_{01}(0)}a^4 + \mathcal{O}(a^5) = \frac{c_{20}'(0)^2}{4c_{01}(0)c_{40}(0)}\nu^2 + \mathcal{O}\left(\nu^3\right).$$

□

Remark 22. *The curve of non-hyperbolic periodic orbits has the following expression when written in terms of the Hamiltonian functions associated with the PSVF $\mathcal{Z}$*

$$\mu = \frac{c_{20}'(0)^2}{4c_{01}(0)c_{40}(0)}\nu^2 + \mathcal{O}\left(\nu^3\right) = \frac{M_1}{M_2}\nu^2 + \mathcal{O}\left(\nu^3\right), \tag{5.27}$$

where

$$\begin{aligned} M_1 = {} & 15H_{xx}^+(p_0)^4H_{xx\nu}^-(p_0)^2H_{xxx}^-(p_0)^2 + 15H_{xx}^-(p_0)^4H_{xx\nu}^+(p_0)^2H_{xxx}^+(p_0)^2 \\ & -30H_{xx}^-(p_0)^2H_{xx}^+(p_0)^2H_{xx\nu}^-(p_0)H_{xx\nu}^+(p_0)H_{xxx}^-(p_0)H_{xxx}^+(p_0) \\ & -30H_{xx}^-(p_0)H_{xx}^+(p_0)^4H_{xx\nu}^-(p_0)H_{xxx}^-(p_0)H_{xxx\nu}^-(p_0) \\ & +30H_{xx}^-(p_0)^3H_{xx}^+(p_0)^2H_{xx\nu}^+(p_0)H_{xxx}^+(p_0)H_{xxx\nu}^-(p_0) \\ & +15H_{xx}^-(p_0)^2H_{xx}^+(p_0)^4H_{xxx\nu}^-(p_0)^2 \\ & +30H_{xx}^-(p_0)^2H_{xx}^+(p_0)^3H_{xx\nu}^-(p_0)H_{xxx}^-(p_0)H_{xxx\nu}^+(p_0) \\ & -30H_{xx}^-(p_0)^4H_{xx}^+(p_0)H_{xx\nu}^+(p_0)H_{xxx}^+(p_0)H_{xxx\nu}^+(p_0) \\ & -30H_{xx}^-(p_0)^3H_{xx}^+(p_0)^3H_{xxx\nu}^-(p_0)H_{xxx\nu}^+(p_0) + 15H_{xx}^-(p_0)^4H_{xx}^+(p_0)^2H_{xxx\nu}^+(p_0)^2, \end{aligned}$$

$$\begin{aligned} M_2 = {} & -80H_{x\mu}^+(p_0)H_{xx}^-(p_0)H_{xx}^+(p_0)^3H_{xxx}^-(p_0)^3 + 80H_{x\mu}^-(p_0)H_{xx}^+(p_0)^4H_{xxx}^-(p_0)^3 \\ & +120H_{x\mu}^+(p_0)H_{xx}^-(p_0)^2H_{xx}^+(p_0)^2H_{xxx}^-(p_0)^2H_{xxx}^+(p_0) \\ & -120H_{x\mu}^-(p_0)H_{xx}^-(p_0)H_{xx}^+(p_0)^3H_{xxx}^-(p_0)^2H_{xxx}^+(p_0) \\ & -120H_{x\mu}^+(p_0)H_{xx}^-(p_0)^3H_{xx}^+(p_0)H_{xxx}^-(p_0)H_{xxx}^+(p_0)^2 \\ & +120H_{x\mu}^-(p_0)H_{xx}^-(p_0)^2H_{xx}^+(p_0)^2H_{xxx}^-(p_0)H_{xxx}^+(p_0)^2 \\ & +80H_{x\mu}^+(p_0)H_{xx}^-(p_0)^4H_{xxx}^+(p_0)^3 - 80H_{x\mu}^-(p_0)H_{xx}^-(p_0)^3H_{xx}^+(p_0)H_{xxx}^+(p_0)^3 \\ & +60H_{x\mu}^+(p_0)H_{xx}^-(p_0)^2H_{xx}^+(p_0)^3H_{xxx}^-(p_0)H_{xxxx}^-(p_0) \\ & -60H_{x\mu}^-(p_0)H_{xx}^-(p_0)H_{xx}^+(p_0)^4H_{xxx}^-(p_0)H_{xxxx}^-(p_0) \\ & -60H_{x\mu}^+(p_0)H_{xx}^-(p_0)^4H_{xx}^+(p_0)H_{xxx}^+(p_0)H_{xxxx}^+(p_0) \\ & +60H_{x\mu}^-(p_0)H_{xx}^-(p_0)^3H_{xx}^+(p_0)^2H_{xxx}^+(p_0)H_{xxxx}^+(p_0) \\ & -18H_{x\mu}^+(p_0)H_{xx}^-(p_0)^3H_{xx}^+(p_0)^3H_{xxxxx}^-(p_0) + 18H_{x\mu}^-(p_0)H_{xx}^-(p_0)^2H_{xx}^+(p_0)^4H_{xxxxx}^-(p_0) \\ & +18H_{x\mu}^+(p_0)H_{xx}^-(p_0)^4H_{xx}^+(p_0)^2H_{xxxxx}^+(p_0) - H_{x\mu}^-(p_0)H_{xx}^-(p_0)^3H_{xx}^+(p_0)^3H_{xxxxx}^+(p_0), \end{aligned}$$

and $p_0 = (0, 0, 0, 0)$.

In the following theorem we obtain the bifurcation diagram of $\mathcal{Z}$ for one case when the fourth

Lyapunov coefficient is nonzero. The other cases can be studied similarly.

Theorem 19. *Consider the family of PWSVFs $\mathcal{Z}$ given in* (5.1) *satisfying the assumptions* (5.4)*, $\mathcal{T} < 0$ and $L_2^{*\prime}(0) > 0$. Moreover, suppose that the fourth Lyapunov coefficient $L_4^* > 0$. For (μ, ν) sufficiently close to the origin the vector field $\mathcal{Z}$ undergoes the following bifurcations (see Figure 5.4):*

1. *There exist bifurcations of Type III (see Figure 5.3) for $\mu = 0$ and $\nu > 0$.*

2. *There exist bifurcations of Type IV (see Figure 5.3) for $\mu = 0$ and $\nu < 0$.*

3. *There exist saddle-node bifurcations of periodic orbits for parameters on the curve*

$$\left\{(\nu, \mu) : \mu = \frac{c_{20}'(0)^2}{4c_{01}(0)c_{40}(0)}\nu^2 + \mathcal{O}\left(\nu^3\right) \text{ for } \nu < 0\right\}.$$

Proof. If $\mathcal{T} = \gamma'(0) < 0$, then $x_0^+(\mu) > x_0^-(\mu)$, for $\mu < 0$ and $x_0^+(\mu) < x_0^-(\mu)$, for $\mu > 0$. On the other hand, since $c_{20}(0) = 0$ and $c_{20}'(0) > 0$ we get that the function $c_{20}(\nu)$ is positive for $\nu > 0$ and negative for $\nu < 0$ small enough. The displacement function has the form

$$\Delta(a, \mu, \nu) = c_{01}(\nu)\mu + c_{20}(\nu)a^2 + c_{11}(\nu)a\mu + c_{02}(\nu)\mu^2 + \cdots .$$

So, for $\mu = 0$, we get $\Delta(a, 0, \nu) = c_{20}(\nu)a^2 + c_{30}(\nu)a^3 + \cdots$. For $\nu > 0$, we conclude that $\Delta(a, 0, \nu) > 0$, that is, the invisible fold-fold is repelling. The invisible fold-fold is attracting for $\nu < 0$ since $\Delta(a, 0, \nu) < 0$. For $\nu = 0$, we obtain $\Delta(a, 0, 0) = c_{40}(0)a^4 + \mathcal{O}\left(a^5\right)$. Since $c_{40}(0) > 0$ we conclude that the origin is a repellor invisible fold-fold for $\nu = \mu = 0$. By Proposition 41 we get

$$\mu = \alpha(a, \nu) = -\frac{c_{20}(\nu)}{c_{01}(\nu)}a^2 + \frac{c_{11}(\nu)c_{20}(\nu) - c_{01}(\nu)c_{30}(\nu)}{c_{01}(\nu)^2}a^3 + \cdots$$

(see (5.13)) giving the zeroes of the displacement function Δ. Since $\mathcal{T} < 0$ it follows that $c_{01}(\nu) < 0$, for all $\nu \in I_\nu$. If $\nu > 0$, then $c_{20} > 0$, which implies that $\mu > 0$, for small a. On the other hand, if $\nu < 0$, then $\mu < 0$, for small a. So, for $\mu \neq 0$ the periodic orbits are defined either for $\nu > 0$ and $\mu > 0$ or $\nu < 0$ and $\mu < 0$. The stability of those periodic orbits are given by

$$\Pi_a(a, \alpha(a, \nu), \nu) = 1 + 2c_{20}(\nu)a + \left(3c_{30}(\nu) - \frac{c_{11}(\nu)c_{20}(\nu)}{c_{01}(\nu)}\right)a^2 + \cdots .$$

Therefore, for $\nu > 0$, we get $\Pi_a(a, \alpha(a, \nu), \nu) > 1$ and the crossing limit cycle is repelling. For $\nu < 0$, we have $\Pi_a(a, \alpha(a, \nu), \nu) < 1$ and the crossing limit cycle is attracting. The Taylor series of $\mu = \alpha(a, \nu)$ around $(a, \nu) = (0, 0)$ when $c_{20}(0) = c_{30}(0) = 0$ is given by

$$\mu = -\frac{c'_{20}(0)}{c_{01}(0)}a^2\nu - \frac{c_{40}(0)}{c_{01}(0)}a^4 + \cdots = a^2\left(-\frac{c'_{20}(0)}{c_{01}(0)}\nu - \frac{c_{40}(0)}{c_{01}(0)}a^2 + \cdots\right) = a^2 g(a, \nu). \qquad (5.28)$$

Observe that, for $\nu = 0$, μ has the form

$$\mu = \alpha(a, 0) = -\frac{c_{40}(0)}{c_{01}(0)}a^4 + \cdots .$$

We conclude that, for $\nu = 0$, there exists a periodic orbit for $\mu > 0$ which is a repellor since $\Pi_a(a, \alpha(a, 0), 0) = 1 + 4c_{40}(0)a^3 + \cdots$ is greater than one. Since $g(0, 0) = 0$ and $\partial g/\partial\nu(0, 0) \neq 0$ by Implicit Function Theorem there exists $\nu = \nu(a)$ such that $\nu(0) = 0$ and $\mu = \alpha(a, \nu(a)) = 0$. Furthermore,

$$\nu(a) = -\frac{c_{40}(0)}{c'_{20}(0)}a^2 + \mathcal{O}\left(a^3\right).$$

So, for $\mu = 0$, there exists a periodic orbit defined for $\nu < 0$. The Taylor series of Π_a given by Equation (5.14) around $(a, \nu) = (0, 0)$ evaluated on $\nu = \nu(a)$ when $c_{20}(0) = c_{30}(0) = 0$ has the expression

$$\Pi_a(a, \alpha(a, \nu(a)), \nu(a)) = 1 + 2c_{40}(0)a^3 + \mathcal{O}\left(a^4\right)$$

which is greater than one since $c_{40}(0) > 0$. So, for $\mu = 0$, there exists a repelling crossing limit cycle defined for $\nu < 0$ which persists for $\mu \neq 0$ since it is hyperbolic.

For parameters in the set $\{(\nu, \mu) : \mu < 0, \nu > 0\}$ there exists an escaping set $\Sigma^e = \{(x, 0) \in \Sigma : x_0^- < x < x_0^+\}$ that behaves like a repellor and there are no periodic orbits. For parameters in the set $\{(\nu, \mu) : \mu = 0, \nu > 0\}$ we get a repelling invisible fold-fold while for parameters in the set $\{(\nu, \mu) : \mu > 0, \nu > 0\}$ there is a sliding set $\Sigma^s = \{(x, 0) \in \Sigma : x_0^+ < x < x_0^-\}$, contained in the region bounded by a repelling crossing limit cycle, that behaves like an attractor. See Figure 5.4. So, there exists a bifurcation of type III (see Figure 5.3) when the parameters cross the set $\{(\nu, \mu) : \mu = 0, \nu > 0\}$.

By the previous calculations, the above repelling crossing limit cycle persists for $\mu > 0$ and $\nu = 0$. Due to its hyperbolicity it persists for $\nu < 0$ and $\mu > 0$. In this way, in the set $\{(\nu, \mu) : \mu = 0, \nu < 0\}$ we have an attracting invisible fold-fold at the origin contained in the region bounded by this repelling crossing limit cycle. So, a bifurcation of type IV (see Figure 5.3) occurs when the parameters cross the set $\{(\nu, \mu) : \mu = 0, \nu < 0\}$. Therefore, close to this set there exists one repelling crossing limit cycle for $\mu > 0$ and $\nu < 0$ and there are two crossing limit cycles of opposite stabilities for $\mu < 0$ and $\nu < 0$. See Figure 5.4. It is clear that a bifurcation leading to the disappearance of the above periodic orbits (that corresponds to a double zero of the displacement function Δ) takes place in the set $\{(\nu,\mu):\mu<0,\nu<0\}$. By Equation (5.24), there exists

$$\nu=\eta(a)=-\frac{2c_{40}(0)}{c_{20}'(0)}a^2+\mathcal{O}(a^3)$$

such that $\Delta_a(a,\alpha(a,\eta(a)),\eta(a)) = 0$. Therefore, by Proposition 42, the curve on which saddle–node bifurcations of periodic orbits takes place is given by

$$\mu=\frac{c_{20}'(0)^2}{4c_{01}(0)c_{40}(0)}\nu^2+\mathcal{O}\left(\nu^3\right)$$

which is well defined for $\mu<0$ and $\nu<0$. The bifurcation diagram is depicted in Figure 5.4. □

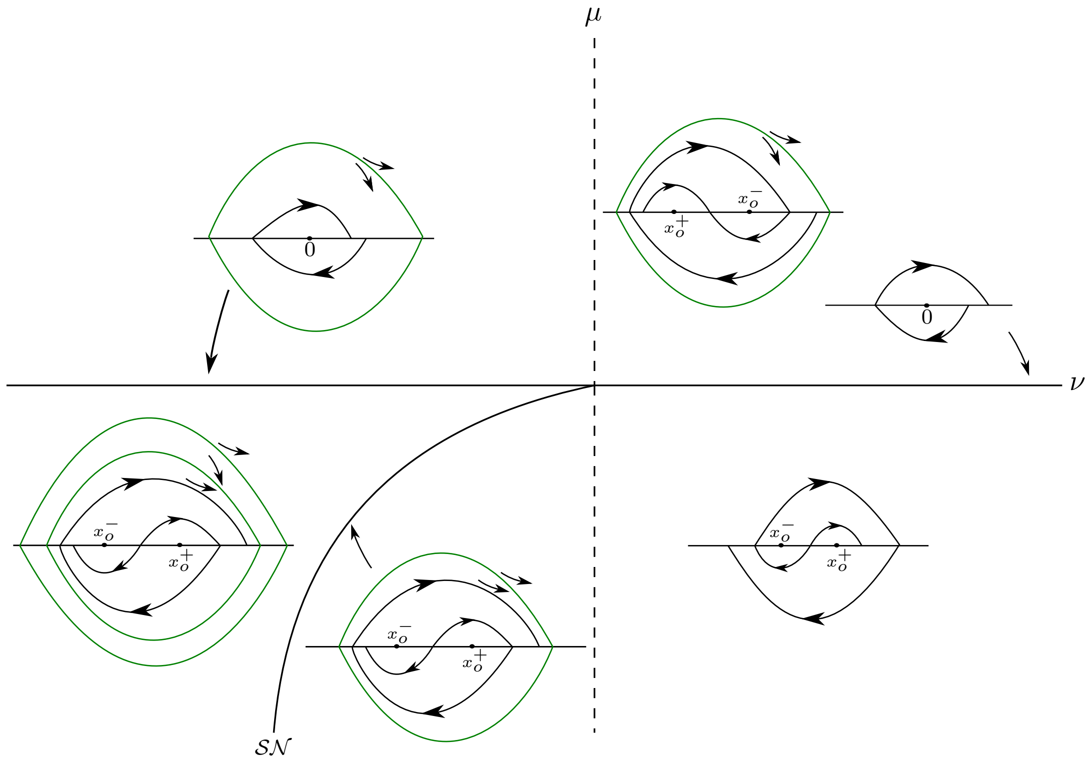

Figure 5.4: Bifurcation diagram of the PSVF $\mathcal{Z}$ under the hypotheses of Theorem 19.

The cases for different signs of the hypothesis considered in Theorem 19 can be treated similarly. An example of the bifurcation studied is shown in the sequel where we apply the formulas obtained in this work to a family of two parameters presenting an unfolding of an invisible fold-fold singularity. Consider the following family of PSVFs

$$Z(x,y,\mu,\nu)=\left\{\begin{array}{lcll} X_\nu(x,y) & = & \left(1,-x+\nu x^2+x^4\right), & y\geq 0,\\ Y_\mu(x,y) & = & \left(-1,-x+\mu\right), & y\leq 0,\end{array}\right. \tag{5.29}$$

where $(x,y)\in\mathbb{R}^2$ are the state variables and $(\mu,\nu)\in\mathbb{R}^2$ are real parameters. Again the separation line is $\Sigma=h^{-1}(0)$ where $h(x,y)=y$. Such a family is relevant in the literature and has been already studied in [62] where the bifurcation diagram were exhibited.

Proposition 43. *Consider the PSVF Z given by* (5.29). *The point* $(0,0)$ *is an invisible fold point of* X_ν *with* Σ.

Proof. Indeed, the derivative of h in the direction of the vector field X_ν is given by

$$X_\nu f(x,y) = X_\nu(x,y)\cdot\nabla f(x,y) = -x+\nu x^2+x^4$$

which vanishes for $x=0$. Furthermore, $X_\nu^2 f(x,y) = X_\nu(x,y)\cdot\nabla X_\nu f(x,y) = -1+2\nu x+4x^3$. So, $X_\nu^2 f(0,0) = -1 < 0$ and therefore $(0,0)$ is an invisible fold point of X_ν. □

Proposition 44. *Consider the PSVF Z given by* (5.29). *The point* $(\mu,0)$ *is an invisible fold point of* Y_μ *with* Σ.

Proof. The first Lie derivative is given by $Y_\mu f(x,y) = Y_\mu(x,y)\cdot\nabla f(x,y) = -x+\mu$ which vanishes for $x=\mu$. Furthermore, $Y_\mu^2 f(x,y) = Y_\mu(x,y)\cdot\nabla Y_\mu f(x,y) = 1$. So, $Y_\mu^2 f(0,0) > 0$ and thus $(\mu,0)$ is an invisible fold point of Y_μ. □

We observe that $\Sigma^s = \{(x,0)\in\Sigma : 0<x<\mu\}$ for $\mu>0$ and $\Sigma^e = \{(x,0)\in\Sigma : \mu<x<0\}$ for $\mu<0$. For $\mu=0$ the invisible fold points of X_ν and Y_μ coincide. In this case, it is easy to see that $(0,0)\in\Sigma$ is a crossing invisible fold-fold singularity. Moreover, X_ν and Y_μ are both Hamiltonian vector fields whose Hamiltonian functions are, respectively, given by

$$\mathcal{H}^+(x,y,\mu,\nu) = -y+\frac{x^5}{5}+\frac{\nu x^3}{3}-\frac{x^2}{2}$$

and

$$\mathcal{H}^-(x,y,\mu,\nu) = -\frac{x^2}{2}+\mu x+y.$$

In this case, the function γ given by (5.5) has the expression $\gamma(\mu)=-\mu$. So, we have that the transversality condition (5.6) is given by $\mathcal{T}=\gamma'(0)=-1$. Therefore, the hypotheses of Theorem 15 are satisfied. Calculating the second Lyapunov coefficient of Z at $(0,0,0,\nu)$ given by (5.18) we obtain

$$L_2^* = \frac{1}{3}\left(\frac{H^-_{xxx}(0,0,0,\nu)}{H^-_{xx}(0,0,0,\nu)} - \frac{H^+_{xxx}(0,0,0,\nu)}{H^+_{xx}(0,0,0,\nu)}\right) = \frac{2\nu}{3}.$$

Since $\mathcal{T}<0$, if $L_2^*\neq 0$, then the bifurcation associated with the PSVF Z of type III given by Theorem 17 for $L_2^*>0$. For $L_2^*<0$ it occurs a bifurcation of type IV, also described in Theorem 17. Furthermore, when the second Lyapunov coefficient vanishes, that is, when $\nu=0$, we obtain, from (5.20), the fourth Lyapunov coefficient

$$L_4^* = \frac{2}{5}.$$

Note that $L_4^* > 0$ and $L_2^{*'}(0) = 2/3 > 0$. Then, near the crossing invisible fold-fold at the origin the family of PSVFs Z undergoes the bifurcations described in Theorem 19 and depicted in Figure 5.4.

Our results are in accordance with those found in [62] where the first return map Π_Z associated with Z was explicitly computed. When $\mu = 0$ the map Π_Z is given by

$$\begin{aligned} \Pi_Z : \quad \Sigma \quad &\longrightarrow \quad \Sigma \\ x_0 \quad &\longmapsto \quad \Pi_Z(x_0) = \Pi_{X_\nu} \circ \Pi_{Y_\mu}(x_0) \end{aligned}$$

where $\Pi_{Y_\mu}(x_0) = -x_0$ is the half return map associated with the vector field Y_μ and

$$\Pi_{X_\nu}(x_0) = -x_0 + \frac{2\nu}{3}x_0^2 - \frac{4\nu^2}{9}x_0^3 + \left(\frac{2}{5} + \frac{16}{27}\nu^3\right)x_0^4 + \mathcal{O}(x_0^5)$$

the half return map associated with the vector field X_ν. Thus,

$$\Pi_Z(x_0) = x_0 + \frac{2\nu}{3}x_0^2 + \frac{4\nu^2}{9}x_0^3 + \left(\frac{2}{5} + \frac{16}{27}\nu^3\right)x_0^4 + \mathcal{O}(x_0^5).$$

Also, the curve of non-hyperbolic periodic orbits associated with the vector field Z given by Proposition 42, whose expression is given by Remark 22, has the form

$$\mu = -\frac{5}{36}\nu^2 + \mathcal{O}(\nu^3),$$

which is in conformity with the calculations performed in [62].

We will make a detour by relating our study to those found in the literature. A pioneering work on *degenerate Hopf bifurcations in discontinuous planar systems* were the paper [29], where the authors obtained a general expression for the first three Lyapunov coefficients at points of *parabolic-parabolic type*, that is, the solution of both systems have a second order contact point with the switching manifold, what we call a fold point. In consonance with the computations performed in Theorem 15, their first and third Lyapunov coefficients vanish. In order to present the formula obtained in [29] for the second Lyapunov coefficient let us consider the PSVF Q

given by

$$Q(x,y) = \begin{cases} (X^+(x,y), Y^+(x,y)), & y \geq 0, \\ \\ (X^-(x,y), Y^-(x,y)), & y \leq 0. \end{cases} \tag{5.30}$$

Consider the Taylor series of $X^\pm$ and $Y^\pm$ at the origin

$$\begin{aligned} X^\pm(x,y) &= a^\pm + b^\pm x + c^\pm y + d^\pm x^2 + e^\pm xy + f^\pm y^2 + g^\pm x^3 + \cdots, \\ Y^\pm(x,y) &= l^\pm x + m^\pm y + n^\pm x^2 + o^\pm xy + p^\pm y^2 + q^\pm x^3 + r^\pm x^2 y + \cdots. \end{aligned}$$

We notice that the vector field Q has an invisible fold-fold at the origin when $a^+ < 0$, $a^- > 0$, $l^+ > 0$ and $l^- > 0$. The second Lyapunov coefficient obtained in [29] is given by

$$V_2 = \mu^+ - \mu^-, \quad \text{where} \quad \mu^\pm = \frac{2}{3}\frac{a^\pm n^\pm - (b^\pm + m^\pm)\, l^\pm}{a^\pm l^\pm}.$$

In order to corroborate our results let us analyze if the formulas of V_2 and L_2^* coincide when $(X^+(x,y), Y^+(x,y))$ and $(X^-(x,y), Y^-(x,y))$ are Hamiltonian vector fields. In this case we have that the divergence of both vector fields are zero, that is,

$$\begin{aligned} 0 &= \operatorname{div}\left(X^\pm(x,y), Y^\pm(x,y)\right) \\ &= \left(b^\pm + 2d^\pm x + e^\pm y + 3g^\pm x^2 + \cdots\right) + \left(m^\pm + o^\pm x + 2p^\pm y + r^\pm x^2 + \cdots\right) \\ &= \left(b^\pm + m^\pm\right) + \left(2d^\pm + o^\pm\right) x + \left(e^\pm + 2p^\pm\right) y + \left(3g^\pm + r^\pm\right) x^2 + \cdots. \end{aligned}$$

This implies that $b^\pm + m^\pm = 0$, $2d^\pm + o^\pm = 0$, $e^\pm + 2p^\pm = 0$, $3g^\pm + r^\pm = 0$ and so on. Since $b^\pm + m^\pm = 0$ we obtain

$$\mu^\pm = \frac{2}{3}\frac{n^\pm}{l^\pm}$$

and therefore

$$V_2 = \frac{2}{3}\left(\frac{n^+}{l^+} - \frac{n^-}{l^-}\right).$$

The Hamiltonian functions H^+ and H^- associated with the vector fields $(X^+(x,y), Y^+(x,y))$ and $(X^-(x,y), Y^-(x,y))$, respectively, have the forms

$$H^\pm(x,y) = -a^\pm y + \frac{l^\pm}{2}x^2 - b^\pm xy - \frac{c^\pm}{2}y^2 + \frac{n^\pm}{3}x^3 - d^\pm x^2 y + p^\pm xy^2 - \frac{f^\pm}{3}y^3 - g^\pm x^3 y + \cdots.$$

The second Lyapunov coefficient L_2^* obtained in (5.18) has the form

$$L_2^* = \frac{2}{3}\left(\frac{n^-}{l^-} - \frac{n^+}{l^+}\right).$$

Therefore, $V_2 = -L_2$. The opposite sign is due to the orientations taken in the vector fields.

5.2 Limit cycles bifurcating from an invisible fold-fold singularity in a family of planar piecewise Hamiltonian systems

Adopting the ideas used in the previous section, in which we took advantage of the Hamiltonian functions associated with the components of the discontinuous vector fields to construct a first return map, and consequently, to define the Lyapunov constants, we apply this process in a family of planar piecewise Hamiltonian vector fields presenting an invisible fold-fold singularity and we explore the existence of limit cycles as well as the analysis of its bifurcation diagram.

The first goal of this section is to investigate the existence and positions of limit cycles of an unfolding of the following family of PSVF

$$\mathfrak{Z}_{b,k,\lambda}(x,y) = \begin{cases} \mathfrak{X}_{b,k}(x,y) & = \left(1, -x + bx^{2k}\right), \qquad y \geq 0 \\ Y_\lambda(x,y) & = (-1, -x+\lambda), \qquad y \leq 0, \end{cases} \tag{5.31}$$

where λ is a small parameter, b a nonzero real number and $k = 1, 2, 3, \ldots$. We notice that, in this case, the switching manifold is $\Sigma = f^{-1}(0)$ where $f(x,y) = y$. As we will show in the sequel, for $\lambda = 0$ the piecewise smooth vector field $\mathfrak{Z}_{b,k,\lambda}$ has an invisible fold-fold at the origin that behaves like a repellor or an attractor depending on the sign of the coefficient b. Indeed, if we consider the first return map associated with $\mathfrak{Z}_{b,k,\lambda}$ in a neighborhood of the invisible fold-fold at the origin we conclude that it behaves like a repellor if $b > 0$ or an attractor if $b < 0$.

The unfolding considered is of the form

$$Z_{a,k,\lambda}(x,y) = \begin{cases} X_{a,k}(x,y) & = \left(1, -x + a_2x^2 + \cdots + a_{2k-2}x^{2k-2} + a_{2k}x^{2k}\right), \quad y \geq 0; \\ Y_\lambda(x,y) & = (-1, -x+\lambda), \qquad y \leq 0. \end{cases} \tag{5.32}$$

Such a family is relevant in the literature and has been already studied in [80] and [62] for low codimension, where the bifurcation diagram were exhibited containing one and two limit cycles. In fact, in the last one the authors studied the bifurcation diagram of the piecewise smooth vector fields $Z_{a,2,\lambda}$ and proved that one or two crossing limit cycles can appear in this family. The study of the existence of one crossing limit cycle, as well as the pertinent bifurcation diagram, for a family close related to $Z_{a,1,\lambda}$ can be found in [80]. We intend to generalize these results which can be summarized in the following question: For a fixed $k = 1, 2, \ldots$ there exists $\lambda \in \mathbb{R}$ sufficiently small and $a = (a_2, a_4, \ldots, a_{2k-2}, a_{2k})$ such that $Z_{a,k,\lambda}$ has exactly k crossing limit cycles near the origin?

In what follows we bring some properties of the vector field $\mathfrak{Z}_{b,k,\lambda}$ given by (5.31).

Proposition 45. *Consider the PSVF $\mathfrak{Z}_{b,k,\lambda}$ given by* (5.31)*. The origin* $(0,0)$ *is an invisible fold point of $\mathfrak{X}_{b,k}$.*

Proof. Indeed, $\mathfrak{X}_{b,k}f(x,y) = \mathfrak{X}_{b,k}(x,y)\cdot\nabla f(x,y) = -x + bx^{2k}$ which is clearly zero for $x = 0$. Moreover, $\mathfrak{X}^2_{b,k}f(x,y) = \mathfrak{X}_{b,k}\cdot\nabla\mathfrak{X}_{b,k}f(x,y) = -1 + 2kbx^{2k-1}$. So, $\mathfrak{X}^2_{b,k}f(0,0) = -1 < 0$ and therefore $(0,0)$ is an invisible fold point of $\mathfrak{X}_{b,k}$. □

Proposition 46. *Consider the PSVF $\mathfrak{Z}_{b,k,\lambda}$ given by* (5.31)*. The point* $(\lambda,0)$ *is an invisible fold point of Y_λ.*

Proof. In fact, $Y_\lambda f(x,y) = Y_\lambda(x,y)\cdot\nabla f(x,y) = -x+\lambda$ which is clearly null for $x = \lambda$. Furthermore, $Y^2_\lambda f(x,y) = Y_\lambda(x,y)\cdot\nabla Y_\lambda f(x,y) = 1$. So, $Y^2_\lambda f(0,0) = 1 > 0$ and so $(\lambda,0)$ is an invisible fold point of Y_λ. □

The points of the set $\{(x,y)\in\mathbb{R}^2 : 0 < x < \lambda,\ y = 0\}\subset\Sigma$ (for $\lambda > 0$) are sliding points while the points of the set $\{(x,y)\in\mathbb{R}^2 : \lambda < x < 0,\ y = 0\}\subset\Sigma$ (for $\lambda < 0$) are escaping points. See Figure 5.5. In these sets, we have that the sliding vector field Z^s given by (1) has a pseudo-equilibria. In fact, by (1.2) we have that the zeroes of Z^s correspond to points where $\mathfrak{X}_{b,k}$ and Y_λ are linearly dependent, that is, when it holds $\xi(\lambda,x) = \lambda - 2x + bx^{2k} = 0$. By Implicit Function Theorem there exists a neighborhood A containing zero and $x\colon A\longrightarrow\mathbb{R}$ such that $x(0) = 0$ and $\xi(\lambda,x(\lambda)) = 0$ for all $\lambda\in A$. Therefore, for all $\lambda\neq 0$ sufficiently small there exists $x(\lambda)$ such that the point $(x(\lambda),0)\in\Sigma$ is a pseudo equilibria of Z^s which behaves like an attractor on Σ since the derivative of ξ with respect to x is negative. Then, the pseudo-equilibria is a pseudo-saddle for $\lambda < 0$ and a pseudo-node for $\lambda > 0$. In this way, we need to comprehend the behavior of the invisible fold-fold when $\lambda = 0$.

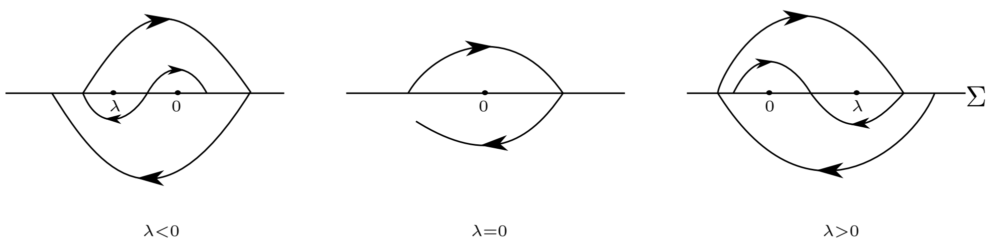

Figure 5.5: Behavior of the vector field $\mathfrak{Z}_{b,k,\lambda}$ near the origin.

Lemma 15. *The vector field $Y_0 = (-1,-x)$ when restricted to Σ is symmetric with respect to y-axis, that is, given $(x_0,0)\in\Sigma$, the orbit of Y_0 through $(x_0,0)$ returns to Σ at $(x_1,0) = (-x_0,0)$.*

Proof. Notice that Y_0 is a Hamiltonian vector field with Hamiltonian function

$$H_0(x,y) = y - \frac{x^2}{2}.$$

Two points $(x_0,0),(x_1,0) \in \Sigma$ belong to the same level curve of H_0 if, and only if, it holds $H_0(x_0,0) = H_0(x_1,0)$. In other words, we have $(x_1-x_0)(x_1+x_0) = 0$. Since we are looking for points such that $x_0 \neq x_1$ we get that $x_1 = -x_0$ is the x-coordinate of the return to Σ of an orbit of Y_0 passing through $(x_0,0)$. $\square$

Lemma 16. *Consider*

$$g(x_0,x_1) = x_1^{2k} + x_1^{2k-1}x_0 + \cdots + x_1 x_0^{2k-1} + x_0^{2k} - \frac{2k+1}{2b}(x_1+x_0).$$

Then there exists $I \subset \mathbb{R}$ containing zero and a function $x_1 \colon I \longrightarrow \mathbb{R}$ such that $x_1(0) = 0$ and $g(x_0,x_1(x_0)) = 0$, for all $x_0 \in I$. Moreover, $x_1'(0) = -1$,

$$x_1^{(i)}(0) = 0, \quad 1 < i < 2k$$

and

$$x_1^{(2k)}(0) = \frac{2b}{2k+1}(2k)!.$$

Proof. Since

$$g(0,0) = 0, \qquad \frac{\partial g(0,0)}{\partial x_1} = -\frac{2k+1}{2b} \neq 0,$$

by Implicit Function Theorem there exists an interval $I \subset \mathbb{R}$ containing zero and a function $x_1 \colon I \longrightarrow \mathbb{R}$ such that $x_1(0) = 0$ and $g(x_0,x_1(x_0)) = 0$, for all $x_0 \in I$. Furthermore,

$$x_1'(0) = -\frac{\dfrac{\partial g(0,0)}{\partial x_0}}{\dfrac{\partial g(0,0)}{\partial x_1}} = -1.$$

Notice that g is the sum of a homogeneous polynomial of degree $2k$ with a linear term. So, the linear term will disappear in the derivatives of order greater than or equal 2 of g. However, the derivatives of g of order i, for $1 < i < 2k$, will have terms of x_0 or x_1 that will vanish at $(0,0)$. Then, the derivative of order i, for $1 < i < 2k$, of $g(x_0,x_1(x_0)) = 0$ at $(0,0)$ with respect to the variable x_0 is of the form

$$0 + \frac{\partial g(0,0)}{\partial x_1} x_1^{(i)}(0) = 0.$$

Therefore $x_1^{(i)}(0) = 0$, for $1 < i < 2k$. Moreover, the derivative of order $2k$ of $g(x_0,x_1(x_0)) = 0$

at $(0,0)$ with respect to x_0 is given by

$$\frac{\partial g(0,0)}{\partial x_1}x_1^{(2k)}(0)+\binom{2k}{0}(x_1'(0))^{2k}\frac{\partial^{2k}g(0,0)}{\partial x_1^{2k}}+\binom{2k}{1}(x_1'(0))^{2k-1}\frac{\partial^{2k}g(0,0)}{\partial x_0\partial x_1^{2k-1}}+$$

$$+\cdots+\binom{2k}{2k}(x_1'(0))^{2k}\frac{\partial^{2k}g(0,0)}{\partial x_0^{2k}}=0.$$

Since $x_1'(0)=-1$ and, for $u+v=2k$, we have

$$\binom{2k}{u}\frac{\partial^{2k}g(0,0)}{\partial x_0^u\partial x_1^v}=(2k)!,$$

it follows that the mixed derivatives of order $2k$ will cancel in pairs in a way that we get

$$\frac{\partial g(0,0)}{\partial x_1}x_1^{(2k)}(0)+\binom{2k}{2k}(x_1'(0))^{2k}\frac{\partial^{2k}g(0,0)}{\partial x_0^{2k}}=0$$

and therefore

$$x_1^{(2k)}(0)=\frac{2b}{2k+1}(2k)!.$$

□

In the next result, the vector field $\mathfrak{Z}_{b,k,0}$ denotes the PSVF $\mathfrak{Z}_{b,k,\lambda}$ for $\lambda=0$.

Proposition 47. *Consider the PSVF $\mathfrak{Z}_{b,k,\lambda}$ given by* (5.31). *$\mathfrak{Z}_{b,k,0}$ has an invisible fold-fold at the origin which is a repellor for $b>0$ or an attractor for $b<0$.*

Proof. The vector field $\mathfrak{X}_{b,k}(x,y)=\left(1,-x+bx^{2k}\right)$ is a Hamiltonian vector field with Hamiltonian function given by

$$H_{\mathfrak{X}}(x,y)=-y-\frac{x^2}{2}+\frac{bx^{2k+1}}{2k+1}.$$

Two points $(x_0,0)$ and $(x_1,0)$ of Σ are on the same level curve of $H_{\mathfrak{X}}$ if, and only if, $H_{\mathfrak{X}}(x_0,0)=H_{\mathfrak{X}}(x_1,0)$. This implies that $g(x_0,x_1)=0$, where g is given by Lemma 16. By Lemma 16 we get

$$x_1(x_0)=-x_0+\frac{2b}{2k+1}x_0^{2k}+\mathcal{O}\left(x_0^{2k+1}\right).$$

So, we can define the first return map associated with $\mathfrak{Z}_{b,k,0}$

$$\begin{array}{rccl}\pi_{\mathfrak{Z}_{k,0}}: & \Sigma & \longrightarrow & \Sigma\\ & x_0 & \longmapsto & \pi_{\mathfrak{Z}}(x_0)=\pi_{Y_0}\circ\pi_{\mathfrak{X}_k}(x_0)\end{array}$$

where $\pi_{Y_0}(x_0) = -x_0$ is the half return map associated with the vector field Y_0 and $\pi_{\mathfrak{X}_k}(x_0) = x_1(x_0)$ the half return map associated with the vector field $\mathfrak{X}_{b,k}$. So,

$$\pi_{\mathfrak{Z}_{k,0}}(x_0) = x_0 - \frac{2b}{2k+1}x_0^{2k} + \mathcal{O}\left(x_0^{2k+1}\right).$$

Therefore, if $b > 0$, then $\pi_{\mathfrak{Z}_{k,0}} < x_0$ which implies that the origin is a repelling fold-fold. If $b < 0$, then $\pi_{\mathfrak{Z}_{k,0}}(x_0) > x_0$ which implies that the origin is an attracting fold-fold. See Figure 5.6. □

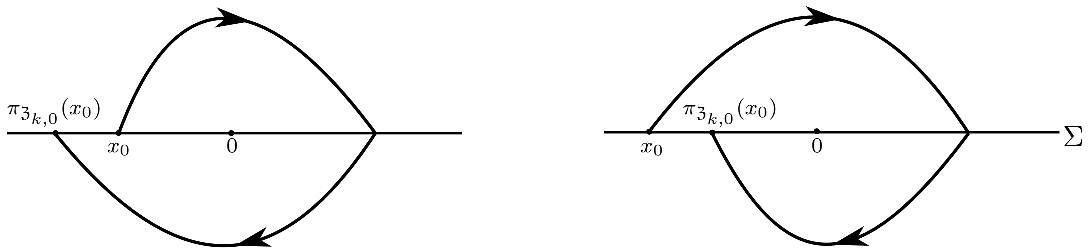

Figure 5.6: repelling or attracting fold-fold that behaves like a focus.

In the following proposition we consider $a_2 > 0$. An analogous result can be obtained for $a_2 < 0$.

Proposition 48. *Consider $a_2 > 0$ fixed and the PSVF*

$$Z_{1,\lambda}(x,y) = \begin{cases} X_1(x,y) &= \left(1, -x + a_2x^2\right), & y \geq 0; \\ Y_\lambda(x,y) &= \left(-1, -x + \lambda\right), & y \leq 0, \end{cases}$$

There exists $\lambda \in \mathbb{R}$ sufficiently small such that $Z_{1,\lambda}$ has one hyperbolic crossing limit cycle near the origin.

Proof. By Proposition 47, for $\lambda = 0$, the first return map associated with $Z_{1,0}$ is given by

$$\pi_{Z_{1,0}}(x_0) = x_0 - \frac{2a_2}{3}x_0^2 + \mathcal{O}(x_0^3).$$

Then the origin is a repellor invisible fold-fold. Observe that for $\lambda < 0$ we have an escaping region that behaves like a repulsor and for $\lambda > 0$ we have a sliding region that behaves like an attractor. Notice that X_1 is Hamiltonian with Hamiltonian function

$$H_1(x,y) = -y - \frac{x^2}{2} + \frac{a_2x^3}{3}.$$

So, from $H_1(x_0, 0) = H_1(x_1, 0)$ we obtain

$$-\frac{a_2}{3}(x_1^2 + x_1x_0 + x_0^2) + \frac{1}{2}(x_1 + x_0) = 0. \tag{5.33}$$

Similarly, Y_λ is Hamiltonian with Hamiltonian function

$$H_Y(x,y) = y - \frac{x^2}{2} + \lambda x.$$

Then, from $H_Y(x_0,0) = H_Y(x_1,0)$ we have

$$x_1 = -x_0 + 2\lambda. \tag{5.34}$$

Substituting (5.34) in (5.33) we get

$$-\frac{a_2}{3}x_0^2 + \frac{2a_2}{3}x_0\lambda - \frac{4a_2\lambda^2}{3} + \lambda = 0 \tag{5.35}$$

whose zeros are given by

$$x_0^{\pm} = \frac{a_2\lambda \pm \sqrt{3}\sqrt{a_2\lambda - a_2^2\lambda^2}}{a_2}$$

The discriminant

$$\Delta = -\frac{4a_2^2\lambda^2}{3} + \frac{4a_2\lambda}{3}$$

is a parabola concave downward with zeroes $\lambda = 0$ and $\lambda = 1/a_2$. In this way, for $\lambda \in \left(0, \frac{1}{a_2}\right)$ the equation (5.35) has two distinct real roots that correspond to a limit cycle. Observe that x_0^+ belongs to the crossing set if $x_0^+ < 1/a_2$, that is, $0 < \lambda < 1/(4a_2)$. Therefore, for $\lambda > 0$ sufficiently small, there exist a repelling crossing limit cycle of $Z_{1,\lambda}$ through x_0^+. See Figure 5.7. $\square$

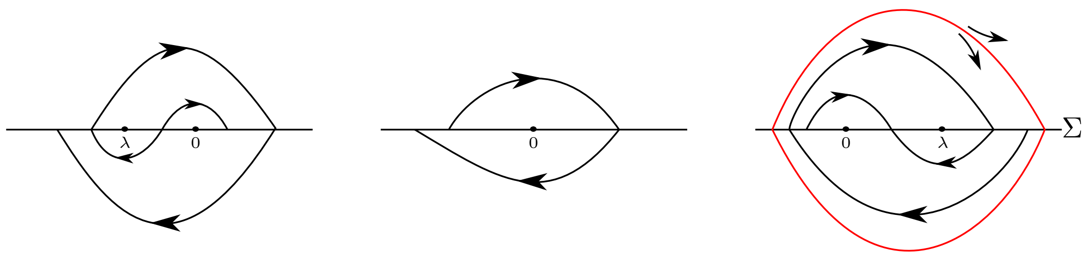

$\lambda < 0$ $\lambda = 0$ $\lambda > 0$

Figure 5.7: Bifurcation diagram of the PSVF $Z_{1,\lambda}$ for $a_2 > 0$.

Figure 5.8 illustrates the bifurcation diagram for the analogous case of Proposition 48 for negative values of a_2.

Remark 23. *In what follows we will consider $a_{2k} > 0$. More precisely, we take the normalization by considering $a_{2k} = 1$ in order to fix the stability of the fold-fold at the origin. Analogous and dual case can be achieved for $a_{2k} < 0$.*

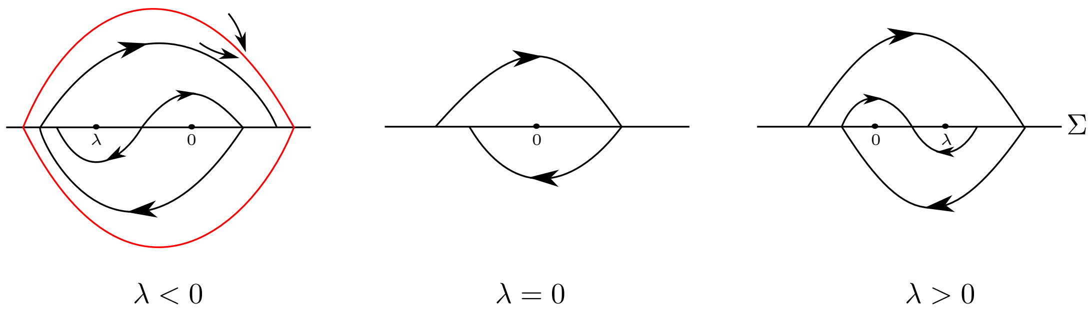

Figure 5.8: Bifurcation diagram of the PSVF $Z_{1,\lambda}$ for $a_2 < 0$.

Proposition 49. *Consider the PSVF*

$$Z_{a,2,\lambda}(x,y) = \begin{cases} X_2(x,y) &= \left(1, -x + a_2x^2 + x^4\right), & y \geq 0; \\ Y_\lambda(x,y) &= (-1, -x + \lambda), & y \leq 0, \end{cases}$$

There exist $\lambda \in \mathbb{R}$ sufficiently small and $a = (a_2, 1)$ such that $Z_{a,2,\lambda}$ has two hyperbolic crossing limit cycles near the origin.

Proof. X_2 is a Hamiltonian vector field with Hamiltonian function

$$H_2(x,y) = -y - \frac{x^2}{2} + \frac{a_2x^3}{3} + \frac{x^5}{5}.$$

So, from $H_2(x_0, 0) = H_2(x_1, 0)$ we obtain

$$g(x_0, x_1) = \frac{1}{2}(x_1 + x_0) - \frac{a_2}{3}(x_1^2 + x_1x_0 + x_0^2) - \frac{1}{5}(x_1^4 + x_1^3x_0 + x_1^2x_0^2 + x_1x_0^3 + x_0^4) = 0. \quad (5.36)$$

Since $g(0,0) = 0$ and $\partial g(0,0)/\partial x_1 = 1/2 \neq 0$, by Implicit Function Theorem there exists an interval I containing zero and $x_1 \colon I \longrightarrow \mathbb{R}$ such that $x_1(0) = 0$ and $g(x_0, x_1(x_0)) = 0$, for all $x_0 \in I$. Moreover, we get

$$x_1(x_0) = -x_0 + \frac{2a_2}{3}x_0^2 - \frac{4a_2^2}{9}x_0^3 + \mathcal{O}(x_0^4).$$

In this way, the first return map associated with $Z_{a,2,\lambda}$ is given by

$$\begin{array}{rccl} \pi_{Z_{2,\lambda}} \colon & \Sigma & \longrightarrow & \Sigma \\ & x_0 & \longmapsto & \pi_{Z_{2,\lambda}}(x_0) = \pi_{Y_\lambda} \circ \pi_{X_2}(x_0) \end{array}$$

where $\pi_{Y_\lambda}(x_0) = -x_0 + 2\lambda$ and $\pi_{X_2}(x_0) = -x_0 + \frac{2a_2}{3}x_0^2 - \frac{4a_2^2}{9}x_0^3 + \mathcal{O}(x_0^4)$. Thus, we have

$$\pi_{Z_{2,\lambda}}(x_0) = 2\lambda + x_0 - \frac{2a_2}{3}x_0^2 + \frac{4a_2^2}{9}x_0^3 + \mathcal{O}(x_0^4).$$

For $\lambda = 0$ we get

$$\pi_{Z_{2,0}}(x_0) = x_0 - \frac{2a_2}{3}x_0^2 + \frac{4a_2^2}{9}x_0^3 + \mathcal{O}(x_0^4).$$

Therefore, the origin is a repelling fold-fold for $a_2 > 0$ and an attracting fold-fold for $a_2 < 0$. Solving the equation $\pi_{Z_{2,0}}(x_0) = x_0$ we can assure the existence of a repelling crossing limit cycle for $a_2 < 0$ passing through

$$x_0^{\pm} = \pm\sqrt{\frac{-5a_2}{3}} + \mathcal{O}(a_2).$$

Then, for $a_2 < 0$ and $\lambda = 0$ there exist a repelling limit cycle that intercepts Σ at the points $\left(x_0^{\pm}, 0\right)$ and which persists for $\lambda \neq 0$ when $a_2 < 0$ since it is hyperbolic. Next to the curve $\{(a_2, \lambda) : \lambda = 0, a_2 > 0\}$ there exists a crossing limit cycle for $\lambda > 0$ and none for $\lambda < 0$ due to the fold-fold bifurcation of Proposition 48. For $a_2 < 0$ and $\lambda = 0$ we have an attracting fold-fold contained in the region bounded by a repelling limit cycle. So, for $\lambda < 0$, we get the appearance of a second limit cycle due to the fold-fold bifurcation of Proposition 48. Let us analyze the region $\{(a_2, \lambda) : \lambda < 0, a_2 < 0\}$ and the bifurcation leading to the disappearance of the limit cycles. Consider the displacement function

$$P(x_0) = \pi_{Z_{2,\lambda}}(x_0) - x_0 = 2\lambda - \frac{2a_2}{3}x_0^2 + \frac{4a_2^2}{9}x_0^3 + \mathcal{O}(x_0^4).$$

We point out that the periodic orbits are given by the fixed points of the return map $\pi_{Z_{2,\lambda}}$ that correspond to the zeroes of the displacement function P. So, the bifurcation that leads to the disappearance of the above limit cycles corresponds to the existence of a double zero of P. Therefore, we want to find the points such that $P(x_0) = 0$ and $P'(x_0) = 0$. From $P(x_0) = 0$ we get

$$\lambda = \frac{a_2}{3}x_0^2 - \frac{2a_2^2}{9}x_0^3 + \mathcal{O}(x_0^4).$$

Also,

$$P'(x_0) = -\frac{4a_2}{3}x_0 + \frac{4a_2^2}{3}x_0^2 + \mathcal{O}(x_0^3) = x_0 \left[\underbrace{-\frac{4a_2}{3} + \frac{4a_2^2}{3}x_0 + \mathcal{O}(x_0^2)}_{r(x_0,a_2)}\right].$$

So, $P'(x_0) = 0$ implies $r(x_0, a_2) = 0$. Since $r(0,0) = 0$ and $\partial r(0,0)/\partial a_2 = -4/3 \neq 0$, by Implicit Function Theorem there exist an interval J containing zero and $a_2\colon J \longrightarrow \mathbb{R}$ such that $a_2(0) = 0$

and $r(x_0, a_2(x_0)) = 0$, for all $x_0 \in J$. Furthermore,

$$a_2(x_0) = -\frac{6}{5}x_0^2 + \mathcal{O}(x_0^3).$$

By Implicit Function Theorem we get

$$x_0^2 = -\frac{5a_2}{6} + \mathcal{O}(a_2).$$

Thus,

$$\lambda = -\frac{5a_2^2}{18} + \mathcal{O}(a_2^3).$$

Therefore, in $\{(a_2, \lambda) : \lambda < 0, a_2 < 0\}$ there exists a curve

$$\lambda = -\frac{5a_2^2}{18} + \mathcal{O}(a_2^3)$$

on which the saddle-node bifurcation of periodic orbits takes place corresponding to a non-hyperbolic limit cycle and leading to the disappearance of the periodic orbits. See Figure 5.9. □

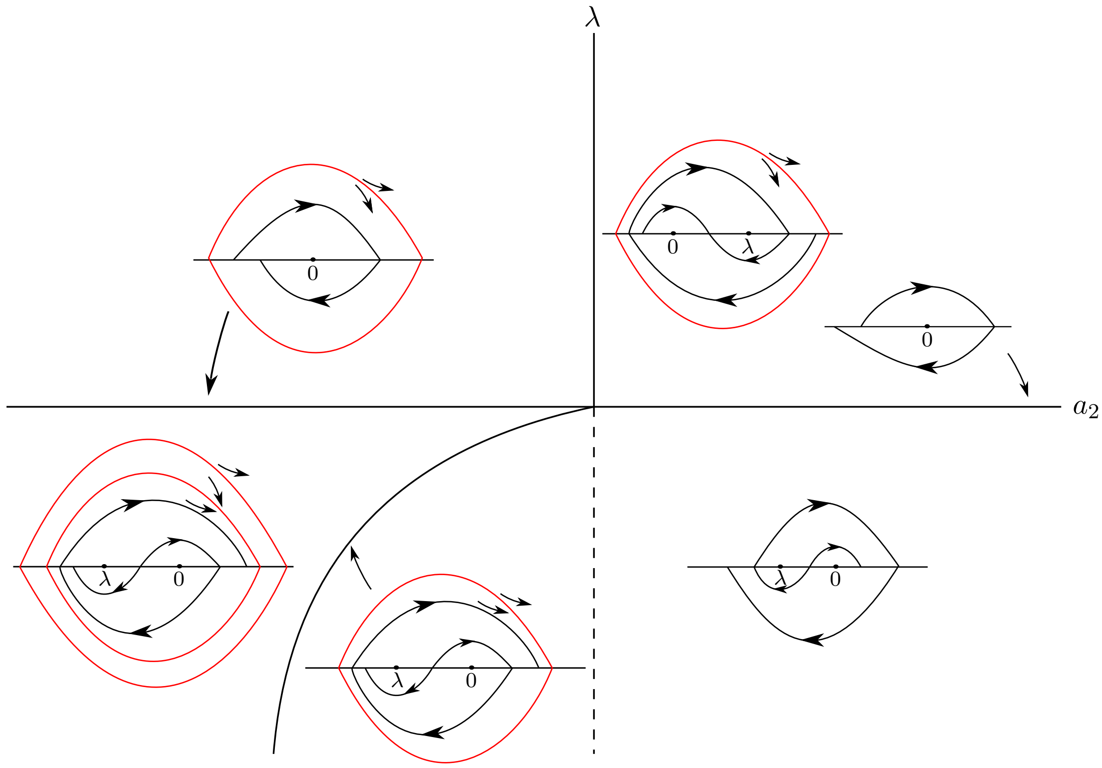

Figure 5.9: Bifurcation diagram of the PSVF $Z_{a,2,\lambda}$.

We point out the similarities between the bifurcation diagrams described in Propositions 48 and 49 with the bifurcation diagrams of Hopf bifurcations of codimension one and two for smooth vector fields, respectively. See [79] and [97] for details.

In this way, let us consider the PSVF

$$Z_{a,3,\lambda}(x,y) = \begin{cases} X(x,y) &= \left(1, -x + a_2x^2 + a_4x^4 + x^6\right), & y \geq 0; \\ Y_\lambda(x,y) &= (-1, -x+\lambda), & y \leq 0, \end{cases} \tag{5.37}$$

where $a = (a_2, a_4, 1)$. Proceeding in an analogous approach like Proposition 49 we can find the bifurcation set $B \in \mathbb{R}^3$ associated with $Z_{a,3,\lambda}$, that is, the set of the points $\zeta = (\lambda, a_2, a_4) \in \mathbb{R}^3$ such that the number of the solutions of $P(\zeta, x_0) = 0$, where P is the corresponding displacement function, is not locally constant. Figure 5.10 presents the bifurcation set associated with $Z_{a,3,\lambda}$.

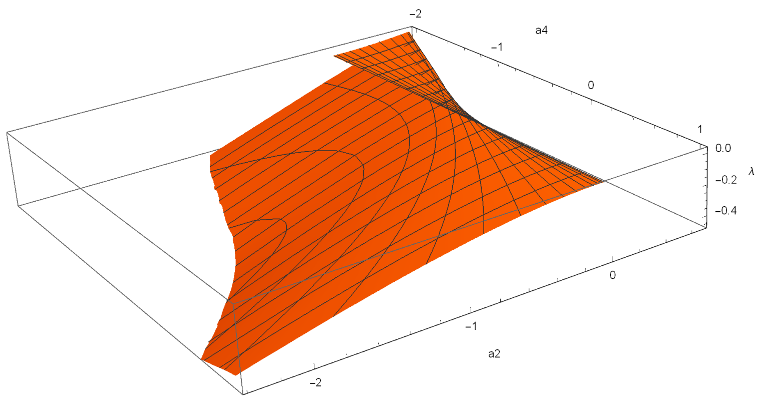

Figure 5.10: Bifurcation set associated with $Z_{a,3,\lambda}$.

We emphasize that the bifurcation set of (5.37) described in Figure 5.10 is also very similar to the bifurcation set found by Takens (see [113]) for smooth codimension three Hopf bifurcations. This bifurcation diagram is also illustrated in [108].

Once the simplest cases have been studied, we will now turn our attention to the general study of the vector field

$$X_{a,k}(x,y) = \left(1, -x + a_2x^2 + a_4x^4 + \cdots + a_{2k-2}x^{2k-2} + x^{2k}\right),$$

where $a = (a_2, a_4, \ldots, a_{2k-2}, 1)$ and system (5.32) which is given by

$$Z_{a,k,\lambda}(x,y) = \begin{cases} X_{a,k}(x,y), & y \geq 0; \\ Y_\lambda(x,y) = (-1, -x+\lambda), & y \leq 0. \end{cases}$$

The vector field $X_{a,k}$ is Hamiltonian whose Hamiltonian function is given by

$$H_k(x,y) = -y - \frac{x^2}{2} + \frac{a_2x^3}{3} + \frac{a_4x^5}{5} + \cdots + \frac{a_{2k-2}}{2k-1}x^{2k-1} + \frac{x^{2k+1}}{2k+1}.$$

So, $H_k(x_0,0) = H_k(x_1,0)$ is equivalent to

$$\tfrac{1}{2}(x_1+x_0) - \tfrac{a_2}{3}(x_1^2 + x_1x_0 + x_0^2) - \cdots - \frac{a_{2k-2}}{2k-1}(x_1^{2k-2} + \cdots + x_0^{2k-2}) - \frac{1}{2k+1}(x_1^{2k} + \cdots + x_0^{2k}) = 0.$$

Let us call $g(x_0,x_1)$ the function described above. Since $g(0,0)=0$ and $\partial g(0,0)/\partial x_1 = 1/2 \neq 0$, by Implicit Function Theorem there exist an interval I containing zero and $x_1\colon I \longrightarrow \mathbb{R}$ such that $x_1(0) = 0$ e $g(x_0, x_1(x_0)) = 0$, for all $x_0 \in I$. Moreover,

$$x_1(x_0) = -x_0 + \frac{2a_2}{3}x_0^2 - \frac{4a_2^2}{9}x_0^3 + \left(\frac{16a_2^3}{27} + \frac{2a_4}{5}\right)x_0^4 + \mathcal{O}(x_0^5).$$

Let $Z_{a,k,0}$ be the PSVF given by system (5.32) when $\lambda = 0$, that is,

$$Z_{a,k,0}(x,y) = \begin{cases} X_{a,k}(x,y) = \left(1, -x + a_2x^2 + \cdots + a_{2k-2}x^{2k-2} + x^{2k}\right), & y \geq 0; \\ Y_0(x,y) = (-1,-x), & y \leq 0. \end{cases} \tag{5.38}$$

The first return map associated with $Z_{a,k,0}$ ($\lambda = 0$) is given by

$$\begin{aligned} \pi_{Z_{k,0}}\colon \Sigma &\longrightarrow \Sigma \\ x_0 &\longmapsto \pi_{Z_{k,0}}(x_0) = \pi_{Y_0} \circ \pi_{X_k}(x_0) \end{aligned}$$

where $\pi_{Y_0}(x_0) = -x_0$ is the half return map associated with the vector field Y_0 (Lemma 15) and $\pi_{X_k}(x_0) = x_1(x_0)$ is the half return map associated with the vector field $X_{a,k}$. Thus,

$$\pi_{Z_{k,0}}(x_0) = x_0 - \frac{2a_2}{3}x_0^2 + \frac{4a_2^2}{9}x_0^3 - \left(\frac{16a_2^3}{27} + \frac{2a_4}{5}\right)x_0^4 + \mathcal{O}(x_0^5)$$

and the corresponding displacement function can be written as

$$P_0(x_0) = \pi_{Z_{k,0}}(x_0) - x_0 = -\frac{2a_2}{3}x_0^2 + \frac{4a_2^2}{9}x_0^3 - \left(\frac{16a_2^3}{27} + \frac{2a_4}{5}\right)x_0^4 + \mathcal{O}(x_0^5). \tag{5.39}$$

We notice that if a_2 is zero then the coefficients of the terms of order two and three of the displacement function vanish and the coefficient of the term of order 4 is a negative multiple of a_4. This process is evidenced in the following lemma.

Lemma 17. *Consider $Z_{a,k,0}$ given by* (5.38) *and let P_0 be the displacement function associated with $Z_{a,k,0}$. Suppose that $P_0(x_0) = V_0 + V_1x_0 + V_2x_0^2 + \cdots + V_ix_0^i + \cdots$. Then $V_0 = V_1 = 0$. Moreover, for $n \geq 3$ if $V_2 = V_4 = \cdots = V_{2n-4} = 0$ then $V_{2n-3} = 0$ and V_{2n-2} is given by*

$$V_{2n-2} = -\frac{2}{2n-1}a_{2n-2}.$$

Proof. From (5.39) it is straightforward that $V_0 = V_1 = 0$. The rest of the proof is given by induction on n. Consider $n = 3$. From (5.39) we get that if $V_2 = 0$ then $V_3 = 0$ and

$$V_4 = -\frac{2}{5}a_4.$$

Suppose that it holds for $n = j-1$, that is, $V_{2j-5} = 0$ and

$$V_{2j-4} = -\frac{2}{2j-3}a_{2j-4}$$

when $V_2 = \cdots = V_{2j-6} = 0$. We need to show that it holds for $n = j$, that is, if $V_2 = \cdots = V_{2j-6} = V_{2j-4} = 0$ then $V_{2j-3} = 0$ and

$$V_{2j-2} = -\frac{2}{2j-1}a_{2j-2}.$$

If $V_2 = \cdots = V_{2j-6} = V_{2j-4} = 0$ we have that $a_2 = \cdots = a_{2j-6} = a_{2j-4} = 0$ and

$$X_{a,k}(x,y) = \Big(1, -x + a_{2j-2}x^{2j-2} + \cdots + a_{2k-2}x^{2k-2} + x^{2k}\Big).$$

Thus, $H_k(x_0, 0) = H_k(x_1, 0)$ is equivalent to

$$\frac{1}{2}(x_1 + x_0) - \frac{a_{2j-2}}{2j-1}(x_1^{2j-2} + \cdots + x_0^{2j-2}) - \cdots - \\ \frac{a_{2k-2}}{2k-1}(x_1^{2k-2} + \cdots + x_0^{2k-2}) - \frac{1}{2k+1}(x_1^{2k} + \cdots + x_0^{2k}) = 0.$$

Let us call $g(x_0, x_1)$ the function described above. Since $g(0,0) = 0$ and $\partial g(0,0)/\partial x_1 = 1/2 \neq 0$, by Implicit Function Theorem there exist an interval I containing zero and $x_1 \colon I \longrightarrow \mathbb{R}$ such that $x_1(0) = 0$ e $g(x_0, x_1(x_0)) = 0$, for all $x_0 \in I$. Furthermore, $x_1'(0) = -1$ and the derivatives $x_1^i(0) = 0$ for $1 < i < 2j-2$ since g is the sum of linear terms with homogeneous polynomials of even degree between $2j-2$ and $2k$. Moreover, the derivative of order $2j-2$ of $g(x_0, x_1(x_0)) = 0$

with respect to the variable x_0 evaluated on the origin is of the form

$$\frac{\partial^{2j-2}g(0,0)}{\partial x_0^{2j-2}} + x_1^{(2j-2)}(0)\frac{\partial g(0,0)}{\partial x_1} = 0$$

and we get

$$x_1^{(2j-2)}(0) = \frac{2(2j-2)!}{2j-1}a_{2j-2}.$$

Hence,

$$P_0(x_0) = -\frac{2}{2j-1}a_{2j-2}x_0^{2j-2} + \mathcal{O}\left(x_0^{2j-1}\right).$$

Therefore, if $V_2 = \cdots = V_{2j-6} = V_{2j-4} = 0$ then $V_{2j-3} = 0$ and

$$V_{2j-2} = -\frac{2}{2j-1}a_{2j-2}.$$

□

The next result will be very useful in the sequel.

Lemma 18. *Consider the real polynomial $p(r) = a_2r^2 + a_4r^4 + \cdots + a_{2n}r^{2n}$, where $a_{2n} > 0$. If $a_{2j}a_{2j+2} < 0$, for $j = 1, \ldots, n-1$ and $|a_2| << |a_4| << \cdots << |a_{2n}|$ then p has exactly $2n-2$ nonzero real roots being $n-1$ positive and $n-1$ negative.*

Proof. We remark that $r = 0$ is a double zero of p. Also, $p(r) = p(-r)$ and consequently if r is a zero of p then $-r$ is also a zero of p. Initially, suppose that $a_2 = a_4 = \cdots = a_{2n-2} = 0$. Then the graph of $p_0(r) = a_{2n}r^{2n}$ is a parabola concave upward in which the origin $r = 0$ is a multiple zero of p_0. Consider now $a_2 = a_4 = \cdots = a_{2n-4} = 0$ and $a_{2n-2} < 0$ so that $|a_{2n-2}| << |a_{2n}|$. Thus, we get

$$p_1(r) = a_{2n-2}r^{2n-2} + a_{2n}r^{2n} = r^{2n-2}\left(a_{2n-2} + a_{2n}r^2\right) = r^{2n-2}q_1(r).$$

Observe that the graph of q_1 is a parabola concave upward, symmetric to the vertical axis, passing through it in a negative point, and presenting two nonzero real roots. So, $p_1(r)$ is the product of a non-negative function and q_1 so that p_1 has the same sign of q_1 except at the origin. Now take $a_2 = a_4 = \cdots = a_{2n-6} = 0$ and $a_{2n-4} > 0$ so that $|a_{2n-4}| << |a_{2n-2}|$. Then we get

$$p_2(r) = r^{2n-4}\left(a_{2n-4} + r^2(a_{2n-2} + a_{2n}r^2)\right) = r^{2n-4}q_2(r)$$

The graph of q_2 is similar to the graph of p_1 translated in the positive way of the vertical axis, that is, it is a small perturbation of p_1 in a way that it preserves the earlier zeroes and generate a new pair of ones. Thus, p_2 is the product of q_2 by a non-negative function and consequently it preserves the sign of q_2 except at the origin. Proceeding in this way it is possible to choose $a_2, a_4, \dots, a_{2n-2}$ so that p has $2n-2$ nonzero roots. $\square$

In the result below we show that the PSVF $Z_{a,k,0}$ given by (5.38) has at most $k-1$ crossing limit cycles. Also, there exists choices of the parameters for which the limit cycles exist.

Theorem 20. *Consider the PSVF $Z_{a,k,0}$ given by* (5.38)*. Then there are at most $k-1$ hyperbolic crossing limit cycles in a suitable neighborhood of the origin. Moreover, if $a_2, a_4, \dots, a_{2k-2}$ are chosen such that*

(1) $a_{2k-2} < 0, a_{2k-4} > 0, \dots, a_2$ is negative or positive if k is even or odd, respectively;

(2) $|a_2| << |a_4| << \cdots << |a_{2k-2}|$;

then $Z_{a,k,0}$ has exactly $k-1$ hyperbolic crossing limit cycles in a suitable neighborhood of the origin.

Proof. By the previous analysis, the vector field $X_{a,k}$ is Hamiltonian whose Hamiltonian function is given by

$$H_k(x,y) = -y - \frac{x^2}{2} + \frac{a_2x^3}{3} + \frac{a_4x^5}{5} + \cdots + \frac{a_{2k-2}}{2k-1}x^{2k-1} + \frac{x^{2k+1}}{2k+1}.$$

So, $H_k(x_0,0) = H_k(x_1,0)$ is equivalent to

$$\frac{1}{2}(x_1+x_0) - \frac{a_2}{3}(x_1^2+x_1x_0+x_0^2) - \cdots - \frac{a_{2k-2}}{2k-1}(x_1^{2k-2}+\cdots+x_0^{2k-2}) - \frac{1}{2k+1}(x_1^{2k}+\cdots+x_0^{2k}) = 0. \tag{5.40}$$

By Lemma 15 the return to Σ of an orbit of Y_0 through x_0 is $x_1 = -x_0$. Substituting $x_1 = -x_0$ in Equation (5.40) we get

$$l(x_0) = -\frac{a_2}{3}x_0^2 - \frac{a_4}{5}x_0^4 - \cdots - \frac{a_{2k-2}}{2k-1}x_0^{2k-2} - \frac{1}{2k+1}x_0^{2k} = 0$$

a polynomial of degree $2k$ with only even exponents of degree less than or equal to $2k$. Therefore l has at most $2k-2$ nonzero roots that corresponds to at most $k-1$ limit cycles. Proceeding in the same way of Lemma 18 it is possible to choose $a_2, a_4, \dots, a_{2k-2}$ so that l has exactly $2k-2$ nonzero roots that corresponds to $k-1$ limit cycles. $\square$

In the next result we give a positive answer to the question that guided this work.

Theorem 21. *Consider $k \in \mathbb{N}$ fixed. Then, there exist $\lambda \in \mathbb{R}$ sufficiently small and $a = (a_2, a_4, \ldots, a_{2k-2}, 1)$ such that $Z_{a,k,\lambda}$ given by* (5.32) *has exactly k hyperbolic crossing limit cycles near the origin.*

Proof. In fact, the vector field $X_{a,k}$ is Hamiltonian and a Hamiltonian function is given by

$$H_k(x, y) = -y - \frac{x^2}{2} + \frac{a_2x^3}{3} + \frac{a_4x^5}{5} + \cdots + \frac{a_{2k-2}}{2k-1}x^{2k-1} + \frac{x^{2k+1}}{2k+1}.$$

So, $H_k(x_0, 0) = H_k(x_1, 0)$ is equivalent to

$$\frac{1}{2}(x_1+x_0) - \frac{a_2}{3}(x_1^2+x_1x_0+x_0^2) - \cdots - \frac{a_{2k-2}}{2k-1}(x_1^{2k-2}+\cdots+x_0^{2k-2}) - \frac{1}{2k+1}(x_1^{2k}+\cdots+x_0^{2k}) = 0. \tag{5.41}$$

Similarly, Y_λ is Hamiltonian whose Hamiltonian function is

$$H_Y(x, y) = y - \frac{x^2}{2} + \lambda x.$$

Then, $H_Y(x_0, 0) = H_Y(x_1, 0)$ is equivalent to $x_1 = -x_0 + 2\lambda$. Substituting $x_1 = -x_0 + 2\lambda$ into Equation (5.41) we get

$$q(x_0) = -\frac{a_2}{3}x_0^2 - \frac{a_4}{5}x_0^4 - \cdots - \frac{a_{2k-2}}{2k-1}x_0^{2k-2} - \frac{1}{2k+1}x_0^{2k} + R(\lambda, x_0) = 0 \tag{5.42}$$

where $R(0, x_0) = 0$, for all $x_0 \in I$. By Theorem 20, for $\lambda = 0$, it is possible to choose $a_2, a_4, \ldots, a_{2k-2}$ so that q has exactly $2k-2$ nonzero roots that corresponds to $k-1$ crossing limit cycles. Fix $a_2, a_4, \ldots, a_{2k-2}$ according Theorem 20. On the other hand, we observe that the limit cycles of $Z_{a,k,\lambda}$ correspond to a pair of intersections between the curves

$$h_\lambda(x_0, x_1) = x_1 + x_0 - 2\lambda = 0$$

and

$$g(x_0, x_1) = \frac{1}{2}(x_1 + x_0) - \frac{a_2}{3}\left(x_1^2 + x_1x_0 + x_0^2\right) - \cdots - \frac{1}{2k+1}\left(x_1^{2k} + \cdots + x_0^{2k}\right) = 0$$

in the x_0x_1-plane. We claim that $g(x_0, x_1) = 0$ has a fold point with $\gamma^{-1}(0)$ at $(x_0, x_1) = (0, 0)$, where

$$\gamma(x_0, x_1) = x_1 + x_0 = h_0(x_0, x_1).$$

In fact, we want to find a vector field F so that an orbit of F is contained in the zero level of

$g(x_0, x_1)$ in order to investigate the quadratic contact with $\gamma^{-1}(0)$. Naturally, just consider

$$F(x_0, x_1) = \left(-\frac{\partial g(x_0, x_1)}{\partial x_1}, \frac{\partial g(x_0, x_1)}{\partial x_0}\right).$$

So, the first and second derivatives of γ in the direction of F at $(x_0, x_1) = (0, 0)$ are, respectively, given by

$$F\gamma(0,0) = F(x_0, x_1) \cdot (1,1)|_{(0,0)} = -\frac{\partial g(0,0)}{\partial x_1} + \frac{\partial g(0,0)}{\partial x_0} = 0$$

and

$$F^2\gamma(0,0) = F(x_0, x_1) \cdot \nabla F\gamma(x_0, x_1)|_{(0,0)} = \frac{a_2}{3}.$$

Consequently, $(0,0) \in \gamma^{-1}(0)$ is a fold point of F that is visible or invisible depending on the sign of a_2. See illustrated at Figure 5.11.

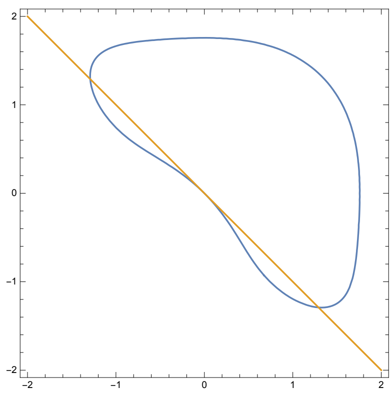

Figure 5.11: Quadratic contact between the vector field F and $\gamma^{-1}(0)$ at $(0,0)$.

Therefore, for a small perturbation of γ, that is, for $\lambda \neq 0$ sufficiently small having the same sign of a_2 and such that $|\lambda| << |a_2|$, we can perturb this fold point in order to generate two more transversal intersections between g and h_λ which correspond to another crossing limit cycle. See Figure 5.12. Thus, there exist $\lambda \in \mathbb{R}$ sufficiently small and $a = (a_2, a_4, \ldots, a_{2k-2})$ such that $Z_{a,k,\lambda}$ given by (5.32) has exactly k hyperbolic crossing limit cycles. □

Example 2. *In order to corroborate our results, we perform a numerical example showing the existence of three hyperbolic crossing limit cycles. Let us consider the piecewise smooth vector field*

$$W(x,y) = \begin{cases} \left(1, -x + \frac{17}{40}x^2 - \frac{29}{20}x^4 + x^6\right), & y \geq 0, \\ \left(-1, \frac{7}{1000} - x\right), & y \leq 0, \end{cases}$$

that is, we take $a_2 = 17/40$, $a_4 = -29/20$ and $\lambda = 7/1000$. In this case, the respective function

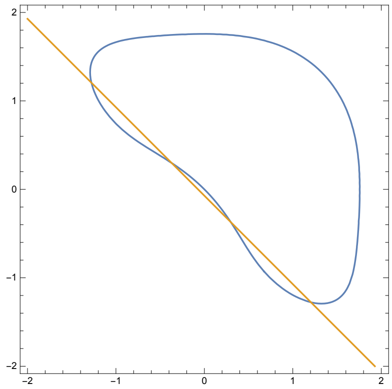

Figure 5.12: Small perturbation of $\gamma^{-1}(0)$ in a way that maintains transversal the earlier intersections.

q obtained in the proof of Theorem 21 is given by

$$-\frac{x_0^6}{7}+\frac{3x_0^5}{500}+\frac{72437x_0^4}{250000}-\frac{1014363x_0^3}{125000000}-\frac{26519881319x_0^2}{187500000000}+\frac{37142745703x_0}{18750000000000}+\frac{326823959667079}{468750000000000000}=0$$

whose negative zeros are given by $x_b=-1.129139$, $x_c=-0.819270$ and $x_d=-0.228449$ with six decimals. The three positives zeros are given by $-x_i+2\lambda$, for $i=b,c,d$. Since λ is positive there is a sliding set between $x=0$ and $x=\lambda$. If we take the trajectories of W passing through the zeros we can notice the existence of three hyperbolic crossing limit cycles whose stability characters alternate between an attractor and a repellor in a way that the smallest limit cycle is repellor due to the attracting sliding set near the origin. See Figure 5.13 for an illustration.

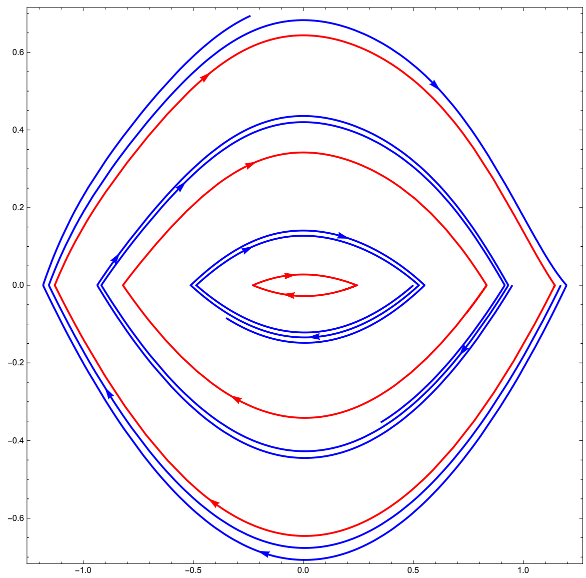

Figure 5.13: Crossing limit cycles (in red) of the vector field W.

By Lemma 17 the coefficients of the displacement function

$$P_0(x_0) = V_0 + V_1 x_0 + V_2 x_0^2 + \cdots + V_i x_0^i + \cdots$$

associated with the family of piecewise smooth vector fields $Z_{a,k,0}$ given by (5.38) are given by $V_0 = V_1 = 0$ and for $n \geq 3$ if $V_2 = V_4 = \cdots = V_{2n-4} = 0$ then $V_{2n-3} = 0$ and

$$V_{2n-2} = -\frac{2}{2n-1} a_{2n-2}.$$

Therefore, we can redefine the *Lyapunov coefficients* associated with $Z_{a,k,0}$ by

$$L_j^* = a_{2j}, \qquad j = 1, 2, 3 \ldots \tag{5.43}$$

that can be seen as the obstruction for the invisible fold-fold point at the origin to be a center. As in the smooth case, it makes sense to define L_j^* just when $L_i^* = 0$ for all $i < j$. Therefore, if $L_j^* > 0$, for some $j \in \mathbb{N}$, then $P_0(x_0) = \phi(x_0) - x_0 < 0$, which implies that the origin is a repelling fold-fold. On the other hand, if $L_j^* < 0$, for some $j \in \mathbb{N}$, then $P_0(x_0) = \phi(x_0) - x_0 > 0$, which implies that the origin is an attracting fold-fold.

We pointed out some similarities between the bifurcation diagrams described in Propositions 48 and 49 with the bifurcation diagrams of Hopf bifurcations of codimension one and two, respectively, for smooth vector fields. So, a natural question can be formulated about the relationship between the PSVF $Z_{a,k,0}$ and its regularization. If there exists a Hopf point in the regularized system where we can compute the Lyapunov coefficients there will be a correlation between them? We exhibit a relation between the Lyapunov coefficients of the nonsmooth family and their regularization.

The idea behind the Regularization method established by Sotomayor and Teixeira in [109] consists to approximate a piecewise smooth vector field $Z = (X, Y)$ given by Equation (1.1) by a one-parameter family of smooth vector fields which agrees with the original PSVF outside a strip around the switching manifold. The expectation is that by applying classical tools in the regularized system we could obtain some information about the behavior of the discontinuous vector field Z when the regularization parameter goes to zero. See [107] for more details.

Definition 19. *A C^∞ function $\varphi\colon \mathbb{R} \longrightarrow \mathbb{R}$ is called a transition function if*

$$\varphi(t) = \begin{cases} 0, & t \leq -1; \\ \varphi'(t) > 0, & -1 < t < 1; \\ 1, & t \geq 1. \end{cases} \tag{5.44}$$

Figure 5.14 shows the behavior of a transition function.

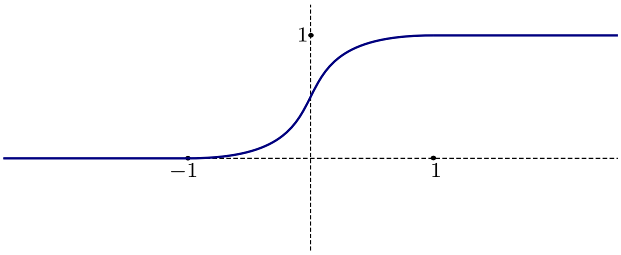

Figure 5.14: Transition function.

Definition 20. *A φ_ε-regularization of $Z = (X, Y)$ is the one parameter family of vector fields Z_ε given by*

$$Z_\varepsilon(q) = \Big(1 - \varphi_\varepsilon(y)\Big)Y(q) + \varphi_\varepsilon(y)X(q) \tag{5.45}$$

where φ is a transition function and $\varphi_\varepsilon(t) = \varphi\left(\frac{t}{\varepsilon}\right)$.

We can notice that inside the strip $\Sigma \times (-\varepsilon, \varepsilon)$, a transition function is used to average the vector fields X and Y. If we apply the above construction to the family of discontinuous vector fields $Z_{a,k,0}$ given by (5.38) we get

$$\begin{aligned} Z_\varepsilon(x, y) &= \Big(1 - \varphi_\varepsilon(y)\Big)Y_0(x, y) + \varphi_\varepsilon(y)X_{a,k}(x, y) \\ &= \Big(-1 + 2\varphi_\varepsilon(y), -x + \varphi_\varepsilon(y)\left(a_2x^2 + \cdots + a_{2k-2}x^{2k-2} + x^{2k}\right)\Big) \\ &= \Big(Z^1_\varepsilon(x, y), Z^2_\varepsilon(x, y)\Big). \end{aligned} \tag{5.46}$$

The equilibrium points of Z_ε must satisfies $Z^1_\varepsilon(x, y) = -1 + 2\varphi_\varepsilon(y) = 0$. So, we have that the y-coordinate of the equilibrium must satisfies $\varphi_\varepsilon(y) = 1/2$. Notice that by the continuity of the transition function there exists y_0 such that $\varphi_\varepsilon(y_0) = 1/2$. In what follows we will consider $y_0 = 0$. In this way, since $Z^2_\varepsilon(0, 0) = 0$ we have that $(x, y) = (0, 0)$ is an equilibrium point of the regularized vector field Z_ε.

The Jacobian matrix of the regularized vector field Z_ε evaluated at $(0, 0)$ is given by

$$DZ_\varepsilon(0, 0) = \begin{bmatrix} 0 & \frac{2\varphi'(0)}{\varepsilon} \\ -1 & 0 \end{bmatrix}.$$

As a result we have that $Tr\,(DZ_\varepsilon(0, 0)) = 0$ and $Det\,(DZ_\varepsilon(0, 0)) = 2\varphi'(0)/\varepsilon > 0$. Therefore the linearization of the vector field Z_ε at the equilibrium point $(0, 0)$ is of center type whose eigenvalues are given by

$$\mu_\pm = \pm i\sqrt{\frac{2\varphi'(0)}{\varepsilon}}.$$

Thus $(0,0)$ is a Hopf point of the regularized system. We study its stability by computing the Lyapunov coefficients. As follows, we will utilize the approach already described in this work and also available in [27] and [69]. An eigenvector associated with the eigenvalue μ_+ of DZ_ε at the origin is given by

$$v = (0,1) + \left(-\sqrt{\frac{2\varphi'(0)}{\varepsilon}}, 0\right) i.$$

Thus, the matrix of transformation to the Jordan canonical form has the expression

$$T = \begin{bmatrix} -\sqrt{\frac{2\varphi'(0)}{\varepsilon}} & 0 \\ 0 & 1 \end{bmatrix}.$$

Consequently, we get $Z_\varepsilon(x,y) = \Big(\mathcal{G}_1(x,y), \mathcal{G}_2(x,y)\Big)$ where

$$\mathcal{G}_1(x,y) = \frac{\varepsilon}{2\varphi'(0)} - \frac{\varepsilon}{\varphi'(0)}\varphi\left(\frac{y}{\varepsilon}\right)$$

and

$$\mathcal{G}_2(x,y) = x + \sqrt{2}\varphi\left(\frac{y}{\varepsilon}\right)\left[\sum_{j=1}^{k} 2^{j-1} a_{2j} x^{2j}\left(\frac{\varphi'(0)}{\varepsilon}\right)^{\frac{2j-1}{2}}\right].$$

We remark that $a_{2k} = 1$. The series expansion of $\mathcal{G}_1$ has the expression

$$\mathcal{G}_1(x,y) = -y - \frac{\varepsilon}{\varphi'(0)}\left(\frac{y^2\varphi''(0)}{2\varepsilon^2} + \frac{y^3\varphi'''(0)}{6\varepsilon^3} + \cdots\right).$$

Thus we can rewrite the vector field Z_ε as $Z_\varepsilon(x,y) = \Big(G_1(x,y), G_2(x,y)\Big)$ where

$$G_1(x,y) = -y - \frac{1}{b_1}\Big(b_2 y^2 + b_3 y^3 + \cdots\Big),$$

$$G_2(x,y) = x + \Big(\alpha_2 x^2 + \cdots + \alpha_{2k} x^{2k}\Big)\Big(b_0 + b_1 y + b_2 y^2 + b_3 y^3 + \cdots\Big),$$

b_i are the coefficients of order i of the series expansion of the transition function φ and, for $j = 1, \ldots, k$,

$$\alpha_j = 2^{j-1}\sqrt{2}\left(\frac{\varphi'(0)}{\varepsilon}\right)^{\frac{2j-1}{2}} a_{2j}.$$

Consider a function V represented formally as the series

$$V(x,y)=\frac{1}{2}\left(x^2+y^2\right)+\sum_{j=3}^{\infty}V_j(x,y)$$

where each V_j is a homogeneous polynomial of degree j. We denote by $V_{n,m}$ the coefficient of x^ny^m in V_j, for $j=n+m$. We say that $V_{n,m}$ is even or odd according to n is even or odd. Computing the derivative of V in the direction of Z_ε we get the expression

$$\dot V=\nabla V\cdot Z_\varepsilon=\Big(x+V_{3x}+V_{4x}+\cdots,y+V_{3y}+V_{4y}+\cdots\Big)\cdot Z_\varepsilon(x,y).$$

Performing the calculations we have

$$\begin{aligned}\dot V &= \Big[-xy+xy\Big]+\Big[-\frac{b_2}{b_1}xy^2+\alpha_2b_0x^2y+xV_{3y}-yV_{3x}\Big]+\cdots\\ &= V_{2,1}x^3+\Big(-3V_{3,0}+\alpha_2b_0+2V_{1,2}\Big)x^2y+\Big(-\frac{b_2}{b_1}-2V_{2,1}+3V_{0,3}\Big)xy^2-\\ &\quad -V_{1,2}y^3+V_{3,1}x^4+\Big(2V_{2,2}-4V_{4,0}\Big)x^3y+\Big(3V_{1,3}-3V_{3,1}+\alpha_2b_1\Big)x^2y^2\\ &\quad +\Big(-\frac{b_3}{b_1}-2V_{2,2}\Big)xy^3-V_{1,3}y^4+\cdots.\end{aligned}\tag{5.47}$$

By Theorem 2 the linear transformation

$$\begin{aligned}T_n:\quad \mathcal{H}^n &\longrightarrow \mathcal{H}^n\\ p(x,y) &\longmapsto T_n(p(x,y))=-y\frac{\partial p}{\partial x}(x,y)+x\frac{\partial p}{\partial y}(x,y).\end{aligned}$$

is an isomorphism for n odd. Thus T_3 is an isomorphism and we can choose the coefficients $V_{3,0},\ldots,V_{0,3}$ so that $\dot V$ determined in (5.47) contains no cubic terms. To do so they must satisfy the following set of equations

$$\begin{cases} V_{2,1}=0,\\ -3V_{3,0}+2V_{1,2}=-\alpha_2b_0,\\ -2V_{2,1}+3V_{0,3}=\frac{b_2}{b_1},\\ -V_{1,2}=0.\end{cases}$$

Consequently, we get $V_{2,1}=V_{1,2}=0$, $V_{0,3}=b_2/(3b_1)$ and $V_{3,0}=\alpha_2b_0/3$. Therefore, there exists

$$V_3(x,y)=\frac{\alpha_2b_0}{3}x^3+\frac{b_2}{3b_1}y^3\in\mathcal{H}^3$$

such that $\dot V$ has order greater than or equal four. Now have to proceed to the quartic terms.

By Theorem 2 the linear transformation T_4 is not an isomorphism. However, since it's kernel is generated by $\left(x^2+y^2\right)^2$, we have that $\dot{V}_4 - \eta_4(x^2+y^2)^2$ belongs to the image of T_4, where $\dot{V}_4$ represents the quartic terms of $\dot{V}$. So, we can seek for $V_{4,0}, \ldots, V_{0,4}$ such that

$$\dot{V} \;\; = \;\; \eta_4\left(x^2+y^2\right)^2 + \cdots .$$

To achieved this the terms of V_4 must satisfy the following set of equations

$$\begin{cases} V_{3,1} - \eta_4 &= 0, \\ -4V_{4,0} + 2V_{2,2} &= 0, \\ -3V_{3,1} + 3V_{1,3} - 2\eta_4 &= -\alpha_2 b_1, \\ -\frac{b_3}{b_1} - 2V_{2,2} &= 0, \\ -V_{1,3} - \eta_4 &= 0. \end{cases}$$

Thus, we may choose

$$V_{0,4} = 0, \quad V_{2,2} = -\frac{b_3}{2b_1}, \quad V_{4,0} = -\frac{b_3}{4b_1}, \quad V_{1,3} = -\frac{\alpha_2 b_1}{8} \quad \text{and} \quad \eta_4 = V_{3,1} = \frac{\alpha_2 b_1}{8}.$$

In other words, the first obstruction to the origin be a center is given by

$$\eta_4 = \frac{1}{8}\alpha_2 b_1 = \frac{\sqrt{2}}{8} a_2 \left(\frac{\varphi'(0)}{\varepsilon}\right)^{\frac{3}{2}}.$$

By the previous calculations the following Lemma is proved.

Lemma 19. *Consider the differential system associated with the regularized vector field Z_ε*

$$\begin{cases} \dot{x} = G_1(x,y); \\ \dot{y} = G_2(x,y). \end{cases} \tag{5.48}$$

The following statements hold:

(1) The first Lyapunov coefficient at $(0,0)$ is given by $L_1 = \alpha_2$;

(2) If $\alpha_2 = 0$ then $V_{3,0} = V_{1,2} = V_{1,3} = V_{3,1} = 0$.

Theorem 22. *Consider system (5.48). For $n = 1, \ldots, k$, the Lyapunov coefficient L_n is given by $L_n = \alpha_{2n}$.*

Proof. The proof is given by induction on the following statement P_k: $L_j = \alpha_{2j}$ for $j = 1, \ldots, k$. If $\alpha_{2j} = 0$ for $j = 1, \ldots, k$ the odd coefficients of V_j, for $j \leq 2k+2$ are zero.

By Lemma 19, P_1 is true. Now suppose that P_k is true. Let us show that P_{k+1} is true, that is, $L_{k+1} = \alpha_{2k+2}$ and if $\alpha_2 = \ldots = \alpha_{2k+2} = 0$ then the odd coefficients of V_{2k+3} and V_{2k+4} are zero. When $\alpha_2 = \ldots = \alpha_{2k} = 0$ the odd coefficients of V_{2k+3} are determined by the following set of equations

$$\begin{cases} V_{1,2k+2} = 0, \\ -3V_{3,2k} + (2k+2)V_{1,2k+2} = 0, \\ -5V_{5,2k-2} + (2k)V_{3,2k} = 0, \\ \vdots \\ -(2k+1)V_{2k+1,2} + 4V_{2k-1,4} = 0, \\ -(2k+3)V_{2k+3,0} + 2V_{2k+1,2} = -b_0\alpha_{2k+2}. \end{cases}$$

If $\alpha_2 = \ldots = \alpha_{2k} = \alpha_{2k+2} = 0$ then the right–hand sides of these equations are zero and, consequently, the odd coefficients of V_{2k+3} are zero. On the other hand, the odd coefficients of V_{2k+4} are determined by the following set of equations

$$\begin{cases} -\eta_{2k+4} - V_{1,2k+3} = 0, \\ -\binom{k+2}{k+1}\eta_{2k+4} - 3V_{3,2k+1} + (2k+3)V_{1,2k+3} = 0, \\ -\binom{k+2}{k}\eta_{2k+4} - 5V_{5,2k-1} + (2k+1)V_{3,2k+1} = 0, \\ \vdots \\ -\binom{k+2}{1}\eta_{2k+4} - (2k+3)V_{2k+3,1} + 3V_{2k+1,3} = -\alpha_{2k+2}b_1, \\ -\eta_{2k+4} + 2V_{2k+3,1} = 0. \end{cases}$$

Working backwards through the equations, we see that η_{2k+4} is a positive multiple of α_{2k+2}, and each odd coefficient is a negative multiple of α_{2k+2}. We deduce that, if P_k is true, then $L_{k+1} = \alpha_{2k+2}$ and if $\alpha_2 = \ldots = \alpha_{2k+2} = 0$ then the odd coefficients of V_{2k+3} and V_{2k+4} are zero. □

In this way, we have achieved the next result that establishes the equality between the signs of the Lyapunov coefficients of the family of discontinuous vector fields $Z_{a,k,0}$ and its regularization Z_ε.

Theorem 23. *For $\varepsilon > 0$ sufficiently small, the Lyapunov coefficients of the family of PSVFs $Z_{a,k,0}$ and the Lyapunov coefficients of its regularization Z_ε have the same sign.*

Proof. It follows from Equation (5.43) and Theorem 22. □

Combining Theorem 23 with Proposition 13 of [107] we obtain the following Theorem which states the existence of a hyperbolic limit cycle of the regularized systems in a suitable small neighborhood of each hyperbolic crossing limit cycle of the discontinuous ones.

Theorem 24. *Given $k \in \mathbb{N}$, consider the family of piecewise smooth vector fields $Z_{a,k,\lambda}$ and its regularization Z_ε. Then there exist $a = (a_2, a_4, \dots, a_{2k-2}, a_{2k}) \in \mathbb{R}^k$, $\lambda \in \mathbb{R}$ and $\varepsilon_0 > 0$ sufficiently small such that, for every transition function, Z_ε has k hyperbolic limit cycles in a suitable neighborhood of the origin, for each $0 < \varepsilon < \varepsilon_0$.*

Example 3. *We perform a numerical example showing the existence of three hyperbolic limit cycles for the family of regularized systems W^ε in a neighborhood of the hyperbolic crossing limit cycles of the piecewise smooth vector field W given in Example 2. In this simulation we consider a transition function φ of class C^2 given by*

$$\varphi(y) = \begin{cases} 0, & y \leq -1, \\ p(y), & -1 < y < 1, \\ 1, & y \geq 1, \end{cases}$$

where

$$p(y) = \frac{1}{2} + y - \frac{13y^3}{16} + \frac{3y^5}{8} - \frac{y^7}{16}.$$

In this way, the regularization of the PSVF W in Example 2 produces the family of smooth vector fields

$$W^\varepsilon(x,y) = \left(-1 + 2\varphi\left(\frac{y}{\varepsilon}\right), \frac{7}{1000} - x + \left(x^6 - \frac{29x^4}{20} + \frac{17x^2}{40} - \frac{7}{1000}\right)\varphi\left(\frac{y}{\varepsilon}\right)\right).$$

The vector field W^ε has an equilibrium point near the origin that is an attracting focus for each small value of ε. In particular, we consider $\varepsilon_1 = 0.1$ and $\varepsilon_2 = 0.3$. In the first case, we notice the existence of hyperbolic limit cycles of W^{ε_1} near the points $(0.273220, 0)$, $(0.846184, 0)$ and $(1.153989, 0)$ with six decimals. In the last one, we observe the existence of hyperbolic limit cycles of W^{ε_2} close to the initial conditions $(0.279302, 0)$, $(0.869197, 0)$ and $(1.170542, 0)$ with six decimals. The smooth limit cycles are getting close to the crossing ones as ε decreases. See Figure 5.15.

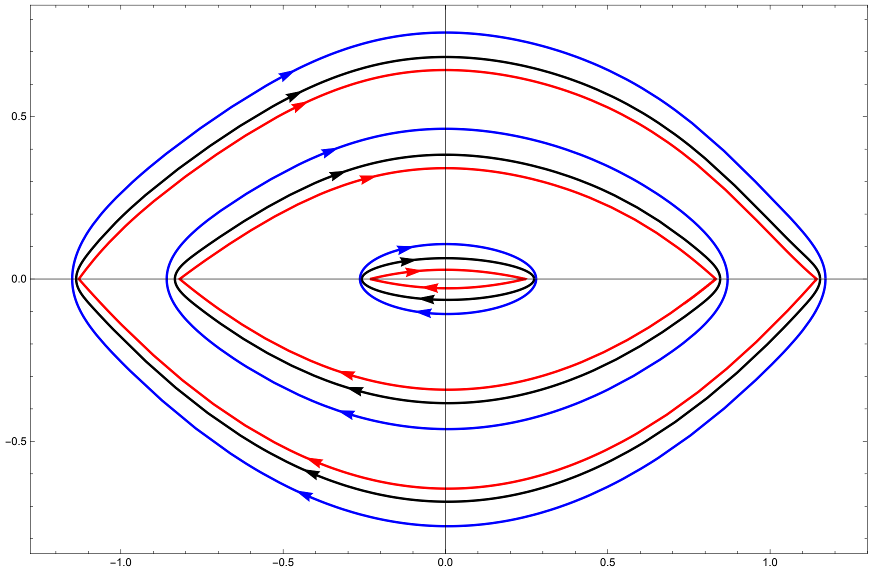

Figure 5.15: The three hyperbolic crossing limit cycles of the PSVF W given in Example 2 are depicted in red solid lines. Smooth hyperbolic limit cycles of the regularized system W^ε are depicted in black (blue, respectively) solid lines for $\varepsilon = 0.1$ ($\varepsilon = 0.3$, respectively).

We can ask if the relation between the signs of the Lyapunov coefficients of the nonsmooth vector field and its regularization holds in general. We will see in the next example that the stability of the invisible fold-fold associated with a piecewise Hamiltonian vector field can be distinct from the stability of the equilibrium point of the regularized one. This example contradicts our intuition that the regularization process just "smooth" a small neighborhood of the switching manifold and that this process could not affect the equilibrium stability.

Let us consider a discontinuous vector field $\mathcal{F}$ given by

$$\mathcal{F}(x,y) = \begin{cases} \mathcal{F}_1(x,y), & y \geq 0; \\ \mathcal{F}_2(x,y) = (-1, -x+\lambda), & y \leq 0, \end{cases} \tag{5.49}$$

where $\mathcal{F}_1(x,y)$ is given by

$$\mathcal{F}_1 = \left(1 + a_{11}x + a_{21}x^2 + 2a_{02}y + 2a_{12}xy + 3a_{03}y^2, -2x - 3a_{30}x^2 - a_{11}y - 2a_{21}xy - a_{12}y^2\right).$$

By a straightforward calculation we get that both vector fields $\mathcal{F}_1$ and $\mathcal{F}_2$ have an invisible fold-fold singularity at the origin when $\lambda = 0$. Moreover, $\mathcal{F}_1$ and $\mathcal{F}_2$ are Hamiltonian vector fields and the discontinuous vector field $\mathcal{F}$ is in the hypotheses of Theorem 15. So, applying the formula given by (5.18), the second Lyapunov coefficient (using the nomenclature of Section

5.1) is $L_2^* = -a_{30}$. Indeed, the first return map associated with $\mathcal{F}$ has the expression

$$\pi_{\mathcal{F}}(x_0) = x_0 - a_{30}x_0^2 + a_{30}^2 x_0^3 + \mathcal{O}\left(x_0^4\right).$$

Therefore the invisible fold-fold at the origin is repelling for $a_{30} < 0$ and attracting for $a_{30} > 0$. The regularized vector field associated with the PSVF $\mathcal{F}$ is given by

$$\begin{aligned} \mathcal{F}_\varepsilon(x,y) &= \Big(1 - \varphi_\varepsilon(y)\Big)\mathcal{F}_2(x,y) + \varphi_\varepsilon(y)\mathcal{F}_1(x,y) \\ &= \Big(\mathcal{F}_\varepsilon^1(x,y), \mathcal{F}_\varepsilon^2(x,y)\Big). \end{aligned} \tag{5.50}$$

where

$$\mathcal{F}_\varepsilon^1(x,y) = -1 + \varphi_\varepsilon(y)\left(2 + a_{11}x + a_{21}x^2 + 2a_{02}y + 2a_{12}xy + 3a_{03}y^2\right)$$

and

$$\mathcal{F}_\varepsilon^2(x,y) = -x + \varphi_\varepsilon(y)\left(-x - 3a_{30}x^2 - a_{11}y - 2a_{21}xy - a_{12}y^2\right).$$

Let us consider $\varphi(0) = 1/2$. In this way we get that the origin $(0,0)$ is an equilibrium point of $\mathcal{F}_\varepsilon$. The Jacobian matrix of the regularized vector field $\mathcal{F}_\varepsilon$ evaluated on $(0,0)$ is given by

$$D\mathcal{F}_\varepsilon(0,0) = \begin{bmatrix} \frac{a_{11}}{2} & a_{02} + \frac{2\varphi'(0)}{\varepsilon} \\ -\frac{3}{2} & -\frac{a_{11}}{2} \end{bmatrix}.$$

As a result we have that $Tr\left(D\mathcal{F}_\varepsilon(0,0)\right) = 0$ and

$$Det\left(D\mathcal{F}_\varepsilon(0,0)\right) = \frac{3a_{02}}{2} - \frac{a_{11}^2}{4} + \frac{3\varphi'(0)}{\varepsilon},$$

which is positive, for $\varepsilon > 0$ sufficiently small. Therefore, the linearization of $\mathcal{F}_\varepsilon$ at the equilibrium point $(0,0)$ is of center type. Given a smooth vector field $Z_\varepsilon(x,y) = \left(Z_\varepsilon^1(x,y), Z_\varepsilon^2(x,y)\right)$ where

$$Z_\varepsilon^1(x,y) = A_{10}x + A_{01}y + A_{20}x^2 + A_{11}xy + A_{02}y^2 + \cdots$$

and

$$Z_\varepsilon^2(x,y) = B_{10}x + B_{01}y + B_{20}x^2 + B_{11}xy + B_{02}y^2 + \cdots,$$

with $k = i + j$ for $i,j = 0,1,2,\ldots$,

$$A_{ij} = \frac{1}{k!}\binom{k}{i}\frac{\partial^k}{\partial x^i \partial y^j}Z_\varepsilon^1(x,y), \quad B_{ij} = \frac{1}{k!}\binom{k}{i}\frac{\partial^k}{\partial x^i \partial y^j}Z_\varepsilon^2(x,y)$$

the first Lyapunov coefficient of smooth systems, following the work of Andronov (see [4] or [97, 79]), has the expression

$$\begin{aligned}
L_1 &= -\frac{\pi}{4A_{01}(A_{10}B_{01}-A_{01}B_{10})^{3/2}}\left\{A_{01}^2(-(2A_{20}B_{20}+B_{11}B_{20}))\right.\\
&+ \left(A_{01}B_{10}-2A_{10}^2\right)\left(B_{02}B_{11}-A_{11}A_{20}\right)-\left(A_{01}B_{10}+A_{10}^2\right)\cdot\\
&\cdot \quad (3(B_{03}B_{10}-A_{01}A_{30})-A_{01}B_{21}+2A_{10}(A_{21}+B_{12})\\
&+ A_{12}B_{10})+A_{01}A_{10}\left(A_{11}B_{20}+A_{20}B_{11}+B_{11}^2\right)-2A_{01}A_{10}\cdot\\
&\cdot \quad \left(A_{20}^2-B_{02}B_{20}\right)+A_{10}B_{10}\left(A_{02}B_{11}+A_{11}^2+A_{11}B_{02}\right)-\\
&- \left. 2A_{10}B_{10}\left(B_{02}^2-A_{02}A_{20}\right)+B_{10}^2(A_{02}A_{11}+2A_{02}B_{02})\right\}.
\end{aligned}$$

Applying this formula to vector field $\mathcal{F}_\varepsilon$ it is straightforward that the denominator of L_1 is positive for $\varepsilon > 0$ sufficiently small. Therefore, the sign of L_1 is given by its numerator. Notice that the formula for L_1 involves terms of up to third order. So, for $\varepsilon > 0$ sufficiently small, the sign of L_1 is given by the coefficient of $1/\varepsilon^3$, that is, the sign of L_1 is given by

$$2\left(a_{11}-6a_{30}\right)\pi\varphi'(0)^3-\frac{3}{2}a_{11}\pi\varphi'(0)\varphi''(0).$$

Therefore, it is possible to choose values such that the stability of the equilibrium point at the origin of the regularized vector field $\mathcal{F}_\varepsilon$ is distinct from the stability of the invisible fold-fold at the origin associated with the discontinuous vector field $\mathcal{F}$. Another example can be found in [11] where the authors construct a family of piecewise smooth vector fields so that, for some parameter values, the family of PSVFs has an invisible fold-fold at the origin that behaves like an attractor but the Hopf point of the respective regularized system is repelling.

Bibliography

[1] P. A. Abrams and H. Matsuda. Population dynamical consequences of reduced predator switching at low total prey densities. *Population Ecology*, 45(3):175–185, 2003.

[2] J. A. Allen, J. J. D. Greenwood, B. C. Clarke, L. Partridge, and A. Robertson. Frequency-dependent selection by predators. *Philosophical Transactions of the Royal Society B: Biological Sciences*, 319(1196):485–503, 1988.

[3] J. Ananworanich, A. Gayet-Agernon, and M. Le Braz. CD4 guided scheduled treatment interruption compared to continuous therapy: Results of the stacato trial. *The Lancet*, 368(9534):459–465, 2006.

[4] A. Andronov, E. A. Leontovich, I. I. Gordon, and A. G. Maier. *Theory of bifurcations of dynamic systems on a plane.* Israel Program for Scientific Translations, 1971.

[5] A. Andronov, A. Vitt, and S. Khaikin. *Theory of Oscillators.* Adiwes International Series in Physics. Pergamon Press, 1966. Translated from the Russian by F. Immirzi. Translation edited and abridged by W. Fishwick.

[6] J. Aroesty, T. Lincoln, N. Shapiro, and G. Boccia. Tumor growth and chemotherapy: Mathematical methods, computer simulations, and experimental foundations. *Mathematical Biosciences*, 17(3-4):243–300, 1973.

[7] M. Atiyah. The art of mathematics. *Notices of the American Mathematical Society*, 57(1):8, 2010.

[8] E. Bäuerle and U. Gaedke. *Lake Constance: Characterization of an ecosystem in transition.* Schweizerbart Science Publishers, Stuttgart, Germany, 1999.

[9] R. Bellman. *Mathematical Methods in Medicine*, volume 1 of *Modern Applied Mathematics.* World Scientific, 1983.

[10] S. Benzekry, C. Lamont, A. Beheshti, A. Tracz, J. M. L. Ebos, L. Hlatky, and P. Hahnfeldt. Classical mathematical models for description and prediction of experimental tumor growth. *PLOS Computational Biology*, 10(8):1–19, 2014.

[11] C. Bonet-Reves, J. Larrosa, and T. M-Seara. Regularization around a generic codimension one fold-fold singularity. *Journal of Differential Equations*, 265(5):1761–1838, 2018.

[12] D. C. Braga, T. Carvalho, and L. F. Mello. Limit cycles bifurcating from discontinuous centers. *IMA Journal of Applied Mathematics*, 82(4):849–863, 2017.

[13] D. C. Braga, A. F. Fonseca, and L. F. Mello. Study of limit cycles in piecewise smooth perturbations of Hamiltonian centers via regularization method. *Electronic Journal of Qualitative Theory of Differential Equations*, 79:1–13, 2017.

[14] D. C. Braga and L. F. Mello. Limit cycles in a family of discontinuous piecewise linear differential systems with two zones in the plane. *Nonlinear Dynamics*, 73(3):1283–1288, 2013.

[15] D. C. Braga and L. F. Mello. More than three limit cycles in discontinuous piecewise linear differential systems with two zones in the plane. *International Journal of Bifurcation and Chaos*, 24(4):1450056, 2014.

[16] B. Brogliato. *Nonsmooth Mechanics: Models, Dynamics and Control.* Communications and Control Engineering Series. Springer-Verlag London, second edition, 1999.

[17] L. E. J. Brouwer. On continuous vector distributions on surfaces. In *Proceedings of the Royal Netherlands Academy of Arts and Sciences (KNAW)*, volume 11, pages 850–858, 1909.

[18] C. A. Buzzi, T. Carvalho, and R. D. Euzébio. Chaotic planar piecewise smooth vector fields with non-trivial minimal sets. *Ergodic Theory and Dynamical Systems*, 36(2):458–469, 2016.

[19] C. A. Buzzi, T. Carvalho, and R. D. Euzébio. On Poincaré-Bendixson Theorem and non-trivial minimal sets in planar nonsmooth vector fields. *Publicacions Matemàtiques*, 62(1):113–131, 2018.

[20] C. A. Buzzi, T. Carvalho, and M. A. Teixeira. On 3-parameter families of piecewise smooth vector fields in the plane. *SIAM Journal on Applied Dynamical Systems*, 11(4):1402–1424, 2012.

[21] C. Camacho and A. Lins Neto. *Geometric Theory of Foliations*. Birkhauser, first edition, 1985.

[22] T. Carvalho. A recíproca do Teorema de Denjoy-Schwartz. Master's thesis, Universidade de São Paulo, 2007.

[23] T. Carvalho. On the closing lemma for planar piecewise smooth vector fields. *Journal de Mathématiques Pures et Appliquées*, 106(6):1174–1185, 2016.

[24] T. Carvalho and M. A. Teixeira. Basin of attraction of a cusp-fold singularity in $3D$ piecewise smooth vector fields. *Journal of Mathematical Analysis and Applications*, 418(1):11–30, 2014.

[25] T. Carvalho and M. A. Teixeira. On piecewise smooth vector fields tangent to nested tori. *Journal of Differential Equations*, 261(7):4008–4029, 2016.

[26] T. Carvalho, M. A. Teixeira, and D. J. Tonon. Asymptotic stability and bifurcations of $3D$ piecewise smooth vector fields. *Zeitschrift für angewandte Mathematik und Physik*, 67(2):31, 2016.

[27] C. Chicone. *Ordinary Differential Equations with Applications*, volume 34 of *Texts in Applied Mathematics*. Springer-Verlag New York, first edition, 1999.

[28] L. Chua, M. Komuro, and T. Matsumoto. The double scroll family. *IEEE Transactions on Circuits and Systems*, 33(11):1072–1118, 1986.

[29] B. Coll, A. Gasull, and R. Prohens. Degenerate Hopf Bifurcations in discontinuous planar systems. *Journal of Mathematical Analysis and Applications*, 253(2):671–690, 2001.

[30] A. Colombo, M. di Bernardo, E. Fossas, and M. R. Jeffrey. Teixeira singularities in $3D$ switched feedback control systems. *Systems & Control Letters*, 59(10):615–622, 2010.

[31] A. Colombo and M. R. Jeffrey. Nondeterministic chaos, and the two-fold singularity in piecewise smooth flows. *SIAM Journal on Applied Dynamical Systems*, 10(2):423–451, 2011.

[32] R. Cristiano, T. Carvalho, D. J. Tonon, and D. J. Pagano. Hopf and Homoclinic bifurcations on the sliding vector field of switching systems in $\mathbb{R}^3$: A case study in power electronics. *Physica D: Nonlinear Phenomena*, 347:12–20, 2017.

[33] R. Cristiano, D. J. Pagano, E. Freire, and E. Ponce. Revisiting the Teixeira singularity bifurcation analysis. Application to the control of power converters. *International Journal of Bifurcation and Chaos*, 28(9):1850106, 2018.

[34] L. G. de Pillis and A. E. Radunskaya. A mathematical tumor model with immune resistance and drug therapy: An optimal control approach. *Journal of Theoretical Medicine*, 3(2):79–100, 2001.

[35] L. G. de Pillis, A. E. Radunskaya, and C. L. Wiseman. A validated mathematical model of cell-mediated immune response to tumor growth. *Cancer Research*, 65(17):7950–7958, 2005.

[36] A. Denjoy. Sur les courbes définies par les équations différentielles à la surface du tore. *Journal de Mathématiques Pures et Appliquées*, 11:333–376, 1932.

[37] M. di Bernardo, C. J. Budd, A. R. Champneys, and P. Kowalczyk. *Piecewise-smooth Dynamical Systems: Theory and Applications.* Number 163 in Applied Mathematical Sciences. Springer-Verlag London, first edition, 2008.

[38] M. di Bernardo, A. Colombo, and E. Fossas. Two-fold singularity in nonsmooth electrical systems. In *2011 IEEE International Symposium of Circuits and Systems (ISCAS)*, pages 2713–2716, 2011.

[39] M. di Bernardo, K. H. Johansson, and F. Vasca. Self-oscillations and sliding in relay feedback systems: Symmetry and bifurcations. *International Journal of Bifurcation and Chaos*, 11(04):1121–1140, 2001.

[40] D. D. Dixon. Piecewise deterministic dynamics from the application of noise to singular equations of motion. *Journal of Physics A: Mathematical and General*, 28(19):5539–5551, 1995.

[41] R. T. Dorr and D. D. Von Hoff. *Cancer Chemotherapy Handbook.* Appleton & Lange, Norwalk, 1994.

[42] N. M. Drissa. *Fixed point, game and selection theory: from the Hairy Ball Theorem to a non hair-pulling conversation.* PhD thesis, Université Paris 1 Panthéon–Sorbonne, 2016.

[43] F. Dumortier, J. Llibre, and J. Artés. *Qualitative Theory Of Planar Differential Systems.* Universitext. Springer-Verlag Berlin Heidelberg, 2006.

[44] A. Dutta and P. K. Gupta. A mathematical model for transmission dynamics of HIV/AIDS with effect of weak CD4$^+$T cells. *Chinese Journal of Physics*, 56(3):1045–1056, 2018.

[45] S. N. Elaydi. *Discrete Chaos: With Applications in Science and Engineering*. Chapman and Hall/CRC, second edition, 2007.

[46] Y. Emvudu, D. Bongor, and R. Koïna. Mathematical analysis of HIV/AIDS stochastic dynamic models. *Applied Mathematical Modelling*, 40(21–22):9131–9151, 2016.

[47] A. F. Filippov. *Differential Equations with Discontinuous Righthand Sides*, volume 18 of *Mathematics and its Applications*. Springer Netherlands, first edition, 1988.

[48] E. Freire, E. Ponce, F. Rodrigo, and F. Torres. Bifurcation sets of continuous piecewise linear systems with two zones. *International Journal of Bifurcation and Chaos*, 8(11):2073–2097, 1998.

[49] R. P. Gendron. Models and mechanisms of frequency-dependent predation. *The American Naturalist*, 130(4):603–623, 1987.

[50] L. F. Gonçalves, D. C. Braga, A. F. Fonseca, and L. F. Mello. Limit cycles bifurcating from an invisible fold-fold in planar piecewise Hamiltonian systems. Submitted preprint, 2019.

[51] L. F. Gonçalves, D. C. Braga, A. F. Fonseca, and L. F. Mello. Lyapunov coefficients for an invisible fold-fold singularity in planar piecewise Hamiltonian systems. *Journal of Mathematical Analysis and Applications*, online, 2019. doi: 10.1016/j.jmaa.2019.123692.

[52] L. F. Gonçalves and T. Carvalho. Combing the Hairy Ball using a vector field without equilibria. *Journal of Dynamical and Control Systems*, 2019. doi: 10.1007/s10883-019-09446-5.

[53] L. F. Gonçalves and T. Carvalho. Creation of limit cycles in piecewise smooth vector fields tangent to nested tori. Submitted preprint, 2019.

[54] L. F. Gonçalves and T. Carvalho. A flow on S^2 presenting the ball as its minimal set. Submitted preprint, 2019.

[55] L. F. Gonçalves, T. Carvalho, R. Cristiano, and D. J. Tonon. Global analysis of the dynamics of a mathematical model to intermittent HIV treatment using sliding mode control. Submitted preprint, 2019.

[56] L. F. Gonçalves, T. Carvalho, and D. D. Novaes. Sliding shilnikov connection in prey switching model. Preprint. Available in `https://arxiv.org/abs/1809.02060`, 2019.

[57] L. F. Gonçalves, D. S. Rodrigues, P. F. A. Mancera, and T. Carvalho. A mathematical model for chemoimmunotherapy of chronic lymphocytic leukemia. *Applied Mathematics and Computation*, 349:118–133, 2019. doi:10.1016/j.amc.2018.12.008.

[58] L. F. Gonçalves, D. S. Rodrigues, P. F. A. Mancera, and T. Carvalho. Sliding mode control in a mathematical model to chemoimmunotherapy: the occurrence of typical singularities. *Applied Mathematics and Computation*, in press, 2019. doi:10.1016/j.amc.2019.124782.

[59] L. F. Gonçalves, D. C. Vicentin, P. F. A. Mancera, and T. Carvalho. Mathematical model of an antiretroviral therapy to HIV via Filippov theory. Submitted preprint, 2019.

[60] R. M. Granich, C. F. Gilks, C. Dye, K. M. D. Cock, and B. G. Williams. Universal voluntary HIV testing with immediate antiretroviral therapy as a strategy for elimination of HIV transmission: a mathematical model. *The Lancet*, 373(9669):48–57, 2009.

[61] J. J. D. Greenwood and R. A. Elton. Analysing experiments on frequency-dependent selection by predators. *Journal of Animal Ecology*, 48(3):721–737, 1979.

[62] M. Guardia, T. M. Seara, and M. A. Teixeira. Generic bifurcations of low codimension of planar Filippov Systems. *Journal of Differential Equations*, 250(4):1967–2023, 2011.

[63] C. Gutierrez. Smoothing continuous flows on two-manifolds and recurrences. *Ergodic Theory and Dynamical Systems*, 6(1):17–44, 1986.

[64] H. Guven, M. Gilljam, B. J. Chambers, H. G. Ljunggren, B. Christensson, E. Kimby, and M. S. Dilber. Expansion of natural killer (NK) and natural killer-like T (NKT)-cell populations derived from patients with B-chronic lymphocytic leukemia (B-CLL): a potential source for cellular immunotherapy. *Leukemia*, 17:1973–1980, 2003.

[65] D. Hilbert. Mathematical problems. *Bull. Amer. Math. Soc.*, 8(10):437–479, 07 1902.

[66] Y. Hirata, K. Morino, K. Akakura, C. S. Higano, and K. Aihara. Personalizing Androgen Suppression for Prostate Cancer Using Mathematical Modeling. *Scientific Reports*, 8(1):2673, 2018.

[67] M. W. Hirsch, S. Smale, and R. L. Devaney. *Differential Equations, Dynamical Systems, and an Introduction to Chaos*. Pure and Applied Mathematics. Elsevier Academic Press, second edition, 2004.

[68] B. Hirschel and T. Flanigan. Is it smart to continue to study treatment interruptions? *AIDS*, 23(7):757–759, 2009.

[69] J. H. Hubbard and B. H. West. *Differential Equations: A Dynamical Systems Approach*, volume 5 of *Texts in Applied Mathematics*. Springer-Verlag New York, first edition, 1991.

[70] C. Imai, S. Iwamoto, and D. Campana. Genetic modification of primary natural killer cells overcomes inhibitory signals and induces specific killing of leukemic cells. *Blood*, 106(1):376–383, 2005.

[71] A. Jacquemard and D. J. Tonon. Coupled systems of non-smooth differential equations. *Bulletin des Sciences Mathématiques*, 136(3):239–255, 2012.

[72] M. R. Jeffrey and A. Colombo. The two-fold singularity of discontinuous vector fields. *SIAM Journal on Applied Dynamical Systems*, 8(2):624–640, 2009.

[73] D. Kirschner and G. F. Webb. A model for treatment strategy in the chemotherapy of AIDS. *Bulletin of Mathematical Biology*, 58(2):367–390, 1996.

[74] J. M. Kneitel and J. M. Chase. Trade-offs in community ecology: linking spatial scales and species coexistence. *Ecology Letters*, 7(1):69–80, 2004.

[75] A. Korobeinikov. Global properties of basic virus dynamics models. *Bulletin of Mathematical Biology*, 66:879–883, 2004.

[76] T. Kousaka, T. Kido, T. Ueta, H. Kawakami, and M. Abe. Analysis of border-collision bifurcation in a simple circuit. In *2000 IEEE International Symposium on Circuits and Systems. Emerging Technologies for the 21st Century. Proceedings (IEEE Cat No.00CH36353)*, volume 2, pages 481–484, 2000.

[77] V. S. Kozlova. Structural stability of a discontinuous system. *Vestnik Moskovskogo Universiteta. Seriya I. Matematika, Mekhanika*, 5:16–20, 1984.

[78] V. Krivan. Optimal foraging and predator–prey dynamics. *Theoretical Population Biology*, 49(3):265–290, 1996.

[79] Y. A. Kuznetsov. *Elements of Applied Bifurcation Theory*, volume 112 of *Applied Mathematical Sciences*. Springer-Verlag New York, second edition, 1998.

[80] Y. A. Kuznetsov, S. Rinaldi, and A. Gragnani. One-parameter bifurcations in planar Filippov systems. *International Journal of Bifurcation and Chaos*, 13(08):2157–2188, 2003.

[81] P. Leenheer and H. L. Smith. Virus dynamics: a global analysis. *SIAM J. Appl. Math.*, 63(4):1313–1327, 2003.

[82] R. Leine and H. Nijmeijer. *Dynamics and Bifurcations of Non-Smooth Mechanical Systems*, volume 18 of *Lecture Notes in Applied and Computational Mechanics.* Springer-Verlag Berlin Heidelberg, first edition, 2004.

[83] A. Liapounoff. *Problème général de la stabilité du mouvement*, volume 17 of *Annals of Mathematics Studies.* Princeton University Press, 1947.

[84] J. Llibre and E. Ponce. Three nested limit cycles in discontinuous piecewise linear differential systems with two zones. *Dynamics of Continuous, Discrete and Impulsive Systems Series B: Applications & Algorithms*, 19(3):325–335, 2012.

[85] H. Lüllmann, K. Mohr, A. Ziegler, and D. Bieger. *Color Atlas of Pharmacology.* Thieme Stuttgart, New York, 2000.

[86] R. Lum and L. O. Chua. Global properties of continuous piecewise linear vector fields. part I: Simplest case in $\mathbb{R}^2$. *International Journal of Circuit Theory and Applications*, 19(3):251–307, 1991.

[87] F. Maggiolo, M. Airoldi, A. Callegaro, C. Martinelli, A. Dolara, T. Bini, G. Gregis, G. Quinzan, D. Ripamonti, V. Ravasio, and F. Suter. CD4 cell-guided scheduled treatment interruptions in HIV-infected patients with sustained immunologic response to HAART. *AIDS*, 23(7):799–807, 2009.

[88] J. C. Medrado and J. Torregrosa. Uniqueness of limit cycles for sewing planar piecewise linear systems. *Journal of Mathematical Analysis and Applications*, 431(1):529–544, 2015.

[89] J. D. Meiss. *Differential Dynamical Systems*, volume 14 of *Mathematical modeling and computation.* Society for Industrial and Applied Mathematics (SIAM), 2007.

[90] J. Milnor. Analytic proofs of the "hairy ball theorem" and the brouwer fixed point theorem. *The American Mathematical Monthly*, 85(7):521–524, 1978.

[91] W. W. Murdoch. Switching in general predators: Experiments on predator specificity and stability of prey populations. *Ecological Monographs*, 39(4):335–354, 1969.

[92] D. D. Novaes and E. Ponce. A simple solution to the Braga–Mello Conjecture. *International Journal of Bifurcation and Chaos*, 25(1):1550009, 2015.

[93] D. D. Novaes, G. Ponce, and R. Varão. Chaos induced by sliding phenomena in Filippov systems. *Journal of Dynamics and Differential Equations*, 29(4):1569–1583, 2017.

[94] D. D. Novaes and M. A. Teixeira. Shilnikov problem in Filippov dynamical systems, 2015.

[95] M. Nowak and R. M. May. *Virus Dynamics: Mathematical Principles of Immunology and Virology*. Oxford University Press, UK, 2000.

[96] A. S. Perelson and P. W. Nelson. Mathematical analysis of HIV-1 dynamics in vivo. *SIAM Review*, 41:3–4, 1999.

[97] L. Perko. *Differential Equations and Dynamical Systems*, volume 7 of *Texts in Applied Mathematics*. Springer-Verlag New York, third edition, 2001.

[98] C. Pessoa and D. J. Tonon. Piecewise smooth vector fields in $\mathbb{R}^3$ at infinity. *Journal of Mathematical Analysis and Applications*, 427(2):841 – 855, 2015.

[99] S. H. Piltz, M. A. Porter, and P. K. Maini. Prey switching with a linear preference trade-off. *SIAM Journal on Applied Dynamical Systems*, 13(2):658–682, 2014.

[100] H. Poincaré. Mémoire sur les courbes définies par une équation différentielle (I). *Journal de Mathématiques Pures et Appliquées*, 7(3):375–422, 1881.

[101] A. J. Schwartz. A generalization of a Poincaré-Bendixson Theorem to closed two-dimensional manifolds. *American Journal of Mathematics*, 85(3):453–458, 1963.

[102] P. A. Schweitzer. Counterexamples to the Seifert Conjecture and opening closed leaves of foliations. *Annals of Mathematics*, 100(2):386–400, 1974.

[103] L. P. Shilnikov. A case of the existence of a denumerable set of periodic motions. *Doklady Akademii Nauk SSSR*, 160:558–561, 1965.

[104] L. P. Shilnikov. The generation of a periodic motion from a trajectory which is doubly asymptotic to a saddle type equilibrium state. *Mat. Sb. (N.S.)*, 77(119):461–472, 1968.

[105] D. J. W. Simpson. A compendium of Hopf-like bifurcations in piecewise-smooth dynamical systems. *Physics Letters A*, 382(35):2439–2444, 2018.

[106] H. E. Skipper, F. M. Schabel Jr, and W. S. Wilcox. Experimental evaluation of potential anticancer agents. XIII: On the criteria and kinetics associated with "curability" of experimental leukemia. *Cancer Chemotherapy Reports*, 35:1–111, 1964.

[107] J. Sotomayor and A. L. F. Machado. Structurally stable discontinuous vector fields in the plane. *Qualitative Theory of Dynamical Systems*, 3(1):227–250, 2002.

[108] J. Sotomayor, L. F. Mello, and D. C. Braga. Bifurcation analysis of the Watt governor system. *Computational and Applied Mathematics*, 26(1):19–44, 2007.

[109] J. Sotomayor and M. A. Teixeira. Regularization of discontinuous vector fields. In *International Conference on Differential Equations, Lisboa, 1995*, pages 207–223. World Scientific Publishing, 1998.

[110] J. S. Spratt, J. S. Meyer, and J. A. Spratt. Rates of growth of human neoplasms: Part II. *Journal of Surgical Oncology*, 61(1):68–83, 1996.

[111] D. W. Stephens and J. R. Krebs. *Foraging Theory.* Monographs in Behavior and Ecology. Princeton University Press, 1987.

[112] T. Suzuki, N. Bruchovsky, and K. Aihara. Piecewise affine systems modelling for optimizing hormone therapy of prostate cancer. *Philosophical Transactions of the Royal Society A: Mathematical, Physical and Engineering Sciences*, 368(1930):5045–5059, 2010.

[113] F. Takens. Unfoldings of certain singularities of vectorfields: Generalized Hopf bifurcations. *Journal of Differential Equations*, 14(3):476–493, 1973.

[114] B. Tang, Y. Xiao, R. A. Cheke, and N. Wang. Piecewise virus-immune model with HIV-1 RNA-guided therapy. *Journal of Theoretical Biology*, 377:36–46, 2015.

[115] S. Tang, Y. Xiao, N. Wang, and H. Wu. Piecewise HIV virus dynamic model with CD4$^+$T cell count-guided therapy: I. *Journal of Theoretical Biology*, 308(7):123–134, 2012.

[116] M. A. Teixeira. Generic bifurcation in manifolds with boundary. *Journal of Differential Equations*, 25(1):65–89, 1977.

[117] M. A. Teixeira. Generic singularities of discontinuous vector fields. *Anais da Academia Brasileira de Ciências*, 53(2):257–260, 1981.

[118] M. A. Teixeira. Stability conditions for discontinuous vector fields. *Journal of Differential Equations*, 88(1):15–29, 1990.

[119] M. A. Teixeira. Perturbation theory for non-smooth systems. In *Encyclopedia of Complexity and Systems Science*, pages 6697–6709. Springer New York, New York, 2009.

[120] K. Tirok and U. Gaedke. Regulation of planktonic ciliate dynamics and functional composition during spring in Lake Constance. *Aquatic Microbial Ecology*, 49(1):87–100, 2007.

[121] K. Tirok and U. Gaedke. Internally driven alternation of functional traits in a multispecies predator–prey system. *Ecology*, 91(6):1748–1762, 2010.

[122] C. Tresser. Un théorème de Shilnikov en $C^{1,1}$. *Comptes Rendus des Séances de l'Académie des Sciences. Série I. Mathématique*, 296(13):545–548, 1983.

[123] E. van Leeuwen, Å. Brännström, V. A. A. Jansen, U. Dieckmann, and A. G. Rossberg. A generalized functional response for predators that switch between multiple prey species. *Journal of Theoretical Biology*, 328:89–98, 2013.

[124] R. A. Weinberg. *The biology of cancer.* Garland Science, New York, 2006.

[125] E. T. Whittaker and G. Robinson. *The Calculus of Observations: A Treatise on Numerical Mathematics.* Blackie & Son limited, fourth edition, 1954.

[126] S. Wiggins. *Introduction to Applied Nonlinear Dynamical Systems and Chaos.* Texts in Applied Mathematics. Springer-Verlag New York, second edition, 2003.

[127] Wolfram Research, Inc. Mathematica, Version 11. Champaign, IL, 2018.

[128] World Health Organization. Consolidated guidelines on the use of antiretroviral drugs for treating and preventing HIV infection, 2016. `https://www.who.int/hiv/pub/arv/arv-2016/en/`.

[129] World Health Organization. Data and statistics, 2019. `https://www.who.int/hiv/data/en/`. Accessed: September, 2019.